OCS Study
MMS 2009-024

Coastal Studies Institute

# Environmental Investigation of the Long-Term Use of Ship Shoal Sand Resources for Large Scale Beach and Coastal Restoration in Louisiana

## Final Report

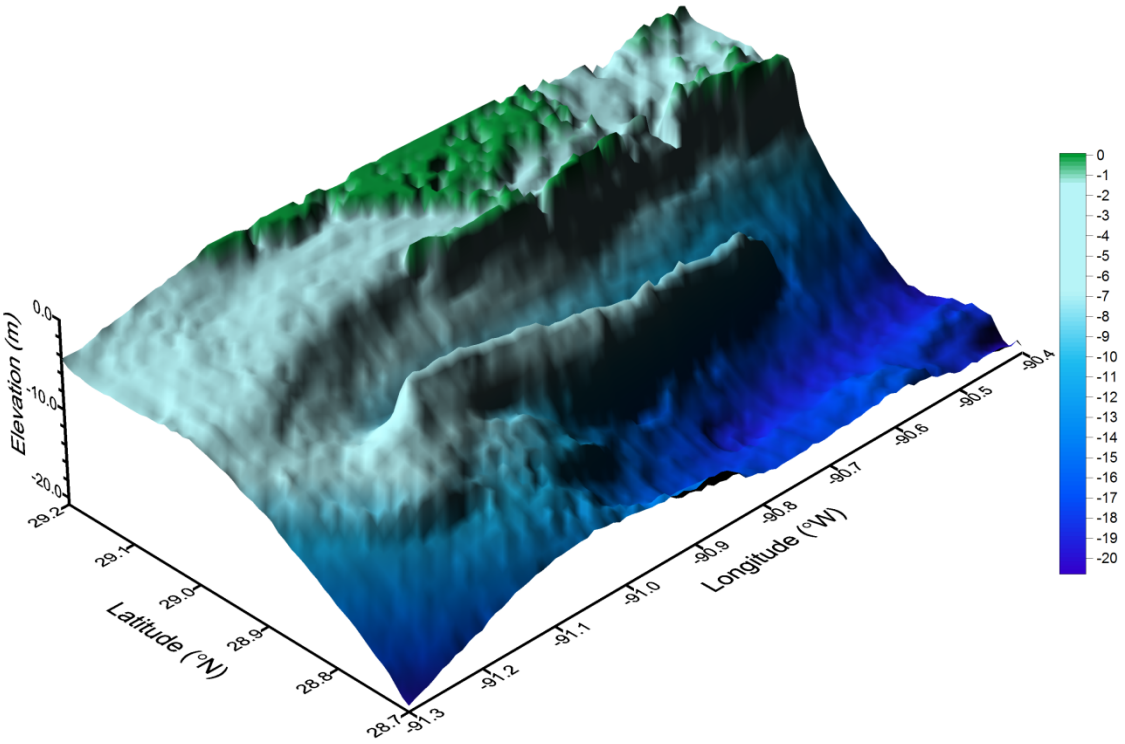



MMS U.S. Department of the Interior
Minerals Management Service

Louisiana Applied Coastal Engineering & Science Division
Office of Coastal Protection & Restoration

LSU Coastal Studies Institute
Louisiana State University

OCS Study
MMS 2009-024

Coastal Studies Institute

# Environmental Investigation of the Long-Term Use of Ship Shoal Sand Resources for Large Scale Beach and Coastal Restoration in Louisiana

## Final Report

**Principal Investigator** Dr. Gregory W. Stone
**Co-Pi** Dr. Richard E. Condrey
**Co-Pi** Dr. John W. Fleeger
**Co-Pi** Syed M. Khalil

**Contributors**

Dr. Daijiro Kobashi
Dr. Felix Jose
Elaine Evers
Dr. Stanislas Dubois
Dr. Baozhu Liu
Sara Arndt

**Current Doctoral Students**

Carey Gelpi
Mark A. Grippo
Yixin Luo
Seyed M. SiadatMousavi
Yuliang Chen
Marjo Alavillamo
Francois Reynal

Prepared under MMS Contract
1435-01-04-CA-35162
and
LCPRA Contract
2503-07-10
by
Coastal Studies Institute & Department of Oceanography and Coastal Sciences and Department of Biological Sciences, Louisiana State University
Baton Rouge, LA 70803
Louisiana Applied Coastal Engineering & Science Division, Office of Coastal Protection & Restoration, Baton Rouge, LA 70804

Published by

**U.S. Department of the Interior**
**Minerals Management Service** **April 2009**

## DISCLAIMER

This report was prepared under contract between the Minerals Management Service (MMS), Louisiana Applied Coastal Engineering & Science Division, Office of Coastal Protection & Restoration and Louisiana State University. This report has been technically reviewed by the MMS, and it has been approved for publication. Approval does not signify that the contents necessarily reflect the views and policies of the MMS, nor does mention of trade names or commercial products constitute endorsement or recommendation for use. It is, however, exempt from review and compliance with the MMS editorial standards.

## REPORT AVAILABILITY

Extra copies of this report may be obtained from the Public Information Office (Mail Stop 5034) at the following address: U.S. Department of the Interior Minerals Management Service:

U.S. Department of the Interior
Minerals Management Service
Gulf of Mexico OCS Region
Public Information Office (MS 5034)
1201 Elmwood Park Boulevard
New Orleans, Louisiana 70123-2394

Telephone: (504) 736-2419 or
1-800-200-GULF

## CITATION

Suggested citation:

Stone, G.W. et al. 2009. Environmental Investigation of the Long-Term Use of Ship Shoal Sand Resources for Large Scale Beach and Coastal Restoration in Louisiana. U.S. Dept. of the Interior, Minerals Management Service, Gulf of Mexico OCS Region, New Orleans,LA. OCS Study MMS 2009-024. 278 pp.

# Acknowledgements

We would like to thank Minerals Management Service (MMS), Department of Interior, for providing us the funding support in order to pursue this multi-disciplinary research. We greatly benefited from the advice provided by the Louisiana Sand Management Working Group. Also, we would like to extend our appreciation to the Office of Research and Economic Development at LSU and the supporting staff at respective departments for providing the necessary administrative support.

The Physical group acknowledges the essential role of the Coastal Studies Institute Field Support Group in carrying out the extensive field surveys. DHI Water and Environment® is acknowledged for granting the permission to use their Hydrodynamic models for this study. The Meiofauna and Macrofauna groups wish to thank the captains and crew of Louisiana Universities Marine Consortium's RV *Acadiana* and RV *Pelican*, for the extraordinary part they played in making each biological sampling trip a success.

The Meiofauna group sincerely appreciates the critical review and comments of its chapters by Drs. Kevin Carman, Brian Fry and Nancy Rabalais. Also, Laboratory support was extended by Alana Cleland, Monissa Duvai, Ross del Rio and Lea Macarthy. Technical advice on light and pigment measurement was provided by Mike Murrell and Soraya Silva.

The Macroinfauna/blue crab group greatly benefited from the advice and assistance of the Coastal Ecology Group of the Louisiana Department of Wildlife and Fisheries, Sara Lecroy, and Talat Farooqi, and Drs. Nancy Rabalais, J. Geaghan, Herbert Boschung, Darryl Felder and Richard Shaw. Amy Spaziani, Puneeta Naik, Chris Baker and Heather Drucker assisted in data collection. Dr. D. B. Eggleston provided us with a prepublication copy of Eggleston et al. (in review) and Dr. R. M. Overstreet with an early draft of Shields and Overstreet (2007). S. Wells in Dr. J. R. McConaugha's lab provided valuable insight on procedures for estimating number of eggs in a blue crab sponge. Dr. T. Wolcott, S. Wells, and Gerald Adkins provided valuable reviews of our blue crab manuscript. We benefited from blue crabs discussions with Drs. M. Ogburn and R. A. Tankersley, D. L. Dudley, Harriet Perry, and Vince Guillory.

# Table of Cotents

# LIST OF FIGURES

# LIST OF TABLES

# LIST OF ABBREVIATIONS

| | |
|---|---|
| mg $O_2$/L | milligram of Oxygen in 1 liter of sea water |
| CSI | Coastal Studies Institute |
| WAVCIS | wave current surge information ystem |
| ADV | Acoustic Doppler Velocimeter |
| PC ADP | Pulse coherent Acoustic Doppler Profiler |
| ADCP | Acoustic Doppler Current Profiler |
| $\rho_f$ | fluid density |
| Hz | unit of frequency (number of cycles per second) |
| $H_s$ | significant wave height, unit (meters) |
| $T_p$ | peak wave period, unit (second) |
| k | wave number in $m^{-1}$ |
| $U_b$, $u_{ob}$ | wave orbital velocity at the bottom |
| $U_{100}$ | mean current at 1 m above the bottom |
| $f_p$ | peak frequency |
| $u_{*w}$ | shear velocity at the bed due to waves |
| $\tau$ | wind stress on the sea surface |
| $\tau_w$ | shear stress at the bottom due to waves |
| $\tau_c$ | shear stress at the bottom due to current |
| $\nu$ | kinematic viscosity |
| OBS | optical backscatter intensity, measured in NTU units |
| NTU | nephelometric turbidity units |
| SSC | suspended sediment concentration |
| $\phi$ | unit of sediment size |
| $ms^{-1}$ | velocity, in meters/second |
| $C_f$ | surface drag coefficient |
| $C_D$ | bottom drag coefficient |
| cfs | cubic feet per second, river gauge data |
| ANOVA | analysis of variance |
| BPP | benthic primary production |
| BWC | bottom-water chl *a* |
| Chl *a* | chlorophyll *a* |
| D.O. | dissolved Oxygen (mg/L) |
| HPLC | high Performance Liquid Chromatography |
| Iz | percent of surface light reaching sediment surface |
| $I_o$ | surface PAR |
| $K_{PAR}$ | light attenuation coefficient |
| LCS | Louisiana continental shelf |
| PAR | Photosynthetically Active Radiation |
| SEAMAP | Southeast Area Monitoring and Assessment Program |
| *z* | bottom depth (m) |
| WCI | integrated water-column chl *a* |

| | |
|---|---|
| ppt | parts per thousand |
| AH | abdominal hairs located on the pleopods of a female blue crab |
| ANCOVA | analysis of covariance |
| ANOSIM | analysis of similarities |
| BACI | before-after, control-impact |
| BB | blue crab carapace width at the base of lateral spines |
| BC | acorn barnacle exoskeleton coverage of a blue crab |
| BW | acorn barnacle weight on a blue crab |
| C | blue crab body weight without tail |
| D | largest acorn barnacle diameter on a blue crab |
| E | number of eggs in a blue crab sponge |
| G | gooseneck barnacle intensity on blue crab gills |
| GN | presence/absence of nemerteans on blue crab gills |
| H | blue crab carapace height |
| H’ | Shannon-Wiener diversity |
| HSD | honestly significant differences |
| L | blue crab carapace length |
| SI | Simpson’s index |
| N0 | species richness |
| N1 | exp (H’) |
| N2 | 1/SI |
| nMDS | non-metric multidimensional scaling |
| O | blue crab ovary fullness on a three-point scale |
| $O_{SC}$ | ovarian condition as a function of blue crab sponge color |
| P | presence or absence of a sponge on a mature female blue crab |
| $R^2$ | residual sum of squares |
| S | blue crab spermathecae |
| S.E. | standard error |
| SC | blue crab sponge color |
| SIMPER | similarity percentage |
| SN | nemertean intensity on blue crab sponge |
| SNK | Student-Newman-Keuls test |
| STTSC | Ship/Trinity/Tiger Shoal Complex |
| T | blue crab tail weight |
| t | time |
| TT | blue crab carapace width between the lateral spines |
| V | volume |
| W | blue crab weight without acorn barnacles |
| X | linear estimate of volume |

*CONTRIBUTORS FOR INDIVIDUAL CHAPTERS*

**Executive Summary**

Gregory W. Stone
Richard E. Condrey
John W. Fleeger
Syed M. Khalil
Daijiro Kobashi
Stanislas Dubois
Felix Jose
Carey Gelpi
Mark A. Grippo
Baozhu Liu

**Chapter 1**

Gregory W. Stone
Richard E. Condrey
John W. Fleeger
Carey Gelpi
Daijiro Kobashi
Mark A. Grippo
Felix Jose
Stanislas Dubois
Syed M. Khalil

**Chapter 2**

Syed M. Khalil
Charles W. Finkl
Jeff Andrews
Christopher P. Knotts

**Chapter 3**

Daijiro Kobashi
Gregory W. Stone

**Chapter 4**

Daijiro Kobashi
Gregory W. Stone
Felix Jose

Yixin Luo

**Chapter 5**

Felix Jose
Daijiro Kobashi
Gregory W. Stone

**Chapter 6**

Daijiro Kobashi
Gregory W. Stone

**Chapter 7**

Daijiro Kobashi
Gregory W. Stone
Syed M. Khalil
Seyed M. SiadatMousavi

**Chapter 8**

Mark A. Grippo
John W. Fleeger
Richard E. Condrey

**Chapter 9**

John W. Fleeger
Mark A. Grippo

**Chapter 10**

Stanislas Dubois
Carey Gelpi
Richard E. Condrey
John W. Fleeger
Sara Arndt
Marjo Alavillamo
Francois Reynal
Elaine Evers

**Chapter 11**

Mark A. Grippo

Richard E. Condrey
Carey Gelpi
John W. Fleeger

**Chapter 12**

Richard E. Condrey
Carey Gelpi
Stanislas Dubois
John W. Fleeger
Elaine Evers
Sara Arndt
Marjo Alavillamo
Francois Reynal

**Chapter 13**

Gregory W. Stone
Richard E. Condrey
John W. Fleeger
Felix Jose
Mark A. Grippo
Daijiro Kobashi
Carey Gelpi
Stanislas Dubois
Syed M. Khalil
Baozhu Liu

# EXECUTIVE SUMMARY

Ship Shoal is one of the largest offshore sand resources along the northern Gulf of Mexico, containing 1.6 billion cubic yards (1.22 billion $m^3$) of fine sand. This shoal may be mined and used in beach reinforcement and coastal stabilization projects designed to mitigate coastal erosion due to storm damages and prevent extensive coastal wetland loss due to anthropogenic activities. However, Ship Shoal is poorly known in terms of its hydrodynamics as well as the biological abundance associated with the shoal. In anticipation of sand mining, we initiated field surveys and shoal monitoring in 2005 that continued until 2008 to more adequately describe existing physical and biological conditions on Ship Shoal and to better predict the biological impacts of and recovery from sand mining. A substantial amount of hydrodynamic modeling was also undertaken to this effect.

Sand resources along the southern Louisiana coast are relatively scarce given the large volumes of sand required for restoration of the rapidly degrading barrier island chains, mainland beaches and other ecologically sensitive coastal systems. During this study, vibracores were obtained along the eastern end of Ship Shoal, commonly known as South Pelto, to estimate sand resources. It is estimated that the eastern flank of the shoal encompasses very clean sand (less than 5% silt in the upper shoal units) that ranged in thickness from 4 to 6 m. Approximately 21.6 x $10^6$ $m^3$ of clean sand has been estimated in total for the three potential borrow areas identified along the shoal. Buffers around oil and gas infra-structure and other magnetic anomalies occurring in and around the study area were avoided during borrow area design to ensure quality of the borrow sediments and to enhance the safety of dredging operations. Sand deposits identified along South Pelto in this study have significant potential to support large-scale coastal restoration along coastal regions within the vicinity of eastern Ship Shoal. Sand from this borrow area is proposed to be used for restoration of the Caminada-Moreau headland restoration project.

Wind fields associated with tropical and extra-tropical storms decisively contributed towards fluvial sediment dispersal and transport on the inner shelf off the Louisiana coast. The voluminous debouchments of sediment from the Atchafalaya River, especially during the spring flood season, occasionally coincided with post-frontal phases of cold front events so that material being transported is deposited farther south onto the inner shelf and its shallow shoals. The prevailing westward dispersal pattern during the winter-spring season is shifted to the southeast, following strong post-frontal northwesterly winds, which in turn facilitated generation of southeastward currents and further transport of fluvially-derived fine sediments from the Atchafalaya River/Bay farther southeast. Under some conditions, a portion of these terrigenous materials eventually settle, at least ephemerally, on Ship Shoal, located approximately 50 km southeast from the river mouth. Sediment transport events occurred in pulses and in tandem with high fluvial sediment discharge during spring floods and/or when local sediment re-suspension peaked. While, during tropical cyclones, fluvially-derived sediment transport occurred based on strong local sediment re-suspension and mixing, and was possibly in part based on high suspended sediment concentration (SSC) from both the lower Atchafalaya River and the Wax

Lake Outlet, and being redistributed onto the Atchafalaya Shelf and to adjacent transgressive shoals.
Our modeling efforts to relate the Atchafalaya River sediment plume structure to storm winds and its consequent effects on the offshore shoal, corroborated the results of *in-situ* measurements by demonstrating a strong response of the dispersal to various wind conditions, illustrating conspicuous shifts in sediment dispersal patterns during post-frontal wind conditions. For the model case with northwest winds, illustrated in C*hapter 3*, sediments transported southeastward did not reach the shoal after 20 days of the model duration under all storm wind conditions; while, the case with combined no wind and northwest wind provided that sediment plumes transported further southeastward and reached the shoal within 3 days of post-frontal winds. Modeling studies further confirmed that sediment supply from offshore may not be significant except during strong storms, given the fact that sediment re-suspension off the shoal is significantly lower than that on the shoal.

Frequencies of the dispersal shifts (approximately once every 8 days) and the sediment plume that reached the shoal (approximately once every 19 days) had no correlation with monthly mean river discharge; however the latter was strongly correlated with monthly mean wind stress, suggesting the importance of storm winds in relation to the dispersal shifts rather than river discharge, although increased river discharge likely contributes high fluvial sediment supply into the Atchafalaya Bay and farther offshore to the inner shelf.

Based on our field surveys and sediment sample analysis it is suggested that an occasional sediment plume shift from the Atchafalaya River/Bay to the southeast may result in accumulation of a thin fluid mud layer on patchy portions of the shoal with a maximal thickness of approximately 2 - 4cm. In an isolated case, during the 2006 deployment, a thickness of 15 cm and 30 cm for unconsolidated and partially consolidated fluid mud, in the waning phase of storms, was measured from a location along the eastern flank of the shoal. The accumulated fluid mud layer strongly interacted with bottom sediment through the process of sediment re-suspension, vertical mixing, hindered settling, and re-distribution, resulting in a maximum of 20 cm of erosion followed by 30 cm of accumulation at the deployment site. Ship Shoal, although comprised primarily of sediment in the sand range, appears to undergo short-lived but important changes in sediment type in the bottom boundary layer with an as yet undetermined portion of its surficial sediments being comprised of predominantly fine silts and clays during portions of the spring flood season. The data during the 2008 deployment showed that the bottom sediments were composed primarily of material in the sandy range and hence the bottom boundary layer dynamics were estimated following conventional approaches.

It was estimated that the rate of transport for cohesive sediment was more than an order of magnitude higher than those numerically derived non-cohesive sediment transport as calculated for fine sand sampled during the retrieval cruise in 2006, suggesting the importance of fluid mud transport. The accumulation of fluid mud may be ephemeral and non-uniform on the shoal given the frequencies of the dispersal shifts (once every 19 days) and more frequent sediment re-suspension events associated with winter storms (once every 6.0 days).

Results obtained from numerical modeling of waves, currents and sediment transport were in general agreement with *in-situ* observational data and satellite images except during peak storm conditions. Simulated currents also agreed with *in-situ* currents; however, bottom cross-shore currents were poorly correlated with *in-situ* bottom currents and are probably due to the inaccuracy of shoal bathymetry despite depth corrections. From the seaward to the landward flank of the shoal, significant wave height attenuation of 22% was computed for southerly waves and 28% for northerly waves. The dissipation of wave energy over the shoal resulted in re-suspension and transport of shoal sediment during storm events. This level of wave energy attenuation also points to the effectiveness of the shoal in shielding the already vulnerable coast against frequent cold fronts and occasional hurricanes. The evolution of the energy spectra, when the cold front crosses the study area, was abrupt and the dominant direction shifted from southwest to north across the shoal. This shift is attributed to wave refraction due to the shoal as well as veering of the wind direction. In spite of the influences of freshwater and fluvial sediments from the Atchafalaya River, a barotropic hydrodynamic model performed reasonably well on examining currents over the shoal and the surrounding inner shelf.

Waves and wave-induced sediment re-suspension significantly changed between the two extreme scenarios, viz., with and without the shoal. While, for the case of partial removal of the shoal, more realistic in terms of the scope of the proposed mining projects, the variability in the waves and wave-induced sediment re-suspension were computed as insignificant. Although there are differences in magnitudes for the model results with and without the shoal, large-scale targeted sand mining did not result in abrupt changes in current patterns.

Sediment re-suspension intensity (RI) was high across the inner shelf and the shoal during severe and strong storms; in general, it was spatially different and dependent upon physical forcing (i.e. wind and deep water waves). The RI decreased from the shallowest western portion of the shoal to the deepest eastern flank of the shoal; the RI off the shoal was significantly lower than that on the shoal. The results suggest that the deeper eastern flank of the shoal is in favor of fluid mud accumulation. This suggestion was supported by *in-situ* measurements;

The distribution of fluid mud, based on repeated sediment sampling and *in-situ* measurements, may be considered as patchy and ephemeral. The patchiness of the fluid mud distribution is extremely difficult to resolve within the scope of this study, given the unavailability of seasonal sediment data from the entire shoal environment. The *in situ* data suggest that as storm intensity varies, strongest in January and decreases toward Spring, the eastern portion of the shoal tends to be more susceptible to the accumulation of fluid mud than the middle and western portions of the shoal; moreover, sediment re-suspension and re-distribution tend to outweigh sediment supply during Spring and results in the formation of a sandy surface layer on the shoal by the end of the winter storm season, in May. Numerical modeling studies suggest that large-scale sand dredging would have spatially profound impacts on waves and sediment suspension on the shoal, however, no abrupt changes to current patterns. The changes in wave transformation and sediment suspension suggest that large-scale sand dredging may enhance fluid mud accumulation on the shoal.

The sedimentology of bottom sediments in addition to water chemistry, were also evaluated as part of this study. Spatial gradients in depth and grain size were found on Ship Shoal. Depths across the shoal ranged from 5 to 11 m and generally increased from west (5 to 8 m) to east (9 to 10 m). Sediments on Ship Shoal were well sorted fine- to very-fine sand (mean grain size ranged from 120 to 200 μm (2.32 -3.06ϕ) with a low silt/clay content (usually < 2%). Mean grain size generally increased from west to east, a pattern attributable to the higher percentage of shell hash (measured as percent gravel) on the eastern end. Sediment organic carbon values were generally less than 0.2% across all stations. Bottom-water dissolved oxygen (D.O.) concentrations on Ship Shoal were above hypoxic levels (2 mg/l) at all stations and seasons.

We determined that Ship Shoal is a high-relief sub-aqueous shoal composed of fine sand. Benthic macroinfauna species diversity is high and community taxonomic composition is very different on Ship Shoal compared to the surrounding deeper, muddier sediments. Thus, Ship Shoal may be an important and previously unrecognized biodiversity hot spot and potentially serve as a "stepping stone" for gene flow and dispersal of macroinfauna with affinities to sandy sediments in the northern Gulf (serving as a link between sandy habitats along the coasts of Florida and Texas).

Based on measurements of bottom water and faunal composition, Ship Shoal does not appear to be subject to frequent or intense hypoxia. Ship Shoal macroinfauna likely contribute larvae as a type of "seed bank" for an annual recolonization of surrounding areas influenced by seasonal hypoxia. During the surrounding hypoxia events most nekton do not appear to aggregate on Ship Shoal as a refuge from hypoxia. The abundance of several important nekton species, e.g., white and brown shrimp and croaker, is relatively low on Ship Shoal compared to surrounding, oxygen-sufficient areas and their residency on Ship Shoal appears to be short. On the other hand, female blue crab form important spawning and feeding aggregations with long residency on Ship Shoal (see below). We found that all demersal nekton collected on Ship Shoal use local benthic resources in their diet.

Light reaches the seafloor on Ship Shoal in sufficient intensity to potentially stimulate benthic primary production year round. The biomass of benthic algae is high and the high proportion of benthic diatoms (compared to settled phytoplankton) suggests that benthic primary production may comprise a large fraction of the total (benthic plus pelagic) primary production on Ship Shoal. Benthic algae may contribute to Ship Shoal food webs as basal resources to macrofauna which are, in turn, prey to nekton. Sand mining will reduce light intensity on the seafloor (by making the water deeper and increasing turbidity) and may increase the concentration of fine-grain sediments. These factors will likely diminish the abundance and productivity of benthic algae. This is expected to affect food webs relying on benthic algae as the basal resource.

Meiofauna communities are known to have intimate relationships with sediments. On Ship Shoal, meiofauna live as interstitial animals, living and moving between sand particles. Their taxonomic composition differs from surrounding sediments and their abundance and diversity is relatively low. Meiofauna will likely be removed by sand mining, however their recovery will depend on the method and extent of sand mining.

Macroinfauna on Ship Shoal are diverse taxonomically and occur in a very high biomass. The most prominent species contributing to the high biomass are large-bodied cephalochordates, crustaceans and mollusks that require access to the sediment surface for feeding, while polychaetes and crustaceans contribute most to species diversity. There are gradients of diversity and biomass on Ship Shoal in both east-west and north-south directions (highest abundances occur on the southern and western sides of Ship Shoal). In addition, diversity and abundance were positively correlated with bottom dissolved oxygen and negatively correlated with sediment grain size. Sediment deposition associated with turbidity flows from the nearby Atchafalaya River does not appear to have significant negative effects on the macroinfauna of Ship Shoal. Macrofauna on Ship Shoal have their highest biomass in the spring and decrease into the autumn, probably as a response to predation by nekton (especially blue crabs). Sand mining effects will likely be strong on macrofauna and recovery may take months to years. Mining disturbance may cause a change in the community such that smaller-bodied, disturbance specialists (e.g., polychaetes) will become more common. This change may reduce energy flow to demersal nekton.

Ship Shoal is an important offshore spawning/hatching/foraging ground for a large segment of the Gulf of Mexico blue crab fishery from at least April – October. During this time, mature female blue crabs appear to be in a continuous spawning cycle, producing new broods approximately every 21 days while actively foraging on the Shoal to supply the necessary energy for this continuous reproductive activity. Egg production apparently declines slightly as the season progresses, perhaps reflecting some ingestion-limited growth of the ovary as infaunal prey densities on the Shoal decline. Despite the Shoal's comparatively higher salinities, Ship Shoal's crabs are as fecund and 'meaty' as those from any known U.S. blue-crab spawning ground. Sand mining on the Shoal is expected to result in some decline in blue crab fecundity and condition factor through a reduction in food supply. In addition, increases in suspended sediments associated with sand mining may increase the mortality of crab larvae. Sand mining practices which minimize these negative impacts should be carefully considered.

# CHAPTER 1
# INTRODUCTION

In Louisiana, where large portions of coastal land is being eroded due to natural processes including land subsidence, Mississippi River deltaic processes and anthropogenic activities including engineering structures. However, while there was little to no anthropogenic intervention, sediment supply from the Mississippi River through natural levees and regular flooding had kept up with high land subsidence, one of the highest rates in the US (National Research Council (NRC) 2006); Over the last half century, heavily engineered structures such as artificial levees and dams substantially prevent natural sediment supply from the river to replenish the flood plains along the coast. This, in turn, causes imbalances in the sediment budget, and further accelerates land loss (National Research Council (NRC) 2006). In addition, the northern Gulf coasts are hurricane-prone and a major hurricane strikes the Louisiana coast approximately once every 3 years (Neumann *et al.* 1993; Stone *et al.* 1997). The tropical cyclones certainly contribute to and exacerbate land loss, which are already at alarming rate (~34.9 $mi^2$/yr (90.4 $km^2$) for the 1978 - 1990 time periods).

The Louisiana coast is characterized by (1) a very shallow and wide shelf, (2) predominantly muddy seabed along with transgressive sand bodies and various reefs (Penland *et al.* 1988; Roberts 1997; Kjerfve *et al.* 2002), (3) located along the mouth of the Mississippi River basin, the largest drainage basin in the entire North America (Mossa 1996), (4) high discharge of freshwater and sediments from the Mississippi River (Roberts 1997), (5) the largest wetlands in the contiguous lower 48 states, (6) wide varieties of wildlife habitats (Coast 2050 1998; Louisiana Department of Wildlife and Fisheries (LDWF) 2005), (7) important commercial fishery production (crabs, shrimp, fish) (O'Connel *et al.* 2005), (8) a low-energy environment, and (9) frequent passage of winter storms and occasional hurricane landfalls or approaches (Hsu 1988; Stone *et al.* 2004a). The above features create unique coastal dynamics and an ecosystem over the Louisiana shelf, which can rarely be seen on other coasts worldwide.

One of the notable characteristics on the northern Gulf coast is barrier island chains stretching along the Gulf coast from western Florida on the east to southern Texas on the west. Barrier islands are narrow, elongated shore-parallel unconsolidated accumulations of detrital sediments separated from the mainland and formed by waves, tide and aeolian processes (Hesp and Short 1999; Davis and Fitzgerald 2004). In contrast to the relatively stable barrier islands on the eastern Gulf coast, Louisiana barrier islands have been disintegrated at an unprecedented rate, mainly due to high relative sea level rise - rates as high as 1 cm/year compared to 0.02 cm/year worldwide- as well as due to tropical and extra-tropical storms (Stone and McBride 1998; Douglas *et al.* 2001).

The barriers have been known to provide valuable functions and habitats to coastal environments. First, the barriers are the first line of defense against hurricane storm surges and high waves, a critical role to protect low lying inland areas and wetlands (McBride and Byrnes 1997; Stone and McBride 1998; Stone *et al.* 2003a; Watzke 2004; Roland and Douglass 2005).

The barriers also reduce salt water intrusion into estuaries and bays, and play a vital role in protecting inland marshes and associated habitats (Howard and Mendelssohn 1999; Hester *et al.* 2005). The barriers also provide an important habitat for nursery and nesting to migrating birds such as brown pelicans and waterfowl (O'Connel *et al.* 2005). The barriers also provide a significant influence on nationally important fisheries (i.e., white and brown shrimp, Gulf menhaden, red drum, Atlantic croaker, spotted seatrout) by indirectly enhancing tidal exchange through narrow inlets and by contributing to transport of larvae/juveniles into estuaries from offshore waters (O'Connel *et al.* 2005). The aforementioned factors clearly indicate that barrier islands provide valuable habitats and critical functions for coastal and inland environments and the deterioration of the barriers could result in substantial alteration of wetland habitats, regionally and nationally important fisheries, and consequently the Louisiana coastal ecosystem.

When the present study began, there was a paucity of biological information which would permit a proper assessment of dredging impacts on the local biology given the probable long-term use of Ship Shoal as a sand resource area. Lessons being learned in other areas emphasized the need for ecosystem understanding/management (e.g., Ocean Studies Board 2002; Thrush and Dayton 2002). Given the limited historic studies and current catch statistics, we hypothesized that Ship Shoal supported major demersal fisheries for white and brown shrimp. White and brown shrimp are dominant members of the nearshore ecosystem of the northern Gulf of Mexico and are likely dependent upon benthic macro- and meiofaunal (infaunal) communities. We expected sand mining to adversely affect the existing benthic communities and to result in altered communities for an unknown period of time after initial recovery with an unknown impact on the nutritional requirements of Ship Shoal's shrimp. As such, we reasoned that sand mining could have adverse impacts on Ship Shoal's shrimp and the important fisheries which these shrimp support. However, before the present study, our inadequate understanding of Ship Shoal's benthic-based shrimp food chain prevented forecast of the rate or pattern of recovery. Therefore we adopted a ecosystem-based BACI plan of integrated surveys of Ship Shoal's meio/macrofaunal communities (using box cores) and demersal shrimp community (using trawls). We saw this as the most cost-effective method to understand a) the existing relationships between Ship Shoal's surface geology and its benthic and demersal shrimp communities; b) the impacts of sand mining on Ship Shoal's benthic communities; and c) the ability of the recolonized benthic communities to support shrimp.

## 1.1. CONCEPTUAL FRAMEWORK FOR PHYSICAL STUDIES

Recently, in response to the rapid deterioration of Louisiana barrier islands and beaches, and to demands to protect barrier islands and associated habitats in the Louisiana coastal zone, U.S. Minerals Management Service (MMS), who administers mineral leases within the U.S. federal waters and conducts environmental studies under the National Environmental Policy Act which regulates major federal actions that significantly impact on environment, are seeking potential sand resources as more and more sand becomes necessary to restore the Louisiana coastal zone (Drucker *et al.* 2004).

In spite of limited sand resources in the Louisiana coastal zone and the immediate inland, there are several sand resources further offshore, viz., submerged river channels, surrounding beaches, and offshore transgressive sand bodies. The former two sources may not be suitable for large scale barrier island restoration because of insufficient sand volume available to the restoration. Thus, the sand resources from outer continental shelf (OCS) have been considered as one of the plausible sand resources for re-nourishment of the barrier islands and beaches because of the available sand volume, proximity to target restoration areas and sand quality (Drucker *et al.* 2004; Khalil *et al.* 2007). Ship Shoal, the largest offshore sand body along the Louisiana coast and located at approximately 20 km offshore from Isles Dernieres, is a high priority target sand resource to restore Isles Dernieres barrier chain, and Caminada-Moreau headland and Timbalier Islands system, both of which are among the highest vulnerable coasts in Louisiana (Williams *et al.* 1992; Drucker *et al.* 2004; Khalil *et al.* 2007). However, there are serious concerns with the sand dredging from the offshore sand resources, particularly in terms of environmental impacts (Michel *et al.* 2001; Nairn *et al.* 2004).

A significant number of studies have been undertaken to evaluate not only available sand volume and its quality (Penland *et al.* 1986; Kulp *et al.* 2001; Khalil *et al.* 2007), but also for the potential impacts of sand dredging on wave transformation and sediment transport (Stone and Xu 1996; Stone *et al.* 2004b). In terms of the physical studies initiated first in 1994, concerned impacts are twofold: (1) changes in wave transformation and subsequent shoreface erosion of barrier islands, and (2) changes in circulation and sediment flux, and associated morphological changes due to sand dredging (Nairn *et al.* 2004). For (1), Stone and Xu (1996) implemented a spectral wave model to investigate how complete sand removal from the shoal could modify the wave transformation processes. Stone *et al.* (2004b) further implemented the same wave model to examine impacts of partial sand removal from the shoal on the wave transformation and consequent impacts on barrier islands, based on a hypothetical bathymetric condition. For (2), Pepper (2000), and Pepper and Stone (2002, 2004) examined wave, current, bottom boundary layer, and sediment transport dynamics on the western flank of Ship Shoal by deploying various arrays of the bottom boundary layer instruments in 1998 and 2000 to examine hydrodynamics and bottom boundary layer characteristics associated with winter storms; some of the important results obtained through the studies are as follows.

(1) Hydrodynamics, bottom boundary layer and sedimentary processes on the Louisiana inner shelf during the winter-spring season are characterized by quasi-periodic cycles of recurring extra-tropical storm passages.

(2) Sediments are transported landward at the north edge of the shoal and seaward at the south edge of the shoal, suggesting the importance of the shoal on current modification

(3) Their analysis based on non-cohesive sediments concluded that sediment transport rates were significant mostly during winter storms, but high sediment transport also occasionally occurred during fair weather also, showing the importance of winter storms on shoal BBL and morphological changes.

(4) The wave records show that waves propagating over the shoal were attenuated as much as 36

percent possibly as a result of frictional energy dissipation, suggesting the shoal mitigates significant amount of wave energy.

(5) Wave transformation significantly varies comparing the model of the pre-sand mining configuration to that of the post-mining configuration. However, the effects of the wave transformation on the shoreface of barrier islands were negligible.

The above results produced the important cornerstone for wave transformation over shallow shoals and the bottom boundary layer and sediment transport studies over the shoal as well as the low-energy Louisiana shelf and identified unique hydrodynamics over the shoal, both of which had poorly been understood (Wright *et al.* 1997b; Friedrichs *et al.* 2000). However, the above results are qualitative and preliminary, and suggest that the shoal physical environment can be more complicated than previously recognized particularly regarding the following issues.

(1) Divers have often taken mud samples on the bottom of Ship Shoal and satellite images also support fluvial fine sediment transport to Ship Shoal during spring (Walker and Hammack 2000); however, such a mechanism is still qualitative and all of the previous studies are limited to the dynamics for non-cohesive sediment (i.e. sand).

(2) Inner shelf shoals seem to have unique hydrodynamics and wave characteristics. These valuable functions were addressed by Pepper (2000), but have still been poorly understood, particularly wave dissipation effects and response of wind to inner shelf currents and bathymetric modification.

(3) Potential impacts of sand dredging on physical process to date are limited to spectral wave model implementation (e.g., Stone *et al.* 2004b). Short-term impacts of sand dredging on waves, currents and sediment transport using pre- and hypothetical post-sand mining scenarios are very important for decision-making on potential sand dredging and implications for the interplay between physical and biological processes.

Arrays of bottom boundary layer instruments, *in-situ* observing network, and state-of-the-art numerical modeling used in this study make it possible to examine pertinent issues relevant to this work. This report was made through research efforts in a collaborative project funded by the U.S. Minerals Management Service and Louisiana Department of Natural Resources as a part of a large-scale coastal restoration project entitled long-term use of Ship Shoal sand resources for restoration of Louisiana barrier islands and beaches, which play a vital role to protect highly valuable habitats on the Louisiana coastal zone as already mentioned in the previous section. Through the project comprising physical and benthic biological studies, unique, but complex physical processes and their interactions with benthic habitats have been first revealed and potential impacts of sand dredging on physic environemtnts have been quantified. The focuses of the study are given to demonstrate physical processes which may affect future potential sand dredging, particularly the following issues: (1) impacts of fluvial sediments on the shoal physical environment, (2) wave-current-fluid mud interactions, (3) coastal hydrodynamics associated with various storm winds, and (4) physical functions of the shoals and quantify potential impacts of sand dredging on such functions, dynamics of the shoal sediments over the shoals.

This report provides critical information regarding physical processes over shallow shoals as well as the low-energy inner shelf. It also provides important implication for the interplay between physical processes and benthic biological habitat over the shoal, which is a primary concern of MMS for future potential sand mining; this collaborative study comprising physical and benthic biological study first enabled us to addresses the issue. Such comprehensive studies have little been reported in the scientific literature to date. Furthermore, most of the information obtained through this study can be transferrable to similar studies and provide valuable case studies, for example, impacts of offshore mineral mining.

Task 1 is covered Chapters 2-7. Chapter 2 deals with the restoration-quality sand associated with Ship Shoal; Chapter 3, response of fluvial fine sediment dispersal to storm wind-current effects; Chapter 4, wind-driven dispersal of fluvially-derived fine sediment; Chapter 5, spectral wave transformation; Chapter 6, two contrasting morphodynamics over recurring sandy and muddy bottoms of the shoal; Capter 7, modeling of waves and currents and its transformation due to the proposed sand mining. Various sand mining scenarios are considered in this study to quantify the hydrodynamic impact in the region. Overall conclusions for both Tasks are addressed in Chapter 13.

## 1.2. CONCEPTUAL FRAMEWORK FOR BIOLOGICAL STUDIES

Our biological study was designed to address the following questions: 1. What is the abundance, taxonomic composition and community structure of Ship Shoal's meiofaunal community? 2. What are the abundance, taxonomic composition and community structure of Ship Shoal's macrofaunal community? 3. How are Ship Shoal's meio/macrofaunal communities affected by surface geology (e.g. substrate composition, water depth, currents, position on the shoal), and water quality (e.g. temperature, salinity, oxygen concentration, turbidity)? 4. What is the relationship between the dominant members of Ship Shoal's benthic communities and the gut contents/fullness of its white and brown shrimp? 5. What are the impacts of sand mining on the taxonomic composition and community structure of the macro- and meiobenthic communities? (How rapidly will these communities recover and how will the taxonomic composition of the recolonized areas compare with pre-impact conditions). 6. What is the relationship between the dominant members of these recolonized benthic communities and the gut contents/fullness of white and brown shrimp and the nutritional requirements of these shrimp as evidenced by their condition factors and stages of maturation. 7. Are the absolute or relative abundances of white and brown shrimp affected by sand mining?

When our project began we expected sand mining to begin on South Pelto Block 13 (SP 13) in May of 2004 and continue for four months; then shift to Ship Shoal Block 88 (SS 88) in May of 2005 and continue for another four months. Based on these expectations, we developed a biological box-core and trawl sampling program (spring, summer, and fall) designed around the life cycles of white and brown shrimp. Our box-core plan contained two related components: a) a shoal-wide grid of sampling stations to provide a basic understanding of the system and serve

as a series of system-wide controls and b) a series of experimental stations within the sand mining sites. A CTD profile, three replicate box-core samples, and three meiobenthic subcores per box core were taken at each station. Our trawl plan consisted of four trawls associated with our box core stations and sites to be mined for sand.

During the conduct of our study it became obvious that sand mining on the shoal would be delayed while sand mining needs might expand onto the adjacent Trinity and Tiger Shoals. In response to these management conditions our experimental stations were relocated to enhance our ecological understanding of Ship Shoal and our overall study expanded. At the same time our studies were revealing that Ship Shoal was an important and unrecognized spawning/hatching/foraging ground for blue crabs; had environmental conditions which favored benthic microalgae production; did not have an abundance of white and brown shrimp; and might be a hypoxia refuge and biodiversity hotspot for macroinfauna. As such our study shifted its focus from shrimp to blue crabs and a consideration of the importance of benthic microalgae in the Ship Shoal food web.

Task 2 is covered in Chapters 8 – 12. Our benthic microalgae findings are given in Chapter 8; meiofauna in Chapter 9; macrobenthos in Chapter 10; shrimp and croaker in Chapter 11; and blue crab in Chapter 12. Overall conclusions for both Tasks are addressed in Chapter 13.

# CHAPTER 2
# GEOTECHNICAL INVESTIGATION FOR SAND FOR RESTORATION OF BARRIER ISLAND FROM SOUTH PELTO BLOCKS OF SHIP SHOAL

## 2.1 INTRODUCTION

The non-availability of easily accessible compatible sediment results in the populace and ecosystem of coastal Louisiana at risk and adversely impacts the nation's oil and gas industries (Khalil and Finkl 2009 (in press)). Further, Khalil *et al.* (2007) states that the degradation of mainland Gulf coast and delta-front barrier islands jeopardizes the vitality of strategic economic and biological resources (including aquatic habitat) as well as the protection of coastal residents from storm surge and wave damage (Stone et al. 2005). Unless significant efforts are made to restore barrier islands and coastal wetlands, Louisiana will lose productive and protective islands (beaches, dunes) and marshes (Campbell *et al.* 2005; Hester *et al.* 2005; Laska *et al.* 2005; Penland *et al.* 2005). The primary objective of mitigation is to attempt to stabilize the landward retreat of the barrier islands by adding sediment to the system and translating the barriers into various types of modified morpho-sedimentary environments (Khalil *et al.* 2006), as most of the barriers are thinning in space and are on the verge of disintegration. In order to promote large-scale restoration (*e.g*. beach nourishment, dune development, marsh creation) of the Louisiana coast, appropriate sand resources must be identified and quantified as these restoration efforts primarily depend on the emplacement of sand and suitable sediment to build up barrier and deltaic systems (Khalil *et al.* 2006). Large accumulations of offshore sand provide a valuable resource for supply of the volume-needs required for building the first line of defense in shore protection. These integrated beach-dune-marsh environments, which, in themselves, comprise a fragile coastal system, can protect the immediate Louisiana hinterland by absorbing wave impacts and diminishing the effects of surge flooding. Stone *et al.* (2005c) provided the role of barrier islands, muddy shelf and the reefs in mitigating the wave fields along this coast, particularly during the high energy events.

There is a need for very large quantities (hundreds of millions of cubic meters) of sediments for coastal and wetland restoration in Louisiana. Sand is needed for beach nourishment, muddy sediments for wetland restoration, and clay for levee construction (Khalil and Finkl 2009 (in press)). The need is likely to increase significantly in future decades as sea-level rise accelerates and storminess increases as a result of global climate change (Hayden 1999). Restoration of Louisiana's barrier islands requires large volumes of sand (for beaches and dunes) and mixed sediments (for marshes). While muddy sediments are most abundant, sand is mostly limited to shoals and buried relict paleo-channel deposits. However, such large volumes can only be obtained from offshore sources and consequently, marine sand searches originally focused on reconnaissance surveys in efforts to ascertain general trends in sediment distribution on the seabed. Preliminary, or reconnaissance efforts (Suter *et al.* 1991; Kindinger *et al.* 2001), resulted in the discovered of potential sand sources in a range of depositional systems that include spit

platforms, delta sheet sands, ebb-tidal deltas, distributary mouth bars, and distributary-channel fills, in addition to inner shelf shoals. Although these types of deposits occur on the continental shelf, a single large deposit is attractive for island restoration because it is cohesive, not dispersed, and not covered by muddy overburden. According to the MMS (2004), estimates of total sand volumes comprising Ship Shoal are on the order of $1.2 \times 10^9$ $m^3$. The drowned barrier sediments range from very fine- to medium-grained sand that in volume are comprised of $112 \times 10^6$ $m^3$ in the shoal crest, $430 \times 10^6$ $m^3$ in the shoal front, and $640 \times 10^6$ $m^3$ within the shoal base. Kulp *et al.* (2001) estimate that there is an additional $123 \times 10^6$ $m^3$ of sand in distributary channel fill deposits under the shoal. As promising as these volumes estimates are, based on reconnaissance data, more detailed studies of the Ship Shoal sands indicate a scope that is limited by subsea infrastructures placed by the oil and gas industries, environmental concerns over dredging, and variability of deposits in the shoal. Nevertheless, these sediments are required for restorative purposes, as indicated below, however constrained by competing needs and restrictive human activities.

## 2.2. GEOLOGICAL SETTING OF THE STUDY AREA

Most of the seafloor beneath the study area consists of a large, submarine sand body that is locally known as Ship Shoal, the largest shoal off Louisiana. The potential of Ship Shoal as a source of sand for restoring parts of Louisiana's rapidly eroding coastline has been summarized by various researchers including Krawiec (1966), Suter *et al*. (1985), Penland *et al*. (1985; 1986), Williams *et al*. (1989), Kulp *et al*. (2001), Stone (2001), Finkl *et al.* (2005). A 40- to 45-m thick wedge of deltaic sediments, deposited by the Mississippi River during the Holocene, underlies the Ship Shoal region. Although processes of Mississippi River Delta formation have been intensively studied (e.g., Coleman and Gagliano 1964; Frazier 1967; Saucier 1994), they are briefly summarized here as they relate to the formation of the Ship Shoal environs. The shoal crest, with surface sand thickness >1 m occupying an area of approximately 560 $km^2$, forms an ancient barrier shoreline that has been modified by processes related to transgression and submergence of the Maringouin delta complex (Krawiec 1966; Frazier 1967; Minerals Management Service (MMS) 2004).

Ship Shoal (Figure 1) is the largest and easternmost of a series of sand shoals on the inner continental shelf of Louisiana resulted due to deltaic abandonment and marine transgression (Kulp *et al.* 2001). The elongated shoal, lying parallel to the coast approximately 12 to 19 km off Terrebonne Parish, measures approximately 50 km long in an east-west direction (Khalil *et al.* 2007). The central portion of the shoal ranges 5 to 12 km in width, but its distal margins narrow to points.

The study area in South Pelto is located on the eastern segment of Ship Shoal, approximately 14 to 20 km offshore the eastern part of the Isles Dernieres barrier chain (Figure 1). The area encompasses portions of five MMS lease blocks (12, 13, 14, 18, and 19) (Minerals Management Service (MMS) 2004). For a better appreciation of the deposit geometry of South Pelto, sedimentary geology, and geomorphology, it is necessary to understand the stratigraphic implications of river diversion (avulsion and branching) and delta switching in major deltaic depositional environments. These processes contribute to the formation of transgressive sand

bodies, such as Ship Shoal, and evolution of modern barrier islands such as those lying landward of the Shoal (*e.g.* Isles Dernieres and Timbalier).

Ship Shoal was formed approximately 7,000 years ago (mid Holocene) in association with the abandonment and reworking of distal sediments from the Maringouin Delta Complex. The Isles Dernieres, located landward of Ship Shoal, are associated with the winnowing and reworking of sediments from the abandonment and submergence of the Caillou Bay headland (abandoned approximately 600 to 800 years ago) of the Lafourche delta complex (Penland *et al.* 1988).

Deltas are dynamic depositional systems that exhibit a wide range of depositional features. The Mississippi deltaic plain is characterized by major river diversions that promote large-scale delta lobes. These delta complexes occur on millennial scales. Bay fills are built and abandoned in centennial time frames, whereas the smallest sub-deltas exist only for two centuries, on average (Coleman and Gagliano 1964).

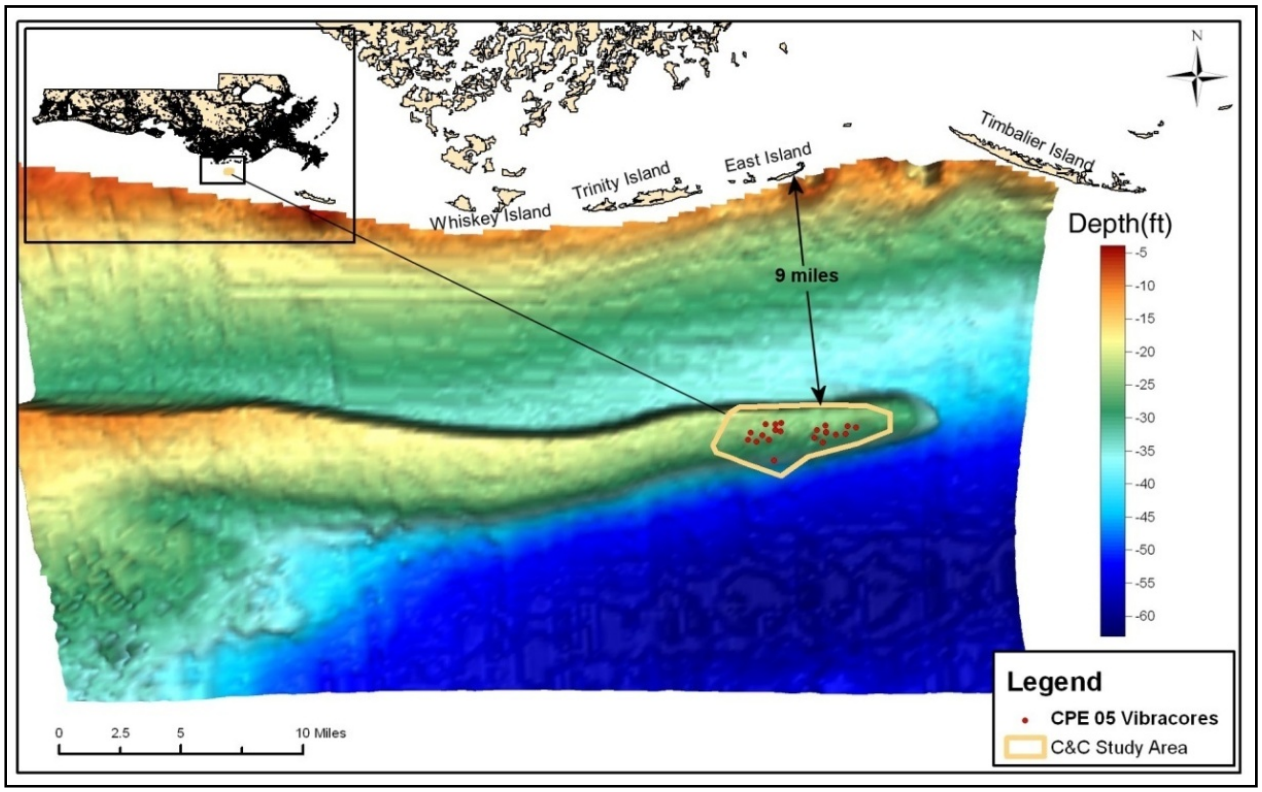


Figure 2.1 Location of the study area (South Pelto) on the eastern margin of Ship Shoal, in relation to the Isles Dernieres (Whiskey, Trinity, and East Islands) and regional bathymetry of Ship Shoal.

Scruton (1960) employed the term *delta cycle* in reference to alternating phases in deltaic sedimentation. Each delta cycle is initiated by (1) sedimentation and rapid growth (a constructional-progradational phase) that is followed by (2) systematic loss of flow efficiency,

(3) sediment dispersal and abandonment of the delta by the sediment delivery system (delta switching), and concludes with (4) a destructional phase in the form of delta deterioration. The coastal plain of Louisiana exhibits all stages of the delta cycle, from the newly constructed Atchafalaya-Wax Lake bayhead deltas to abandoned destructive deltas (*e.g*. Lafourche) (Roberts 1997). At the present time (Holocene epoch), eighteen delta lobes coalesce within six major delta complexes to make up the Holocene deltaic plain of Louisiana (Coleman *et al.* 1998; Kulp *et al.* 2005). The entire deltaic plain is transgressive, with the exception of the Birdfoot (Balize complex) and the Atchafalaya River delta complex. The most recent abandoned lobes are the Laforche and Plaquemines lobes of the modern Balize-Birdfoot delta.

Older lobes of the Mississippi delta began to accumulate sediment about 7,000 YBP (years before present), when the rate of sea-level rise decelerated and MSL (mean sea level) approached present levels (Fisk *et al.* 1954; Roberts 1997). River avulsion (rapid channel switching) and diversion, which often result in delta switching, are responsible for the present complex and diverse geomorphology and stratigraphy of the Mississippi deltaic plain. Study of the sedimentary record suggests that delta building occurred at different locations about every 1000 to 2000 years (Roberts 1997; Coleman *et al.* 1998). The Mississippi River has thus built a broad and complex coastal plain by these basic processes. Throughout the current deltaic plain, late Pleistocene mud-rich and stiff clay deposits underlie Quaternary depositional deltaic sequences. Typically, the Pleistocene facies is denser than overlying Quaternary sediments (compaction occurs mostly in Quaternary sediments). During late (destructive) stages of a delta cycle, abandoned delta complexes subside due to compaction (dewatering of clastic sediments and oxidation of organic-rich materials). As coastal processes rework the seaward margin, the delta lobe enters a transgressive-destructive phase where erosional headlands, flanking barriers, barrier island arcs and erosional headlands develop, as described by Penland *et al.* (1988). A mechanism for the genesis and evolution of transgressive depositional systems in the Louisiana deltaic plain is suggested by Penland *et al.* (1988) in a three-stage geomorphic model. This evolution begins when marine processes transform the abandoned delta complex into a Stage 1 erosional headland with flanking barriers. At this stage, sediment is supplied to flanking barrier development by shoreface erosion. Relative sea-level rise, land loss, and shoreface erosion leads to submergence of back barrier lands and the separation of the Stage 1 barrier from the mainland shoreline, forming the Stage 2 barrier island arc. When relative sea-level rise and overwash processes overcome the ability of the barrier island arc to maintain its subaerial integrity, submergence initiates the formation of inner shelf shoals under Stage 3. Following submergence, the drowned barrier islands continue to be re-worked by marine/coastal processes to form a marine sand body in the inner shelf. This is the last stage in the evolution of transgressive depositional systems. These evolutionary processes were collectively subsumed under the heading of "transgressive submergence" by Penland *et al*. (1988). According to Penland *et al.* (1988) Ship Shoal is an inner shelf shoal that represents Stage 3 of the model.

The controlling variables that differentiate transgressive submergence (Penland *et al.* 1988) from other models of shoreline sand formation such as shoreface retreat (Fisher 1961; Swift 1975) and in-place drowning (Sanders and Kumar 1975) are: (1) high rates of relative sea-level rise, (2) low gradients of continental shelves with limited local sand sources, and (3) a storm-dominated environment. Formation of barrier islands and shoals by mainland detachment processes and

regression generally results in a coarsening upwards stratigraphic sequence (sediment grain size increases upwards from the bottom of the deposit toward the top) that is commonly found in barrier islands arc sequences and inner shelf shoals. Reworked inner shelf shoals exhibit a stratigraphic sequence that grades rapidly from silt and sand in the base, to shoal front sand capped by shoal crest sand and shell on the surface (Penland *et al.* 1988). The sedimentology and stratigraphy of Ship Shoal is further discussed as follows.

## 2.3. SHIP SHOAL - SEDIMENTOLOGY AND STRATIGRAPHY

Penland *et al*. (1988) and Suter *et al*. (1991) have characterized the Ship Shoal system as a sandy submerged barrier island that is approximately 50 km long by 8 km wide in the central area to approximately 5 and 10 km on eastern and western margins, respectively. Local relief varies from approximately 7 m on the western margin to about 5 m elsewhere. Water depths range from 3 m on the west to 5 m on the eastern margin (Kulp *et al.* 2005). According to Penland *et al*. (1988), Ship Shoal has migrated to its present position under conditions of sea-level rise, shoreface erosion, and submergence. Landward asymmetry and stratigraphic position of the shoal indicates that it is a transgressive sand body that is migrating landward.

Penland *et al*. (1988) described seven lithofacies on Ship Shoal that were based on texture, sedimentary structures, faunal assemblages, and stratigraphic position. However the upper three facies that are most relevant to sand resources and include the (1) shoal crest, (2) lower shoal or shoal front, and (3) shoal base. The shoal crest, the facies to explore over the short term, is located in the upper 5 m of the deposit and is comprised by very well sorted quartz sand (99% sand) that ranges from 0.13 mm to 0.16 mm in size. Sediments are very well sorted and coarser on the crest, associated with a general coarsening upward trend in a high-energy active zone where sediments are winnowed and sorted by waves and currents. The shoal front, subsequently overridden by the migrating crest, is slightly thinner (1.2 to 3.4 m thick) and contains finer-grained sand (0.12 to 0.15 mm) compared to the crest. The base of the shoal, underlying the shoal front, contains poorly sorted finer-grained sand that are interbedded with layers of silt and clay. Penland *et al.* (1988) estimates that the shoal crest unit alone contains more than $7.6 \times 10^6$ $m^3$ of sandy sediment. Although there may be large sediment volumes in Ship Shoal, the presence of oil infrastructure and obstructions (pipelines, flow lines, rigs, abandoned pipes, wrecks) may preclude exploration of in many areas.

It is inferred on the basis of available evidences that majority of Holocene sediments (about 45 m thick) underlying the study area is associated with the Maringouin Delta Complex and has been deposited over the last 7,500. These thick Holocene deposits rest on weathered, Pleistocene Prairie terrace deposits that represent floodplain, deltaic and open shelf sediments deposited between about 120,000 and 20,000 years BP (Frazier 1974; Saucier 1994). During low sea-level stands, large expanses of these Pleistocene surfaces were subaerially exposed and streams extended an extensive network of channels across them. Several relict channels trending northwest to southeast are incised into this deeply buried Pleistocene surface near the study area. These relict channels terminate at the head of Mississippi

Canyon and represent channels of an ancestral Mississippi River course (Moore *et al.* 1978). About 18,000 to 20,000 years BP (Last Glacial Maximum in Wisconsinan time), shorelines stood approximately 90 m lower than present and approximated the edge of the outer continental shelf. Since that time, sea level has gradually risen and Pleistocene surfaces were drowned and buried by Holocene marine and deltaic sediments.

Analyses of sediments from Ship Shoal and the Isles Deniers indicates compatibility of grain sizes and sorting viz. 2.64-3.72 phi (0.165-0.076 mm) and 2.73-3.94 phi (0.149-0.063 mm) for Isle Dernieres sediment and Ship Shoal, respectively (based on Krawiec 1966, and reported in MMS 2004). Both areas contain fine to very fine sand that is very well to well sorted, making the deposits compatible and the Ship Shoal sand ideal for beach nourishment (Khalil *et al.* 2007).

## 2.4. METHODS

In order to evaluate available sand reserves, detailed high resolution geophysical surveys were undertaken in 2003 by the Environmental Protection Agency and Louisiana Department of Natural Resources to address archaeological and hazard concerns in South Pelto Blocks 12 &13 (Coastal Environment Incorporated (CEI) 2003a) and Ship Shoal Blocks 88 & 89 (Coastal Environment Incorporated (CEI) 2003b). Such surveys are required by MMS as a pre-requisite for application for leases for future dredging in these areas. In both these study areas about 26 square kilometers of the area was covered by high resolution geophysical surveys (bathymetric, seismic, sonar, and magnetic) along approximately 660 line kilometers of track lines almost all trending east-west with a spacing of 50 m and a few north-south with 900 m spacing (Coastal Environment Incorporated (CEI) 2003a, b). Odom Echo Trac DF 3200 bathymetric system, EdgeTech 500 kHz side scan sonar, Edgetech Geostar SB 512i subbottom profiler, and Geometrics 880 cesium magnetometer were used for the geophysical surveys with C-Nav globally corrected GPS for positioning in both these areas (Coastal Environment Incorporated (CEI) 2003a, b). CEI (2003a) identified twelve sonar targets and eleven magnetic clusters in the South Pelto Blocks 12 &13. This section of the report details offshore geotechnical investigations in the South Pelto Blocks 12 &13. The results of this geotechnical investigation summarize the deposit in terms of its submarine geomorphology, sedimentology, and stratigraphy. Sediments in the study area appear to be suitable for barrier island restoration. Although good quality sediments occur in the Ship Shoal environment, the occurrence of cultural resources and petroleum industry infrastructure impede development of sand resources (Khalil *et al.* 2007). The problem of locating sand resources for barrier island restoration is thus not simply a matter of marine exploration but also being cognizant of hazards to dredging and awareness of potential hazards posed by borrows to existing structures. Complex patterns of pipeline corridors and other infrastructures restrict exploration for sand resources and reduce potential volumes that can be dredged. Eight pipelines transit the study area and seven occur adjacent to it (Coastal Environment Incorporated (CEI) 2003a). Six production platforms and two wells (Coastal Environment Incorporated (CEI) 2003a) also exist just outside the bounds of the study area. These pipelines and structures are protected by 150 m buffer zones within which no dredging can occur.

Cost effective exploration for offshore sand in deltaic environment needs a systematic approach (Khalil 2004; Finkl and Khalil 2005a). As stated previously,most of the tasks associated with the phase-wise approach in sand sediment searches (Khalil 2004) was undertaken during 2003 when a detailed geophysical survey was conducted in Ship Shoal Blocks 88 and 89 (Coastal Environment Incorporated (CEI) 2003b), in addition to South Pelto Blocks 12 and13 (Coastal Environment Incorporated (CEI) 2003a). Based on the interpretation of bathymetric, seismic, sonar, and magnetic data, a geotechnical investigation was undertaken by collecting vibracores (Finkl and Khalil 2005b).

Geophysical/geotechnical equipment and techniques used during this investigation included (Finkl *et al.* 2005):

- Differential Global Positioning System (DGPS) – Trimble GPS and Coast Guard Navigation Beacon (Provides accurate positioning of the survey vessel).
- Navigation/Survey Integration System – Hypack Inc.'s "HYPACK® MAX" (Integrates DGPS data with data collected during the survey).
- Vibracore Acquisition.
- Sediment-Size Analysis.

The technical methods, analytical tools, and equipment used in this geotechnical investigation for evaluation of sand deposits in the study area are described below.

### 2.4.1. Navigation System

The navigation and positioning system used during the survey was a Trimble DGPS Global Positioning System (GPS) that was interfaced to Hypack Inc.'s HYPACK® MAX. A Pro Beacon receiver provided differential GPS correction from the U.S. Coast Guard Navigational Beacon located at English Turn, Louisiana. The DGPS initially receives the civilian signal from the global positioning system (GPS) NAVSTAR satellites. The locator automatically acquires and simultaneously tracks the NAVSTAR satellites, while receiving precisely measured code phase and Doppler phase shifts, which enables the receiver to compute the position and velocity of the vessel. The receiver then determines the time, latitude, longitude, height, and velocity ten times per second. The GPS accuracy, with differential correction used in this study, provides for a position accuracy of 0.3 to 1.2 m, which is within the accuracy needed for geotechnical investigations for sediment sources. The U.S. Army Corps of Engineers (USACE) test of the U.S. Coast Guard beacons found an accuracy of at least 1.5 m approximately 94% of the time.

### 2.4.2. Survey Integration via Hypack Inc.'s HYPACK® MAX

The navigation system was interfaced with an onboard computer, and the data integrated in real time using Hypack Inc.'s HYPACK® MAX. HYPACK® MAX is a state-of-the-art navigation and hydrographic surveying system. Online screen graphic displays include the pre-plotted survey

lines, the updated boat track across the survey area, adjustable left/right indicator, as well as other positioning information such as boat speed, quality of fix, and line bearing. All data were recorded on the computer's hard disk and transferred to a USB memory stick each day during the survey to back-up raw survey data. After post-processing, the navigation data (locational) stored in the HYPACK® MAX system was then exported to a *.dxf* file and imported into ArcGIS 8 in order to create a GIS shapefile for analysis and report preparation.

### 2.4.3. Vibracore Acquisition

A 271B Alpine Pneumatic Vibracore, configured to collect undisturbed sediment cores 6.1m in length, was used for this project. This self-contained, freestanding pneumatic vibracore unit contains the following components: An air-driven vibratory hammer assembly, an aluminum H-beam which acts as the vertical beam upright on the seafloor, a steel coring pipe (with a plastic core liner), and a drilling bit with a cutting edge. An air hose array provided compressed air from the compressor on deck to drive the vibracore. If penetration refusal occurred at less than 80% of expected penetration, the sampled portion was removed from the pipe, a new liner inserted, and a jet pump hose was attached just below the vibracore head. After lowering the rig to the bottom and jetting to 0.3 - 0.6 m above the refusal depth, the jet was turned off and the vibrator turned on in order to collect the remaining core. The vibracore unit was deployed by a crane from the "liftboat" M/V *Stingray*.

### 2.4.4. Sediment-Size (Mechanical) Analysis

Sieve analyses were conducted for samples obtained by vibracoring in accordance with American Society for Testing and Materials Standard Materials Designation D422-63 for particle size analysis of soils (ASTM 1987). This method covered the quantitative determination of the distribution of sand size particles. Results of the particle-size analyses were entered into gINT® software, which computes the mean and median grain size, sorting, and silt/clay percentages for each sample using the moment method described by Folk (Folk 1974).

## 2.5. RESULTS

Twenty vibracores were obtained in the South Pelto study area (Khalil *et al.* 2007). The core locations were selected on the basis of results from preliminary geophysical investigations conducted by CEI (2003a). Vibracore locations were overlaid on a three-dimensional (3D) bathymetric image (using NOAA-NOS historic bathymetric data mostly from 1979) to show the relationship between vibracore locations and morphology whereas the latest bathymetric data (Coastal Environment Incorporated (CEI) 2003a) collected were used to plan the vibracore acquisition. In the study area occurring on the eastern tip of Ship Shoal (Figure 1), water depths decrease from east (mostly between 6 to 9 m isobaths) to west (9 m isobath on the crest) as this

inner-shelf ridge increases in width. Shoreward-facing (north) slopes are steeper than the seaward (south) side slopes. Vibracores were located on the eastern shoal crest and concentrated in two main areas (Figure 1). Vibracore #20 obtained off the south margin of the main shoal contained mostly clay and probably represented lagoonal sediments from the Marogouin delta that underlies the shoal base. Other vibracores on the shoal crest recovered predominantly sand in surface layers and mixed fine sediments (sand, silt, and clay) in basal layers.

Potential borrow sites, targeted by results of prior work, were reported to be free from dredging obstructions. Figure 2 shows the location of the design borrow sites, buffers (no-dredge zones as defined by cultural resource surveys), vibracore locations (Finkl *et al.* 2005), location of fence diagrams, and MMS lease block boundaries. Potential borrow areas are labeled A, B and C in Figure 2.2.

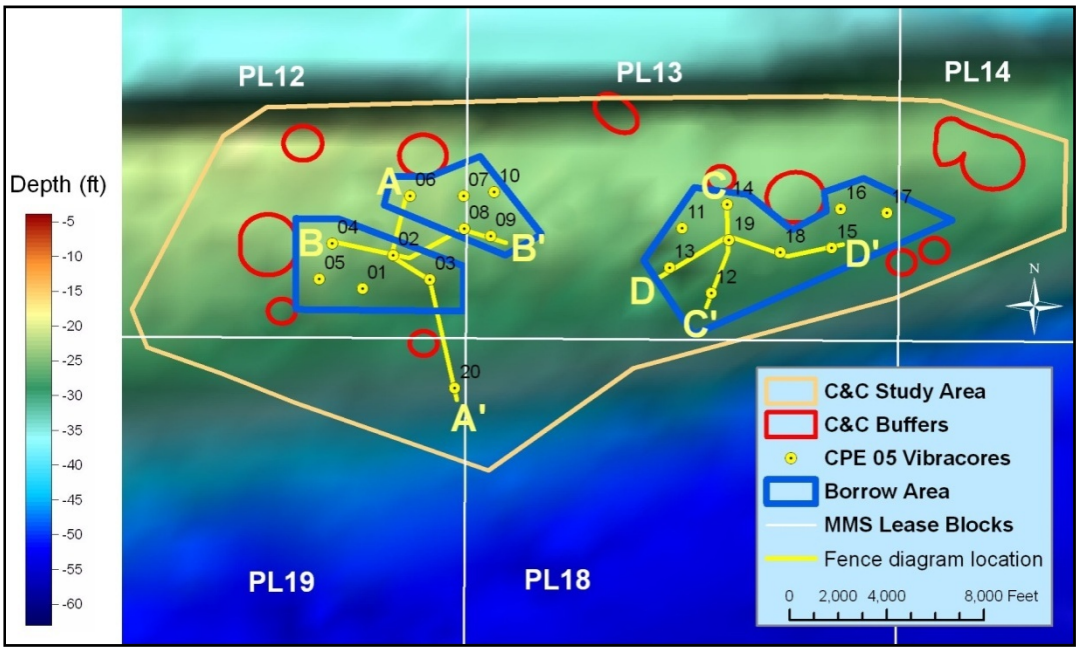


Figure 2.2 Detailed view of Ship Shoal study area showing the location of borrows.

Potential borrow area A contains five vibracores (Cores # 01, 02, 03, 04 and 05). Sand thickness varies from 3.6 to 4.8 m (Khalil *et al.* 2007) with greater thickness occurring in the vibracore closest to the center (#04). Figure 2.3 a fence diagram drawn perpendicular to the shoal crest, shows how the sand deposit thickens to the offshore as the shoal relief decreases and the underlying mud layer outcrops in the shoal seaward (south) side. Upper portions of vibracores generally contained clean sand with mean grain size ranging from 0.15 to 0.22 mm whereas bottom layers contained clay and silty sand with mean grain size ranging from 0.12 to 0.15 mm (Khalil *et al.* 2007). Figure 4, a schematic fence diagram drawn parallel to the shoal's crest, illustrates how the sand thickness is constant along the shoal crest (W-E) in contrast to a rapid

thinning offshore (N-S).

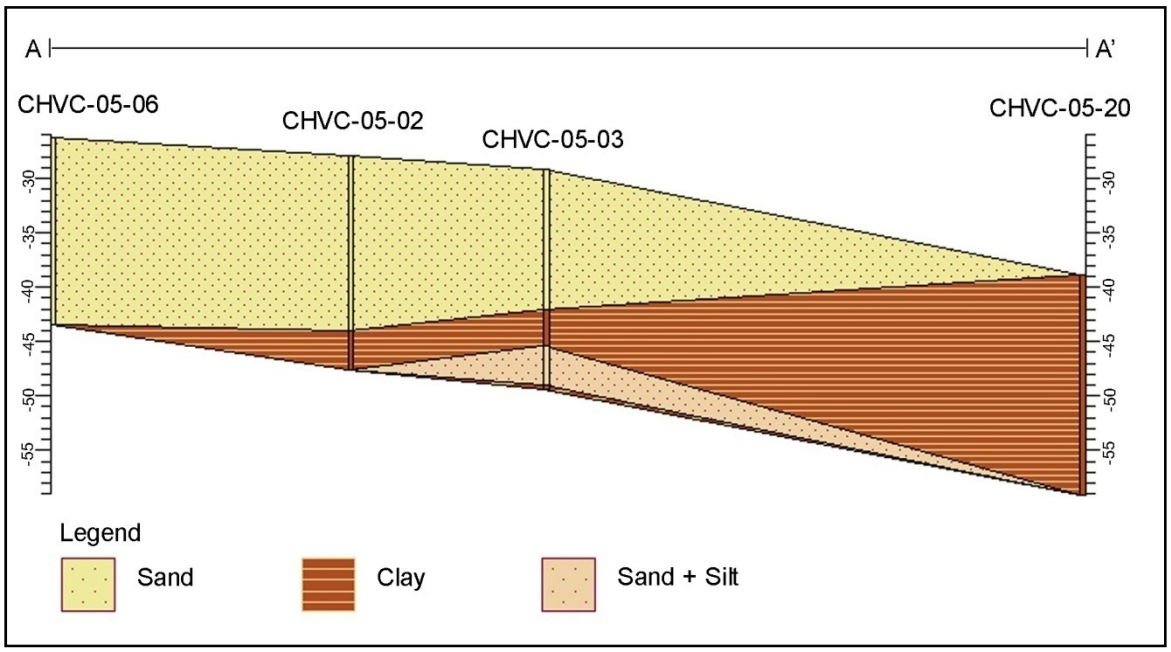


Figure 2.3 Schematic fence diagram perpendicular to the shoal crest showing a decrease of sand thickness towards the offshore (vibracore 20). Vertical scale is in feet. For horizontal scale refer Figure 2.2.

Five vibracores were obtained in potential Borrow Area B (cores # 06, 07, 08, 09 and 10). Sand thickness ranged from 4.6 to 6 m with the greatest thickness occurring in vibracore 07 (Khalil *et al.* 2007). The fence diagram in Figure 3 illustrates that vibracore 06 contained clean sand from the top of the core, down to the core base; an identical pattern is observed in cores 08 and 09 illustrated in Figure 4. Thus, all vibracores along this area contained sand from the shoal crest and displayed a slight coarsening upward trend. Grain sizes range from finer grain sizes (0.15 to 0.18 mm) in the base of the core to slightly coarser sand sizes (0.19 to 0.51 mm, but mostly around 0.2 mm) near the top (Khalil *et al.* 2007). Shell fragments and whole shells in the top 0.6 m of vibracore #10 accounted for coarser grains (0.51 mm).

Nine vibracores were obtained within potential Borrow Area C. Sand thickness ranged from 3.9 to 5.7 m but mostly occurred in the 5 m range (see Figures 5 and 6). Silt decreased and mean grain size increased from the core base to the top. Sediments in the upper 3 m were generally cleaner and contained coarser-grained sand than basal layers. Vibracore #12, the seaward most core, contained the thinnest sand layer that at 4 mtransitioned to clay (Figure 5). Clayey sediments occurred in basal layers of 7 out of the 9 vibracores from this area (Khalil *et al.* 2007). Most clay layers occurred 5 m below the shoal surface.

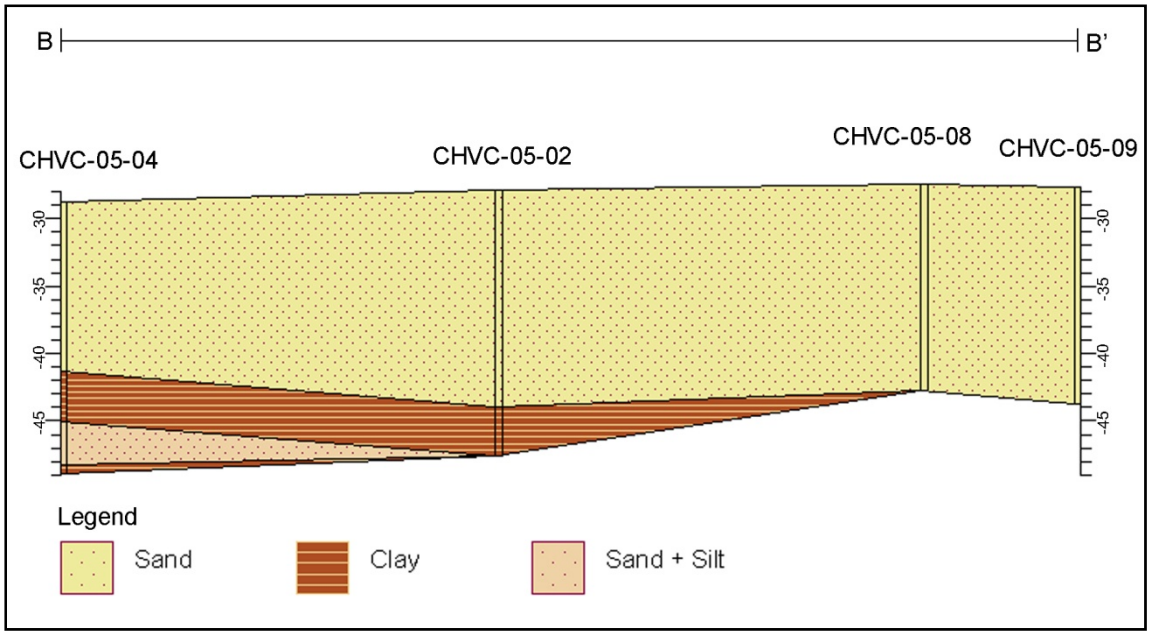


Figure 2.4 Schematic fence diagram drawn parallel to the shoal base showing relatively homogeneous sand thickness throughout the shoal base unit. Vertical scale is in feet. For horizontal scale refer Figure 2.2.

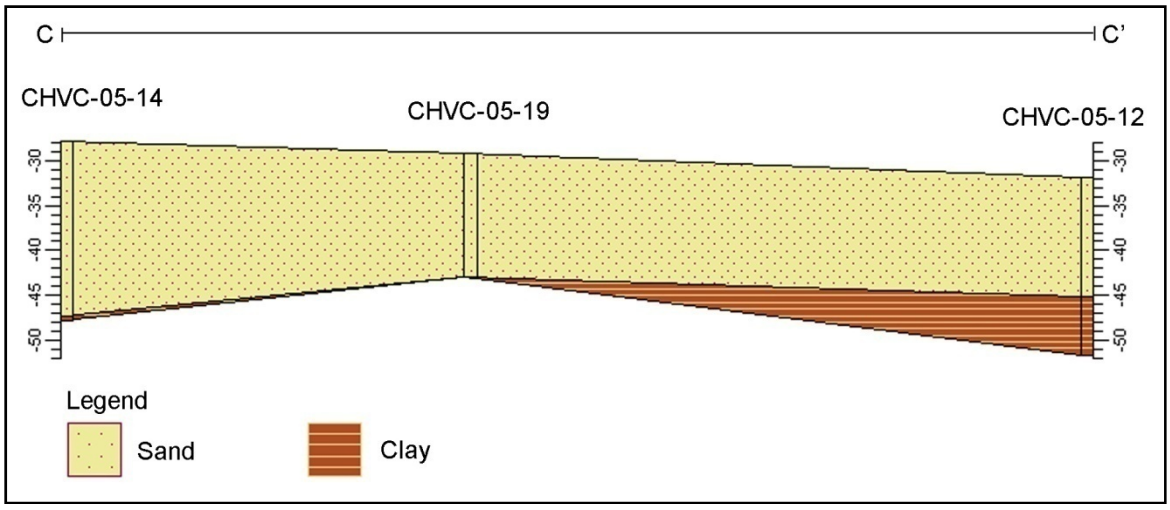


Figure 2.5 Schematic fence diagram drawn perpendicular to the shoal crest in Borrow Area C. The cleaner upper sand layers thin seaward (to the south). Vertical scale is in feet. For horizontal scale refer Figure 2.2.

Based on the interpretation of seismic data compared with historical cores, CEI (2003a) prepared a sand isopach map for the project area. The isopach indicated that sand thickness in the study area varies from 5.7 m on the shoal's crest to 0.3 m on the seaward (south) side of the shoal. Sand thickness decreases abruptly towards the south compared to a more gradual decrease

observed to the north. Sand thickness in the Borrow Area C is slightly thinner than borrow areas A and B and ranges from 3.5 to 5.4 m (Khalil *et al.* 2007).

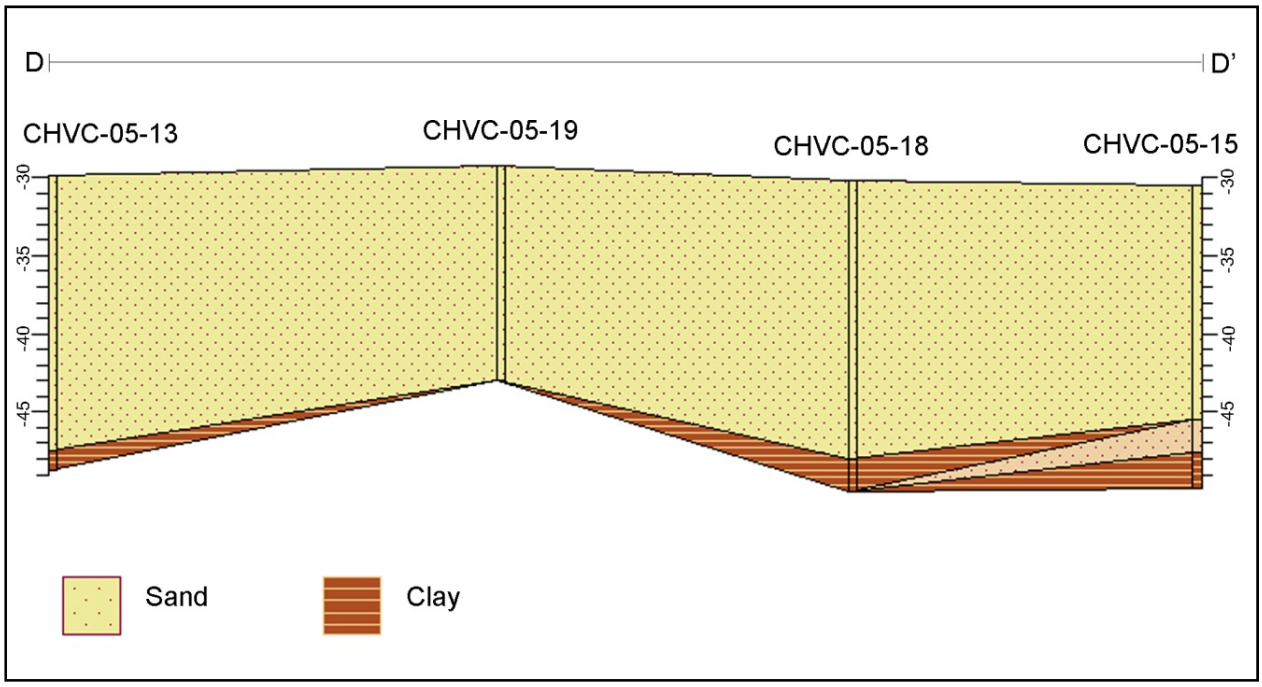


Figure 2.6 Schematic fence diagram drawn parallel to the shoal crest in Borrow Area C. Clean sandy sediments are associated with upper units (shoal crest and front). Vertical scale is in feet. For horizontal scale refer Figure 2.2

Borrow area cuts were calculated using the isopach data provided by CEI (2003a) compared with vibracore results (thickness of clean sand and textural properties). Sand volume estimated in Borrow Area A is about $6.95 \times 10^6$ m$^3$, in Borrow Area B about $4.9\ 10^6$ m$^3$ and in Borrow Area C approximately $9.75\ 10^6$ m$^3$ with a total of about $21.6 \times 10^6$ m$^3$ of sand available from all these three borrow sites (Khalil *et al.* 2007).

## 2.6. CONCLUSIONS

Restoration of Louisiana's barrier islands requires large volumes of sand (for beaches and dunes) and mixed sediments (for marshes). Such large volumes can only be obtained from offshore sources and consequently, marine sand searches originally focused on reconnaissance surveys in efforts to ascertain general trends in sediment distribution on the seabed (Finkl and Khalil 2005a). The success of Louisiana restoration effort depends on locating sufficient volumes of sand that are suitable for placement on beaches and for building dunes and marshes and thus location of potential borrows with suitable sand that are extractable at acceptable costs are crucial to the success of the overall project (Finkl and Khalil 2005a).

Sand resources along the southern Louisiana coast are relatively scarce given the large volumes of sand required for restoration of the rapidly degrading barrier systems. During this investigation, twenty vibracores were obtained from Ship Shoal, a well-known sand source offshore of the Isles Dernieres (Khalil *et al.* 2007). The study area along the eastern end of Ship Shoal, commonly known as South Pelto mainly contained very clean sand (less than 5% silt in the upper shoal units) that ranged in thickness from 4 to 6 m and generally ranged in grain size from 0.15 to 0.2 mm. Approximately $21.6 \times 10^6$ $m^3$ of clean sand is estimated to occur in three borrow areas ((Khalil *et al.* 2007). Buffers around oil and gas infrastructures and other magnetic anomalies occurring in and around the study area were avoided during borrow area design to ensure quality of borrow sediments and safety of dredging operations. The sand deposits identified along South Pelto in this study have great potential to support large-scale coastal restoration of Lafourche Coastal segments. Sand from this borrow area is proposed to be used for restoration of Caminada Headland restoration project which is approximately 48 kilometers. Transporting sand over this distance will be expensive. However in absence of any suitable deposit with adequate quantity of sand in the vicinity of the project area, this is likely the only option.

# CHAPTER 3
# RESPONSE OF FLUVIAL FINE SEDIMENT DISPERSAL TO STORM WIND-CURRENT EFFECTS ON A HOLOCENE TRANSGRESSIVE SHOAL: A NUMERICAL SIMULATION

## 3.1. INTRODUCTION

River plumes (both positive and negative buoyancy currents) are important forcing for local hydrodynamics and consequent linking to coastal ecosystem (e.g., Chao 1987; Wright and Nittrouer 1995; Murray 1997). It has long been known that Atchafalaya River sediments are transported westward during most of the year (cf. Wells and Kemp 1981), following the prevailing wind and consequent coastal circulation pattern. However, recent studies show that during high river discharges, sediment dispersal often shifts in direction from westward to southeastward (cf. Walker and Hammack 2000; Kobashi *et al.* 2007b). Although not all the storms contribute to it, this shift likely accompanies the cold front-induced extra-tropical storms, which frequent the Louisiana coast every three to 10 days between October and May (DiMego *et al.* 1976; Hsu 1988). A Holocene transgressive shoal, Ship Shoal, which is on the pathway of the shifted dispersal and is predominantly characterized as having a sandy bottom, could be covered with fluid mud and dramatically alter its bottom sediment characteristics from sand to heterogeneous bottom sediments, which in turn alter its diverse benthic habitat and local sediment dynamics (Stone *et al.* 2006; Kobashi *et al.* 2007a, b). However, not all post-frontal winds trigger the dispersal shift and the impacts on the shoal have not been understood (Kobashi *et al.* 2009a).

The purpose of this paper is preliminarily to show the response of the fluvial fine sediment dispersal to extra-tropical storms by implementing a three dimensional numerical model with varying wind fields. Such an effort has not been undertaken to date in this environment and has an important implication for the shoal ecosystem and hydrodynamics including potential wave-current attenuation over cohesive sediment on the shoal and inner shelf.

## 3.2. EXPERIMENTAL SETUP

A coupled three dimensional hydrodynamic and advection-dispersion model, MIKE 3 HD/TR was implemented for the study. The HD/TR model solves incompressible Reynolds-averaged Navier-Stokes equation and advection-dispersion equation, respectively (DHI 2005). The model uses the unstructured triangular mesh grid and finite volume method; vertical discretization was equidistant and the number of the vertical layers was selected as 10. Detailed model description is elaborated on in DHI (2005). The model domain covered the Atchafalaya Bay and Shelf and three transgressive shoals, Ship Shoal and Tiger/Trinity shoals (Figure 3.1). The computational grid consisted of fine-resolution meshes near the Atchafalaya River mouth (maximal grid area as

6.1 × 105 $m^2$) and coarser-resolution meshes for the rest of the domain (maximal grid area as 4.9 × 106 $m^2$) (Figure 3.1).

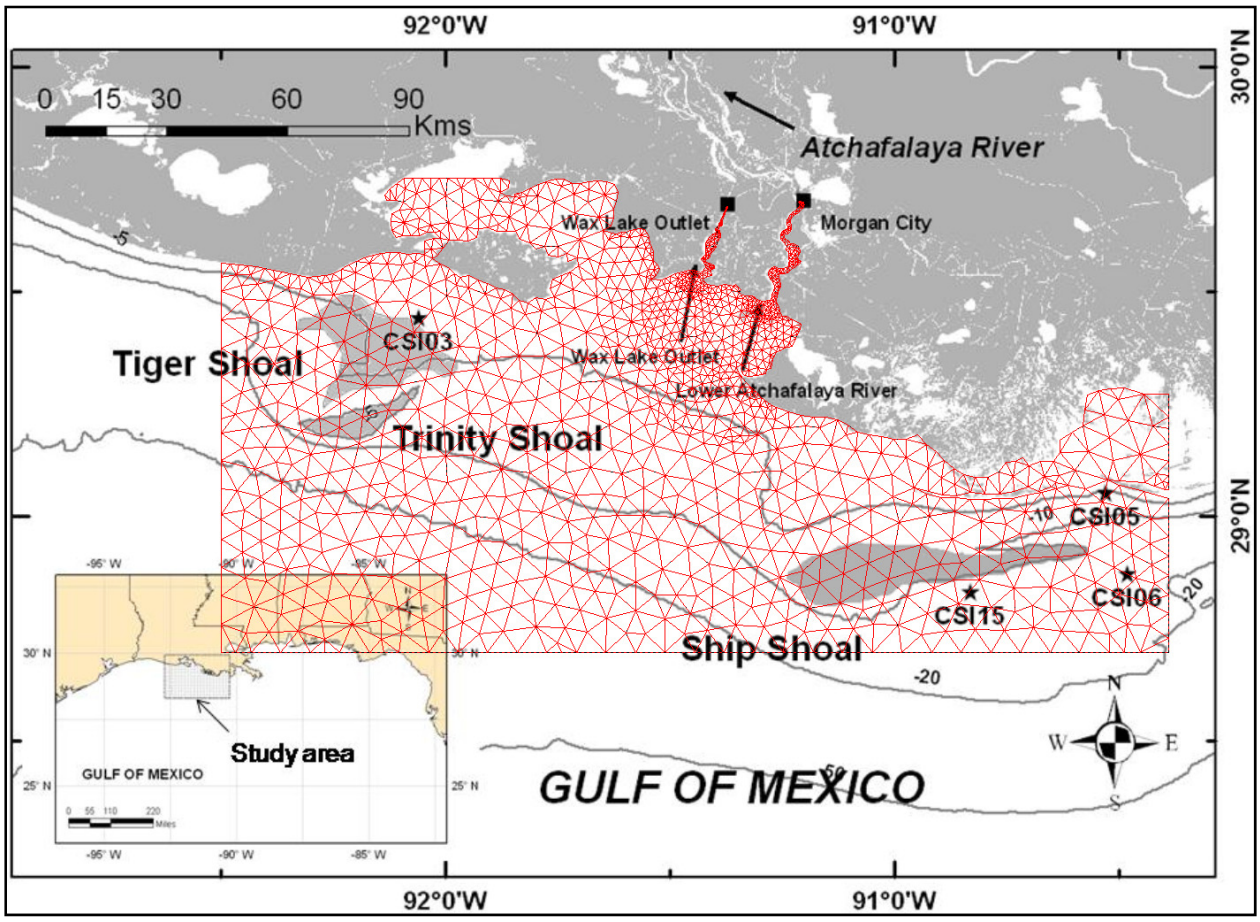


Figure 3.1 Map of study area and computational grids overlaid on the map. Ship Shoal and Tiger/Trinity shoals are shaded.

Four model cases were selected, representing the wind pattern associated with fair weather and extra-tropical storms: (1) no wind, (2) 10 m $s^{-1}$ constant wind from the southeast (135 degrees), (3) 10 m $s^{-1}$ constant wind from the northwest (315 degrees), and (4) 10 days with no wind followed by 3 days of 10 m $s^{-1}$ northwest wind (see Table 3.1). The model duration is 20 days for all cases except case 4, which is 13 days. River discharges at the mouths of the Lower Atchafalaya River and Wax Lake Outlet (Figure 3.1) were selected as constant 3,000 $m^3$ $s^{-1}$ and 1,500 $m^3$ $s^{-1}$, respectively. Suspended sediment concentration (SSC) was selected as constant 140 mg $l^{-1}$ and 45 mg $l^{-1}$ at the mouths of the Lower Atchafalaya River and Wax Lake Outlet, respectively (Figure 3.1). Sediments debouched from both rivers comprise primarily of fine-grained silt and clay; according to Wells and Kemp (1981), the fluvial sediment composition is comprised of montmorillonite, illite and kaolinite.

Those input parameters were determined with reference to in-situ data from the U.S. Geological Survey national water data reports at Morgan City and Wax Lake Outlet (e.g., Baumann *et al.*

2006) and considered as moderately high discharge of the lower Atchafalaya River mouths during spring. Initial temperature, salinity, and the SSC were set up as 25°C, 35 PSU, and 0 mg $l^{-1}$, respectively. Input parameters including river point sources are summarized in Tables 2.1 and 2.2. The purpose of this preliminary study is to examine the response of fluvial sediment dispersal to varying storm winds. Therefore, waves, water level fluctuations, and the Coriolis force were not included in the modeling. The concepts presented here will be tested using comprehensive numerically-derived and in situ data.

Table 3.1

Model cases

| Cases | Wind Speed | Wind Direction | Duration |
|---|---|---|---|
| Case 1 | NA | NA | 20 days |
| Case 2 | 10 m $s^{-1}$ | 135 degrees | 20 days |
| Case 3 | 10 m $s^{-1}$ | 315 degrees | 20 days |
| Case 4 | NA | NA | 10 days |
| | 10 m $s^{-1}$ | 315 degrees | 3 days |

Table 3.2

Input parameters of river discharge, temperature, salinity and SSC

| Parameters | LAR*[1] | WLO*[2] | Domain |
|---|---|---|---|
| River discharge | 3000 $m^3$ $s^{-1}$ | 1500 $m^3$ $s^{-1}$ | NA*[3] |
| Temperature | 20 °C | 20 °C | 25 °C |
| Salinity | 0 PSU | 0 PSU | 35 PSU |
| SSC | 145 mg $l^{-1}$ | 45 mg $l^{-1}$ | 0 mg $l^{-1}$ |

*[1]LAR: Lower Atchafalaya River mouth
*[2]WLO: Wax Lake Outlet mouth
*[3]NA: Not applicable

## 3.3. RESULTS AND DISCUSSION

In Figure 3.2, model results pertaining to the SSC distribution for each scenario after 20 days (13 days for case 4) of simulations are shown. All of the figures clearly showed the effects of wind on fluvial sediment dispersal.

For case 1, which was run with no wind input, the plume abruptly lost its momentum once discharged into the Atchafalaya bay/nearshore and was dispersed over approximately the 5 m isobath and was laterally distributed (Figure 3.2a).

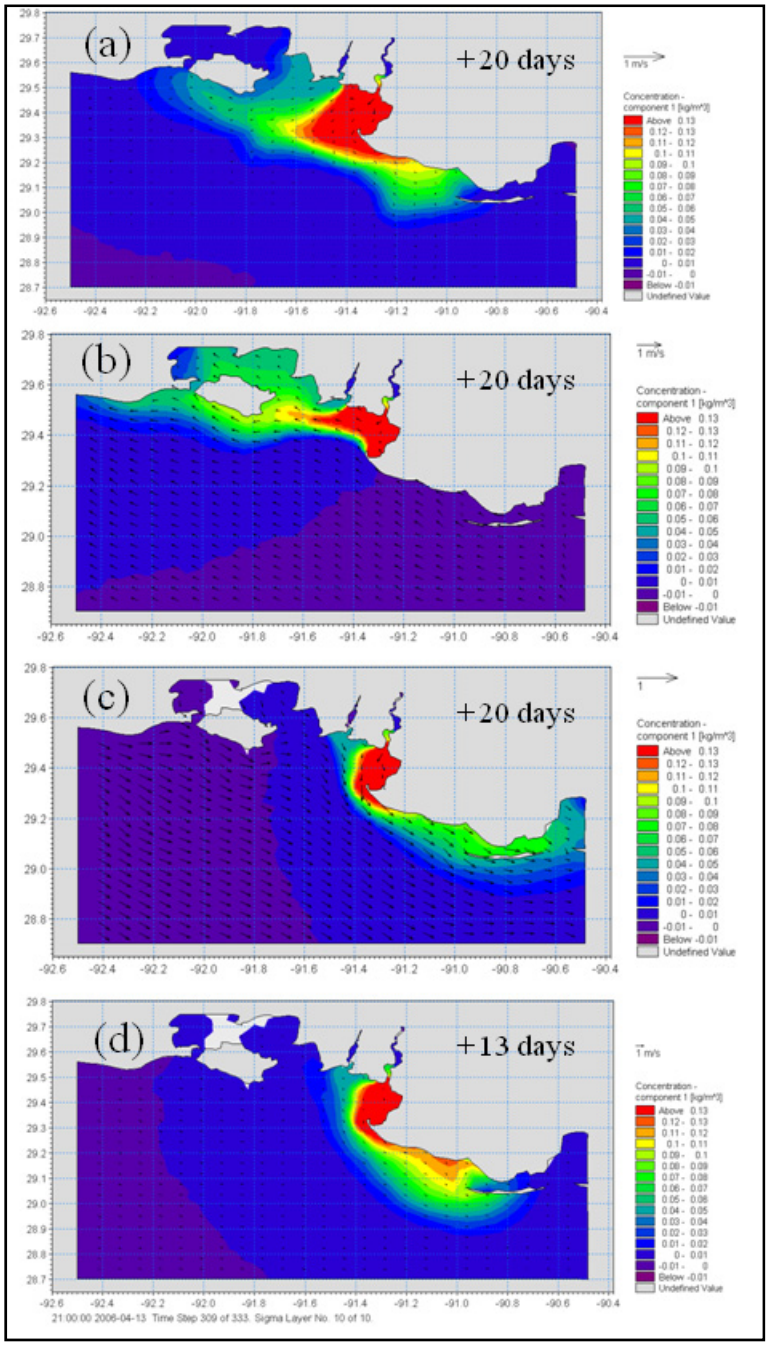


Figure 3.2 Distribution of sediment concentration: (a) Case 1 (No wind), (b) Case 2 (10 m $s^{-1}$ SW wind), (c) Case 3 (10 m $s^{-1}$ NW wind), and (d) Case 4 (No wind + 10 m $s^{-1}$ NW wind).

For case 2, with the uniform southeast wind of 10 m $s^{-1}$, the sediment plume was dispersed toward the west, in consistent with satellite imagery presented for general dispersal patterns (Figures 3.2b, and 3.3 (top left)) as well as results of previous studies (e.g., Wells and Kemp 1981; Walker and Hammack 2000).

For case 3 with the uniform northwest wind of 10 m $s^{-1}$, the fluvial sediment path was shifted from the west and dispersed toward the southeast along the coast and offshore to Ship Shoal, located approximately 50 km southeast of the river mouth (Figures 3.1 and 3.2c). Though the prevailing wind is southeasterly during most of the year along the Louisiana coast (Murray 1997), this shift in direction of the plume dispersion often occurs during post-frontal phase of winter storms, during which wind direction is predominantly from the northern quadrant (Walker and Hammack 2000; Kobashi *et al.* 2007b).

The post-frontal regime lasts for 1 to 3 days depending on the nature and intensity of the storm (Pepper and Stone 2004). The current velocity over the Atchafalaya Bay for all model cases ranged from 0.15 to 0.25 m $s^{-1}$, which was in general agreement with the current velocity observed at CSI-14 (West Cote Blanche Bay, 91°33.41'W, 29°30.96'N) located west of the bay, during winter weather. Since the post-frontal northerly wind lasts for roughly up to 3 days, the sediment plume freshly debouched from the river mouths was not able to reach the shoal during the post-frontal phase (~ 3 days window), as shown in Figure 3.2c, and hence not in conformity with data obtained from satellite imagery (Kobashi *et al.* 2007b). A possible reason is that the source of the fine sediments dispersed southeastward may not be directly dispersed from the river mouths, rather advected and dispersed from the sediments already transported over the Atchafalaya bay/nearshore as illustrated in Figure 3.3 (top left). In order to prove this hypothesis, the case 4 was implemented.

Case 4 was divided into two wind regimes during the 13 day model duration; for the first 10 days the model was run with no wind to determine the initial SSC distribution and was followed by the 3 day simulation with the northwesterly wind (*i.e.*, a total of 13 day model duration) (Table 3.1). The model result showed that the sediments that were already debouched from the river and transported over the bay/nearshore reached the shoal after three days of persistent northwesterly wind (Figure 3.2d). Similar results were obtained from the model results for different wind speeds (20 m $s^{-1}$, 15 m $s^{-1}$, and 12 m $s^{-1}$) though different were the periods which took for the fluvial sediments to reach the shoal. Additionally, the model result generally agreed with the satellite imagery of a typical dispersal pattern during post-frontal phases, obtained from Louisiana State University, Earth Scan Laboratory, as shown in Figure 3.3 (bottom left). *In-situ* observational data from WAVCIS CSI-3 (Stone *et al.* 2001; http://www.wavcis.lsu.edu) during a pre-frontal (Figure 3.3 top right) and post-frontal phase (Figure 3.3, bottom right) showed a complete shift of current profile from northwestward to southeastward throughout the entire water column during the period.

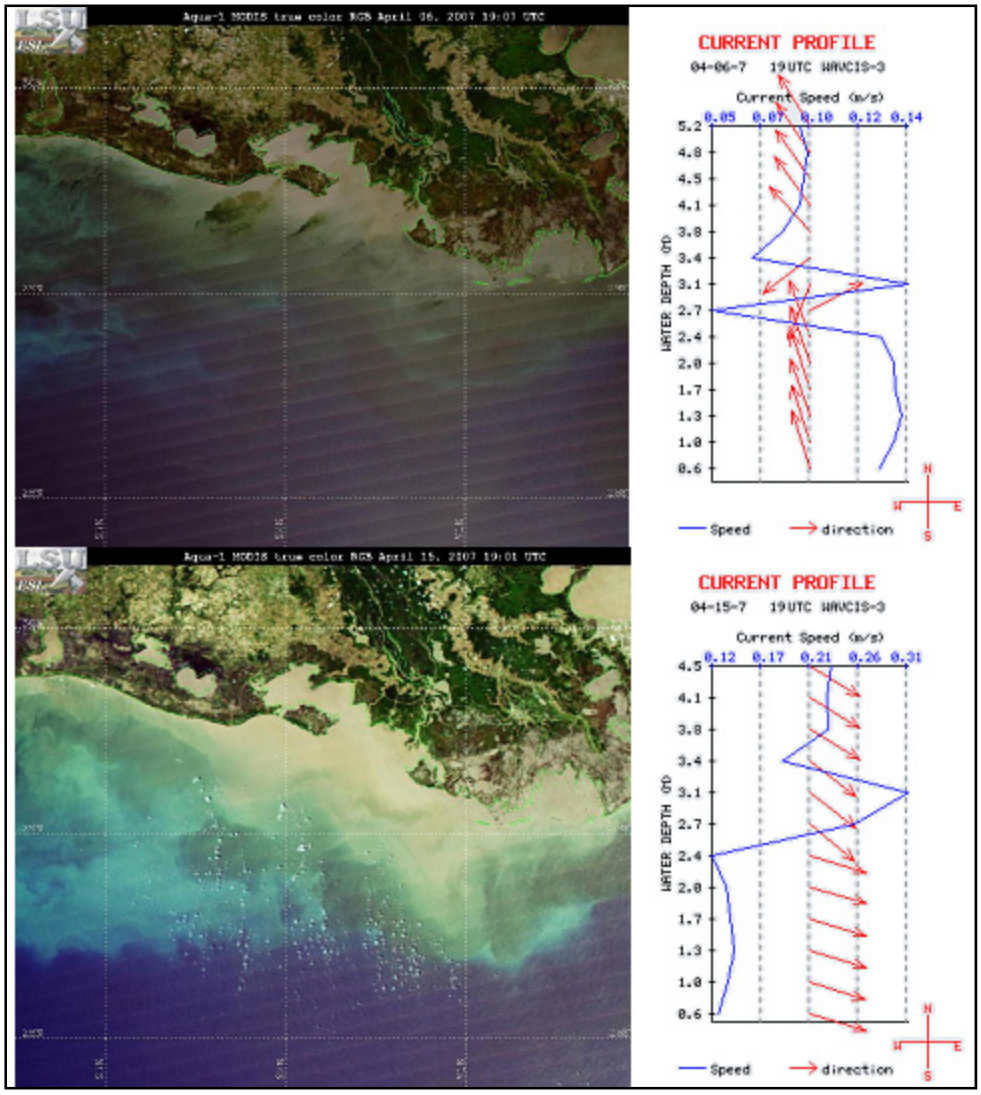


Figure 3.3 MODIS satellite images and current profile of WAVCIS CSI-3 during a pre-frontal (upper) and a post-frontal (bottom) phase (Satellite images obtained from LSU Earth Scan Lab).

Time series of met-ocean data from CSI-3, during the period under study clearly indicated strong storm-wind stress (Figure 3.4a) and associated current shifts (Figure 3.4b) from the northwest to southeast during a storm, supporting our model outputs. In addition, this dispersal shift illustrated in Figure 3.3 likely accompanied wave-induced sediment re-suspension. Wave-induced shear stress above the threshold for sediment suspension (Figure 3.4c, dash line) and the acoustic backscatter signal amplitude (Figure 3.4d), which is a proxy for sediment concentration, clearly illustrated significant re-suspension during the storm, suggesting the importance of sediment suspension and associated dispersal due to storm waves and currents. A similar result was

obtained from CSI-14 data during winter storms in 2005 (Kobashi *et al.* 2009a). It should be noticed that this model study did not include bottom sediment re-suspension and deposition; therefore, these effects, which are also important as shown in Figure 3.4 and are clearly captured by the satellite image over Tiger and Trinity shoals in Figure 3.3 (bottom left) (see location in Figure 3.1), have to be considered for future model implementation, particularly during severe weather such as extra-tropical and tropical storms, the two primary weather events capable of causing bottom sediment re-suspension over the low-energy Louisiana coast (Kobashi *et al.* 2009a).

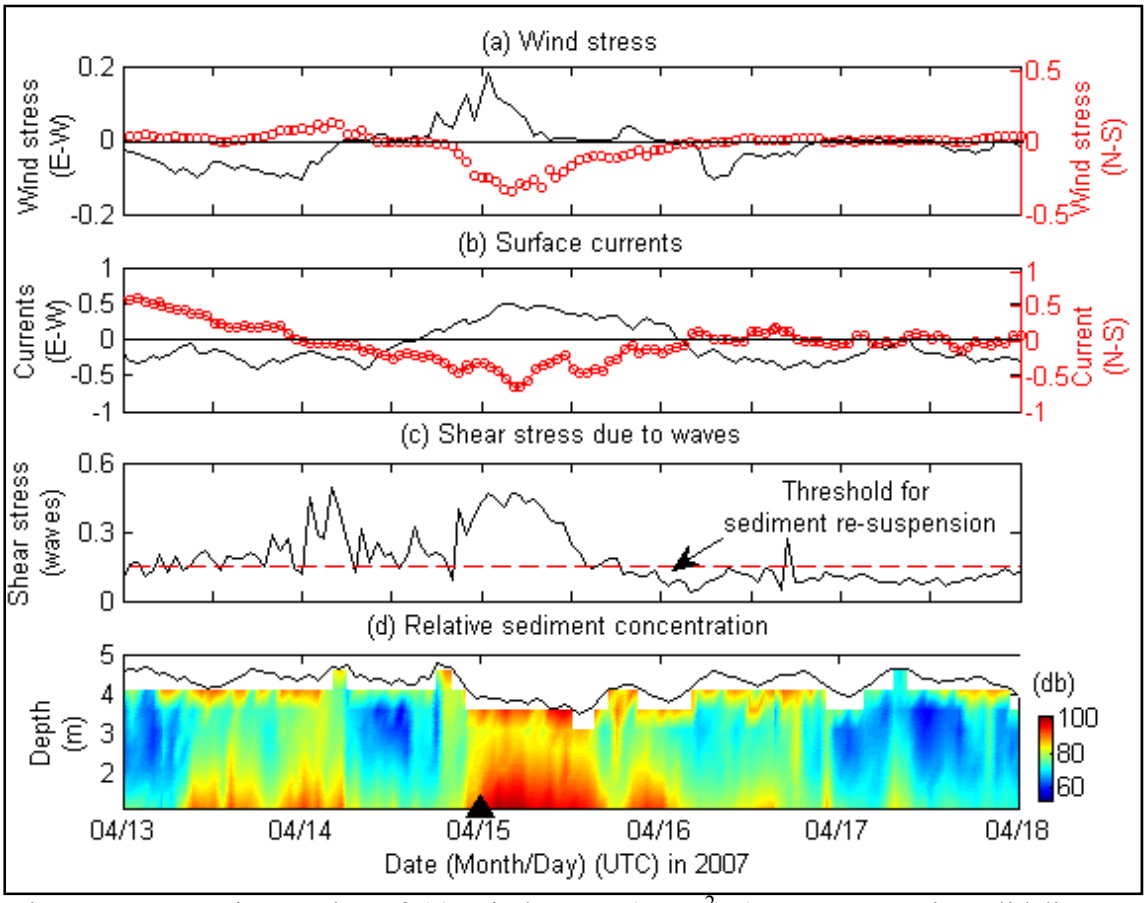


Figure 3.4 Time series of (a) wind stress (N $m^{-2}$) (u-component in solid line, v-component in red circles), (b) near surface currents (m $s^{-1}$) (u-component in solid line, v-component in red circles), (c) wave-induced shear stress (N $m^{-2}$), and (d) acoustic backscatter amplitude (decibel) during a winter storm. A triangle in (d) shows passage of a winter storm. The dashed line in (c) shows threshold for sediment suspension.

Overall, the model results illustrated strong response of fluvial fine sediment dispersal to wind-driven currents associated with the extra-tropical storms and the model simulated plume shifts, as supported by in-situ observing data and satellite images. This simplified model implementation

is preliminary; however, the MIKE3 HD/TR model has the ability to simulate Atchafalaya River sediment dispersal reasonably well if accurate input parameters of wind, sediment sources, and hydrodynamic parameters are included, except for the small scale eddies as seen in the satellite images (Figure 3.3), a consequence of the selected computational grid size. Modeling hydrodynamics and sediment transport, including sediment re-suspension and depositional effects, is currently being pursued.

# CHAPTER 4
# WIND-DRIVEN DISPERSAL OF FLUVIALLY-DERIVED FINE SEDIMENT FOR TWO CONTRASTING STORMS: EXTRA-TROPICAL AND TROPICAL STORMS, ATCHAFALAYA BAY/SHELF, SOUTH-CENTRAL LOUISIANA, U.S.A.

## 4.1. INTRODUCTION

It has long been known that Atchafalaya River fine sediments have been transported westward during most of the year, following Louisiana coastal currents (Wells and Kemp 1981; Cochrane and Kelly 1986; Murray 1997). Dispersal of the fine sediments from the Atchafalaya River, whose sediment load is estimated as approximately 80 million tons $yr^{-1}$ (Milliman and Meade 1983), has contributed to the seaward progradation of the Chenier plain at the rate of 5 to 10 m $yr^{-1}$ (Wells and Kemp 1981; Kemp 1986; McBride *et al.* 2007). Moreover, the westward mud transport and deposition cause unique hydrodynamic behavior including strong wave dissipation over the muddy bottom along the western Louisiana shelf (cf. Kemp 1986; Sheremet and Stone 2003). However, recent studies have shown that during winter-spring season sediment dispersal often shifts the direction from westward to south/southeastward, especially during the spring flood regime (Walker and Hammack 2000; Kobashi *et al.* 2007b). This conspicuous shift in the fine sediment dispersal pattern during spring accompanies winter storms driven by cold front passages across the coast. In addition, tropical cyclones also help to re-distribute inner-shelf sediments further onshore and offshore, even to the continental shelf boundary, as seen from satellite imagery.

River plumes from both the Mississippi River and its main distributary, the Atchafalaya River, have been examined by numerous studies because of their importance on the coastal ecosystem (e.g. water quality, nutrient load, contaminant transport) and also sediment management for restoration (cf. Walker and Rouse 1993; Murray 1997; Walker and Hammack 2000). Walker (2001) and Walker and Hammack (2000) examined the responses of the sediment plume from the Atchafalaya River during storms, based on satellite images and in-situ data, for different winter storm and tropical storm events. Their study showed the response of river-borne sediments to varying storm winds. However, the analysis was solely based on satellite imagery interpretation and limited to short-term in-situ observations of water level, currents and sediment concentration. As a result, the dispersal and transport mechanisms of the fine sediments that originated from the Atchafalaya River and associated coastal hydrodynamics and bottom boundary layer characteristics, are not yet fully understood. Kobashi and Stone (2009) suggested, based on their numerical model study, that wind-induced south-easterly currents during post-frontal phases are a dominant factor for south/southeastward sediment dispersal during winter storms; however, they also suggested that local sediment re-suspension needs to be considered.
A major motivation for this study has come from the fact that the intermittent sediment dispersal shifts to a south/southeasterly direction strongly alter bottom sediment characteristics of a Holocene transgressive shoal, Ship Shoal, located approximately 50 km southeast of the

Atchafalaya River mouth. This shoal was previously considered as having a sandy bottom year-round, and is in fact intermittently heterogeneous bottoms (i.e., mixture of sand and fluid mud), which in turn likely alters local sediment dynamics and its benthic biological environment (Stone *et al.* 2006; Kobashi *et al.* 2007a, b) (Figure 4.1). In addition, during tropical cyclones, substantial sediment re-distribution can be expected, given the shallow bathymetry of the shoal. This paper addresses this unique wind-driven dispersal and transport mechanisms of the fluvial sediments associated with hydrodynamics and bottom boundary layer characteristics during two contrasting storms, tropical and extra-tropical storms. The paper also addresses the impact of fine sediment depositions on the shoal, based on extended in-situ observations and analysis of satellite imagery for the period between October 2004 and September, 2005.

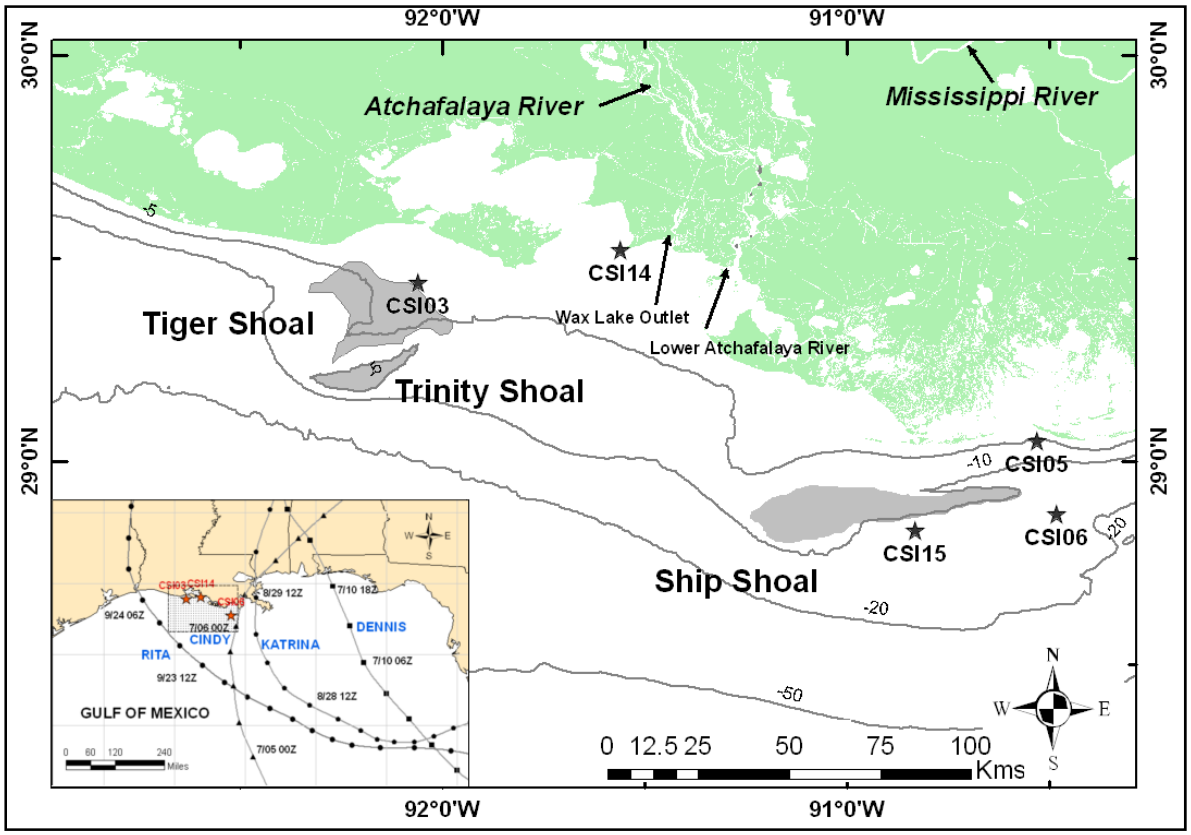


Figure 4.1 Map of study area. Tracks of 2005 Hurricanes that made landfall on northern Gulf of Mexico are shown on bottom left.

## 4.2. WINTER STORMS AND TROPICAL STORMS IN 2005

### 4.2.1. Winter Storms

Winter storms are low pressure systems which originate in the arctic polar region (polar frontal zone). The low pressure accompanies atmospheric fronts (*i.e.*, cold fronts and warm fronts), moving from west to east following westerly; the fronts eventually pass the northern Gulf coast

every 3 to 10 days between October and May (DiMego *et al.* 1976; Hsu 1988). Before the cold fronts pass the Gulf, relatively strong winds blow from the southeast; during post-frontal events, wind direction strongly shifts from the southern quadrant to the northern quadrant and air temperature and barometric pressure abruptly decrease (Figure 4.2, bottom right)(cf. Hsu 1988). These strong wind fields and the rapidly fluctuating wind directionality cause a unique hydrodynamic behavior off the Louisiana shelf. Cold fronts are one of two major driving forces along with tropical cyclones, and significantly affect wave-climate, hydrodynamics and sediment transport along this low-energy shelf (Stone 2000; Kobashi *et al.* 2005; Keim *et al.* 2007). In 2005, approximately 40 cold fronts passed the Louisiana coast. In addition, the year 2005 was the transition period of El Nino to neutral and La Nina. During the El Nino, jet streams shift further to the south and more winter storm activities are expected; while, during La Nina, winter storm activities are expected to be less frequent. On the other hand, tropical cyclones are known to be intensified during neutral or La Nina period (Manty 1993). When Hurricanes Katrina and Rita made landfall, the climatological condition was the neutral to weak La Nina. Discussing the influence of El Nino/La Nina on storm activities is beyond the scope of this paper. More detailed information regarding impacts of El Nino on storm activities is elaborated on in Manty (1993).

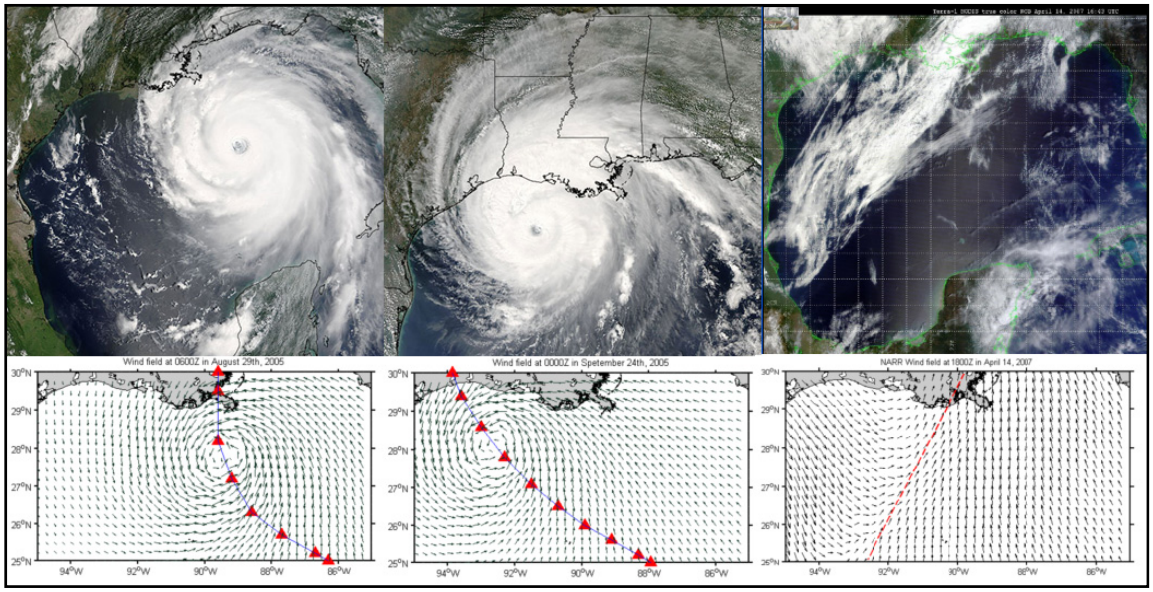


Figure 4.2 MODIS satellite images and NOAA NARR wind field during (Hurricanes Katrina (left) and Rita (middle) and a cold front migrating from a polar region(right) (Images courtesy of MODIS Rapid Response Project at NASA/GSFC and Louisiana State University Earth Scan Lab).

### 4.2.2. Tropical Cyclones

During the 2005 hurricane season, 27 named tropical storms were generated in the Atlantic Basin and out of which 15 developed into hurricanes. The season was the most active in recorded

history (National Climatic Data Center 2006). Three of the season's seven major hurricanes – Dennis, Katrina and Rita- along with Hurricane Cindy caused considerable damage along the coastal Louisiana. Three of them, namely, Katrina, Rita and Cindy, made landfall along the Louisiana coast causing wide spread destruction due to hurricane-forced winds, waves and significant storm surges (Figures 4.1 and 4.2; Table 4.1). The barrier island chains along the coast were either totally eroded due to hurricane waves and storm surges or sustained multiple breaches and overwash (Stone *et al.* 2004a). Freshwater marshes also sustained heavy damage due to the intrusion of salt water, which was accentuated by the presence of dredged channels all along the coastal marshes (Stone *et al.* 2004a). Even though Hurricane Dennis made landfall along Santa Rosa Island in Florida, hurricane-induced winds and waves caused conspicuous damage to the barrier islands along the eastern Louisiana. Table 4.1 shows a brief summary of the hurricanes which made landfall over the northern Gulf of Mexico. More detailed information regarding each hurricane is provided by Knabb *et al.* (2005a; 2005b).

Table 4.1

Summary of 2005 hurricanes that made landfall along the northern Gulf of Mexico (Data source: Knabb (2005a; 2005b).

| Name | Max wind speed | Max storm surge | Min pressure | Time of landfall | Landfall location |
|---|---|---|---|---|---|
| **Cindy** | 34 m/s | 6 ft (1.8 m) | 956 mb | 0300UTC, July 6$^{th}$ | Grand Isles, LA |
| **Dennis** | 64 m/s | 7 ft (2.2 m) | 946 mb | 1930 UTC, July 10$^{th}$ | Santa Rosa Islands, FL |
| **Katrina** | 73 m/s | 28 ft (8.5 m) | 902 mb | 1110 UTC, August 29$^{th}$ | Buras, LA |
| **Rita** | 78 m/s | 15 ft (4.6 m) | 897 mb | 0740 UTC, September 24$^{th}$ | Johnson's Bayou, LA |

## 4.3. LOUISIANA COASTAL CURRENTS

Along the Louisiana/Texas (LA-TX) shelf, the dominant force to drive coastal currents is the prevailing wind, particularly during storms, given the fact that waves and tidal currents are generally low (*i.e.*, low-energy micro-tidal environment) (Cochrane and Kelly 1986; Murray 1997). During most of the year, the wind blows from the southeast and hence, the coastal current direction is mostly westward. Cochrane and Kelly (1986) first showed the strong response of coastal currents to seasonal wind patterns over the LA-TX shelf. Their study revealed that current direction over the LA-TX inner shelf is westward during most of the year; while, the current over the LA-TX shelf in summer reverses from westward to eastward, following a wind reversal from the southeast to west in summer. This seasonal current pattern along the LA-TX shelf was also reported by the Louisiana-Texas Shelf Circulation and Transport Processes Study (LATEX), based on the deployment of numerous meteorological sensors and acoustic Doppler current profilers over the LA-TX shelf (Murray 1997; Nowlin *et al.* 1998). The weekly-averaged wind stress and current velocities (top, middle, and bottom layers) at the WAVCIS CSI-3 station in a depth of approximately 5 m (Figure 4.1) in 2005 have similar results, showing a strong correlation between the wind and current fields (Figure 4.3). The current velocities at top, middle and bottom layers show the same trend and are mostly westward except during April, June, July

and August (Figure 4.3). A detailed discussion of current variation is included in a later section of this paper.

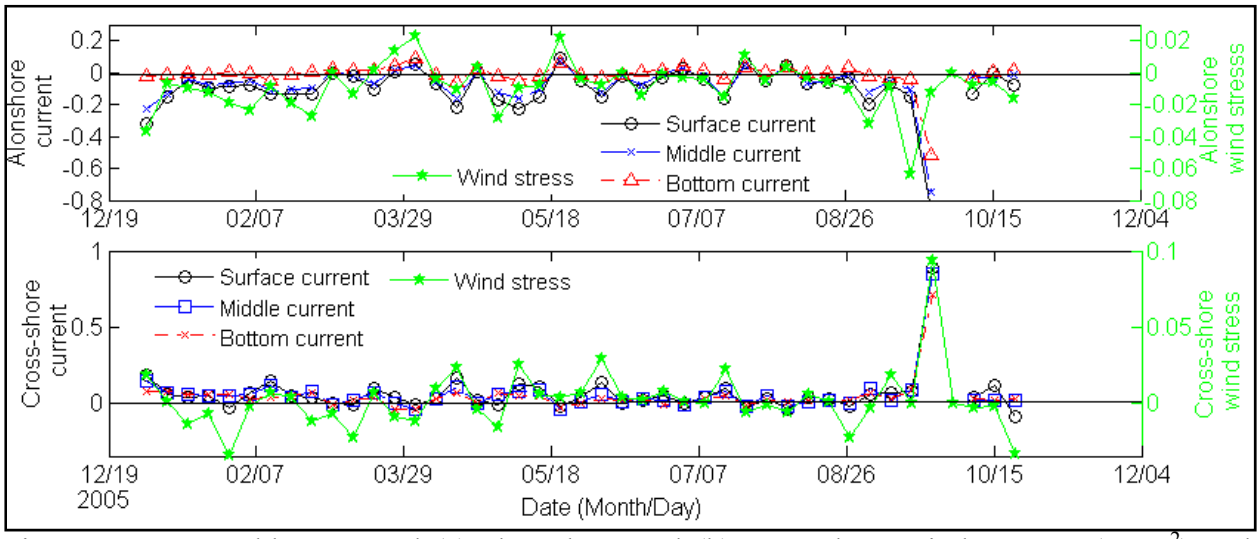


Figure 4.3 Weekly-averaged (a) alongshore and (b) cross-shore wind stresses (N $m^{-2}$) and currents (m $s^{-1}$) of CSI-3 in 2005.

## 4.4. DATA SOURCES AND ANALYTICAL METHODS

Data sources used for analysis include data from in-situ observing stations, WAVCIS (Wave-Current-Surge Information System) CSI's-3, 6, and 14 (see locations in Figure 4.1) and satellite images from the Louisiana State University Earth Scan Laboratory (hereafter referred to as ESL), and hydrological data from the U.S. Geological Survey National Water Information System (Walker and Rouse 1993; Stone *et al.* 2001; Baumann *et al.* 2006). WAVCIS CSI-14 provided hourly directional wave parameters, single-point current, water quality (temperature, salinity and turbidity) all at 1.6 m above the bottom as well as meteorological data. CSI-3 and 6 provided hourly wave parameters, water level, and current profile; water quality data (temperature, salinity, and turbidity) over 1, 2, and 3 m above the bottom were also provided. Detailed information regarding WAVCIS is provided by Stone *et al.* (2001) and Zhang (2003). Satellite imagery of MODIS (Moderate Resolution Image Spectrometer) true color was obtained from the ESL (Walker and Rouse 1993).

Data analysis is mainly based on time series analysis of the in-situ data. Directional wave parameters for CSI-14 and CSIs 3 and 6 were computed using the PUV method (Gordon and Lohrmann 2001) and the standard spectral method developed by the U.S. Army Corps of Engineers Field Wave Gauging Program with the orbital velocity spectrum algorithm developed by RD Instruments Inc. (Earle *et al.* 1995; RD Instruments Inc. 2004), respectively. From the meteorological data, wind stress ($\tau$) was calculated from the following balk equation.

$$\tau = \rho_a C_f U_{10}^2 \text{.....(4-1)}$$

where $\rho_a$ is air density (1.3 kg $m^{-3}$), $C_f$ is surface drag coefficient, and $U_{10}$ is wind speed at 10 m above the surface. The drag coefficient ($C_f$) was computed based on Wu (1982), Holthuijsen (2007), and Hsu (2003, 2006).

$$C_f = \begin{cases} 1.2875 \times 10^{-3} \cdots\cdots\cdots & U_{10} < 7.5(ms^{-1}) \\ (0.8 + 0.065 \times U_{10}) \times 10^{-3} \cdots & 7.5\ (\mathrm{m\ s^{-1}}) \le U_{10} < 20.0(ms^{-1}) \\ 2.5 \times 10^{-3} \cdots\cdots\cdots & U_{10} \ge 20.0(ms^{-1}) \end{cases} \text{..... (4-2)}$$

Suspended sediment concentration (SSC) at CSI-14 (located at West Cote Blanche Bay, see Figure 4.1) was estimated based upon the calibration of the turbidity sensor (optical backscatter sensor, OBS) with sediments and water sampled from the site. A detailed calibration procedure is given in Sheremet *et al.* (2005). The resultant conversion from the OBS to the SSC was obtained as follow ($r^2$=0.998) (Liu, B. Personal communication, 2007).

$$SSC = 0.001 \times OBS - 0.0114 \text{..... (4-3)}$$

For CSI's-3 and 6, acoustic backscatter signal amplitude (ABS) from ADCP (Acoustic Doppler Current Profiler) was given as a proxy for the SSC profile (cf. SonTek Inc. 1997b).

Except for a few isolated sand bodies, bottom sediments of our study area are mainly silt and clay, due to the influx of fine-grained sediments primarily from the Atchafalaya River. Routines for computing the bottom boundary layer parameters (hereafter referred to as BBLP) for many previous studies are applicable for clear water and sandy bottom (cf. Nielsen 1992). For a cohesive bed, which is applicable for our study area, it is known that the algorithms to compute the BBLP for cohesive sediments rely on empirical formulae, which are largely site-specific (e.g., Mehta *et al.* 1989; McAnally *et al.* 2007). Moreover, for turbid waters, bottom drag is strongly reduced and the BBLP using conventional methods such as the von-Karman Plandlt equation, is overestimated (Li and Gust 2000). In addition, waves and currents are interacted with each other and for this reason the BBLP for combined wave-current is not simply the sum of individual BBLP (Grant and Madsen 1986; Nielsen 1992). In this paper, the BBLP for cohesive sediments, namely the bottom shear velocity and stress due to waves ($u_{*w}$, $\tau_w$) and due to currents ($u_{*c}$, $\tau_c$) were estimated using linear wave theory from Madsen (1976) (Equation 4-4) and using the quadratic stress law (Thompson *et al.* 2006) (Equation 4-5), respectively. The wave shear stress was applied to CSI-3, CSI-6, and CSI-14 data, and the current shear stress was applied to CSI-14 data. Solutions are provided as follows.

$$\tau_w = \rho_f u_{ob} \sqrt{\nu \frac{2\pi}{T_P}},\ u_{*W} = \sqrt{\frac{\tau_w}{\rho_f}} \text{..... (4-4)}$$

$$\tau_c = \rho_f C_D U_{100}{}^2,\ u_{*C} = \sqrt{\frac{\tau_C}{\rho_f}} \quad \text{..... (4-5)}$$

$$u_{ob} = \left( \frac{\pi H_S}{T_P \sinh(kh)} \right) \quad \text{..... (4-6)}$$

$$\left( \frac{2\pi}{T_P} \right)^2 = gk \tanh(kh) \quad \text{..... (4-7)}$$

where $\rho_f$ is fluid density (kg $m^{-3}$), ν is viscosity ($1.34 \times 10^{-6}$ $m^2$ $s^{-1}$), g is gravitational acceleration (9.8 m $s^{-2}$), $C_D$ is bottom drag coefficient, $U_{100}$ is mean current velocity at 1 m above the bottom in m $s^{-1}$, $H_S$ is significant wave height in m, $T_P$ is peak wave period in seconds, $u_{ob}$ is near-bottom wave orbital velocity in m $s^{-1}$ (Equation 4-6), k is wave number in $m^{-1}$ estimated by the dispersion relation (Equation 4-7), and h is water depth in m. Pressure and current sensors at CSI-14 were installed at 1.6 m above the seabed; we extrapolated the current to that at the conventional height, 1 m above the bottom, by logarithmic method, assuming flow at the bottom is zero. For the bottom drag coefficient ($C_D$), several studies used a constant drag coefficient to estimate the bed shear stress (Sternberg 1972; Adams *et al.* 1987); however, the coefficient depends on shear velocity, which varies with turbidity in same physical conditions (Li and Gust 2000; Thompson *et al.* 2006). We preliminarily estimated $C_D$ corresponding to sediment concentration (C) based on the result of Thompson *et al.* (2006) using a third order polynomial fit ($r^2 = 0.76$). By comparing $\tau_c$ for varying $C_D$ to that for the constant $C_D$ for a smooth bed, it is found that both results were almost identical. As a result, the constant $C_D$ of 0.0022, following Soulsby (1997), was used in this study.

Fluid density ($\rho_f$) for saline turbid water (10°C and 30 PSU) was estimated from the result of Thompson *et al.* (2006) using linear regression ($r^2 = 1.0$) (Equation 4-8).

$$\rho_f = 0.65 \times C + 1020 \quad \text{..... (4-8)}$$

The critical shear stress for erosion of 0.15 N $m^{-2}$ was selected as the threshold for cohesive sediment re-suspension with reference to Wright *et al.* (1997b). This value is also the same as the maximum threshold value used by the DHI Water and Environment Inc., based on their extensive numerical model studies (Kerper, D.R. personal Communication, 2006).

## 4.5. RESULTS AND DISCUSSION

### 4.5.1. Atchafalaya River Freshwater Discharge and Sediment Load

In Figure 4.4a, we present mean, maximum, and minimum river discharge at Simmesport, upstream Atchafalaya River, between 1997 and 2006, obtained from the U.S. Army Corps of

Engineers, New Orleans District. The Atchafalaya freshwater discharge was maximal in spring (April) due to ice melting from Rocky and Appalachians mountains, and minimum in summer (September). The maximum discharge in spring exceeded 600,000 cubic feet per seconds (cfs) (≈ 17,000 $m^3$ $s^{-1}$). Walker and Hammack (2000) suggest the discharge higher than 200,000 cfs (≈ 5,662 $m^3$ $s^{-1}$) at Simmesport as a high discharge event. Freshwater discharge, sediment load, and the SSC of Morgan City and Wax Lake Outlet obtained from the U.S. Geological Survey (USGS) are shown in Figures 4.4b and 4.4c (Baumann *et al.* 2006). In spring, the freshwater discharge reached 300,000 cfs (≈ 8,493 $m^3$ $s^{-1}$) and 200,000 cfs (≈ 5,662 $m^3$ $s^{-1}$) at Morgan City and Wax Lake Outlet. The sediment load and the SSC during this period were also high, during which significant quantities of fluvial sediments were debouched down to the receiving basin (see Figures 4.4b and 4.4c). One of the noticeable characteristics of the data for both Morgan City and Wax Lake Outlet was that the SSC was abnormally high in summer in spite of low river discharge and low wind energy regime. During this time, freshwater and sediment load in addition to the SSC had no correlation. More discussion is provided in a later section of this paper.

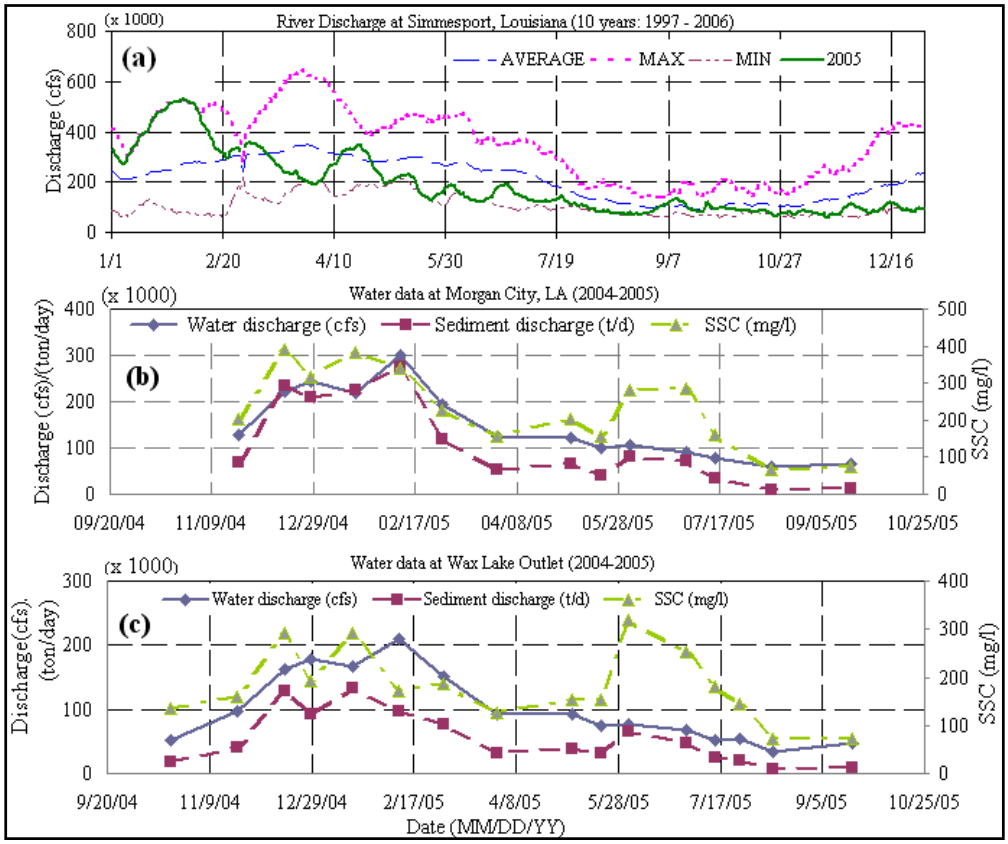


Figure 4.4 (a) Atchafalaya River discharge at Simmesport, LA, between 1997 and 2006 and freshwater discharge, sediment load and SSC at (b) Morgan City, 2005, and (c) Wax Lake Outlet, 2005.

### 4.5.2. Atchafalaya River Fine Sediment Dispersal Patterns

As mentioned in a previous section, the Atchafalaya River fine sediment dispersal and transport are influenced by the prevailing wind and associated coastal currents. The wind-induced westerly currents, during fair weather conditions, transport the sediments westward, and are referred to as the mud stream by Wells and Kemp (1981), as also seen from a MODIS true color image obtained from the ESL (Figure 4.5a). With the onset of a winter storm over the basin, abrupt change of wind direction occurs, which deflects the direction of current and the sediment plumes along the shelf. During spring, concurrent with winter storms, this westward transport occasionally shifts the direction from the west to south/southeast, during the post-frontal northerly wind regime. Such a situation can be clearly seen in Figures 4.5b and 4.5d. It should be noted that not all post-frontal winds yielded this substantial shift in the plume. During tropical cyclones, the transport is dependent upon storm tracks and its intensity. Preliminary analysis of satellite images during the 2005 hurricane season exhibits strong contrasts with respect to sediment dispersal and transport.

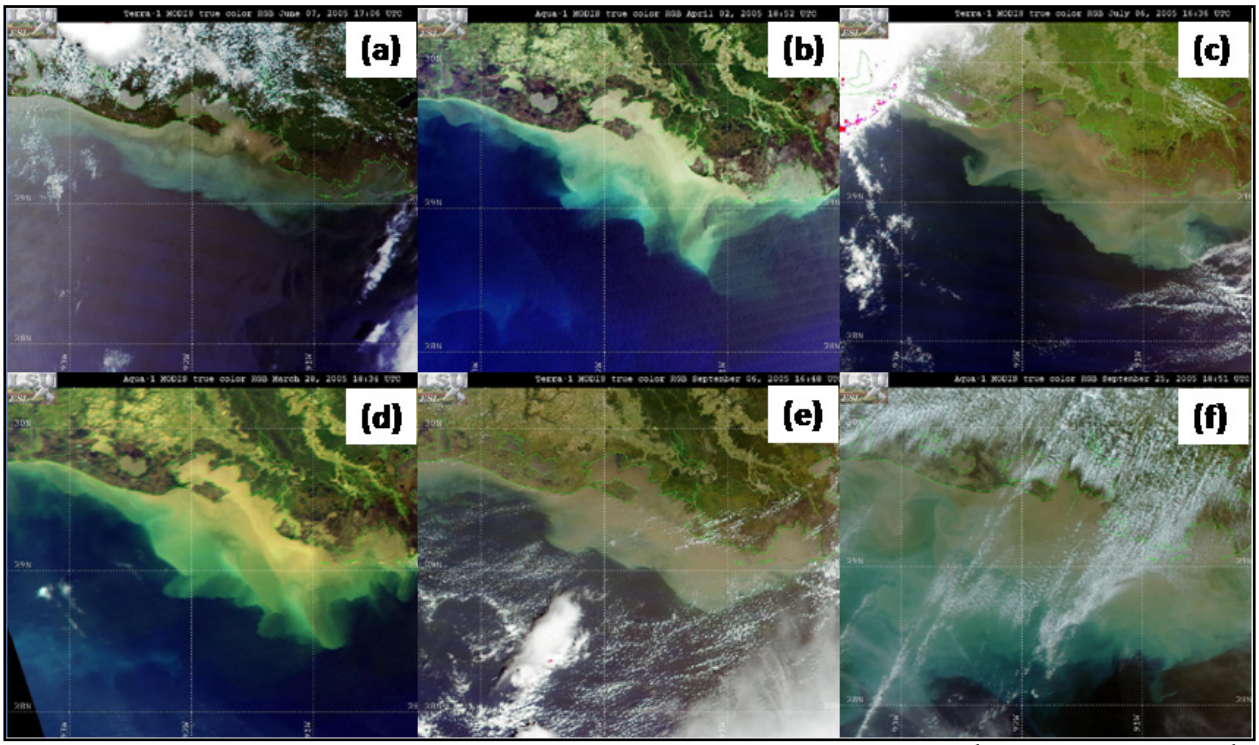


Figure 4.5 MODIS Satellite images in (a) June 7, 2005, (b) April 2nd, 2005, (c) July, 6th, 2005, (d) March 28th, 2005 (e) September, 6th, 2005 (f) September 26th, 2005.

During Hurricanes Cindy (Figure 4.5c), Katrina (Figure 4.5e), and Rita (Figure 4.5f), sediment dispersal patterns driven by the hurricane-induced winds can be clearly seen in spite of low river discharge during summer, implying the importance of local sediment re-suspension. The

mechanism of fluvially-derived sediment dispersal and transport is discussed in the following sections.

### 4.5.3. Wave-climate and Associated Hydrodynamics over the Louisiana Inner Shelf

In Figures 4.6, 4.7 and 4.8 are presented time series of wave-climate, 24 hour moving-averaged currents and SSC (and ABS) at CSI's-3, 6, and 14, respectively. Wave-climate, hydrodynamics and bottom sediment interaction over the Atchafalaya Bay/Shelf are strongly associated with meteorological conditions and river discharge from the Atchafalaya River. As shown in Figure 4.3, alongshore currents at CSI-3 were westward during most of the year 2005, except April, June, July and August during which the prevailing current direction was eastward and the north component was almost zero. The eastward currents in April were associated with the passage of winter storms and the persistent easterly coastal currents during June, July and August were attributed to the reversal in the wind direction to the east, as also reported by Cochrane and Kelly (1986). Cross-shore currents were negative in winter and spring due to strong post-front wind stress and were positive during summer. High positive cross-shore wind stress in late September was associated with Hurricane Rita (Figure 4.3). During fair weather, wave-induced bottom shear stress at CSI-14 was generally lower than the threshold for sediment suspension (Figure 4.6d); while during winter storms and tropical cyclones, shown as shaded triangles in Figure 4.6e, the shear stress due to waves exceeded the critical value, which corresponded to an increase in the sediment re-suspension and in the SSC (Figures 4.6d and 4.6e).

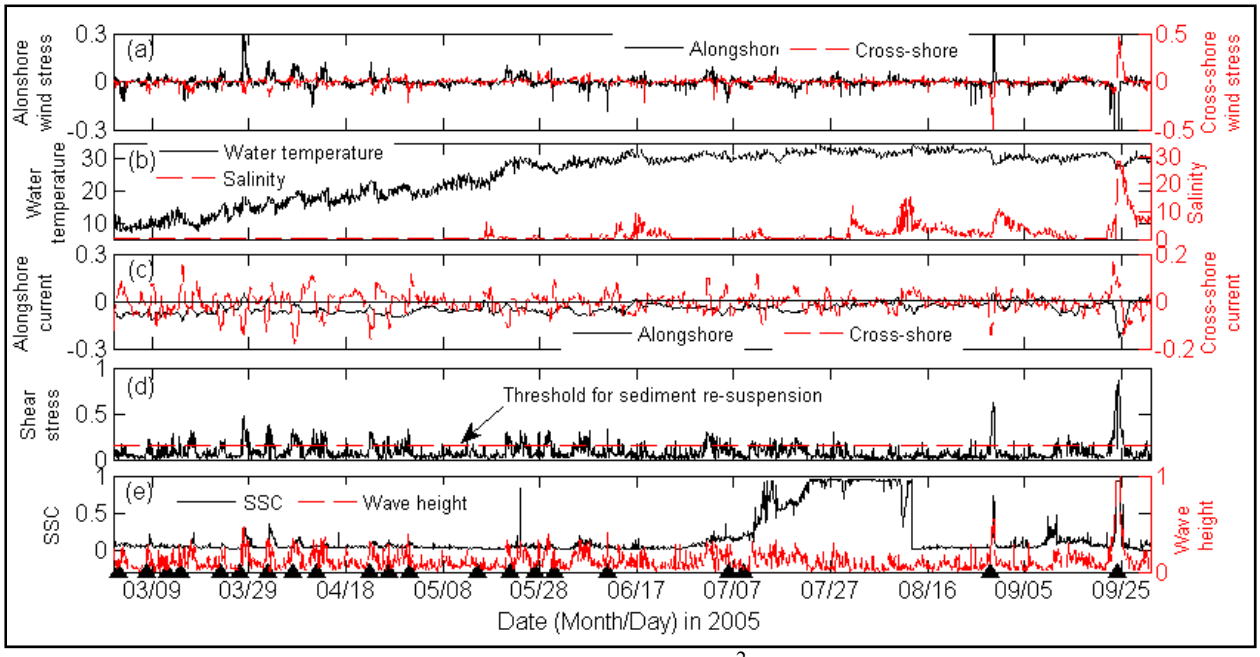


Figure 4.6 Time series of (a) wind stress (N $m^{-2}$), (b) wave height (m) and water depth (m), (c) 24 hr moving-averaged current (m $s^{-1}$), (d) shear stress due to waves (N $m^{-2}$), and (e) SSC (kg $m^{-3}$) at WAVCIS CSI-14 between 2005/03/01-2005/09/30. Passage of winter storms and tropical cyclones are shown with shaded triangles in (e).

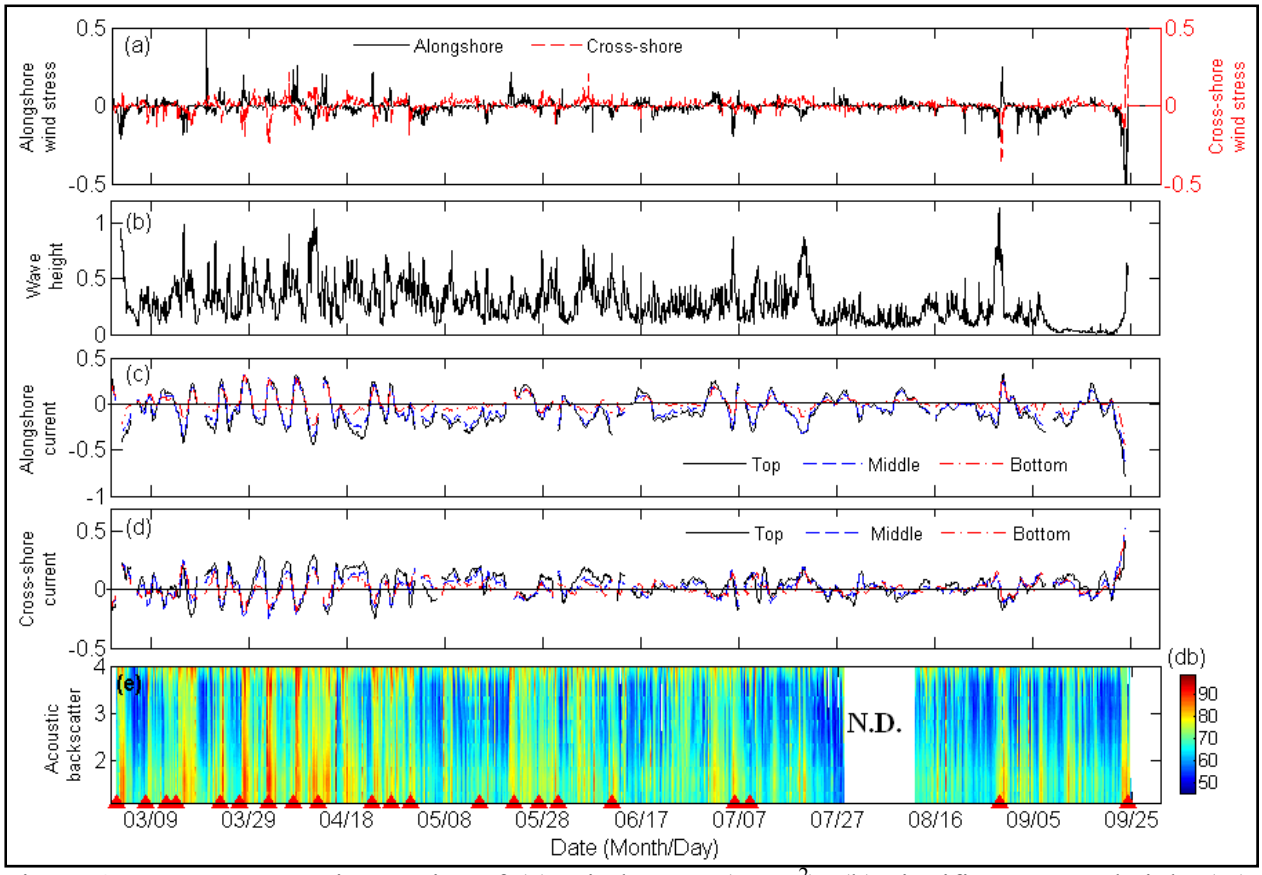


Figure 4.7 Time series of (a) wind stress (N $m^{-2}$), (b) significant wave height (m) and water depth (m), (c) 24 hr moving-averaged alongshore currents (m $s^{-1}$) (top3.75 m, middle: 2.03 m, bottom: 0.63 m), (d) 24 hr moving-averaged cross-shore currents (m $s^{-1}$) (top: 3.75 m, middle: 2.03 m, bottom: 0.63 m), and (e) acoustic backscatter profile (decibel) at WAVCIS CSI-3 between 2005/03/01-2005/09/25. Passage of winter storms and tropical cyclones are shown with shaded triangles in (e). N.D. represents No Data.

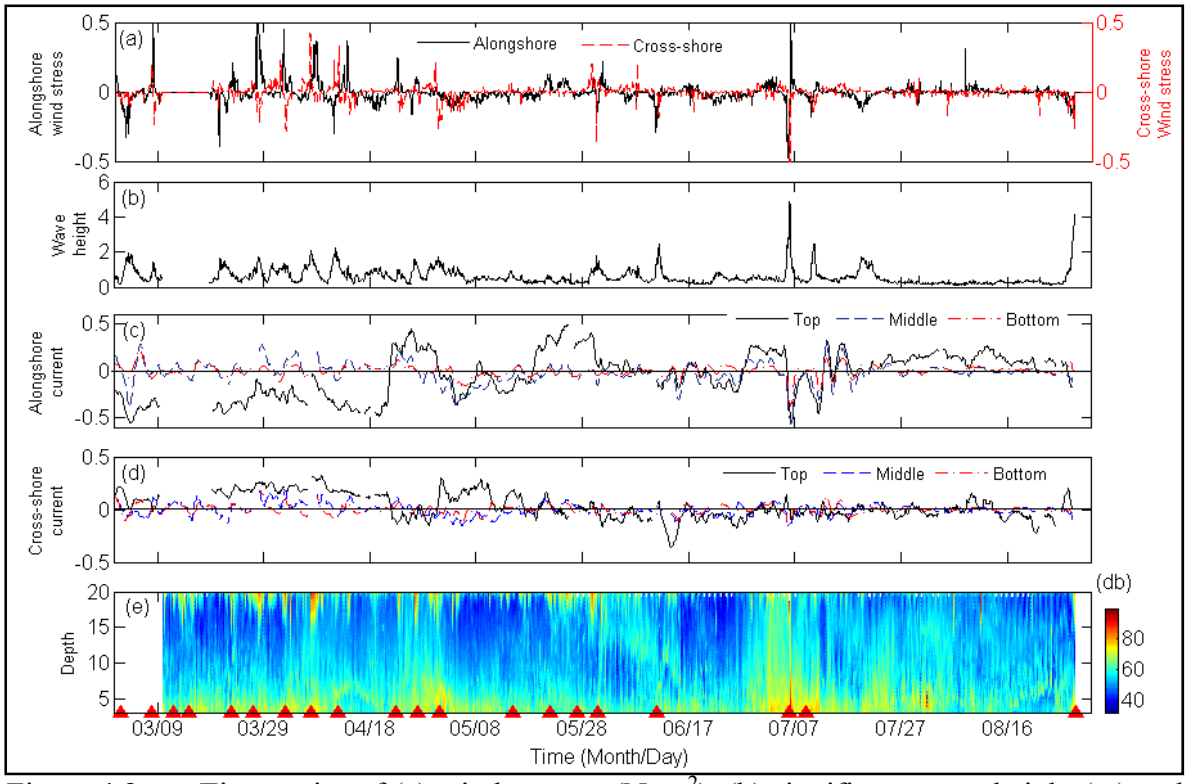


Figure 4.8 Time series of (a) wind stress (N $m^{-2}$), (b) significant wave height (m) and water depth (m), (c) 24 hr moving-averaged alongshore currents (m $s^{-1}$) (top, middle: 10.59 m, bottom: 1.49 m), (d) 24 hr moving-averaged cross-shore currents (m $s^{-1}$) (top, middle: 10.59 m, bottom: 1.49 m), and (e) acoustic backscatter profile (decibel) at WAVCIS CSI-6 between 2005/03/01-2005/08/25. Passage of winter storms and tropical cyclones are shown with shaded triangles in (e).

For CSI-3 located at approximately the 5 m isobath, alongshore and cross-shore currents were oscillated with a period of 3 to 10 days (Figures 4.7c and 4.7d). This oscillation corresponded to variation of wind stress as a result of periodic wind shift due to winter storms (Figures 4.7a and 4.7c). High ABS, thus high SSC, was strongly associated with enhanced wind stress and consequent wave-induced sediment re-suspension. The high SSC was noticed throughout the water column during storms due to sediment suspension and vertical mixing. Significant wave height (hereafter referred to as wave height) at CSI-3 was mostly less than 1 m, which is usually lesser than that of CSI-5 (not in Figure 4.7), in spite of the same isobaths and thus comparable wave energy, but with different bottom sediment configurations (i.e., cohesive bottom). This suggests the significance of wave energy dissipation over muddy bottom as reported by Sheremet and Stone (2003) as well as frictional dissipation over two sand shoals. For CSI-6 located at approximately 20 m isobaths, similar hydrodynamic characteristics can be deciphered. The wave height reached up to 2 m during winter storm period and approximately 5 m during tropical cyclones Cindy and Katrina (Figure 4.8b). There was no wave record during Hurricane Rita at CSI-6 as the station was partially damaged due to high waves and storm surge sustained

from Hurricane Katrina. The ABS, a proxy for the SSC, showed higher values during both winter storms and tropical cyclones. Bottom sediment re-suspension and subsequent mixing events were mostly limited to approximately 10 m above the bottom during winter storms (Figure 4.8e); while, during hurricanes Cindy and Dennis, in early July, the re-suspended sediment clearly reached water surface (around 20 m isobaths) due to strong sediment re-suspension and storm-induced turbulence (vertical velocity over 0.1-0.15 m $s^{-1}$, not in Figure 4.8).

### 4.5.4. Response of the Sediment Dispersal to Two Contrasting Storms

Preliminary satellite image analysis shows the unique response of fluvially-derived sediments to storms (Figure 4.4). The response of the sediment transport to two contrasting storms was examined using in-situ ocean observing data from WAVCIS CSI-14 (Figures 4.9–4.11) as well as from CSI's-3 and 6 (Figures 4.7-4.8). Since hurricanes Cindy, Dennis and Katrina had similar dispersal patterns, only the result during Hurricane Katrina was provided.

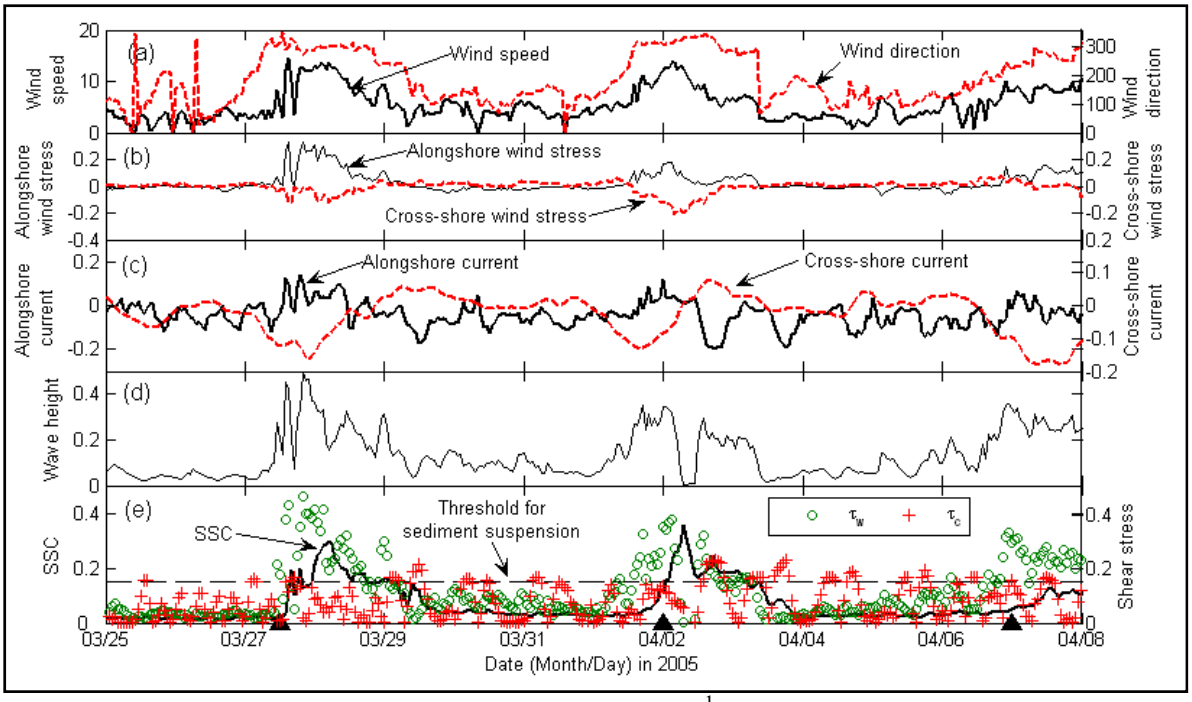


Figure 4.9 Time series of (a) wind speed (m $s^{-1}$) and directions (degree), (b) wind stress (N $m^{-2}$) (alongshore/cross-shore), (c) 24 hr moving-averaged near surface currents (m $s^{-1}$) (alongshore/cross-shore), (d) significant wave height (m), and (e) SSC (kg $m^{-3}$) (left) and shear stress (N $m^{-2}$) (right) at WAVCIS CSI-14 between 2005/03/25 and 2005/04/08.

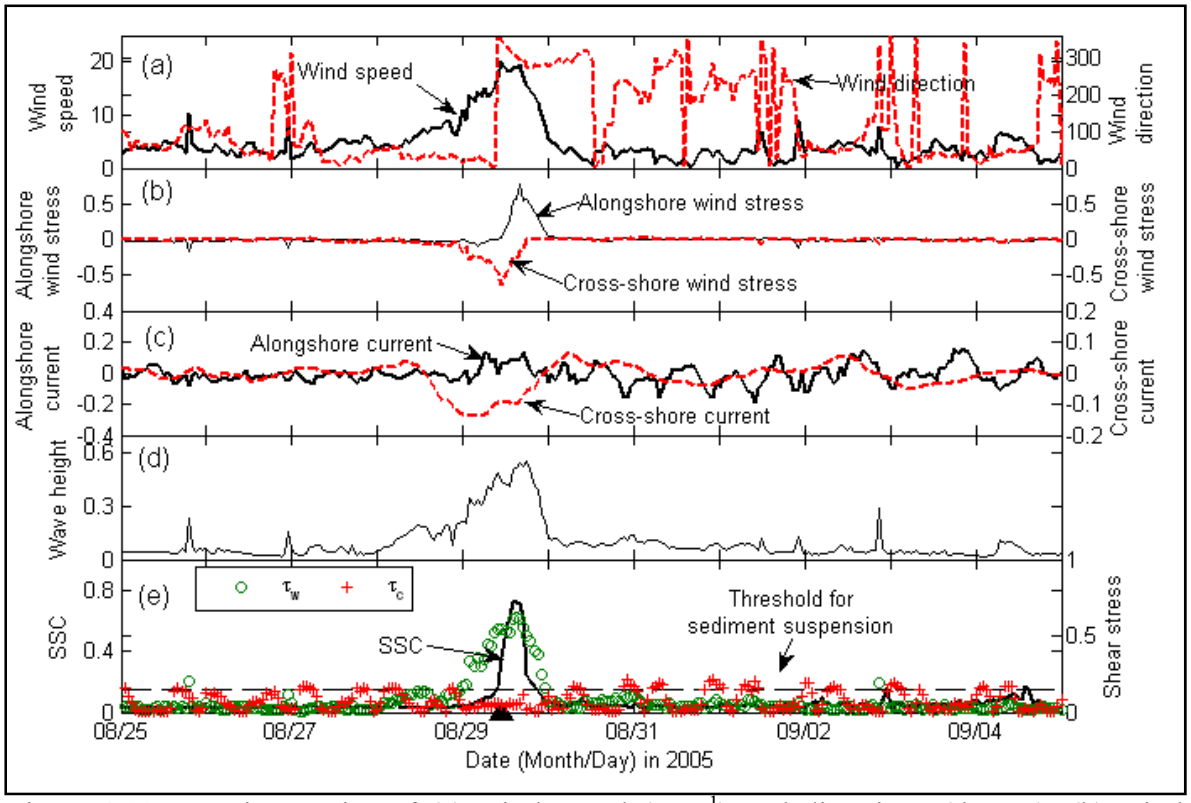


Figure 4.10 Time series of (a) wind speed (m $s^{-1}$) and directions (degree), (b) wind stress (N $m^{-2}$) (alongshore/cross-shore), (c) 24 hr moving-averaged near surface currents (m $s^{-1}$) (alongshore/cross-shore), (d) significant wave height (m), and (e) SSC (kg $m^{-3}$) (left) and shear stress (N $m^{-2}$) (right) at WAVCIS CSI-14 between 2005/08/25 and 2005/09/05.

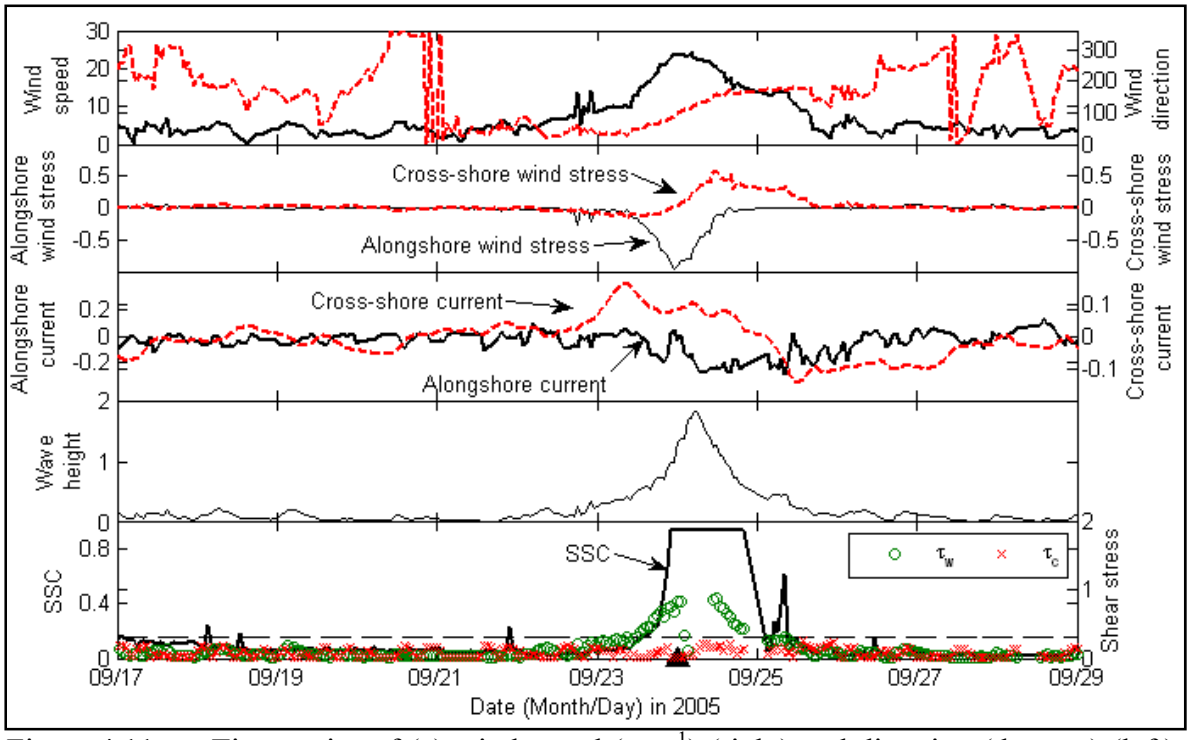


Figure 4.11 Time series of (a) wind speed (m $s^{-1}$) (right) and direction (degrees) (left), (b) wind stress (N $m^{-2}$) (alongshore/cross-shore), (c) 24 hr moving-averaged near surface currents (m $s^{-1}$) (alongshore/cross-shore), (d) significant wave height (m), (e) SSC (kg $m^{-3}$) (left) and shear stress (N $m^{-2}$) (right) at WAVCIS CSI-14 between 2005/09/17 and 2005/09/29.

### *4.5.4.1. Winter Storms*

In Figure 4.9, the time series data at CSI-14 between March 25th and April 8th are shown. During the period, two winter storms crossed the study area: one was on March 27th and the other on April 1st. During each storm, the wind speed exceeded 10 $ms^{-1}$ and the direction of wind strongly shifted from the southeast to north (Figure 4.9c). Wave height reached 0.5 m in March 28th when the bottom shear stress due to waves ($\tau_w$) exceeded the threshold for sediment suspension and was consistent with an increase in the SSC, indicating the sediment re-suspension during the period. Whereas, the shear stress due to currents ($\tau_c$) was not correlated with the SSC during this period which suggests that the waves are a primary factor for sediment re-suspension and the currents contribute to the transport of the suspended sediments. Wind stress was high during post-frontal phases, directing southeastward in consistent with the current direction. As a result, the fine sediments from the river along with re-suspended sediments from the bottom were transported southeastward during this period, as supported by the satellite image in Figure 4.5b and d.

### *4.5.4.2. Tropical Cyclones*

#### 4.5.4.2.1. Hurricane Katrina

Time series data at CSI-14 during Hurricane Katrina are shown in Figure 4.10. Hurricane Katrina made landfall at approximately 200 km east of our study area on August 29$^{th}$, 2005. Wind speed reached 20 ms$^{-1}$ and wave height exceeded 0.5 m at CSI-14, in spite of the fetch-limited wave generation (station was located at the front left quadrant of the hurricane path). Shear stress due to waves reached 0.7 Nm$^{-2}$ during this time, which was more than 4 times higher than the estimated threshold for sediment suspension. While, the stress due to currents was closer to or slightly higher than the threshold, it had no correlation to SSC. The SSC recorded a maximum of 0.7 kgm$^{-3}$ during the landfall and was associated with high wave-induced shear stress, clearly indicating strong sediment re-suspension and mixing during the post-storm phase, given the fact that turbidity sensor was installed at about 1.6 m above the bottom over approximately 3.0 m isobaths. Both alongshore and cross-shore wind stresses during the hurricane landfall were more than 10 times higher than those during fair weather. This high wind stress, whose direction is toward southeast, generates southeast currents and transports the re-suspended and well-mixed sediments toward southeast, validating the dispersal pattern identified from the satellite imagery obtained after the landfall. Hurricanes Cindy and Dennis, both of which made landfall east of the study area, had a similar dispersal pattern to that of Hurricane Katrina.

#### 4.5.4.2.2. Hurricane Rita

In Figure 4.11, we present time series data at CSI-14 during Hurricane Rita, which made landfall at approximately 250 km west of the study area, near the LA-TX border on September, 24$^{th}$, 2005. Data showed that maximal sustained wind speed at CSI-14 reached 24.4 ms$^{-1}$ and wave height attained 1.8 m, approximately 10 times higher than the height during fair weather, due to wave setup by southerly hurricane-force wind. The extremely high waves caused strong sediment re-suspension; the shear stress due to waves reached 0.9 Nm$^{-2}$, 6 times higher than the threshold; while stress due to currents was less than the threshold and had poor correlation to the SSC. The SSC reached 1.0 kgm$^{-3}$, the saturation level and lasted for about a day. During the pre-hurricane landfall, wind direction progressively changed from east, southeast and south as Rita approached the landfall site. Current variation followed the wind pattern. During the approaching phase of the storm, northwesterly currents transported the re-suspended fine sediments towards onshore over most of the Atchafalaya Shelf (Figures 4.5f and 4.11c); while, during the post-landfall phase, southerly return flow was dominated, transporting the sediments back offshore (Figure 4.11).

#### 4.5.4.2.3. Generalized Dispersal Patterns during Cold Fronts and Tropical Cyclones

Analysis of the in-situ data and satellite imagery showed unique hydrodynamics and sediment dispersal patterns for the two contrasting storms, namely, extra-tropical storms (*i.e.*, cold fronts) and tropical cyclones (*i.e.*, tropical storms and hurricanes) that are the two dominant forces to drive sediment transport along the low-energy Louisiana inner shelf (Figure 4.2). Figure 4.12 illustrates typical sediment transport patterns during (i) winter storms (Figures 4.12a and 4.12b),

(ii) tropical cyclones which strike east of the study area (Figures 4.12c and 4.12d), and (iii) tropical cyclones which strike west of the study area (Figures 4.12e and 4.12f), respectively. During fair weather and pre-frontal phases of winter storms, southeasterly wind-induced currents transport the fine sediment westward; while, post-frontal wind shifts current direction from the west to south/southeast and further transport the sediment offshore (Figure 4.12a and b). Sediment sources are likely from both the lower Atchafalaya River and Wax Lake Outlet and also from locally re-suspended sediments in the bay.

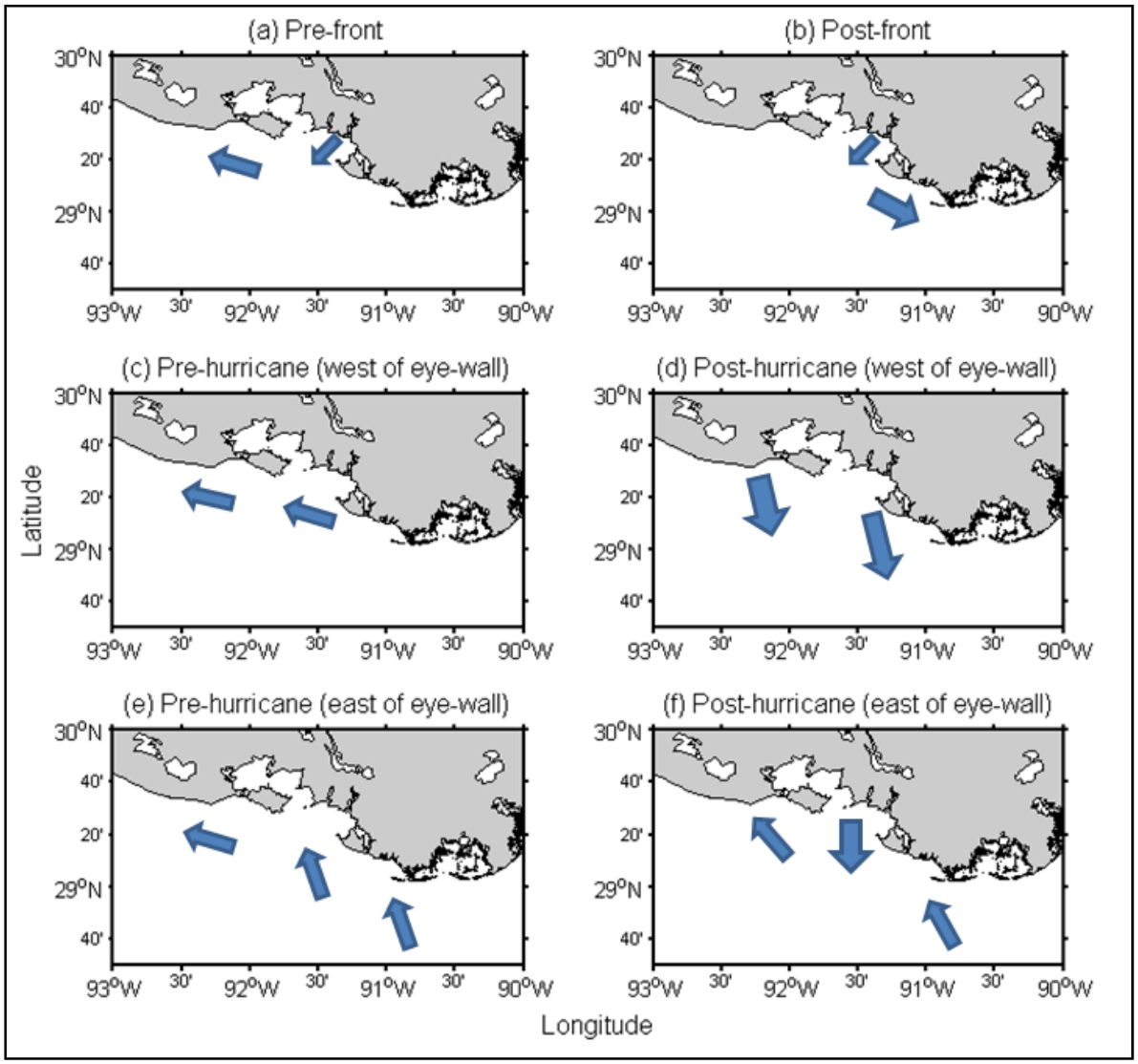


Figure 4.12 General sediment transport patterns for (a&b) winter storms, (c&d) hurricanes made landfall east of the study area, (e&f) hurricanes made landfall west of the study area.

During the period when tropical cyclones approach the coast or make landfall in the vicinity, along the northern Gulf of Mexico, the dispersal and transport patterns depend on the intensity of

the storm and the storm track. For tropical cyclones, which make landfall east of the study area such as Katrina, Cindy and Dennis, strong easterly wind-induced currents transport sediment westward during the pre-hurricane phases and currents due to northerly post-hurricane winds transport sediment south/southeastward (*i.e.*, offshore) (Figure 4.5e and 4.10). This dispersal is likely to accompany strong bottom sediment suspension due to high bottom shear stress and vertical mixing. During the post-hurricane phase, despite relatively lower wind speeds when compared to those east of the right front quadrant of the storm and also fetch-limited onshore waves, sediment re-suspension becomes substantial (Figure 4.10).

During tropical cyclones that make landfall farther west of the study area, such as Hurricane Rita, extremely high waves due to high southerly winds east of the eye-wall strongly re-suspend and mix bottom sediments throughout the entire water column likely over the entire inner shelf, and storm currents subsequently transport the sediments onshore (west/northwest). During the post-landfall phase, the sediments that are already transported to the Atchafalaya Bay/nearshore would be flushed offshore with strong return flow, and are re-distributed onto the Louisiana continental shelf (Figure 4.11).

During spring, when high river discharge coincides with the passage of a cold front across the region, southerly currents during post-frontal phases are capable of transporting fine sediments to the south/southeast. During relatively low river discharge, especially during the summer hurricane season, local re-suspension seems to be the main source of sediment for the dispersal. Thus it is concluded that the sediment dispersal characteristics of the Atchafalaya Bay/Shelf result from either the seasonal existence of high fluvial sediment discharge, local sediment re-suspension or a combination of the two. Kobashi and Stone (2009), based on their preliminary numerical model study, demonstrated that under varying storm winds from northwest along with a moderately high freshwater and sediment discharge from the lower Atchafalaya River and Wax Lake Outlet, sediments originated from the Atchafalaya River and transported over the bay/nearshore can reach up to Ship Shoal, which is located roughly 50 km southeast of the river mouth, in approximately three days during the post-frontal phase.

In spite of low river discharge and generally low wind forcing during summer, the SSC from both lower Atchafalaya River and Wax Lake Outlet as well as at CSI-14 was abnormally high. This high SSC is often measured in summer according to the USGS water data records (Figure 4.4). Strong correlation existed with river discharge during certain years (e.g. 2000, 2003, and 2004); whereas there was no correlation at all in the succeeding year (e.g., 2002, 2005). We have not yet confirmed why the SSC along the river course during summer was so high. Possible reasons may be due to upstream dredging activities, agricultural activities, land clearing etc. Upstream sediment transport from the receiving basin seems not to be realistic since both USGS stations are situated at the significant distance from the mouth of the rivers and also the direction of stream flow was downstream during summer (Walter, D. Personal Communication, 2007). Localized sediment re-suspension along the rivers appears not to occur given the fact that river sediment transport is mainly bed load rather than suspended load during low discharge.

### 4.5.5. Frequencies of Dispersal Shifts and Their Impacts on a Transgressive Shoal

The fluvially-derived sediment transport significantly alters bottom sediment configurations on a Holocene transgressive shoal (Kobashi *et al.* 2007b). As already mentioned, the fine sediment supply from the Atchafalaya River during post-frontal phases and sediment re-distribution during tropical cyclones are likely the major sources of fine sediments onto the shoal since the frequency of winter storms is much higher than those of tropical cyclones. The sediment supply of river-borne sediments mostly occurs during winter and spring. Based on in-situ observing data from WAVCIS CSI-14 and satellite images from the ESL between October 2004 and May 2005, we have investigated how often such dispersal shifts and the shifts which reached Ship Shoal occurred during the period. Figure 4.13 shows a summarized result from the analysis. We define here the dispersal shifts as persistent changes of current direction from west/northwest to south/southeast during post-frontal phases and are sustained for a few days. The number of the shifts which reached Ship Shoal was determined based on satellite images from the ESL. The figure shows that the number of dispersal shifts was maximal in spring with a total of 5 shifts in a month. The average number during the 8 month period was 0.125 times per day (*i.e.*, once every 8 days).

However, not all fluvial sediment associated with dispersal shifts reached the shoal, but the sediment reached the shoal once every 19 days on average compared to once every 6.05 days for the frequency of cold fronts. The number of the shifts had no correlation with monthly mean Atchafalaya river discharge at Simmesport (Figure 4.13, triangle marks); however, it had a strong correlation with monthly mean wind stress (Figure 4.13, square marks). As mentioned in the previous sections, the strong post-frontal winds trigger this dispersal shift; therefore, the correlation between the wind stress and the number of the shifts is reasonable. In spite of relatively cloud-free satellite imagery during post-frontal phases, the analysis was significantly affected by cloud conditions and hence some dispersal shifts were not confirmed from the satellite images although the in-situ data showed the shifts of currents; thus, the result is still qualitative.

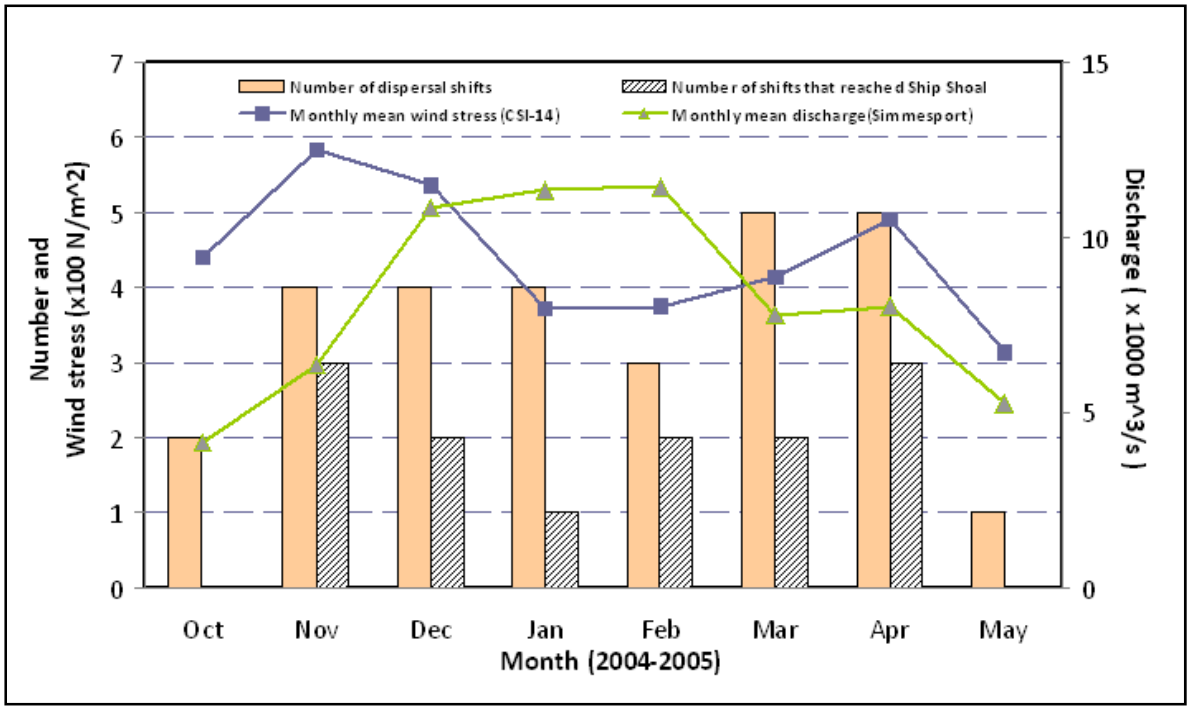


Figure 4.13 Frequencies of dispersal shift and the shifts that reached Ship Shoal between October, 2004 and May, 2005.

Ship Shoal has been found as having diverse benthic habitats and unique sedimentary environment (Stone *et al.* 2006). Distribution of benthic organisms on the shoal is strongly affected by bottom sediment types (Palmer *et al.* 2008) and the species sampled from the entire shoal during biological cruises in spring as well as in summer and fall were generally inhabitable on the bottom in the sandy range and cannot inhabit in and/or on bottoms buried by fluid mud for over a week (Fleeger J., Personal communication, 2007). Possible reasons for this information gap may be because (i) benthic organisms dwelling on unconsolidated fluid mud may have been inadvertently removed due to the sampling technique (Winans, W., Personal Communication, 2007), (ii) sediment distribution may have been patchy so that fine sediment supply may not have significantly affected the benthic communities or, (iii) sediment reworking associated with winter storms was more frequent than fine sediment supply and therefore, fine sediment (*i.e.*, fluid mud) seems to remain temporarily on the bottom and benthic organisms may have been capable of adapting to such intermittent lithological change. In summer and fall when the dispersal shifts are infrequent, shoal bottom sediments seems to be exposed to sand and shells, particularly on the shallower middle and western flank of the shoal unless fine sediments are not flushed out during storms, and/or fine sediments are supplied, for instance, during tropical cyclones. The relationship between benthic habitats and fluvial and bottom boundary layer processes is currently being studied.

# CHAPTER 5
# SPECTRAL WAVE TRANSFORMATION OVER SHIP SHOAL

## 5.1. INTRODUCTION

The Louisiana coast has undergone severe erosion over several decades (Williams *et al.* 1997) and a viable solution put forward to mitigate this problem is to build-up the rapidly disintegrating barrier islands using sand pumped from transgressive shallow shoals located off the coast. One such source, Ship Shoal, is located on the 10 m isobaths in south-central Louisiana adjacent to a rapidly eroding barrier island complex, Isles Dernieres (Figure 5.1). The wave transformation characteristics that can be attributed to this elongated shallow shoal are not fully understood and require further quantification. Stone *et al.* (2004b) reported that the shoal modifies the wave climate of the region, especially during storm weather conditions and that the removal of the shoal would significantly increase wave energy along the leeward flank of the deposits. Not much has been studied on the wave spectral evolution in the region due to the presence of the shoal, especially during high energy events associated with winter and spring extra tropical storms linked to the passage of cold fronts.

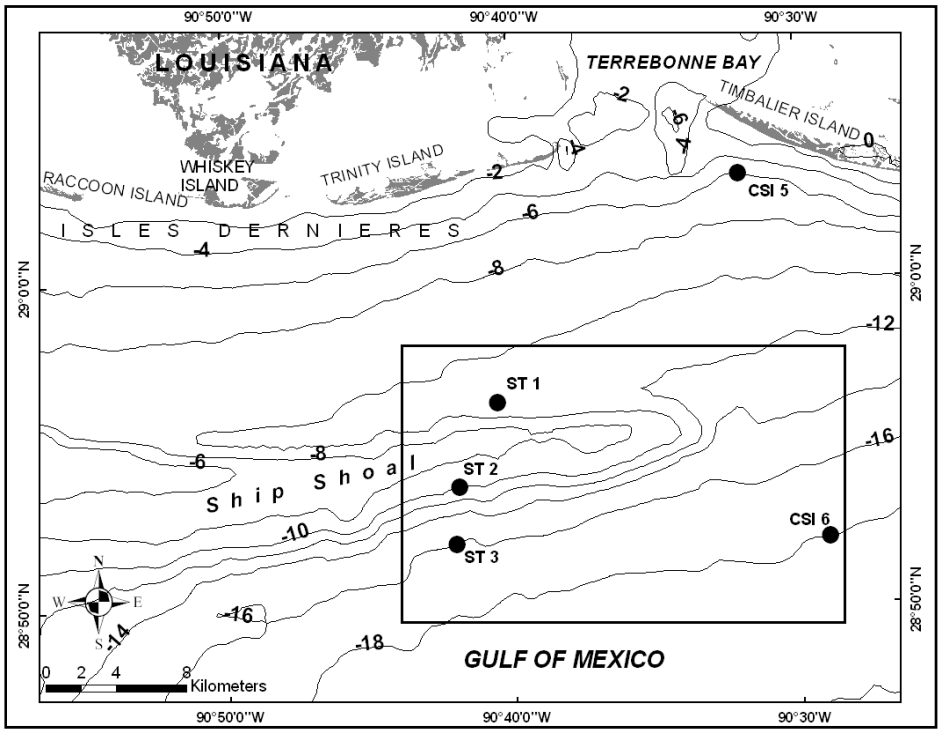


Figure 5.1 Study area. ● showing *in situ* observation stations at Ship Shoal and inshore WAVCIS stations.

As the waves undergo transformation in shallow water, wave energy spectra evolve due to refraction and nonlinear energy transfers to higher and lower frequencies (Elgar *et al.* 1990) and

also energy dissipation caused by wave breaking and bottom friction (Thornton and Guza 1983; Sheremet and Stone 2003). The rapid shift in the wind and wave direction, especially when a cold front passes over the region, significantly influences the wave-wave interaction and hence the wave spectral evolution. The present study is focused on modeling the spectral wave transformation over the eastern half of Ship Shoal during a spring cold front event. Maa *et al.* (2004) also used similar modeling methods to study the impact of sand mining on the wave climate offshore of the Maryland and Delaware coasts.

## 5.2. NUMERICAL MODEL

In order to resolve the characteristic scales of the physical processes in the coastal waters, a fine mesh is required. A high resolution computational grid is also needed to resolve the complex bottom topographies in shallow water environments, such as barrier islands, shallow shoals and submerged bars (Sorensen *et al.* 2004). The need for high resolution local models can be achieved using nesting techniques, where a local model with a fine mesh is embedded in a coarse mesh model.

MIKE 21 Spectral Wave (SW) model is used for the present study, which has also has nesting capabilities. This model was developed by the DHI Water and Environment® and was implemented successfully for modeling coastal wave characteristics in the North Sea (Sorensen *et al.* 2004). Also, the model was applied successfully in San Francisco Bay, USA, to study changes in wave climate associated with a runway expansion project (Kerper, DR., Personal Communication). The model is based on unstructured meshes and it simulates the growth, decay and transformation of wind generated waves and swells in offshore and coastal areas. The discretization in geographical and spectral space is performed using a cell-centered finite volume method. In the geographical domain, an unstructured mesh is used. The integration in time is based on a fractional step approach (Sorensen *et al.* 2004).

The model domain spreads over the eastern section of Ship Shoal and having an area of 26.25 x 13 $km^2$, see the rectangular box inside Figure 5.1. The generated flexible mesh grid (Figure 5.2) had a spatial resolution of ~480 m. A still finer mesh was embedded in this coastal domain to further resolve the wave conditions across a transect of the shoal. This transect was selected based on *in situ* observations from the shoal during spring 2005. The grid resolution for the finer inner mesh was ~220 m. The coastal model was nested with an operational regional wave model for the Gulf of Mexico (Jose and Stone 2006). For this larger domain, along the northern Gulf coast, the grid resolution was ~2 km while for the rest of the boundary a coarser grid of ~30 km was used. The bathymetry data used for generating the computational grid were extracted from the database provided by the National Geophysical Data Centre (NGDC), National Oceanic and Atmospheric Administration (NOAA). Fine scale bathymetry data (6 arc-second resolution) were used for the northern Gulf of Mexico coast and coarse bathymetry for the remainder of the basin. The bathymetry data were referenced to Mean Lower Low Water (MLLW).

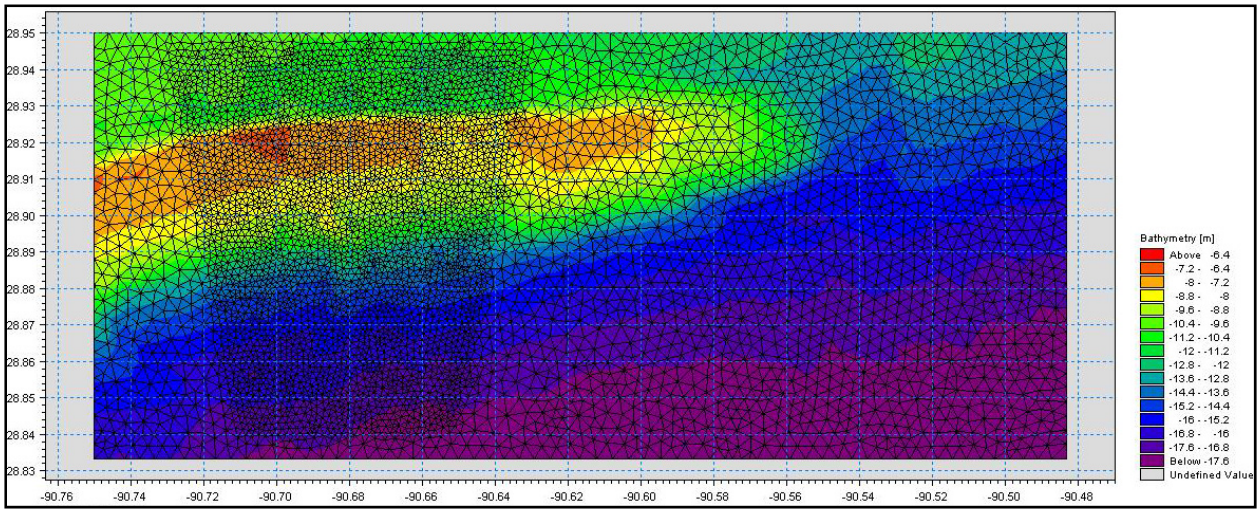

Figure 5.2 Flexible mesh grid generated for the model domain

## 5.3. COLD FRONTS ALONG THE NORTHERN GULF COAST

Hsu (1988) and Roberts *et al.* (1989) provided detailed explanations for the mechanism of cold front generation, sustenance and dissipation in the northern Gulf of Mexico. Once a cold front passes over the northern Gulf coast, wind direction changes from the southern quadrant to the north, wind speed increases and air temperature drops (Kobashi *et al.* 2005). As discussed in Stone (2000), the northern Gulf of Mexico experiences frequent cold front events between October and May and they have played a critical role in the coastal hydrodynamics of the northern Gulf of Mexico coast.

A cold front generated storm event during 5$^{th}$ - 10$^{th}$ April, 2005, was selected for the wave transformation studies. During this period the maximum sustained wind speed and significant wave height measured at a coastal station, CSI 6 (see Figure 5.1), maintained by the WAVCIS program at Louisiana State University (Stone *et al.* 2003b), was 14.2 m/s and 2.1 m respectively. Re-analyzed wind data, input for the wave model, in a grid format, were extracted from the National Center for Environmental prediction (NCEP), NOAA, database. The North American Regional Re-analyzed (NARR) model grid has a horizontal resolution of 32 km and covers the entire continental United States and the Gulf of Mexico region. The u and v components of the wind vector, 10 m above mean sea level (MSL), for the Gulf of Mexico region were extracted from the regional grid using Matlab® routines developed by the authors. For a comparison of the accuracy of the re-analyzed data, the time series data of measured and re-analyzed wind speed and wind direction at the CSI 6 station are presented in Figure 5.3.

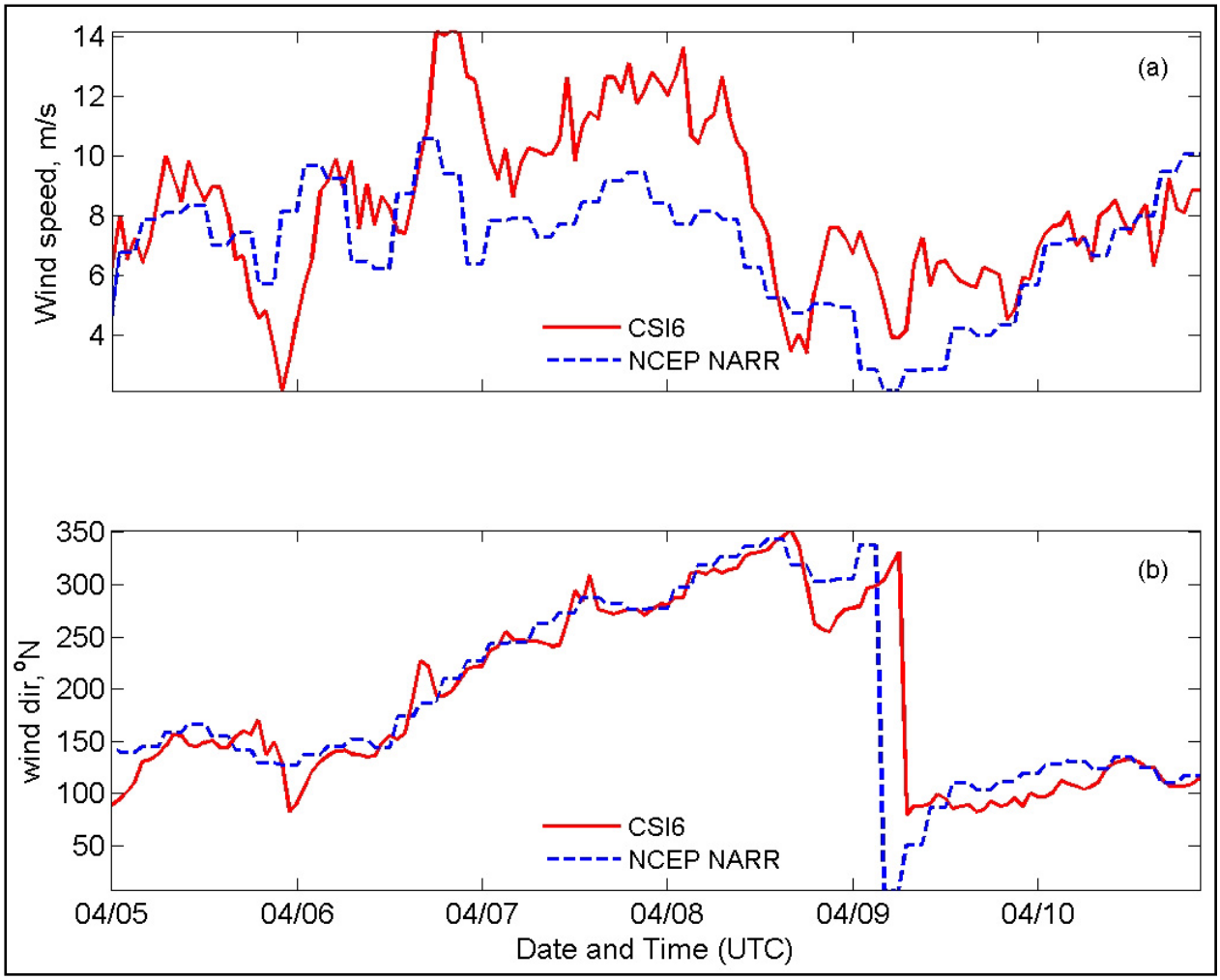


Figure 5.3 (a) wind speed and (b) wind direction at the CSI 6 station. NCEP NARR re-analyzed wind data (broken blue curve) plotted against the measured data.

Tidal elevation data for Wine Island, Timbalier Bay, along the south central Louisiana coast, were extracted from the NOAA tide prediction tables. The tidal data were also referenced with respect to MLLW. The maximum tidal range observed during the study period was 0.48 m, on 5$^{th}$ April, 2005. The tidal elevation data were interpolated into an equal interval time series format using a module provided with the MIKE ZERO software and were included in the coastal wave model to define the water surface elevation (Figure 5.4). Median grain size ($D_{50}$) distribution data for the Ship Shoal region were collected from the United States Geological Survey (USGS) database, usSEABED, and were used for computing the bottom friction parameter.

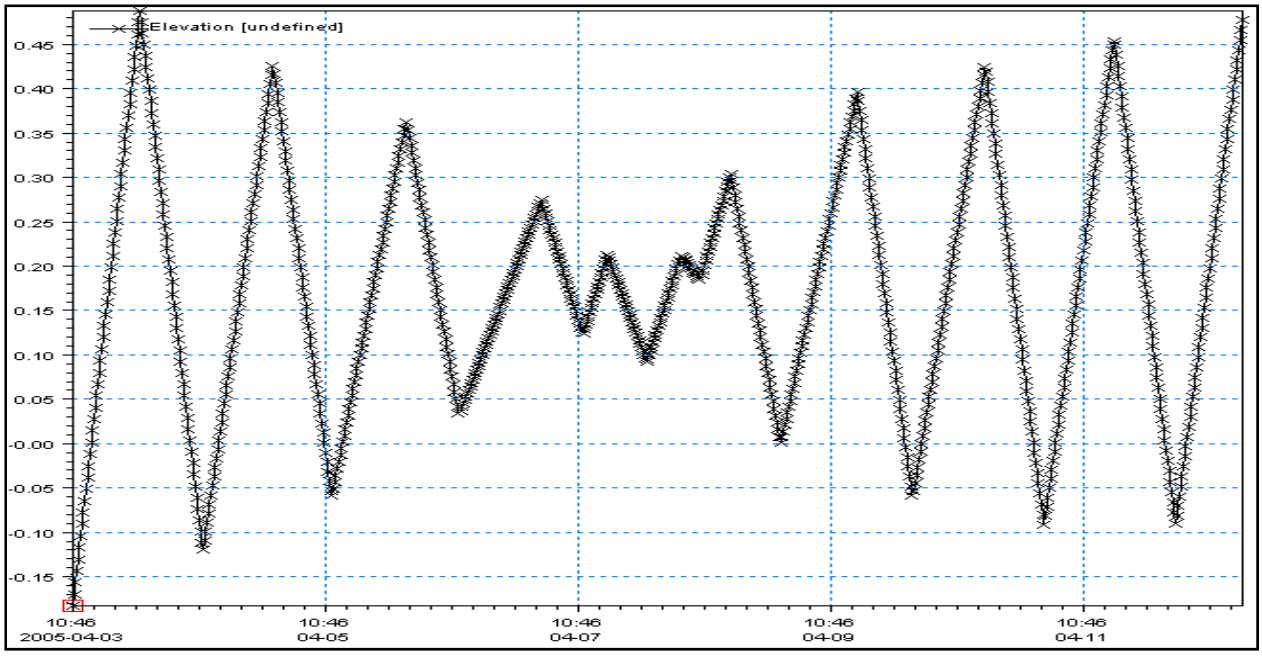


Figure 5.4 Tidal elevation data for Wine Island and Timbalier Bay during the study period (Elevation in meters).

## 5.4. FIELD DATA

This study was conducted in association with a field survey program along eastern Ship Shoal during spring 2005. Three stations were set up across a transect of the shoal (Figure 5.1) and tripods fitted with instruments for measuring wave, current and turbidity were deployed for a period of 34 days in April-May, 2005. Data from an Acoustic Doppler Velocimeter (ADV), deployed at the northern Station ST1, was used for model skill assessment. Also, time series data collected from the CSI 6 station (Figure 5.1) were used for model validation.

## 5.5. SIMULATIONS AND SKILL ASSESSMENT

A fully spectral in-stationary approach was used for the computation of the wave parameters. For the frequency, a logarithmic frequency discretization with 25 frequencies was used. The lowest discrete frequency was $f_{min}$ = 0.04 Hz and the ratio between successive frequencies was chosen as 1.1. The number of discrete directions was chosen as 16. The time step interval chosen for the simulation was 75 s. The white capping parameters were included in the model ($C_{dis}$= 2 and $Delta_{dis}$ = 0.8). For the wave breaking parameter, a constant value of $\gamma$ = 0.8 was used. The model computed the wave parameters using the forecast wind input. Synoptic maps of significant save height (Hs) (Figures 5.5 & 5.6), peak wave period, mean wave direction etc. for the study site were generated. For the purpose of skill assessment of the model, time series outputs of bulk wave parameters were also generated for the 3 stations across the shoal, where the wave and current observations were conducted. Stations ST1, ST2 and ST3 were at depths of 11.6 m, 12.8

m and 16.2 m respectively (Figure 5.1). Time series wave outputs were also generated for the CSI 6 station, located at the eastern end of the domain.

The storm-generated wave fields were simulated by the model. A snap shot of the wave fields during an approaching phase of the cold front is given in Figure 5.5. At the beginning of the simulation the waves were from the south in line with the prevailing wind direction and the maximum wave height computed was 1.5 m. The higher waves were concentrated along the southwestern corner of the domain where the depth-induced shoaling enhanced the wave heights. As the cold front crossed the study area the wind direction rotated and hence the wave fields also switched to the north and north-west (Figure 5.6). The maximum wave height observed during this phase of the storm was 0.6 m. The complex wave energy attenuation along the crest of the shoal during this wave rotation period can also be deciphered from Figure 5.6.

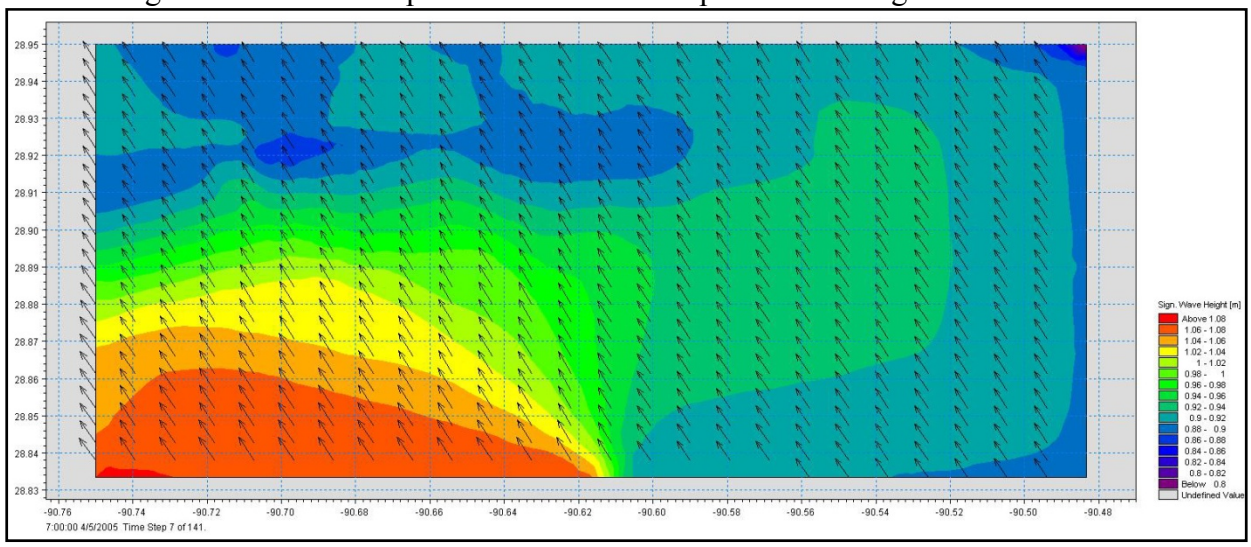


Figure 5.5 Simulated wave fields corresponding to the approaching phase of the cold front.

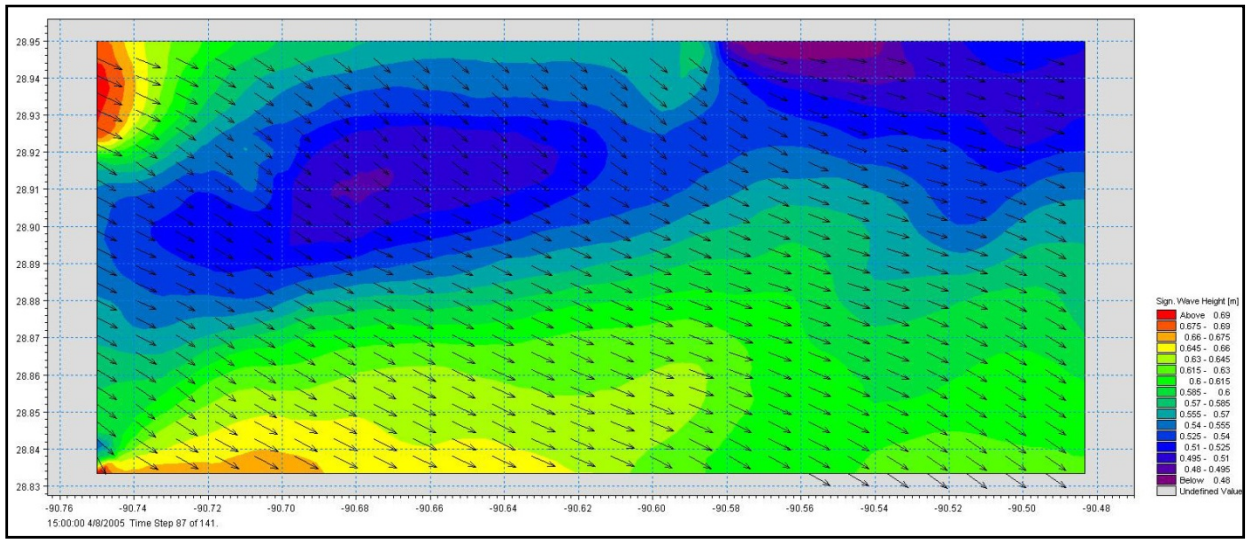


Figure 5.6 Simulated wave fields when the cold front crossed the study area.

The simulated significant wave height, peak wave period and mean wave directions for the three stations are plotted along with measured wave parameters from northern station, ST1 (Figure 5.7). Measured wave data were smoothed using a 5 hour moving average filter. The simulated significant wave height are in good agreement with the measured data except during the peak storm period, prior to the reversal of the wind and wave direction (Figure 5.7a). Time series of peak wave period also shows good correlation with the measured data (Figure 5.7b). Mean wave direction shows good agreement with the measured data except during the reversal of the wave directions (Figure 5.7c), when the simulated wave direction remained northerly for a prolonged period of time.

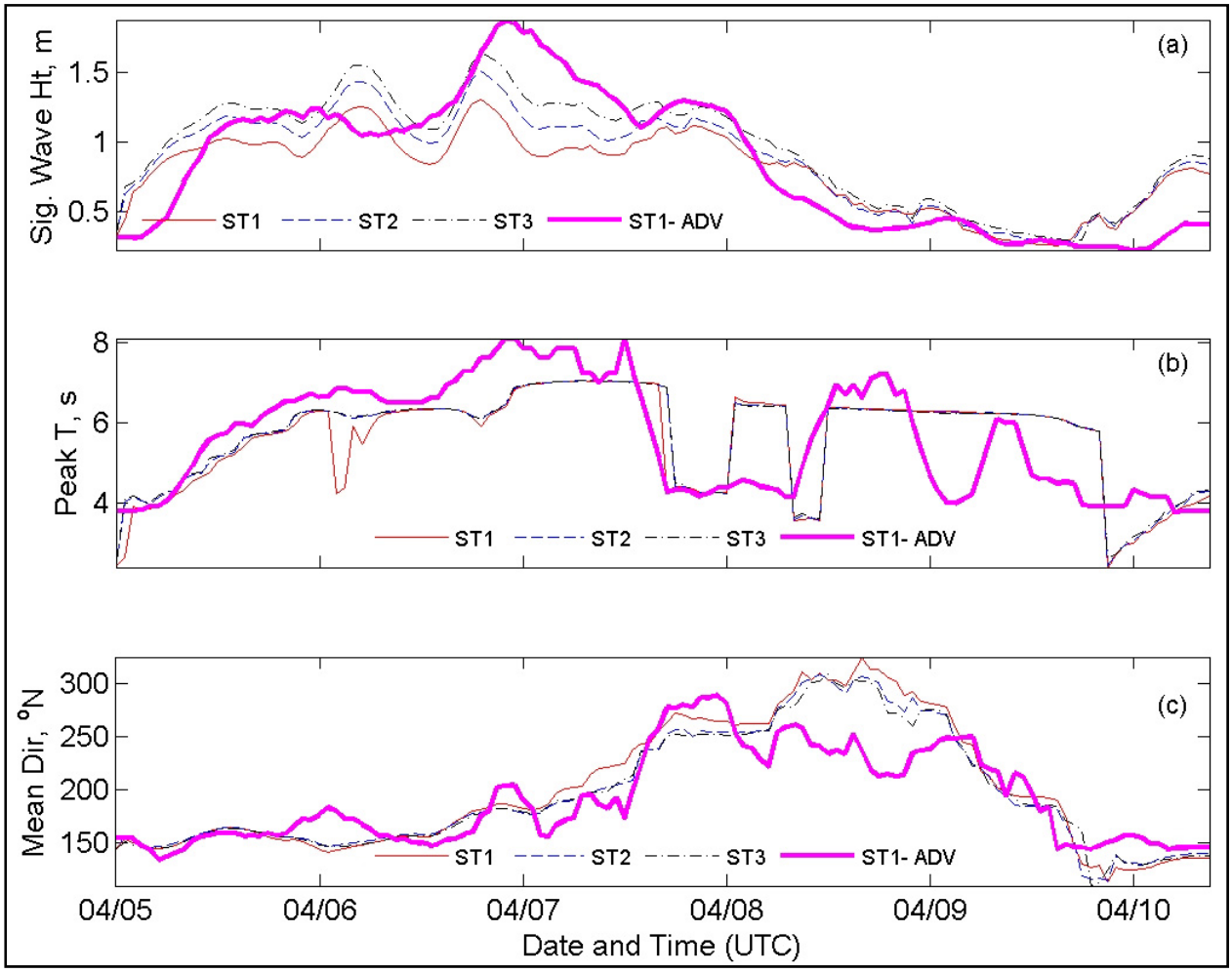


Figure 5.7 Time series of (a) significant wave height, (b) peak wave period and (c) mean wave direction, simulated for the three reference stations. The thick purple line corresponds to the measured data from station ST1.

Model outputs are also compared against the measured data from station CSI 6 (Figure 5.8). Simulated significant wave height values are in good agreement with the measured data (Figure

5.8a) except during the peak storm activity when the model under predicts the wave height. The plot of Peak wave period distribution (Figure 5.8b) shows a very strong correlation between measured and model output.

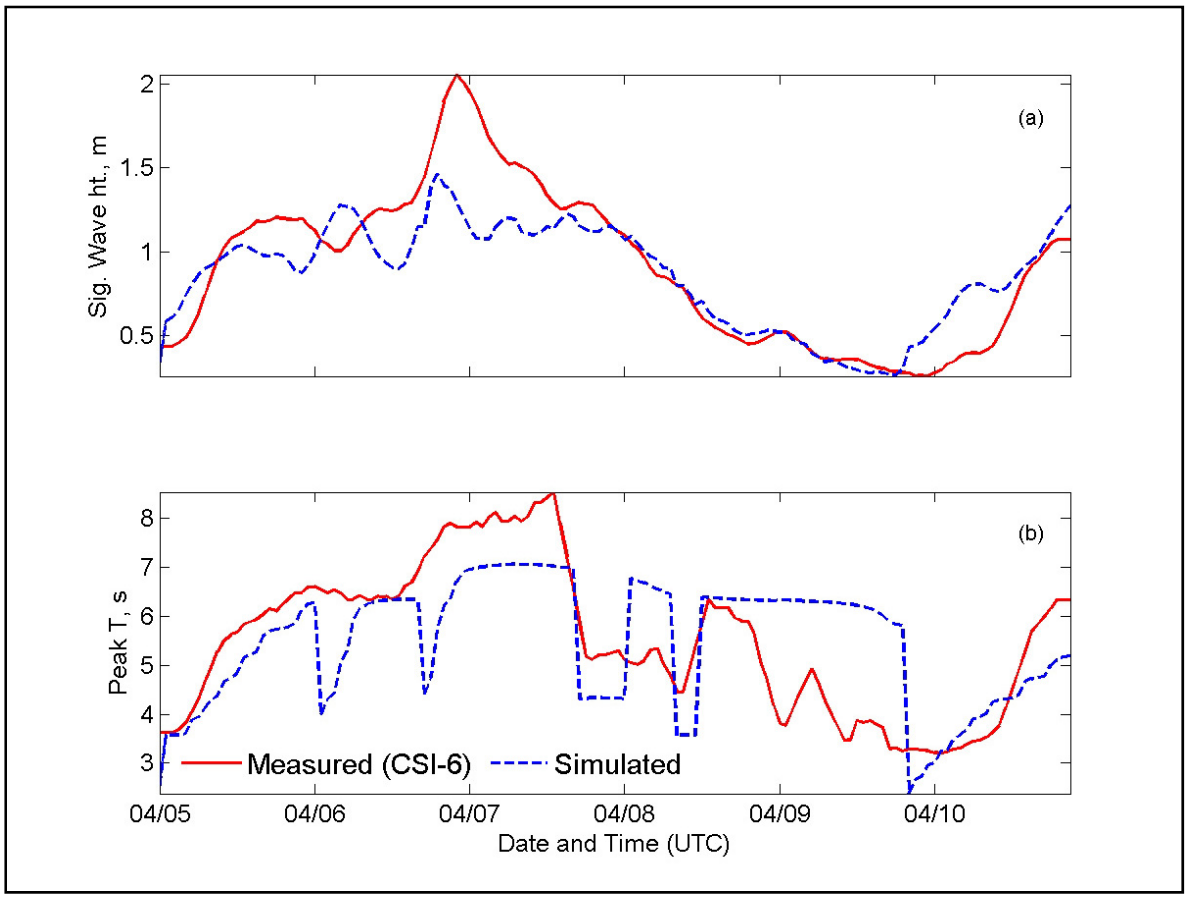


Figure 5.8 Time series of (a) significant wave height and (b) peak wave period at CSI 6.

The discrepancy in the model outputs with that of the measured data can be attributed to the resolution and accuracy of the input wind data. It is clear that wave models are extremely sensitive to wind inputs. For a fully developed sea, sensitivity experiments revealed that small errors in the input wind can result in considerable differences in the computation of wave parameters (Sarkar *et al.* 2000). It can be observed in Figure 5.3a that the NARR model wind data generally under predicts the measured data from station CSI 6. However, for the offshore locations, the model winds are generally in good agreement with the measured data. Jose and Stone (2006) reported very strong correlation between the NARR model wind data and measured data from the National Data Buoy Centre (NDBC) buoys off the Louisiana coast.

## 5.6. WAVE HEIGHT AND SPECTRAL TRANSFORMATION OVER THE SHOAL

The Percentage of attenuation of significant wave height and peak wave period associated with waves crossing the shoal were computed between the three stations (Figure 5.9). As expected, the maximum wave height attenuation occurred between the offshore station and the nearshore station (ST1-ST3). The highest percentage of attenuation calculated was 22.12 for the southerly waves and 27.68 for the northerly waves (Table 5.1). Between stations ST2 and ST3 the corresponding values are 15.67 and 24.13. Between ST1 and ST2 the percentage attenuation values are 15.85 and 13.87 respectively. It is also observed that between stations ST2 and ST3 there is no significant transformation for the peak wave period (Figure 5.9b) while for the ST1-ST2 and the ST1- ST3 stations, the peak wave period also undergoes transformation throughout the study period.

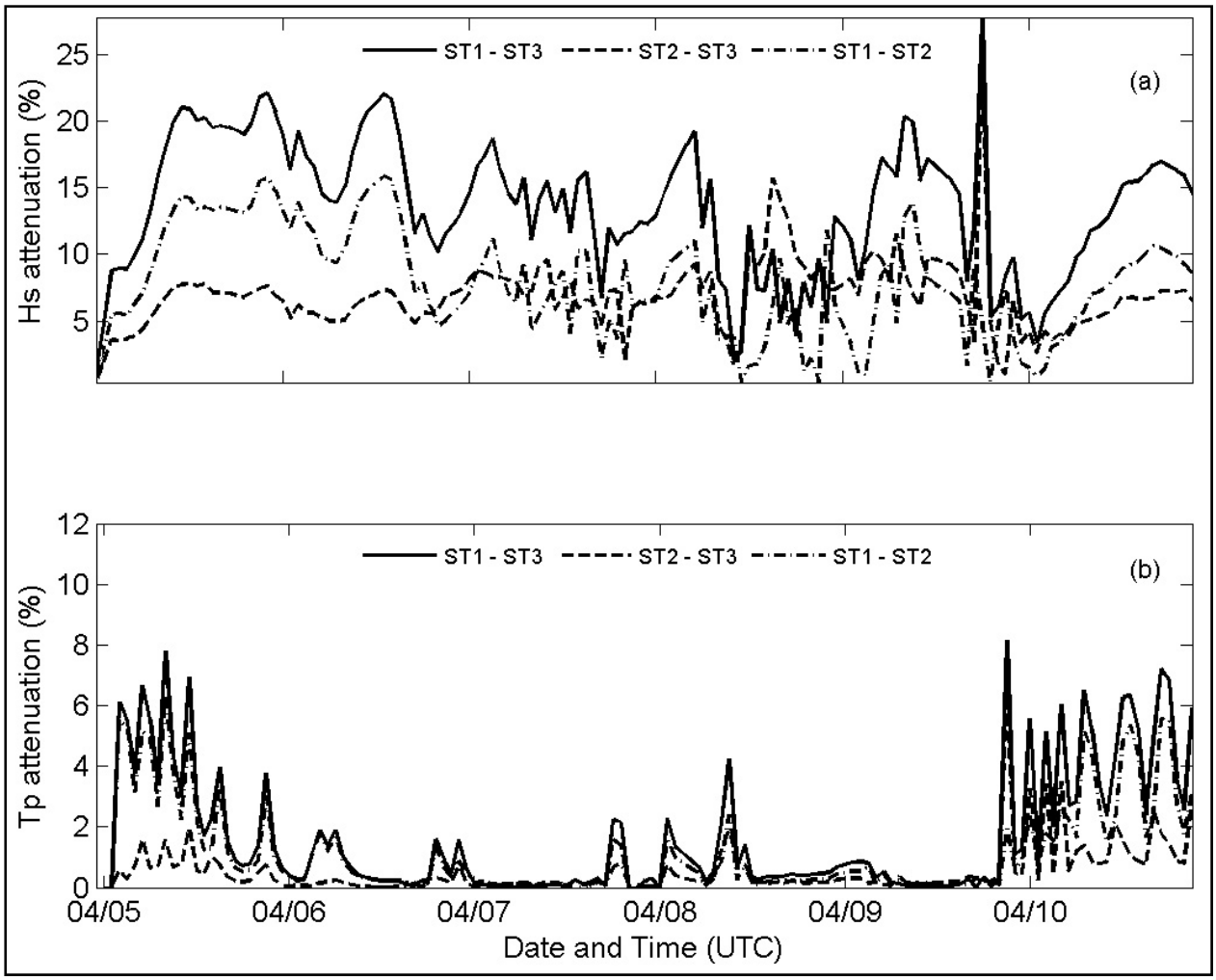


Figure 5.9 Percentage of attenuation of (a) significant wave height and (b) peak wave period, across the three stations.

Table 5.1

Percentage of attenuation of significant wave height across the shoal.

| Station Pair | Distance (km) | Percentage of attenuation | |
|---|---|---|---|
| | | Southerly waves | Northerly waves |
| ST3 – ST1 | 8.37 | 22.12 | 27.68 |
| ST3 – ST2 | 3.22 | 15.67 | 24.13 |
| ST2 – ST1 | 5.29 | 15.85 | 13.87 |

The evolution of wave energy spectra during a cold front generated storm is given in Figure 5.10. Before the cold front passes over the study area,waves are from the south south-easterly direction and the directional spectrum shows an almost similar energy distribution pattern for all three stations (Figures 5.10, a, c and e). Once the cold front passes over the region, a complete rotation of the wave spectra occurs during which waves migrate from south-southeast to north northwest. It is observed that the energy spreads across a wide range of frequencies and direction, following the rapidly shifting wind conditions during this transition phase. For the inshore station (Figure 5.10b) the peak wave energy is centered in the northerly direction and the spectra spread from 45º to 225º. For the middle station, ST2, the wave spectrum is distinctly bimodal (Figure 5.10d) with dominant directions centered at 247.5º and 320º. For the offshore station, ST3, the dominant direction is rotated further to the south (Figure 5.10f) and centered at 225º. This shift in dominant direction of the energy spectra during the passage of the cold front is attributed to the veering of wind direction from southwest to north as well as to the refraction of the waves over the elongated shoal. More field observations across the shoal are required to further explain this wave transformation process.

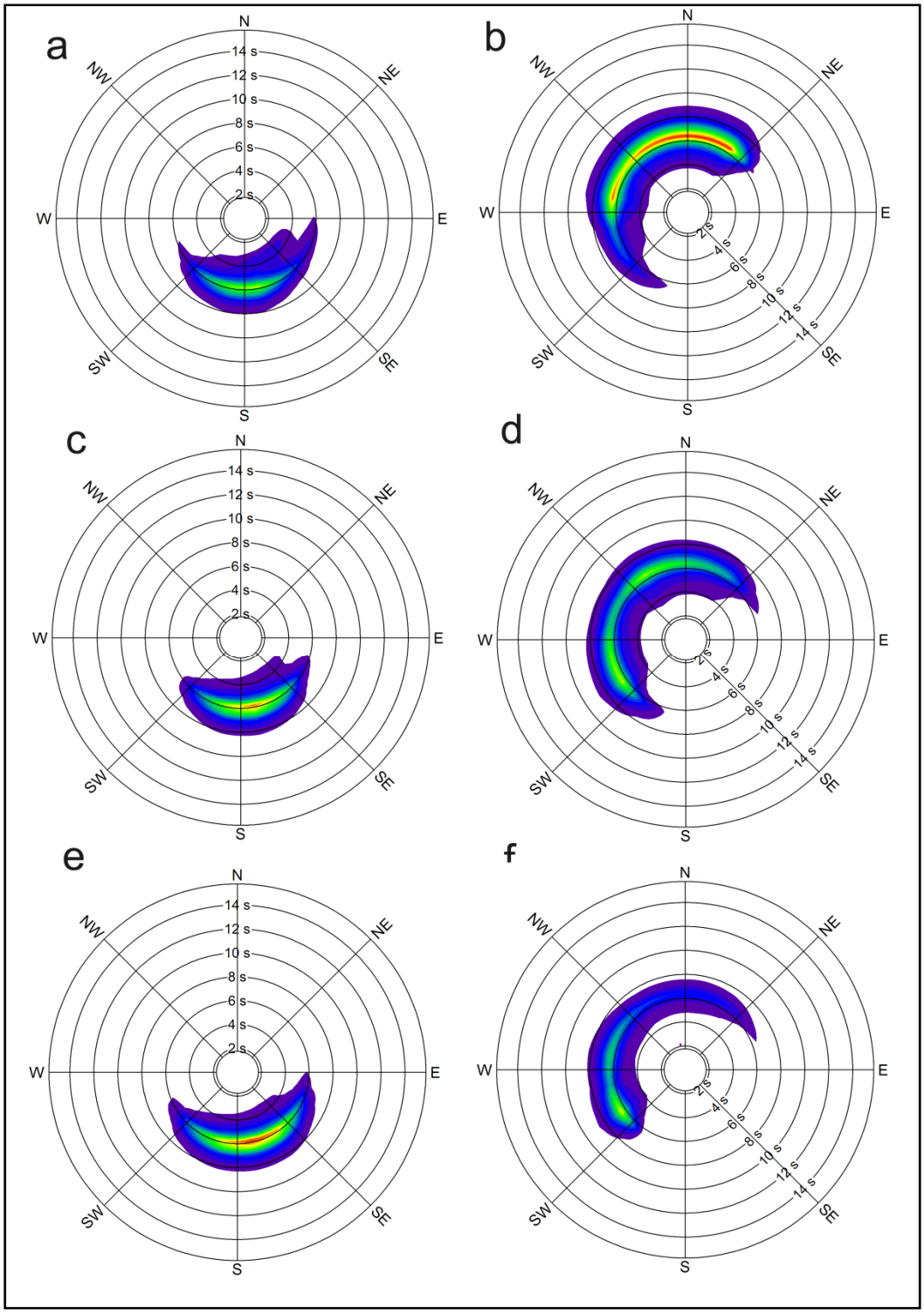


Figure 5.10 Evolution of spectral wave energy at three stations (a and b) station ST1, (c and d) station ST2 and (e and f) station ST3

# CHAPTER 6
# TWO CONTRASTING MORPHODYNAMICS OVER RECURRING SANDY AND MUDDY BOTTOMS OF A SHORE-PARALLEL HOLOCENE TRANSGRESSIVE SHOAL, SOUTH-CENTRAL LOUISIANA, USA

## 6.1. INTRODUCTION

Bottom boundary layer dynamics (BBLDs) over the Louisiana shelf are characterized by low-energy regime; waves and current fields are known to be not strong enough to disturb bottom sediments and cause transport (Adams *et al.* 1987; Wright *et al.* 1997b). However, two energetic weather events, namely tropical and quasi-periodic extra-tropical storms (*i.e.*, winter storms that accompany cold fronts), significantly affect bottom boundary layer (BBL) and sediment transport over this low-energy shelf (Pepper and Stone 2004; Allison *et al.* 2005; Kobashi *et al.* 2005; Sheremet *et al.* 2005; Stone *et al.* 2005b; Kobashi *et al.* 2007b). Several field studies have been conducted in order to understand the BBLDs on various parts of the U.S. continental shelves. Particular attention was paid to investigating the BBLDs during storms during which the BBLDs are reported to be significant across the coasts (Cacchione and Drake 1982, 1990; Green *et al.* 1995; Li *et al.* 1997; Wright *et al.* 1997a; Pepper and Stone 2004; Kobashi *et al.* 2005). Adams *et al.* (1987) studied bottom currents and associated sediment transport over the Louisiana inner shelf near the Southwest Pass in Louisiana in 60 m of water where bottom sediment was predominantly fine-grained silt and clay. Their study revealed that sediment re-suspension was less important on evaluating sediment transport processes. Wright *et al.* (1997b) studied bottom boundary layer characteristics and sediment transport by deploying a tripod off the Louisiana coast along 15.5 and 20.5 m isobaths during summer non-storm conditions in 1992 and 1993. The study concluded that bottom currents were typically weak during fair weather and bed shear stress during fair weather was too weak to re-suspend bottom sediments.

Stone (2000) conducted a detailed BBL study in 1998 and 2000 by deploying various arrays of the BBL instruments on the western flank of Ship Shoal which is also known as a potential offshore sand resource. A strong response of bottom boundary layer processes (BBLPs) for sandy bottoms to winter storms were quantified. In addition, the study qualitatively documented unique flow modulations associated with complex shoal bathymetry. Despite such studies, it was recently revealed that the fluvial sediments from the Atchafalaya located approximately 50 km northwest from the shoal, has a decisive impact on the shoal morphodynamics which has not previously been recognized (Kobashi *et al.* 2007b). Walker and Hammack (2000) investigated the Atchafalaya River sediment plume structure using satellite imagery and limited in-situ data and showed a strong response of the plume to varying wind fields. Kobashi *et al.* (2009a) and Kobashi and Stone (2009) further investigated mechanisms of Atchafalaya sediment plume shifts with respect to rapidly varying wind, particularly during post-frontal phases, based on numerical simulations and prolonged in-situ observational data from stations near Atchafalaya Bay and in deeper water off the Louisiana coast. Both studies led to the conclusion that strong post-frontal northwesterly wind stress generates strong offshore currents, which in turn transport fluvial sediments to the southeast in concert with the sediment re-suspension associated with storm

waves. The results were further corroborated using satellite imagery analysis. In the early Spring of 2006, instrument arrays including a pulse-coherent acoustic Doppler profiler (PCADP) and acoustic Doppler velocimeters (ADV) were deployed at the eastern flank of Ship Shoal in depths ranging from 12-13 m (Figure 6.1); the study unveiled complex interactions of winter storms and fluvial fine sediments from the Atchafalaya River with shoal morphodynamics for the first time (Kobashi *et al.* 2007a, b; Kobashi *et al.* 2008). In order to bolster our findings, further deployments were conducted in winter 2008 along a transect across the middle of the shoal in depths ranging from 7-8 m (Figure 6.1).

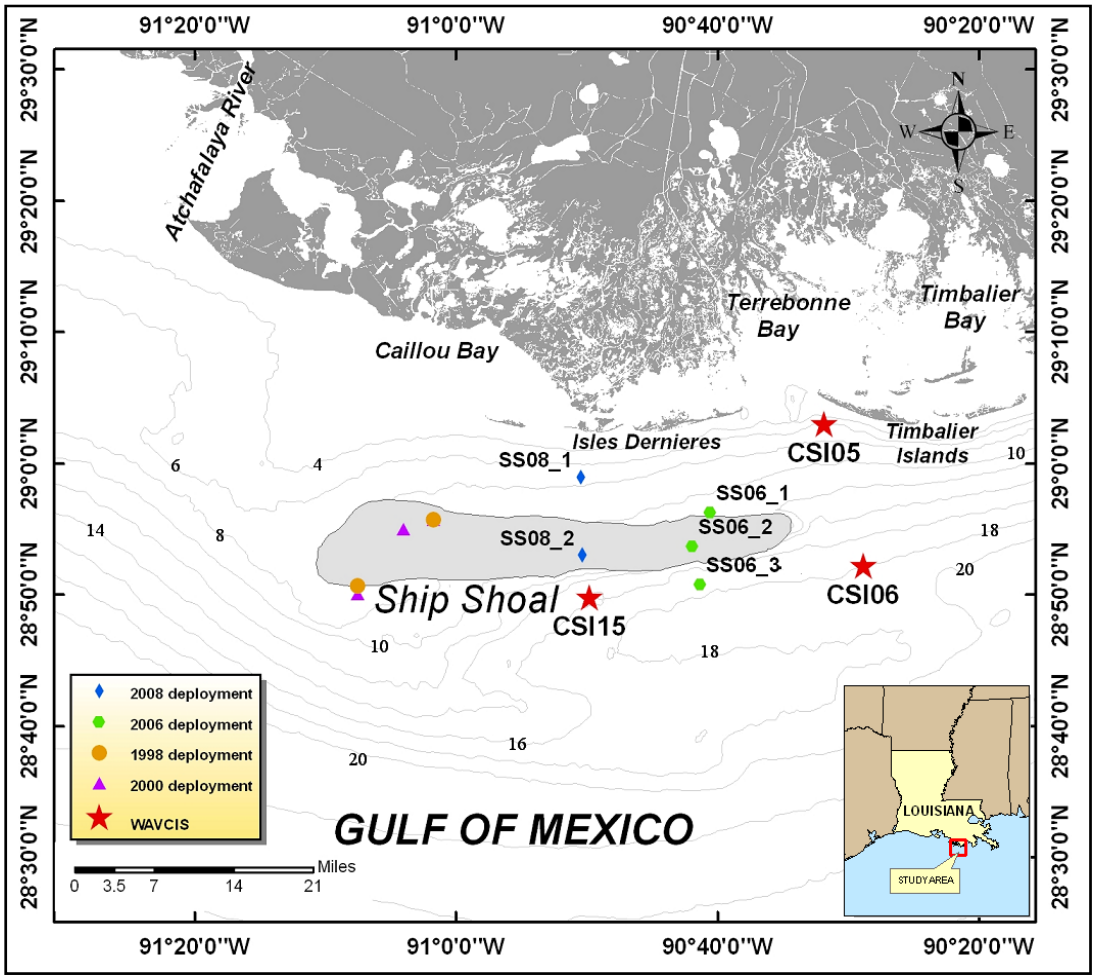

Figure 6.1 Map of study area.

These transect data represented sand-dominated morphodynamics and were in contrast with the 2006 deployments, which represented a low-energy fine sediment environment. Our collaborative study revealed that the shoal may play an important role in commercial fisheries as well as in the life cycle of benthic organisms, for instance, by providing blue crabs with a hatching and foraging ground (Condrey and Gelpi 2008) and also for benthic micro-algae to provide oxygen and food sources (Grippo *et al.* 2009). The benthic habitat distribution strongly correlates with types of sediments and physical parameters such as waves, currents as well as

temperature, salinity, and dissolved oxygen at the bottom (Michel *et al.* 2001; Palmer *et al.* 2008). It has been hypothesized that the morphodynamic features of the shoal has a critical role on the bio-physical interaction of the shoal and consequently on the shoal ecosystem. Such extensive research efforts have little been reported in the scientific literature.

In this paper, an attempt has been made to compare and contrast morphodynamics of two contrasting shoal bottom settings, namely, fluid mud and fine sand, and further to discuss such unique dynamics over the shoal. Implications associated with the morphodynamics for potential impacts on future sand dredging is also briefly discussed.

## 6.2. PHYSICAL SETTING

The Louisiana shelf is characterized as very low gradient, a recipient of substantial quantities of fluvial sediments from both the Mississippi and Atchafalaya rivers, and also a low-energy micro-tidal environment: these are characteristics ideal for the accumulation of fluvial fine sediments onto the continental shelf. In such a low-energy shelf environment, stratification prevails, particularly during summer, when bottom water often demonstrates hypoxic conditions (Rabalais *et al.* 2002). In winter, the recurring passage of extra-tropical storms can break stratification and water density tends to be homogeneous throughout the water column (DiMego *et al.* 1976; Wiseman *et al.* 1986; Rabalais *et al.* 1994; Kobashi *et al.* 2007b). In winter, quasi-periodic passage of winter storms accompanies cold fronts along with sudden veering of the wind from southern to northern quadrants as well as sharp drops in air temperature and barometric pressure (Kobashi *et al.* 2005, see also Figure 4.2).

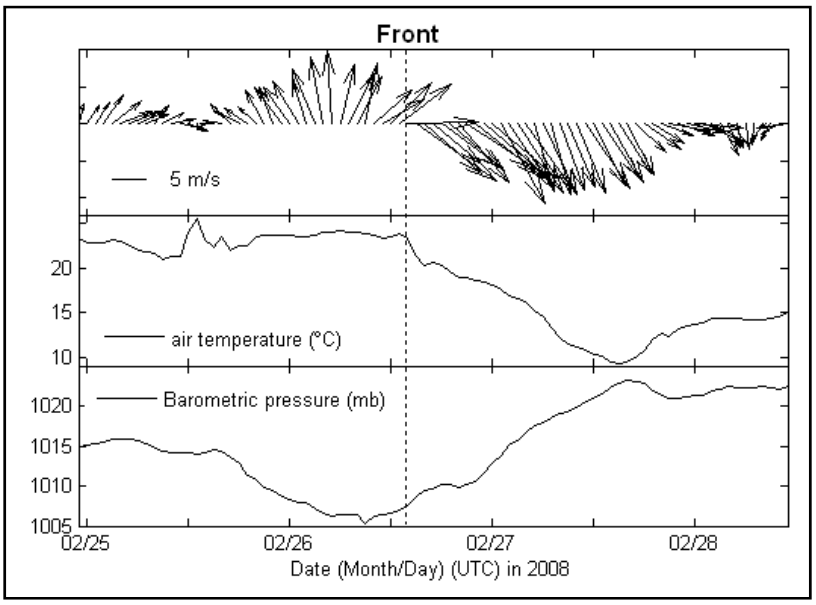


Figure 6.2 Variation of meteorological parameters during a winter storm.

During summer, the coast is exposed to tropical storms. Keim *et al.* (2007) estimated that the return period of tropical storms and hurricanes in southern Louisiana was 3 years. During fair weather conditions, prevailing southeast wind and consequent waves and currents transport materials (sediments and other passive materials) westward (alongshore) (Cochrane and Kelly 1986; Murray 1997; Cipriani and Stone 2001); while, during the post-frontal phase, cross-shore currents generated by persistent cross-shore winds are often dominant (Chuang and Wiseman 1983; Pepper 2000; Kobashi *et al.* 2007a).

The cyclic nature of the Mississippi River delta formation have formed large offshore sand bodies, drowned paleo-barrier islands off Louisiana, on the end phase of the delta cycle (Penland *et al.* 1986; Penland *et al.* 1988; Roberts 1997). Ship Shoal, a shore-parallel elongated sand shoal, located approximately 20 km off the Isles Dernieres, 50 km long and 15 km wide and surrounded by the 10 m isobath, is known as a remnant of the abandoned Maringouin delta that was active approximately 7500 years BP (Penland *et al.* 1986). Bathymetry data show that the western part of the shoal is significantly shallower than the eastern part (Figure 6.1). Historical survey data suggest that Ship Shoal is migrating landward at a rate of 10 to 15 m $yr^{-1}$ under present sea level conditions. This migratory trend of the shoal can be attributed to recurring storm impacts and predominant wave action from the southeast (Kulp *et al.* 2001). In addition, literature and recent bathymetric data suggest that Ship Shoal has been "deepening", given the fact that the shoal has been re-worked extensively during intense storms. Also, the entire Louisiana coast is subsiding in response to the rapid rise in relative sea level (Roberts 1997; Kulp *et al.* 2001).

## 6.3. DATA ACQUISITION

Field measurements were carried out off south-central Louisiana during 2006 and 2008. Various BBL arrays were deployed in spring 2006 on the eastern flank of the shoal (SS06_1 – SS06_3 in Figure 6.1) over a period of 45 days and in winter 2008 on the middle of the shoal (SS08_1 and SS08_2 in Figure 6.1) over a period of 52 days. Three different arrays of oceanographic instruments were deployed on offshore, crest and onshore of the shoal (Figure 6.1). Two ADV tripods and a PCADP system were used for the surveys. In 2006, two ADV systems deployed on the onshore and offshore of the shoal consisted of a pressure sensor and a downward-looking acoustic Doppler velocimeter. For one of the ADV systems deployed on the inshore station, two optical backscatter sensors (OBSs) were also equipped. The PCADP system deployed on the crest in 2006 comprised of a downward-looking pulse-coherent acoustic Doppler profiler, two optical backscatter sensors and a pressure sensor. In 2008, one ADV system with two OBSs was deployed north of Ship Shoal (SS08_1, see location in Figure 6.1) and one ADV system without OBSs and the PCADP system on the crest (SS08_2). The PCADP system deployed in 2008 consisted of a downward looking PCADP, two OBS sensors, two CTD sensors and upward-looking ADCP (Figure 6.3). The above instrument arrays have been widely used to investigate BBL characteristics all over the world (Cacchoine *et al.* 2006). All instruments recorded *in-situ* data discontinuously (*i.e.*, burst mode) to maximize survey duration. Every hour, the instruments

recorded 2048 bursts with sampling frequencies of 2 Hz for the PCADP system, 4 Hz for the ADV system with the OBSs and 10 Hz for the ADV system without the OBSs. Detailed instrument configurations are listed in Table 6.1. Bottom sediments and bottom water samples were collected during all deployment and retrieval cruises. In addition, more sediment samples, plexiglass cores, and underwater camera images (SPI) were taken during collaborative benthic survey cruises.

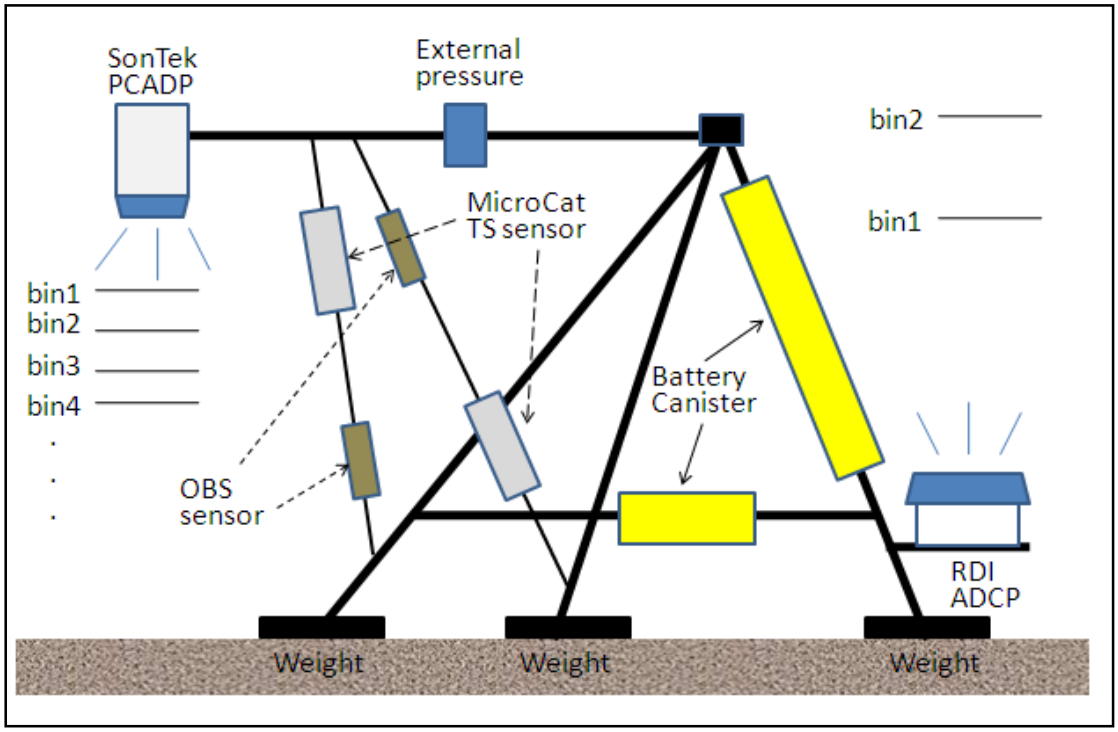


Figure 6.3 Schematic illustration of the PCADP system for 2008 deployment. Sensor heights of all instruments are listed in Table 6.1.

Table 6.1

Instrument configuration

| Year | System | Instruments | Locations | Survey period | Sensor height |
|---|---|---|---|---|---|
| **2006** | **ADV (SS06_1)** | Druck™ Pressure Sensor<br>D&A™ Optical Backscatter<br>SonTek™ Acoustic Doppler Velocimeter | 28º 56.284'N<br>90º 40.523'W | 04/06 00:00 - 05/20 09:00<br>"<br>" | 90 cm<br>19, 78 cm<br>48 cm |
| | **PCADP (SS06_2)** | SonTek™ Pulse-Coherent Doppler Profiler<br>D&A™ Optical Backscatter<br>Druck™ Pressure Sensor | 28º 53.701'N<br>90º 41.893'W | 04/06 00:00 – 05/23 02:01<br>"<br>" | 116 cm<br>30, 61 cm<br>116 cm |
| | **ADV (SS06_3)** | ParoScientific™ Pressure Sensor<br>SonTek™ Acoustic Doppler Velocimeter | 28º 50.808'N<br>90º 41.307'W | 04/06 00:00 -05/25 18:00<br>" | 68 cm<br>47 cm |
| **2008** | **ADV (SS08_1)** | Druck™ Pressure Sensor<br>D&A™ Optical Backscatter<br>SonTek™ Acoustic Doppler Velocimeter | 28 º 58.950' N<br>90 º50.406' W | 02/10 00:00 - 03/23 13:30<br>"<br>" | 78 cm<br>41, 78 cm<br>47 cm |
| | **PCADP (SS08_2)** | SonTek™ Pulse-Coherent Doppler Profiler<br>D&A™ Optical Backscatter<br>Druck™ Pressure Sensor<br>RDI™ ADCP Workhorse 1200 kHz<br>MicroCat™ TS sensors | 90 º 50.298' W,<br>28 º 53.018' N | 02/10 00:00 -03/09 04:00<br>"<br>"<br>02/10 00:00 -04/03 14:20<br>" | 120 cm<br>35, 74 cm<br>120 cm<br>45 cm<br>30, 63 cm |
| | **ADV (SS08_2)** | ParoScientific™ Pressure Sensor<br>SonTek™ Acoustic Doppler Velocimeter | 28 º 53.023' N,<br>90 º50.302' W | 02/10 00:00 03/30 11:30<br>" | 66 cm<br>45 cm |

## 6.4. DATA ANALYSIS

Prior to data analyses of in-situ measurements, all data were inspected regarding QA/QC. For the ADV and PCADP systems, the following criteria were used: (1) mean near bottom current velocity higher than 1.0 m/s were removed since such values are not realistic for the low-energy Louisiana coast even during severe winter storms; (2) all data with less than a 70% correlation (30% for mean currents) were removed; (3) data less than 15 decibel (db) signal-noise ratio (SNR) were removed. Criteria (2) and (3) are recommended by an instrument manufacturer (SonTek Inc. 1997a, 2004). In addition to the automatic screening, all data were visually inspected and apparent outliers were removed.

Bulk wave parameters, spectra of waves and currents, and the BBLPs were computed from field data. Wave parameters and directional waves were computed based on the PUV method (Gordon and Lohrmann 2001). Current signals less than a 40 hour period were filtered out by using the 10th order butterworth filter in order to examine sub-tidal (*i.e.*, wind-induced) currents. The OBSs were calibrated to estimate suspended sediment concentration (SSC) using sampled bottom sediments and water following the procedure by Sheremet *et al.* (Sheremet *et al.* 2005). Acoustic backscatter amplitude (ABS), a by-product of acoustic current meters, is known to be related to the SSC (SonTek Inc. 1997b) and the SSC profile was estimated from the ADV and PCADP ABS by comparing the ABS to the calibrated SSC results (Kobashi *et al.* 2007a). This method contains inevitable noises since the backscatter is corresponding not only to the SSC but also to sediment composition, grain size etc. (Gartner 2002); however, this method has been widely used to estimate the SSC despite such disadvantages because of a cost-effective method and less influence on bio-fouling than the OBS (Gartner 2002; Kobashi *et al.* 2007b). Sediment grain size was analyzed by granulometric analysis and sedigraph (Stone *et al.* 2006).

The BBLPs were calculated based on various algorithms. For the 2006 deployment in which the bottom sediment was predominantly silt and clay, the BBLP, namely shear velocity (u*) and shear stress ($\tau$), due to (1) waves, (2) currents, and (3) combined wave-currents were computed based on (1) linear wave theory (Madsen 1976, equation 4-1), (2) the von-Karman Plandlt equation (equations 4-2&4-3) and quadratic stress law (Sternberg 1972, equation 4-4), and (3) an empirical formulae proposed by Whitehouse *et al.* (2000) (equation 4-5), respectively. For the von-Karman equation, the following criteria were applied: (1) linear regression coefficient (r2) for currents against depth (in log scale) needs to be higher than 0.98 (Wright *et al.* 1997b); (2) maximal differences in current direction between velocity profiles need to be less than 20 degrees (Drake and Cacchione 1992). For stratified water, the BBLP from the von-Karman equation is overestimated and needs to be corrected using a stability parameter (Grant and Madsen 1986; Glenn and Grant 1987). However, because of a lack of available data, in this study, equation (4-2) was used to estimate the BBLPs. Under highly turbid water, it is reported that the bottom drag coefficient reduces significantly, which may cause shear stress to be overestimated (e.g., Li and Gust 2000; Whitehouse *et al.* 2000; Thompson *et al.* 2006). In this study, the drag coefficient at 100 cm above the seabed ($CD_{100}$) for a muddy bottom (*i.e.*, smooth bed) was selected as 0.0022 following Soulsby (1997) and Kobashi *et al.* (Kobashi *et al.* 2009a).

$$\tau_w = \rho_f u_{ob}\left(\nu\frac{2\pi}{T}\right)^{1/2}, u_* = \sqrt{\frac{\tau_W}{\rho}} \quad (6\text{-}1)$$

$$u(z) = \frac{u_*}{\kappa}\ln\left(\frac{z}{z_0}\right) \quad (6\text{-}2)$$

$$\tau_{cl} = \rho_f {u_*}^2 \quad (6\text{-}3)$$

$$\tau_{cq} = \rho_f C_{D100} {u_{100}}^2 \quad (6\text{-}4)$$

$$\tau_{wc\_m} = \tau_c\left[1 + 9.0\left(\frac{\tau_w}{\tau_w + \tau_c}\right)^{9.0}\right] \quad (6\text{-}5)$$

For the 2008 deployment in which the sediment was predominantly sand, the following methods were used: (1) linear wave theory for wave shear stress (equation 6-1), (2) log-linear method (equations 6-2 & 6-3) and quadratic stress law (equation 6-4) for current shear stress, (3) Reynolds stress method (Green 1992; Pepper 2000) and an empirical formulae proposed by Soulsby (1997) (equation 6-6) for combined wave-current. The bottom drag coefficient at 100 cm above the seabed (CD100) for ripple sand was selected as 0.0061 (Soulsby 1997).

$$\tau_{wc\_s} = \tau_c\left[1 + 1.2\left(\frac{\tau_w}{\tau_w + \tau_c}\right)^{3.2}\right] \quad (4\text{-}6)$$

Critical shear stress, above which bottom sediments are expected to be suspended, for non-cohesive sediments was calculated from grain size data based on the modified Yalin parameter (Li *et al.* 1997; Pepper 2000) and was estimated as 0.153 Pa (Pascal) (=$Nm^{-2}$) for the 2008 deployment. Maximum critical shear stress for cohesive sediments in this paper was determined as 0.15 Pa with reference to Wright *et al.* (1997b) and Kerper, D. (personal communication, 2006); this value was used in Kobashi *et al.* (2007b), Kobashi *et al.* (2008) and Kobashi *et al.* (2009a) and shows reasonable results as Kobashi *et al.* (2009a) suggest.

## 6.5. RESULTS

### 6.5.1. Atchafalaya River Hydrology

The Mississippi River system is currently discharging freshwater and fluvial sediments mainly through two rivers, the Mississippi and Atchafalaya Rivers. The main stream, Mississippi River discharges 70 percent of total freshwater and another 30 percent from a distributary, the Atchafalaya River (Mossa 1996; Roberts 1997). Twelve-year records of river discharge at Simmesport, upstream on the Atchafalaya River as illustrated in Figure 6.4, showed high discharge in spring and low discharge during summer. There were two peaks of discharge: one in

January and the other in April. High discharge in April was associated with ice melting in both the Rocky and Appalachian mountains with maximal discharge that exceeded 600,000 cubic feet per second (cfs) (=16,990 $m^3$ $s^{-1}$), which was more than three times higher than the threshold of high river discharge, 200,000 cfs (=5,663.4 $m^3s^{-1}$) reported by Walker and Hammack (2000). While in the summer dry season, discharge was characterized as low.

In 2006, high river discharge occurred in late March and mid May (Figure 6.4). In winter 2008, river discharge was higher than the threshold between February and July with maximal discharge of 626,000 cfs (=17,726.3 $m^3$ $s^{-1}$) in mid April (Figure 6.4). Such high river discharge likely gives rise to debouching large quantity of fluvial sediments down to the receiving basin in spring (Kobashi *et al.* 2009a).

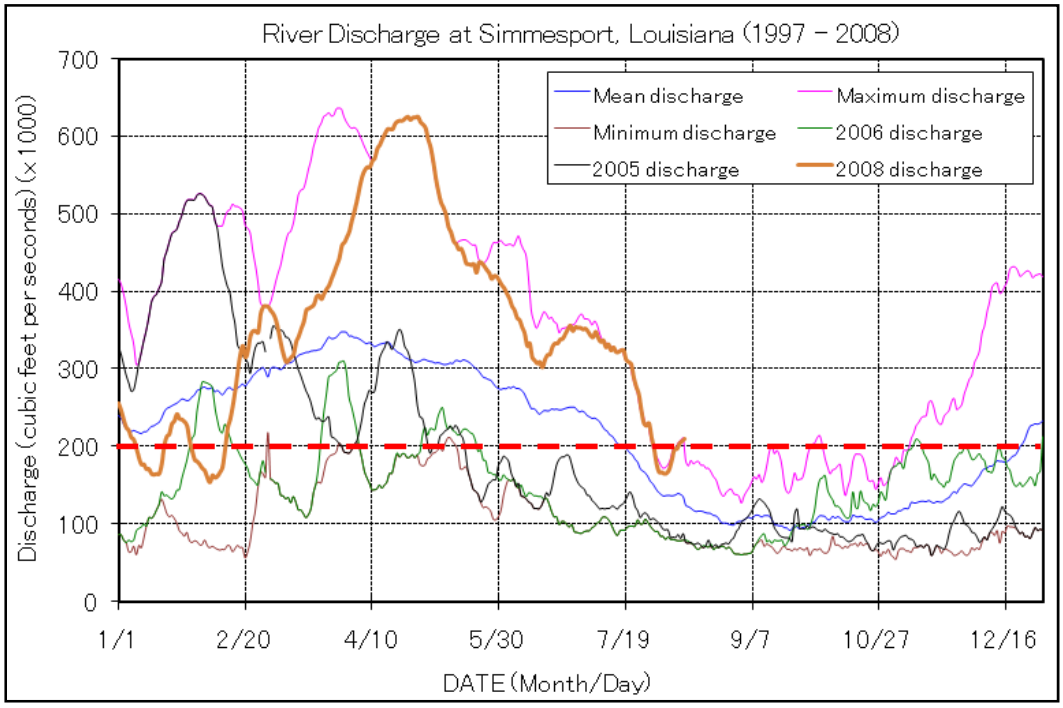


Figure 6.4 River discharge at Simmesport, Louisiana between 1997 and 2008 (Source: the U.S. Army Corps of Engineers, New Orleans District).

### 6.5.2. Bed Characteristics

Bed characteristics for both deployments were analyzed based on bottom sediments sampled on site and plexi-glass cores taken in a 2005 biological cruise (Stone *et al.* 2005a) and sub-surface images from an underwater camera (SPI) taken during a biological cruise in 2006 as well as reports from divers (Stone *et al.* 2006). Figure 6.5 shows grain size distributions during the pre- and post-deployments in spring 2006 and winter 2008. Grain size distributions were remarkably different between the deployments. Sediments sampled when the arrays were deployed in spring 2006, were predominantly clay with the median grain diameter of 1.11 microns ($1.11 \times 10^{-6}$ m)

(Figures 6.5 top and 6.6 bottom); while, sediments during post-deployment were fine sand with a median diameter of 127 microns ($127 \times 10^{-6}$ m) (Figures 6.5 top and 6.6 bottom). In the 2008 deployment, sediments for both pre- and post-deployments were predominantly sandy with a median diameter of 153.4 microns ($153.4 \times 10^{-6}$ m) during the pre-deployment and 148.8 microns ($148.8 \times 10^{-6}$ m) during the post-deployment (Figure 6.5 bottom). However, sediments obtained from post-deployments in 2006 and 2008 also included a small amount of unconsolidated fluid mud on nearby survey locations. Sediments were obtained using plexiglass cores on the western shoal and were predominantly sandy; borrows, shells, and mud lens were evident (not shown). The images from the SPI showed distinct ripple formation and the geometry was determined as approximately 5 cm high and 15 cm long (*i.e.*, ripple steepness ≈ 0.33).

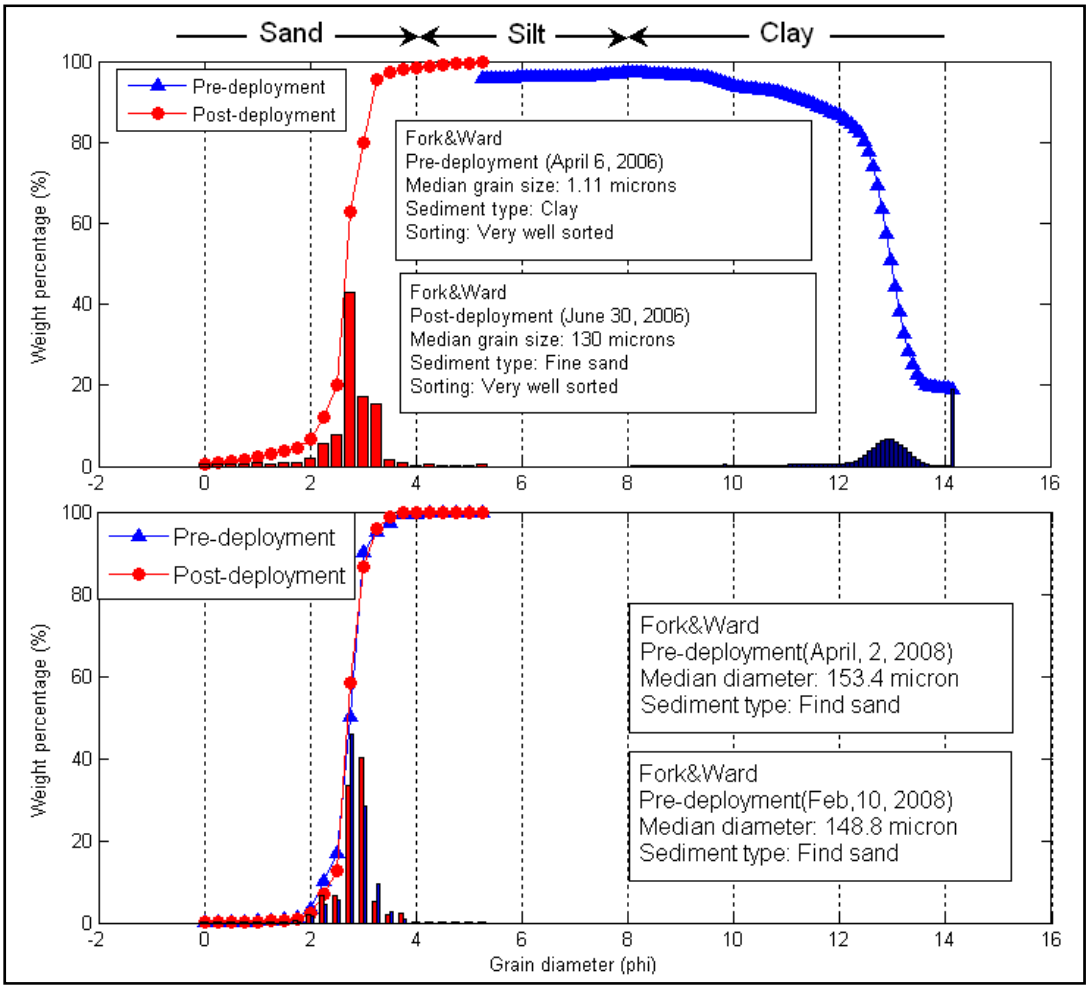


Figure 6.5 Grain size distribution for the samples collected from the crest of the shoal during 2006 (top) and 2008 deployments (bottom).

Figure 6.6 Sampled sediments from the crest of the shoal during the 2006 deployments: (upper) sand and (lower) fluid mud.

### 6.5.3. Wave-Climate, and Variability of Currents and Sediment Concentration

In spring 2006 and winter 2008, over the deployment periods, a total of five and eleven winter storms passed over the study area (Table 6.2). Pepper and Stone (2004) discussed two distinct cold front types: AS storms (type A in Table 6.2) and MC storms (type B in Table 6.2). The AS storms are characterized by weak pre-frontal winds and strong post-frontal winds from northeast. The MC storms are characterized by fairly strong southerly winds during pre-frontal phases followed by strong northwesterly winds (Pepper and Stone 2004). Of the storms, four and six

storms were associated with the AC storms and one and five with the MC storms in the 2006 and 2008 deployments, respectively (Table 6.2). Predominant wind and wave direction was from the southeast during both deployments (Table 6.3); during storms, strong wind stress directed to the southeast, prevailed (Figures 6.7 and 6.8). Maximal wind speed attained 22 m $s^{-1}$ and 19 m $s^{-1}$ during the 2006 and 2008 deployments, respectively. Mean significant wave height was less than 1 m during both deployments; wave height increased as storms approached, exceeding 2 m over the shoal and the inner shelf (Table 6.3); however, the wave height on the inshore station was significantly lower than the height over the crest and offshore (55% and 46% for mean and maximum wave heights in the winter 2008, respectively; see Table 6.3). Low frequency swells ($f < 0.2$ Hz) were dominant during most of the deployment period; however, during the onset of storms and post-frontal phases, wind-induced high frequency seas ($f > 0.2$ Hz) responded quickly to storm winds as illustrated in Figures 6.7 and 6.8 (see also Sheremet *et al.* 2005; Stone *et al.* 2005b; Jose *et al.* 2007).

Table 6.2

Number of winter storms for the 2006 and 2008 deployments. Type A is equivalent to AS storms and Type B is equivalent to MC storms by Pepper and Stone (2004).

| | Total number | Type A | Type B |
|---|---|---|---|
| 2006 deployment | 5 | 4 | 1 |
| 2008 deployment | 11 | 6 | 5 |

Table 6.3

Mean (top) and Maximal (bottom) values of physical parameters (at the shoal crest)

| Year | Wind speed ($m\ s^{-1}$) | Wind direction (degree) | $H_S$ (m) Off, Crest, In | $T_P$ (sec) Off, Crest, In | Wave direction (degree) Off, Crest, In | Bottom $C_{spd}$ ($m\ s^{-1}$) Off, Crest, In | Bottom $C_{dir}$ (degree) Off, Crest, In | $U_{orb}$ ($m\ s^{-1}$) Off, Crest, In |
|---|---|---|---|---|---|---|---|---|
| 2006 | 5.9 | 166.6 | 0.46, 0.58, ND* | 6.2, 6.0, ND* | - , 129.6, ND* | 0.04, 0.02, 0.05 | 142.9, 145.3, 159.2 | 0.09, 0.13, ND* |
| | 22.0 | - | 2.19, 2.32, ND* | 9.8, 10.2, ND* | - | 0.23, 0.26, 0.23 | - | 0.57, 0.81, ND* |
| 2008 | 7.3 | 149.8 | 0.87, 0.83, 0.39 | 6.0, 6.3, 6.6 | 167.5,185.3,167.5 | 0.10,0.05,0.07 | 140.6, 180.3, 159.5 | 0.15,0.22,0.21 |
| | 19.1 | - | 3.42,2.96, 1.85 | 10.7,16.0, 12.8 | - | 0.31,0.30,0.43 | - | 1.02,1.38,1.12 |

*ND: No data. $H_S$: significant wave height, $T_P$: peak wave periods, $C_{SPD}$: Current speed, $C_{dir}$: Current direction, $U_{orb}$: bottom wave orbital velocity.

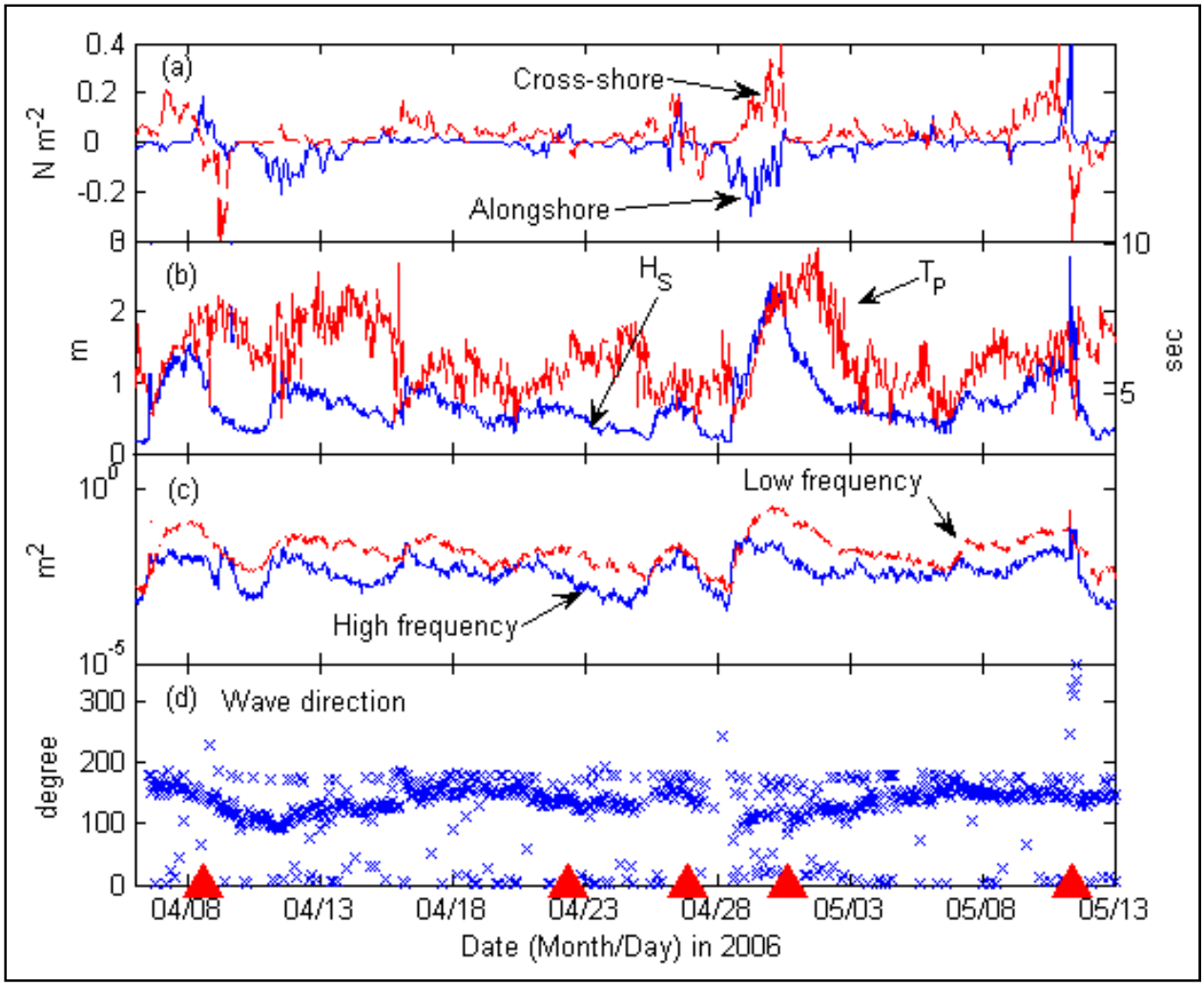


Figure 6.7 Time series of (a) wind stress, (b) wave height and peak period, (c) wave variance (high frequency ($f$>0.2 Hz) and low frequency ($f$<0.2Hz)), and (d) wave direction during the 2006 deployment.

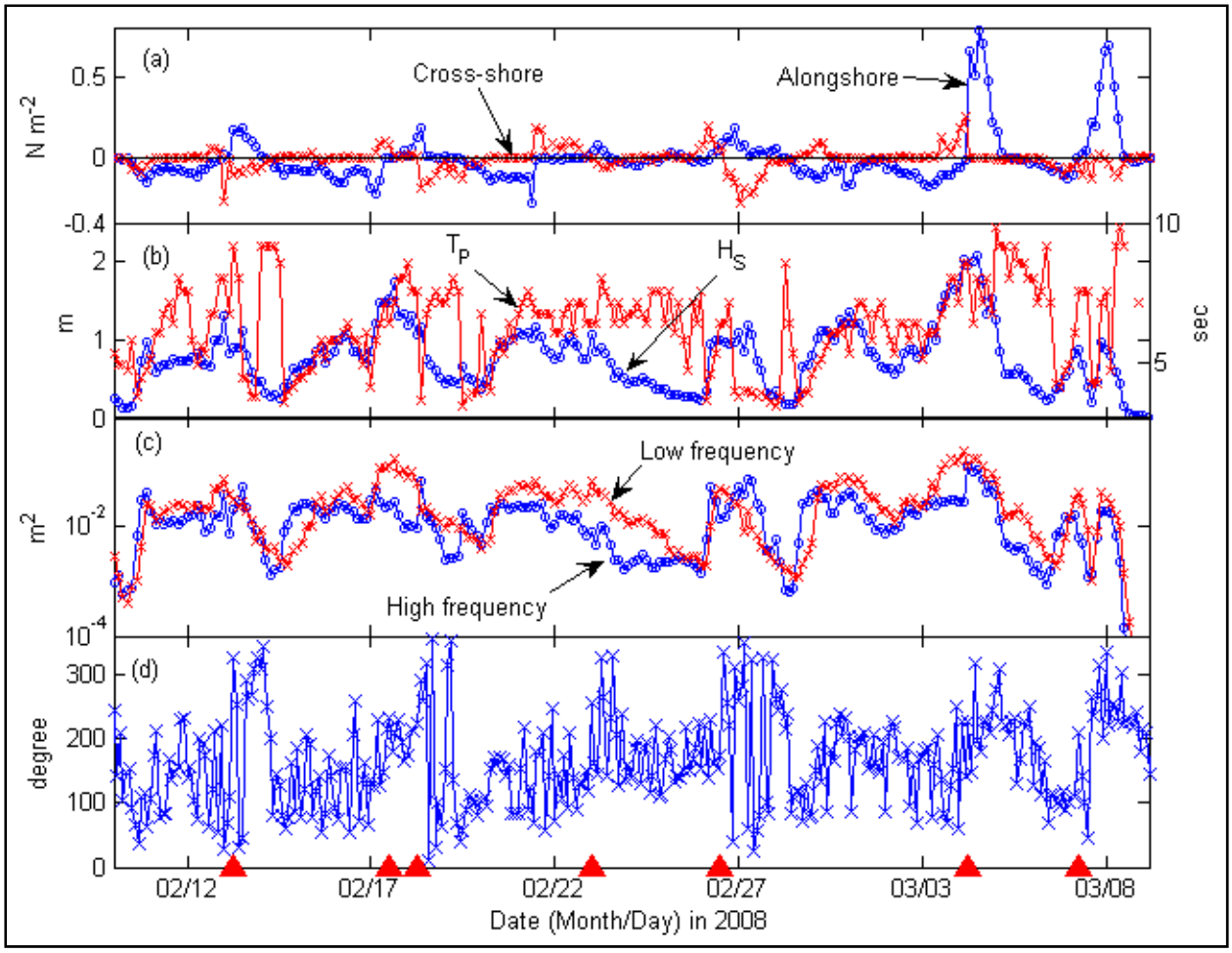


Figure 6.8 Time series of (a) wind stress, (b) wave height and peak period, (c) wave variance (high frequency ($f$>0.2 Hz) and low frequency ($f$<0.2Hz)), and (d) wave direction for the 2008 deployment.

Sea surface slope and currents over the shoal were highly variable, but showed strong response to varying wind directions associated with winter storms for both 2006 and 2008 deployments (Figures 6.9 and 6.10). During the 2006 deployment, the storms passed on April 8th and May 10th and changed sub-tidal water level by 20 cm and 10 cm, respectively; the storm passed in late April and increased the water level by approximately 15 cm. During the former two storms, cross-shore currents (offshore and onshore) were generated. During the storm in late April, cross-shore near bottom currents were generated and yielded total net flux directed offshore. During the 2008 deployment, the sub-tidal water level decreased as fronts passed over the study area. Reduction in the water level was maximal when wind blew alongshore with a maximal change of 40 cm during the winter storm on March 7th and strong offshore currents were generated. This trend was also reported along the Gulf Coast (e.g., Cragg *et al.* 1983; Walker *et al.* 2001). Cross-shore sea surface slope estimated by water level differences between SS06_3 and CSI-5 in 2006 and between CSI-6 and CSI-5 in 2008, showed an influence of surface slope on wind and cross-shore currents. Pepper and Stone (2002) suggested that, based on bottom

current data, that cross-shore sediment flux was offshore and onshore at an offshore and onshore stations, respectively; the net sediment flux during winter storms were directing offshore (Pepper and Stone 2002). Such trends were detected from the data for the 2008 deployment; however, bottom currents varied depending on storm wind direction and consequent sea surface slope as well as due to the bottom topography (Kobashi and Stone 2008b). Turbidity data (and SSC) for both deployments also varied with passages of winter storms. Turbidity increased during the onset of the storms and decreased in the wake of the storms; however, variations in the turbidity (and SSC) were different between the 2006 and 2008 deployments. For the 2006 deployment, a large portion of the bottom OBS sensor recorded values approaching zero during fair weather. This is likely attributed to the sensor burial into fluid mud as discussed in detail in section 4.6.2.1. The upper turbidity concentrations were usually higher than those recorded lower in the water column: for the 2008 deployment, on the other hand, the upper turbidity was almost always lower than lower turbidity levels.

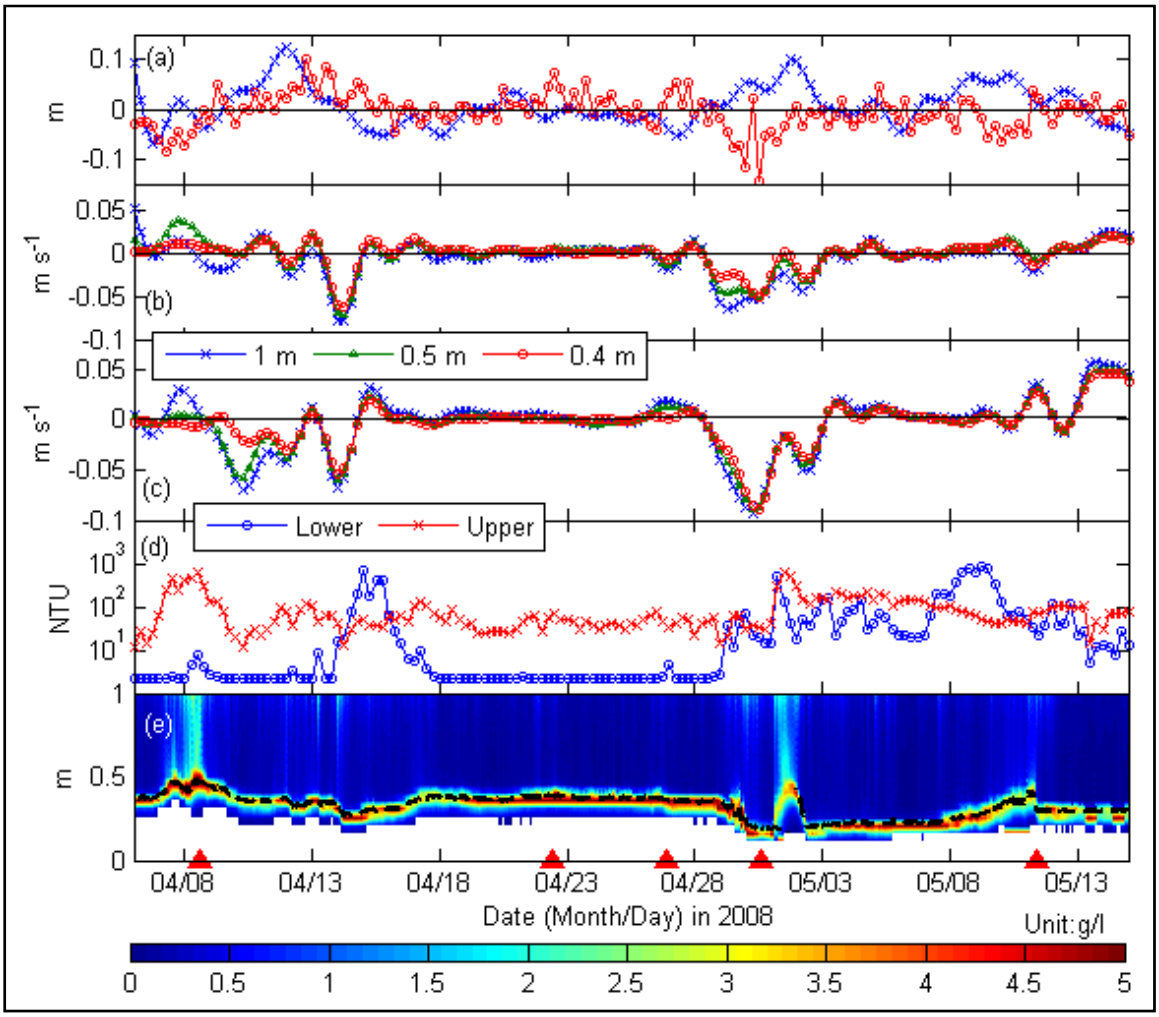


Figure 6.9 Time series of (a) adjusted water level and cross-shore sea surface slope, (b) alongshore current, (c) cross-shore current, (d) OBS (0.3 m and 0.61 m above the bottom) and (e) SSC profile (2006 deployment).

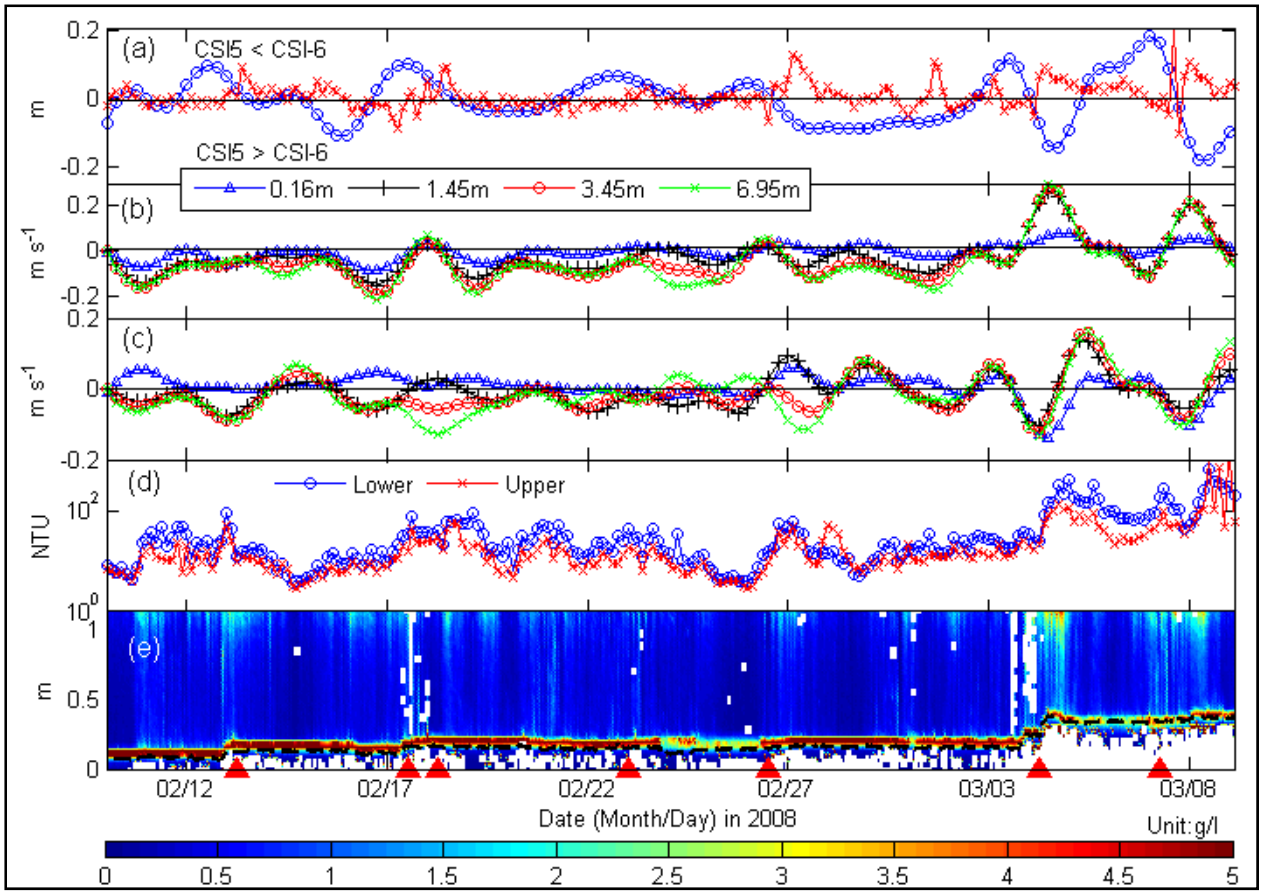


Figure 6.10 Time series of (a) adjusted water level and cross-shore sea surface slope, (b) alongshore current, (c) cross-shore current, (d) OBS (0.35 m and 0.74 m above the bottom) and (e) turbidity profile (2008 deployment).

Bed elevation change was also be directly related to winter storms; increase in the bed elevation corresponded to high river discharge or a post river discharge phase. Decreases in the elevation of approximately 20 cm followed by a 30 cm increase in the elevation, recorded during a storm in late April, 2006. The bed elevation change in winter 2008 was small except on March 5th, 2008 (Figure 6.10). A detailed discussion is presented in section 6.6.1.

### 6.5.4. Bottom Boundary Layer Characteristics

Variations in the BBLPs correspond to the passage of winter storms. Compared to Figures 6.9 and 6.11 and Figures 6.10 and 6.12, there is a strong correlation between changes in the shear stress, particularly wave-induced shear stress ($\tau_w$), and turbidity (and SSC). When the storms passed the study site, shear stress increased as wave height, wave period, and bottom currents increased, and finally reached the threshold value (*i.e.*, critical shear stress) above which bottom sediment was suspended; waves and currents began to re-suspend the bottom sediments. Increase in the shear stress above the threshold value was consistent with increase in the SSC. Shear stress

during fair weather in spring 2006 was largely lower than that during the 2008 deployment. Findings during the 2008 deployment also show similar results; however, the trend during a significant portion of the deployment period in winter 2008 is characterized by higher wave shear stress than the threshold, even during non-storm conditions. A noticeable difference between results of both deployments is that shear stress was higher than the threshold value only during storms during the 2006 deployment; shear stress data obtained from the 2008 deployment was conspicuously higher than the threshold during most of the deployment. The reason for the difference is discussed in section 6.6.2.

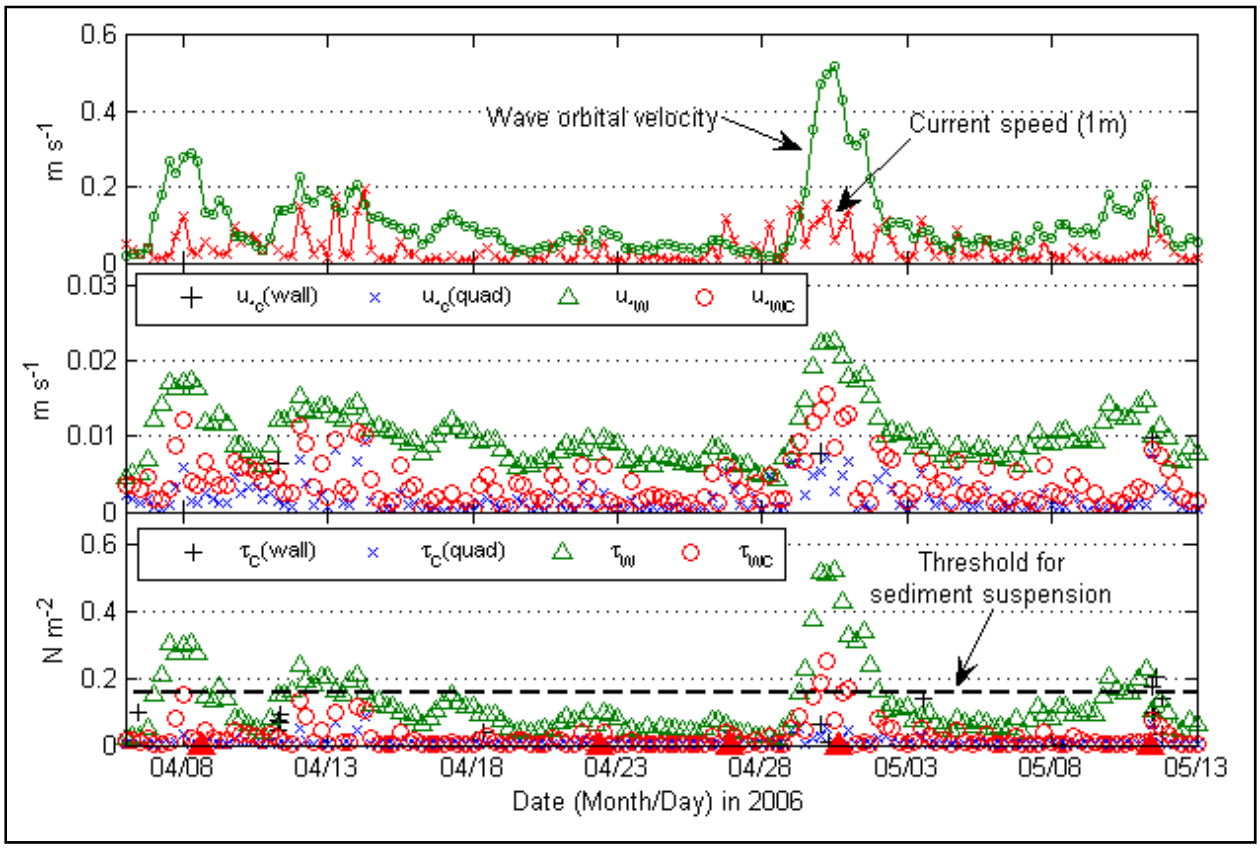


Figure 6.11 Time series of (a) wave orbital velocity and current speed (1m), (b) shear velocity, and (c) shear stress. The dashed line on the bottom figure shows the threshold for sediment suspension. Passage of winter storms is shown as shaded triangle on the bottom figure (2006 deployment).

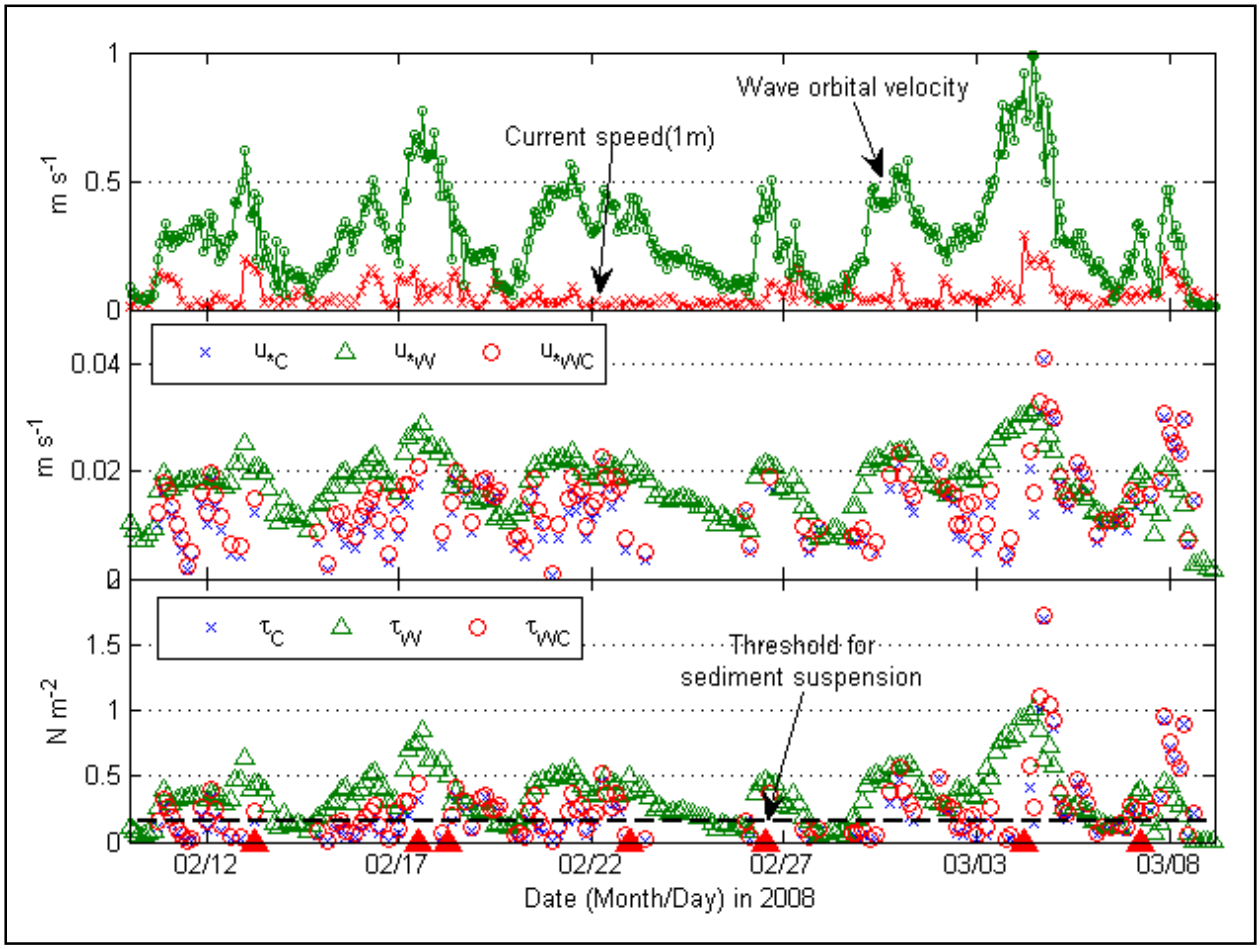


Figure 6.12 Time series of (a) wave orbital velocity and current speed (1m), (b) shear velocity, and (c) shear stress. The dashed line on the bottom figure shows the threshold for sediment suspension. Passage of winter storms is shown as shaded triangle on the bottom figure (2008 deployment).

## 6.6. DISCUSSION

### 6.6.1. Sediment Heterogeneity due to Fluvial Fine Sediments and Winter Storms

Results of grain size analysis in spring 2006 and winter 2008 indicate conspicuous difference in bed characteristics between the two deployments (Figure 6.5). A satellite image during a pre-frontal phase, on April 4th, 2006 (Figure 6.13a), captured westward transport of fluvial sediments. On April 8th, 2006, during a post-frontal phase (Figure 6.13b), the transport trend had shifted from the west to southeast due to the post-frontal wind fields, which generated wind-induced southeast currents that pushed water and sediment offshore and eventually the plumes reached the shoal. During this period ((1) in Figure 6.13d), the PCADP measured approximately

a 15 cm increase in the bed elevation and 2.5 g/l of SSC at SS06_2. A similar situation occurred in mid May, during which approximately a 15 cm increase in the bed elevation and 0.5 g/l of SSC were recorded ((3) in Figure 6.13d&e). Both shifts corresponded to high river discharge at Simmesport, LA, upstream of the Atchafalaya River (Figure 6.13c) following the peak discharge. In late April when a cold front passed over south-central Louisiana ((2) in Figure 6.13), a distinct characteristic was detected; strong winds blew from the southeast, in contrast to the aforementioned two storms resulting in insubstantial fluvial sediment supply as detected by the satellite imagery (not shown). However, during this period, substantial bottom sediment reworking during the pre-frontal phase followed by significant accumulation of the sediment (*i.e.*, fluid mud) during the post-frontal phase occurred. More detailed mechanisms are addressed in section 6.6.2.

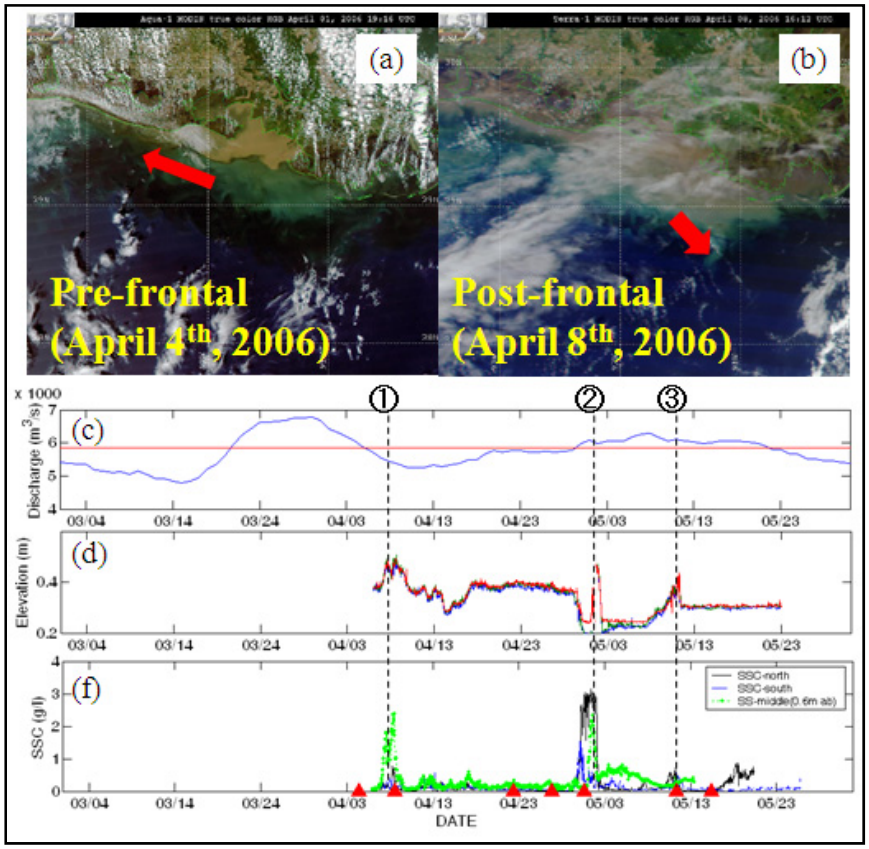


Figure 6.13 Satellite images during a pre-frontal phase (a) and a post-frontal phase (b) along with river discharge (c), bottom elevation at the SS06_2 (d), and SSC (f). Red line in (c) shows the border between high and low discharge suggested by Walker and Hammack (2000). The numbers, (1) and (3) represent passages of winter storms that accompany sediment supply from the Atchafalaya River. The number, (2) represent a passage of winter storms that does not accompany sediment supply from the river.

This pattern of sediment supply was further corroborated by Kobashi *et al.* (Kobashi and Stone 2009) which investigates the dispersal shifts associated with winter storms using prolonged in-situ data collected from the vicinity of the Atchafalaya River and using satellite imagery. The study concluded that post-frontal wind induces strong southeast currents in concert with an enhanced bottom sediment re-suspension, transporting the fluvially-derived sediments further southeast. All aforementioned evidence clearly supports that the post-frontal wind and high river discharge contribute to the sediment heterogeneity on the shoal. During the spring 2006 deployment, a total of five storms passed over the study area and eventually two of them yielded the dispersal shifts which reached the shoal. During the deployment in winter 2008, a total of 11 storms passed over the study area and approximately five of them caused dispersal shifts which eventually reached the shoal. However, during the winter 2008, bottom sediments were predominantly sandy during most of the deployment period given strong meteorological forcing and a shallower water depth except around March 5th when fluid mud accumulation was evident. This likely happened because of strong downwelling currents (not shown) which seems to enforce the accumulation rather than fluid mud settling (see Figure 6.10e).

Fine sediment transport from offshore is another possible factor that has to be addressed here; however, the sediment supply from offshore is not thought as significant as the fluvial sediment supply from the Atchafalaya because sediment re-suspension on the outer shelf is thought to be significant only during severe storms, given the fact that the depth of the surrounding shelf is much deeper than that of the shoal and thus sediment re-suspension offshore is less significant than that on the shoal. We computed sediment re-suspension intensity (RI), defined as the wave shear stress minus the critical shear stress, at CSI-15 off Ship Shoal (17 m isobath) and CSI-6 located southeast of Ship Shoal (20 m isobath); the intensity was on average 70 and 81 percent lower than that on the shoal crest (SS08_2), respectively. The RI was positive during severe storms; net cross-shore sediment flux during winter storms are largely offshore; however, a small portion of fine sediment may have been transported to the shoal during pre-frontal phases, but is not considered to yield significant changes in bed characteristics. This is further corroborated by a numerical model analysis conducted by Kobashi *et al.* (2009b). Thus, it is concluded that sediment supply from the mid-/outer shelf is limited during severe extra- and tropical storms (off-shoal wave height > 4 m according to Kobashi *et al.* 2009b).

Spatial distributions of fluid mud on the shoal are highly complicated given the following reasons; (1) bottom sediment types during the 2006 deployment changed drastically as already mentioned; however, we also found evidence of fluid mud on the proximity of the deployment area during the retrieval cruise. In winter 2008, we also sampled small amounts of fluid mud on the other side of the platform from our tripod on the crest, which is roughly less than 50 meter apart; (2) During our collaborative biological cruises, any evidence of fluid mud from box cores were not found from the shoal bottom although there is a possibility that the box cores did not capture unconsolidated fluid mud (Winans, W., personal communication, 2007); (3) frequencies of winter storms are higher than the frequency of dispersal shifts which eventually reached the shoal (Kobashi *et al.* 2009a). The above reasons suggest that the spatial distribution of fluid mud on the shoal is patchy possibly due to complex shoal bathymetry (*i.e.*, irregularity of the shoal bottom).

### 6.6.2. Wave-Current-Bottom Sediment Interactions over the Shoal during a Storm

As mentioned in the previous sections, shoal bed characteristics and associated bottom boundary layer dynamics are remarkably different depending on the predominant sediment regime. Those differences create two distinct morphodynamic characteristics over the shoal, and which are discussed in the following sub-sections.

#### *6.6.2.1. Fluid Mud Bottom (2006)*

In spring 2006, the instrument arrays and satellite images captured the signal that fluvial fine sediments debouched from the Atchafalaya River, in a form of fluid mud, were accumulated onto the shoal in the wake of storms. The accumulated fluid mud further interacted with hydrodynamic forcing associated with winter storms. In late April, 2006, a strong winter storm passed over the study area and the arrays captured a unique wave-current-fluid mud interaction scenario (Figure 6.14 (a)-(k)).

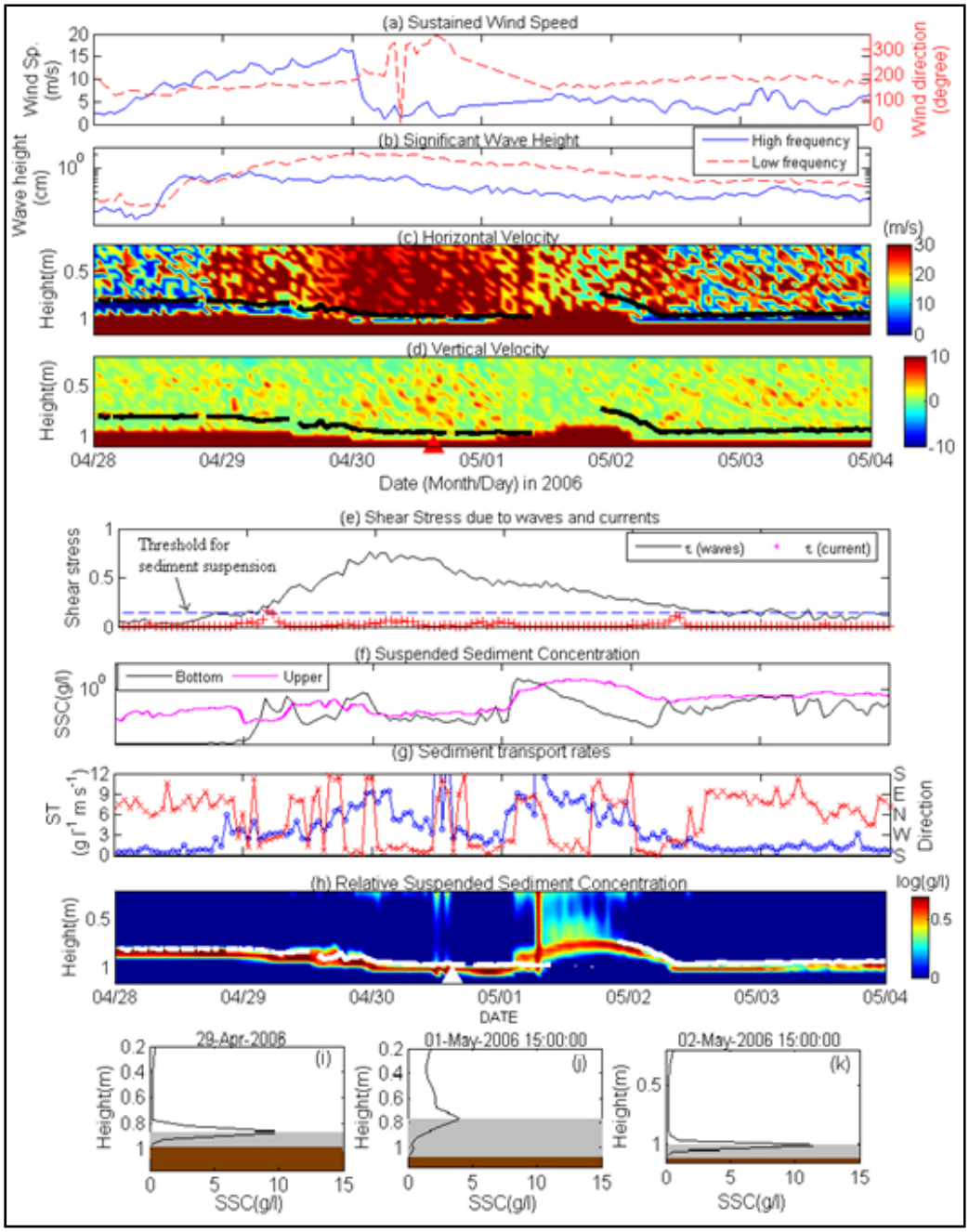


Figure 6.14 Time series of (a) wind speed and direction, (b) wave height, (c) horizontal current profile (d) vertical current profile (e) shear stress, (f) upper and lower SSC (g) sediment transport rates, (h) SSC profile (log scale), and (i)-(k) SSC profiles.

Prior to the storm passage, a thin layer of fluid mud likely existed on the shoal with an approximate thickness of 30 cm and 15 cm for partially consolidated (brown shaded area in Figure 6.14i) and the least consolidated (gray shaded area in Figure 6.14i) fluid mud layer, respectively. This thickness is in general agreement with the report from a diver during the instrument deployment (Depew, D. personal communication, 2006). When the next cold front approached, wave height increased and sediments were re-suspended from the sea floor once the shear stress exceeded the critical value above which bottom sediment was suspended (Fig 4.14e); this was consistent with an increase in the bottom turbidity shown by the OBS sensors (Figure 6.14f).

Sediment transport rates integrated from bottom to the sensor height, approximately 1 m, were then elevated due to increased high storm-induced currents and sediment re-suspension (Figure 6.14c and g), reaching approximately 9.0 kg $m^{-1}$ $s^{-1}$, more than an order of magnitude higher than numerically-derived sand transport rates (~0.1 kg $m^{-1}$ $s^{-1}$) when the bottom sediment is fine sand and ripple steepness is 0.33. Such high sediment transport rates resulted in a 20 cm reduction in the bed elevation (*i.e.*, sediment reworking). When the front passed, strong vertical mixing occurred and suspended sediments were mixed vertically upward due to a positive vertical velocity, resulting in shifting the SSC maxima upward (Figure 6.14d and j) and lowering the upper and bottom SSCs (Figure 4.14f) and consequent transport rates (Figure 6.14g). During the post-frontal phase, the mixed sediment was gradually re-settled out in the wake of the storm as the wave height and current velocity decreased; however, the upper turbidity remained high in spite of a reduction in the lower turbidity; this is probably because settling was significantly hindered due to the formation of large flocs that interfere each other (Figure 6.14f). During this time, the sediment transport rates were high (~10 kg $m^{-1}$ $s^{-1}$) given the high SSC in spite of weak currents. Despite such high transport rates, a portion of the mixed sediments were re-deposited on the bottom with a reduction in thickness of the fluid mud layer than was apparent during the pre-frontal phase (brown and grey areas in Figure 6.14i and k) because a portion of the reworked sediments was likely transported outside of the shoal as indicated by high sediment transport rates during the post-frontal phase (Figure 6.14g). Net fluid mud flux was directed offshore during the storm.

#### *6.6.2.2. Sandy Bottom (2008)*

In contrast to results obtained in spring 2006, bed type on the shoal in winter 2008 was predominantly sandy (Figures 6.5 bottom and 6.6 top). Basic hydrodynamic characteristics were similar to those during the spring 2006 deployment, as illustrated in Figure 6.15. Wave-current-bottom interaction over the sandy bottom was conspicuously different from those in spring 2006. From a limited number of underwater camera images, wave ripples were likely formed on the shoal when the bottom was dominated by sand. In mid February, 2008, when a cold front approached the study area, wave height and current speed increased. Shear stress also increased and finally exceeded the threshold for sediment suspension (see also Figure 6.15e), the sign of incipient bottom sediment suspension. Turbidity values increased as wave height (and shear stress) increased (Figure 6.15b&f). Vertical velocity was highest when the storm passed (Figure

6.15d), and the suspended sediments were vertically mixed, consistent with increases in the upper and lower turbidities (Figure 6.15e&f). Sediment transport rates were high because of high horizontal current speeds and high turbidity; and net transport flux was directed offshore (*i.e.*, south) during the storm (Figure 6.15g). When storms passed the study area, ripples are often washed out due to strong waves and currents (*i.e.*, sheet flow). Soulsby (1997) addressed a ripple washout criterion and estimated that the ripples can be washed out when the mobility number exceeds approximately 150. Taking this into account for the 2008 deployment, the ripples were possibly washed out when near-bottom wave orbital velocity exceeded 0.6 m $s^{-1}$ on the middle shoal crest.

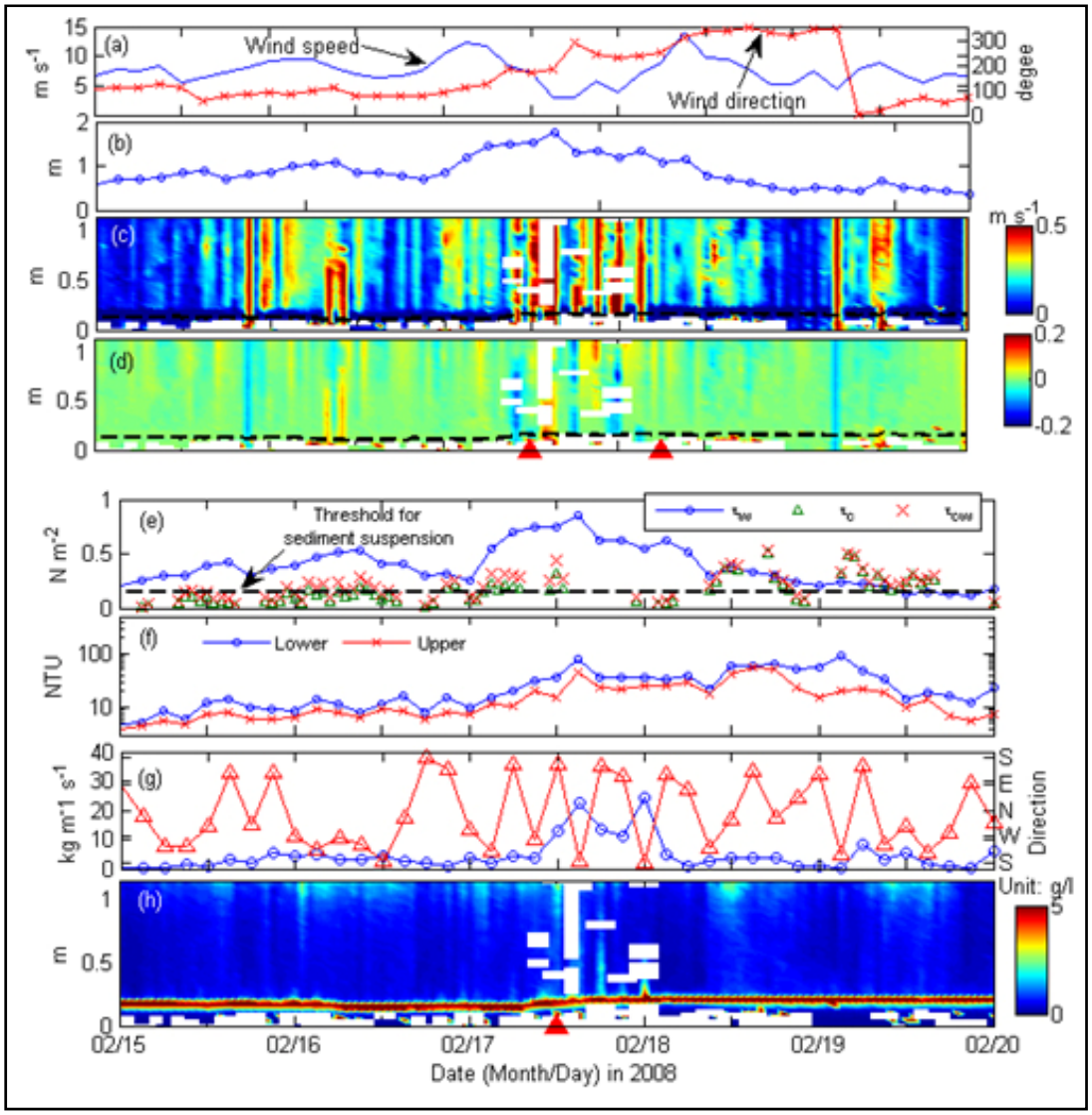


Figure 6.15 Time series of (a) wind speed and direction, (b) wave height, (c) horizontal current profile (d) vertical current profile (e) shear stress, (f) upper and lower SSC (g) sediment transport rates, and (h) SSC profile (log scale).

There were four events during which the orbital velocity exceeded the threshold value, all being consistent with winter storms. In the waning phase of the storm, the re-suspended sediments were re-deposited due to decreasing wave height and current velocities attributable to post-frontal conditions. The ripples that were washed out during the storm were likely reformed during this phase. Grain settling for sand is remarkably different from that for cohesive sediments that undergo three stages: free settling, flocculation and hindered settling (Mehta 1991; Sheremet *et al.* 2005; McAnally *et al.* 2007). Grain settling of sand follows Stokes law and the settling velocity is approximately 0.015 m $s^{-1}$ (*i.e.*, 1.5 cm $s^{-1}$, approximately 100 cm $minute^{-1}$) based on sediments sampled for the 2008 deployment, which is, as a first-order approximation, at least two orders higher than the maximum settling velocity for fluid mud (in the form of flocculation from Sheremet *et al.* 2005). Pepper and Stone (2004) estimated 0.6 kg $m^{-1}$ $s^{-1}$ (AC storms) and 1.0 kg $m^{-1}$ $s^{-1}$ (MC storms) of numerically-derived sand transport rates (Grant-Madsen-Rouse algorithm) based on their deployment on the western flank of Ship Shoal in 1998. In winter 2008, maximum sand transport rates (Engelund-Hansen total transport equation) of 0.015 kg $m^{-1}$ $s^{-1}$ were computed on March, 4th, 2008.

### 6.6.3. Sediment Exchange and Implication for Potential Sand Mining Impacts

Ship Shoal is exposed to recurring sandy and muddy bottoms and shows two contrasting sediment exchange scenarios depending upon predominant bed characteristics, as illustrated in Figures 6.16 and 6.17. Such unique sediment exchange processes are summarized below.

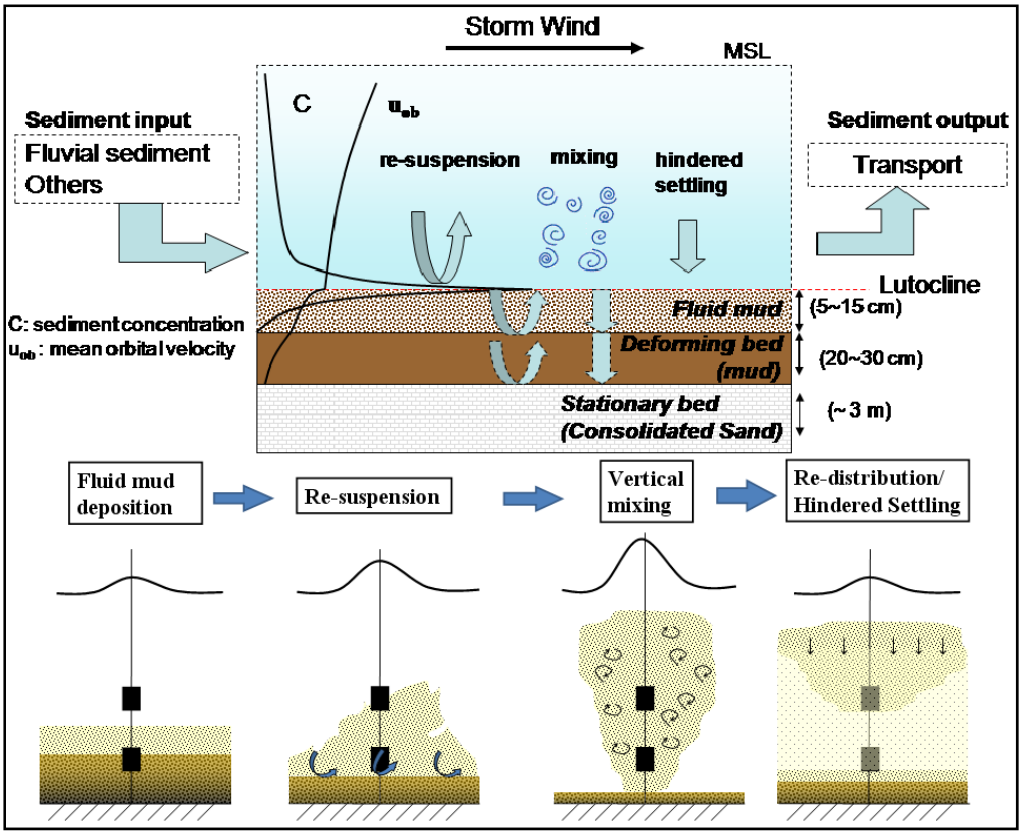


Figure 6.16 Schematic illustration of sediment exchange on Ship Shoal during fluid mud regime.

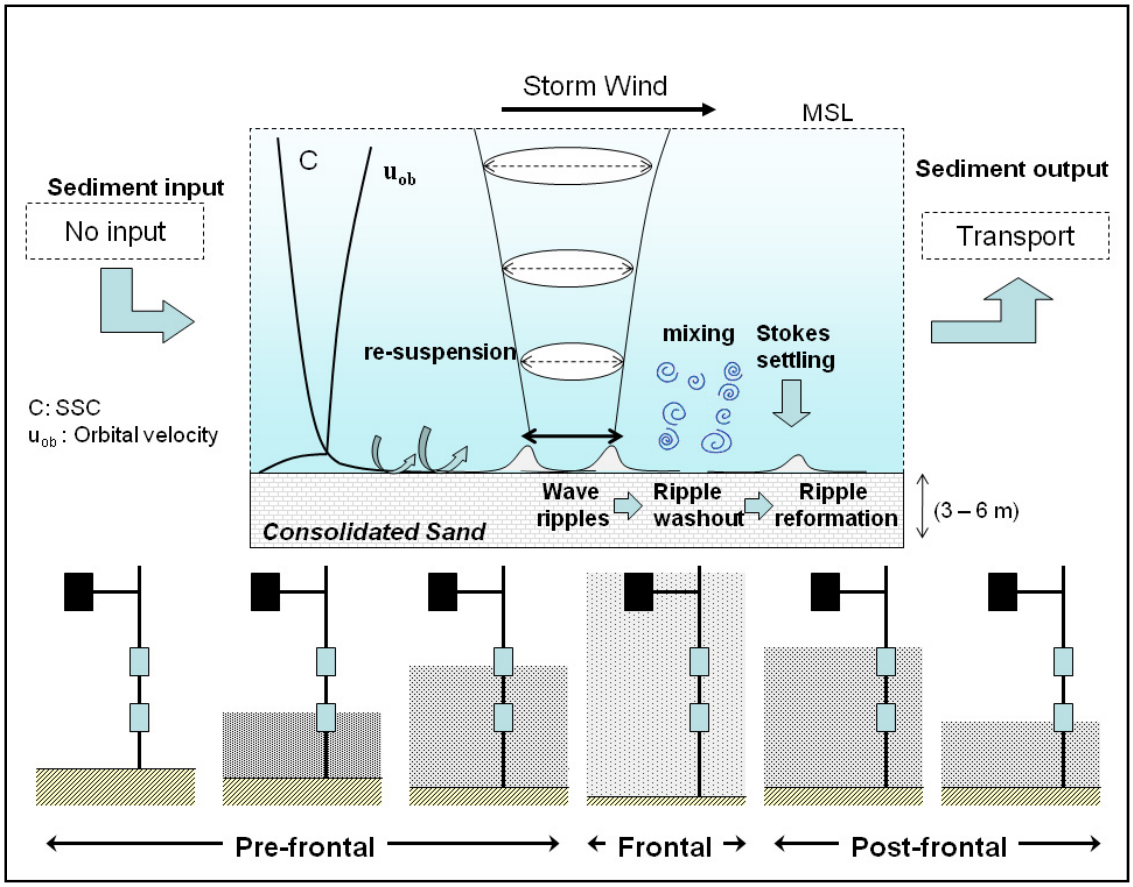


Figure 6.17 Schematic illustration of sediment exchange on Ship Shoal during sand regime.

Whether the sea bed is fluid mud or not is dependent upon the balance between sediment supply and sediment loss (*i.e.*, sediment reworking). Sediment supply, as already discussed above, is associated with fluvial sediment discharge from the Atchafalaya River and winter storm conditions. When the sediment influx from the Atchafalaya River occurs in tandem with the post-frontal phase of the winter storms, sediments are transported further southeast and are occasionally accumulated on the shoal in the wake of the storms. Given the frequency of winter storms, the fluid mud is not likely to get enough time to become permanently consolidated mud and resistant to re-suspension and transport by waves and currents. When another winter storm approaches and then passes over the study area, bottom sediments undergo re-suspension, mixing, hindered settling and re-distribution (Figure 6.16). Settling undergoes three stages: free settling, flocculation and hindered settling depending on sediment concentration (Mehta 1991; McAnally *et al.* 2007).

The morphodynamic processes are dominated by the prevailing waves, bottom currents and the water depth. Measured data suggest that even if waves are not strong enough to suspend fluid mud, weak currents can potentially transport a portion of upper-layer unconsolidated fluid mud during weak storms.

When the sediments are predominantly sandy, shoal bottom undergoes sediment re-suspension, vertical mixing, and settling; the BBLDs follow conventional approaches (cf. Grant and Madsen 1986), though the sediments may contain a small portion of fine-grained materials. Settling follows conventional Stokes settling and the settling velocity is much faster than the fluid mud settling. Another survey data set suggests that wave ripples are formed with an approximate dimension of 5 cm high and 15 cm long on the shoal. Those ripples are disturbed by storm waves and currents and eventually washed out when orbital velocities become high under sheet flow conditions (bottom orbital velocity reached greater than 0.6 m $s^{-1}$ during the 2008 deployment).

The above discussion gives some insight regarding environmental impacts of future potential sand mining from the shoal; especially on the physical processes. As we have discussed above, alteration in water depth is considered to be an important factor for shoal morphodynamics. If large scale dredging is authorized and thus substantially alters the shoal bathymetry, the changes may eventually enhance fluid mud accumulation on the shoal, increasing bottom turbidity and changing bed characteristics and consequently become detrimental for the benthic communities. This is discussed in greater detail in Kobashi *et al.* (Kobashi and Stone 2008b) by means of a-state-of-the-art numerical model implementation and the preliminary results support the above hypothesis. Therefore, it is suggested that sand dredging needs to be carefully planned to minimize physical and biological impacts, particularly in terms of protecting the endemic shoal benthic habitats. The shoal has been recently recognized as a biological hotspot for blue crabs and also an oxygen refugee for benthic organisms, particularly during the summer hypoxia season (Condrey and Gelpi 2008; Grippo *et al.* 2009).

# CHAPTER 7
# IMPACTS OF SAND REMOVAL FROM A SHORE-PARALLEL HOLOCENE TRANSGRESSIVE SHOAL ON HYDRODYNAMICS AND SEDIMENT TRANSPORT, SOUTH-CENTRAL LOUISIANA, U.S.A.

## 7.1. INTRODUCTION

Irregular bottom topography in shallow waters such as sand banks and shoals has been known to influence coastal hydrodynamics and bottom boundary layer dynamics (Stone and Xu 1996; Pepper and Stone 2004). Those offshore sand bodies have been given particular attention as viable sand resources as more sand becomes necessary for large-scale coastal restoration, particularly along the northern Gulf coast (Byrnes *et al.* 1999; Michel *et al.* 2001; Maa *et al.* 2004; Pepper and Stone 2004; Khalil *et al.* 2007). Inner-shelf shoal bathymetry generates unique hydrodynamics which may have a profound influence on the endemic biological and sedimentary environments (Swift 1985; Snedden and Dalrymple 1999; Condrey and Gelpi 2008; Palmer *et al.* 2008). For instance, such bathymetric highs act as submerged breakwaters, mitigating wave energy and hence changing wave refraction, flow patterns, and consequent sediment transport patterns (cf. Stone and Xu 1996; Pepper and Stone 2004; Stone *et al.* 2004b; Jose *et al.* 2007).

Wave transformation studies in shallow waters have been mostly limited to numerical model analysis and laboratory experiments, given the complex nature of dynamics (e.g., Stone and Xu 1996; Byrnes *et al.* 2003; Maa *et al.* 2004; Johnson *et al.* 2005). Stone and Xu (1996) in greater detail investigated wave transformation over a shore-parallel sand body, Ship Shoal, located approximately 20 km off the coast in south-central Louisiana on the approximate 10 m isobath. The authors implemented a spectral wave model, STWAVE (Smith *et al.* 2001), with constant input parameters (*i.e.*, deepwater wave height/directions, wind speeds/directions), based on wave-climate analysis, along with the hypothetical post-dredging bathymetric configuration in which the entire shoal was removed. This work concluded that prevailing southeast waves were impacted the most in terms of wave refraction and dissipation, particularly along the western flank of the shoal; whereas, the ultimate impact of sand removal on the shoreface of barrier islands was insignificant for all model cases. STWAVE is, however, a "half-plane" wave model and this study was limited to waves (both swells and seas) from the southern quadrant, and hence detailed mechanisms of waves, particularly associated with post-frontal winds as well as current variability and sediment transport associated with sand removal, are not fully understood. While Jose *et al.* (2007) implemented a "full-plane" third generation spectral wave model, MIKE21 SW to investigate wave transformation over a shallow shoal and qualitatively addressed the importance of wave dissipation and wave-wave interaction associated with winter cold fronts. There are a growing number of publications which examine hydrodynamics associated with sand mining, particularly waves and their impacts on longshore transport along beaches and barriers (Stone and Xu 1996; Byrnes *et al.* 2003); however little has been discussed regarding the alteration in hydrodynamic and sediment transport over the sand bodies as a consequence to targeted mining.

Ship Shoal, the largest sand body off the Louisiana shelf, was recently recognized as being unique from a sediment dynamic perspective in addition to its biological habitat, and likely has important implications for commercial fisheries (Kobashi *et al.* 2007b; Condrey and Gelpi 2008; Grippo *et al.* 2009; Kobashi *et al.* 2009a). The sand resources from the shoal can be a viable alternative for restoring the rapidly disintegrating Louisiana barriers and beaches (Kulp *et al.* 2001). Without such large-scale intervention Louisiana's barrier islands and marshlands are projected to be lost within the next 50 years or so (Kulp *et al.* 2001; Khalil *et al.* 2007).

Sand mining may cause a profound impact on the local physical and biological environments and hence understanding the prevailing hydrodynamics plays a key role to assess the impacts, given the lack of available scientific literature (Michel *et al.* 2001). Using a state-of-the-art numerical model, an attempt has been made to compare the hydrodynamics of the region corresponding to two contrasting bathymetric configurations: one with shoal and the other with the shoal completely and partially removed. It should be noted that complete sand removal from the shoal is not a realistic mining scenario even if the impacts were minimal, given the fact that there are numerous pipelines underneath the shoal. However, the extreme hypothetical comparison would provide an excellent opportunity to unveil the impact of shoal on the regional hydrodynamics.
We have implemented a coastal ocean model package, MIKE developed by DHI Water and Environment™ to investigate wave transformation and current variations on Ship Shoal (Figure 7.1); the wave model outputs were further used to discuss sediment re-suspension and transport. We also examined wave, current variability, and sediment transport over the shoal with respect to the bathymetry modification that was based on the proposed barrier island restoration scenarios (Table 7.1) (Khalil *et al.* 2007). Two representative energetic events were considered for the computations, namely, winter storms and tropical cyclones. We implemented the models during a winter storm in mid February, 2008 and a tropical cyclone Lili in 2002. Three mining areas on Ship Shoal are currently being proposed: South Pelto 12/13 (area A in Figure 7.1), Ship Shoal block 88/89 (area B in Figure 7.1), and Ship Shoal blocks 84/85/98/99 (area C in Figure 7.1). Those three areas are relatively free of pipelines (Khalil, S., personal communication; see also Figure 7.1 and Table 7.2).

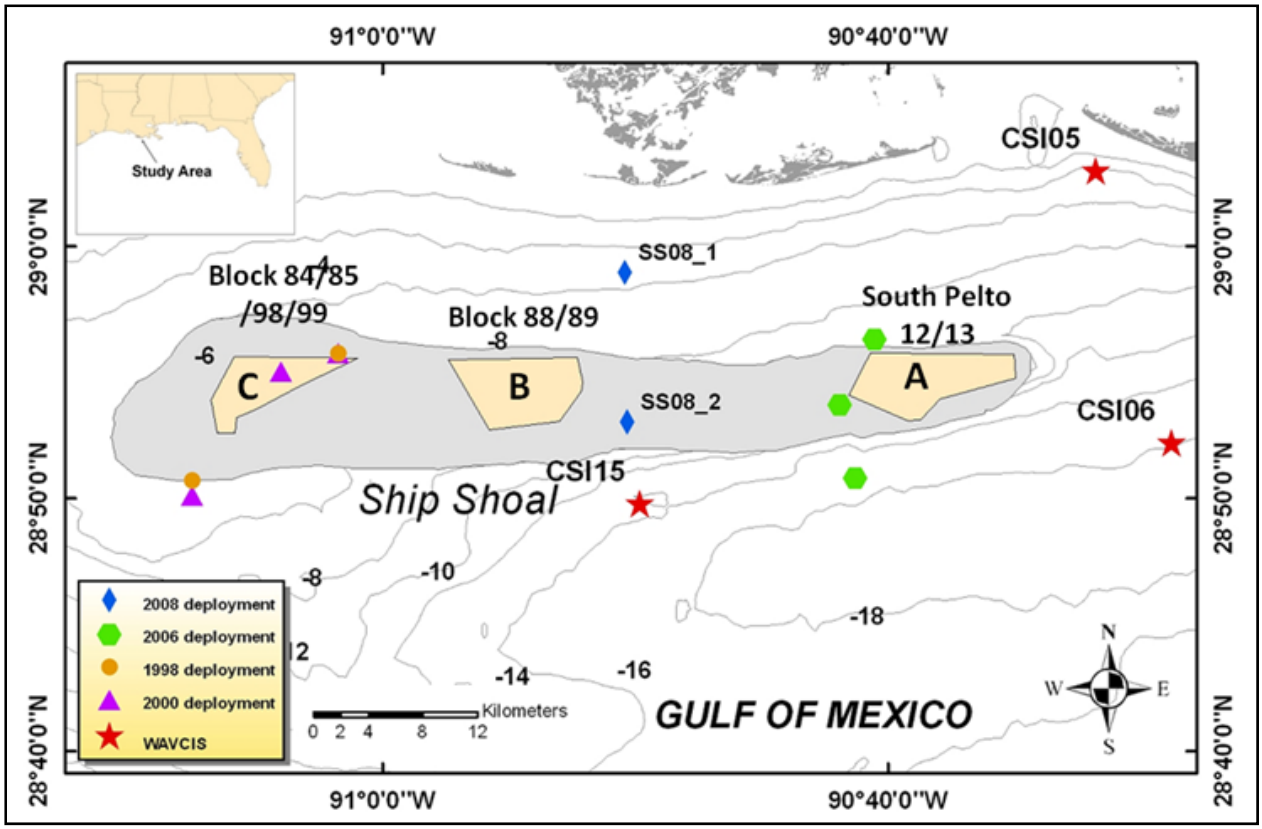


Figure 7.1 Proposed sand mining area: (A) South Pelto 13, (B) Ship Shoal Blocks 88/89, (C) Ship Shoal Blocks 84/85/98/99. Source: Khalil et al (2007).

Table 7.1

Louisiana barrier islands and restoration plans.

| Area | Restoration area | Rate of shoreline change (ft/yr) | Volume needed (yard$^3$) |
|---|---|---|---|
| **Caminada headland** | Caminada headland | -8.6 *[1] | 8.0-10.0 x $10^6$ |
| **Whisley Island** | Isles Dernieres | -89.0 *[1] | 4.0 x $10^6$ *[2] |
| **Trinity Island** | Isles Dernieres | -62.5 *[1] | 4.0 x $10^6$ *[2] |
| **Entire Isles Dernieres** | Isles Dernieres | -61.9 *[1] | 15.2 x $10^6$ *[3] |

*[1]Source: Penland et al (2005)

*[2]Source: Khalil *et al.* (2007)

*[3]Source: van Heeden *et al.* (1992)

Table 7.2

Ship Shoal Sand resources.

| Area | Restoration area | Volume ($yard^3$) | Total area ($m^2$) | Sand thickness (ft) |
|---|---|---|---|---|
| **South Pelto (A)** | Caminada Headland | $28.3 \times 10^6$ | $11.6 \times 10^6$ | 13-20 ft |
| **Blocks 88/89 (B)** | Whiskey/Trinity Islands | $>17.3 \times 10^6$ | $13.4 \times 10^6$ | 12-18 ft |
| **Blocks 84 (C)** | Whiskey/Trinity Islands | $11.2 \times 10^6$ | $24.7 \times 10^6$ | 13 ft |

Source: Khalil *et al.* (2007)

Geological and physical settings pertinent to our study area commonly exist for wide-continental shelves worldwide (e.g. U.S. east coast); hence, our findings and inferences can be extended to such similar environments.

## 7.2. WAVE-CLIMATE AND CURRENT VARIABILITY OVER THE INNER SHELF

Wave-climate and regional current variability were analyzed using in-situ data from various parts of the shoal and inner shelf prior to the model implementation. Data sources included instrument tripods deployed on the shoal and WAVCIS stations, CSIs-6 and 15 (Zhang 2003). The wave-climate for the study area is characterized by low-energy (e.g., Georgiou *et al.* 2005). The in-situ data from WAVCIS CSI-15 (2007/01/01-2008/10/01, 639 days) showed that approximately 89 percent of time (568.7 days) wind speed was less than 10 m $s^{-1}$, 11 percent (70.3 days) between 10 and 20 m $s^{-1}$, 0.13 percent (8.3 days) above 20 m $s^{-1}$ (severe storms). Wind predominantly blew from the northeast to the southeast (39 percent), but its direction was variable (Figure 7.2). Significant wave height (hereafter wave height) was mostly less than 1.0 m (68.3 percent) and only 2.0 percent of the wave height exceeded 1.5 m. Wave direction was mostly between the east and south (67.8 percent). The direction from the northern quadrant was associated with winter storms and to some extent with sea and land breeze interaction (Hsu 1988; Kobashi *et al.* 2005; Stone *et al.* 2005a). Current velocity was more spatially variable than waves and winds. Bottom and surface currents from the WAVCIS CSI-6 (2004/06/03-2008/09/01) was directed predominantly westward; the near bottom currents (1.5 m above the bottom) were varying directionally rapidly when compared to the surface currents (Figure 7.3c&d). Near bottom currents on Ship Shoal were more dynamic than the current fields off-shoal. The bottom current direction on the western flank of the shoal during winter 1998, directed predominantly north/south (cross-shore); the bottom currents on the eastern flank during spring 2006 prevailed to the north. For the near bottom currents on the middle shoal during winter 2008, predominant bottom current direction was westward.

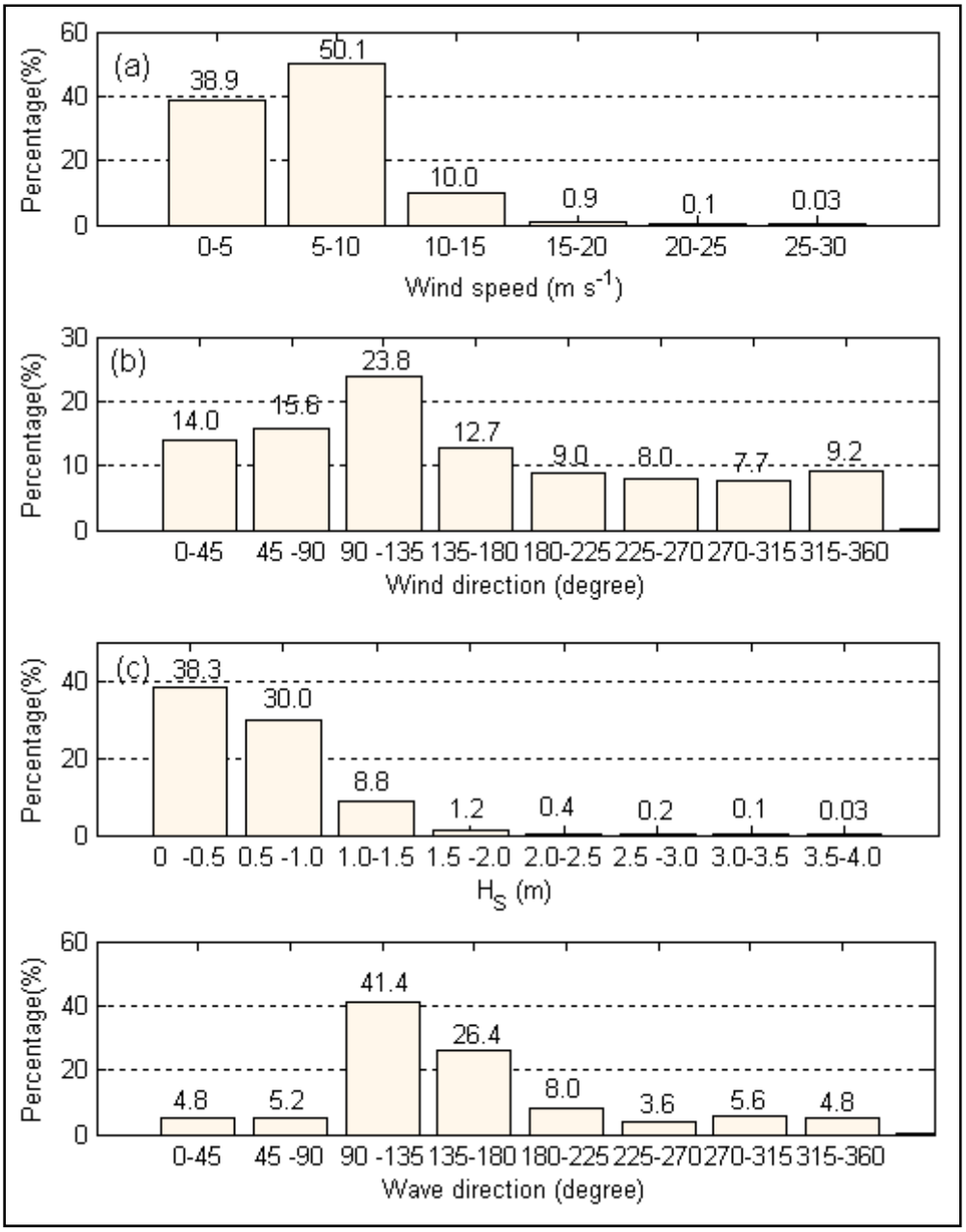


Figure 7.2 Histogram of wave-climate parameters: (a) Wind speed, (b) Wind direction, (c) Wave height, and (d) Wave directions between 2007/01/01 and 2008/10/01, 639 days. The numbers in the figure show percentages.

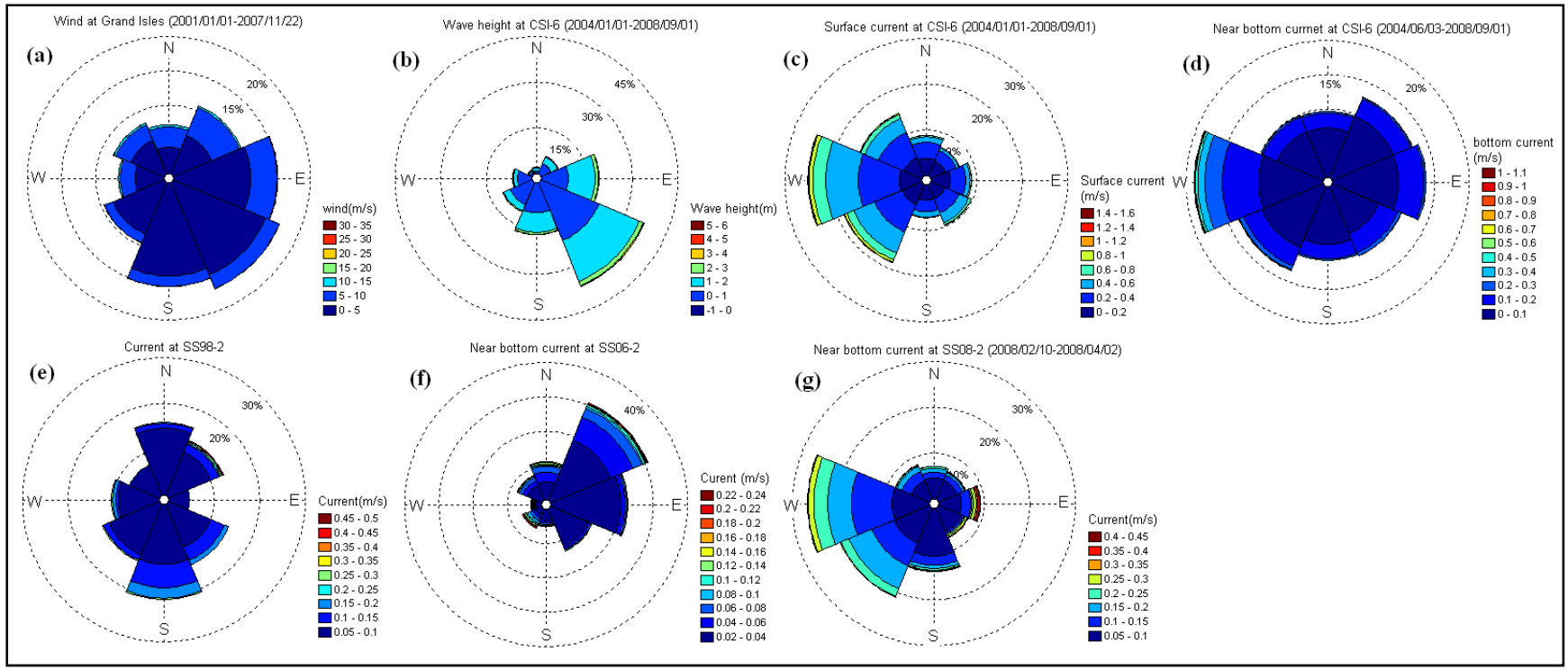


Figure 7.3 Polar plots pertaining to (a) winds at Grand Isle, (b) waves at CSI-6, (c) surface currents at CSI-6, (d) near bottom currents at CSI-6, (e) near bottom currents at SS98_2, (f) near bottom currents at SS06_2, (g) near bottom currents at SS08_2.

The observations indicate that current fields associated with the shoal are highly complicated, depending on the coastal boundary, wind conditions (speed, direction, storm intensity and duration), Coriolis force, and bottom topography (Csanady 1982; Swift and Niedoroda 1985; Kobashi and Stone 2008b). Detailed discussion on three- dimensional current variability over the inner shelf and the shoal is made in Kobashi and Stone (2008b).

## 7.3. MODEL EXPERIMENT

A third-generation spectral wave model, MIKE21 SW (hereafter SW) and a three-dimensional hydrodynamic model, MIKE3 HD (hereafter HD) were implemented in this study. Both models have been developed by DHI Water and Environment™. The SW model has been successfully implemented for the Gulf of Mexico and the Louisiana shelf (Jose and Stone 2006; Jose *et al.* 2007), as part of a wave forecasting study. The HD model has not been utilized for the Louisiana shelf to date. Detailed model descriptions including the models, domain, and input parameters as well as initial conditions are briefly described in the following sections.

### 7.3.1. SW Module

SW is a third-generation spectral wind wave model based on unstructured meshes. The unstructured mesh approach gives the model high degree of flexibility. The model solves the wave action balance equation, the spatial discretization of which is performed using an unstructured finite volume method. The integration over time is based on a fractional step approach, where the propagation steps are solved using an explicit method (Sorensen *et al.* 2004). The wind input, the main source function in the equation, is based on Janssen's quasi-linear theory of wind-wave generation (Janssen 1989; Janssen 1991) and implemented as in WAM Cycle 4. The non-linear energy transfer through the four-wave interaction is represented by the discrete interaction approximation (DIA) proposed by Hasselmann *et al.* (1985) (see also Komen *et al.* 1994). The dissipation due to white capping is implemented according to Hasselmann (1974) and further tuned according to Janssen (1989). Detailed description of all the source functions and the numerical methods used in the model are discussed in Sorensen *et al.* (2004).

### 7.3.2. HD Module

The HD module simulates water level variations and flows in response to a wide variety of forcing in lakes, estuaries, bay and coastal areas (DHI 2005). The module solves three dimensional incompressible Reynolds-averaged Navier-Stokes equation. The model consists of momentum and continuity equations. The model solves horizontal terms explicitly and vertical term implicitly (DHI 2005). Horizontal and vertical eddy viscosities were based on Smagorinsky formulation and k-ε equation, respectively (DHI 2005). Bed resistance is computed based on the

quadratic stress law. Vertical discretization can be selected from either equidistant, layer thickness, or variable grids, which consists of a uniform distribution, user specified distribution, and stretched and top/bottom specified distribution, respectively (DHI 2005). In the study, the equidistant discretization was used. More detailed model information is elaborated on in DHI (2005).

### 7.3.3. Model Domains

The model domain (origin: -91.25º W, 28.75º N) covered Ship Shoal, south of the Isles Dernieres barrier island chain, and three ocean observing stations (Figure 7.4). Two bathymetries were used: one with Ship Shoal (Figure 7.5 top) and the other without the shoal (Figure 7.5 bottom). The bathymetry without the shoal was developed based on the linear interpolation between the north and south edges of the shoal. The computational grids were unstructured triangular mesh grids with an embedded high resolution mesh grid encompassing the shoal boundary (Figure 7.4). The mesh size was based on the volume of grid each with maximal size of $2.0 \times 10^{-5}$ degree2 ($2.5 \times 10^{5}$ m$^2$) over the shoal and $2.0 \times 10^{-4}$ degree2 ($2.5 \times 10^{6}$ m$^2$) for the surrounding areas. For the HD, offshore mesh size was selected as $2.0 \times 10^{-3}$ degree2 ($2.5 \times 10^{7}$ m$^2$). In addition, a fine-resolution mesh was created for another case study embedded with finer resolution grids over the three proposed mining areas, with a maximal area of $5.0 \times 10^{-6}$ deg2 ($6.2 \times 10^{4}$ m$^2$) (not shown in Figure 7.4).

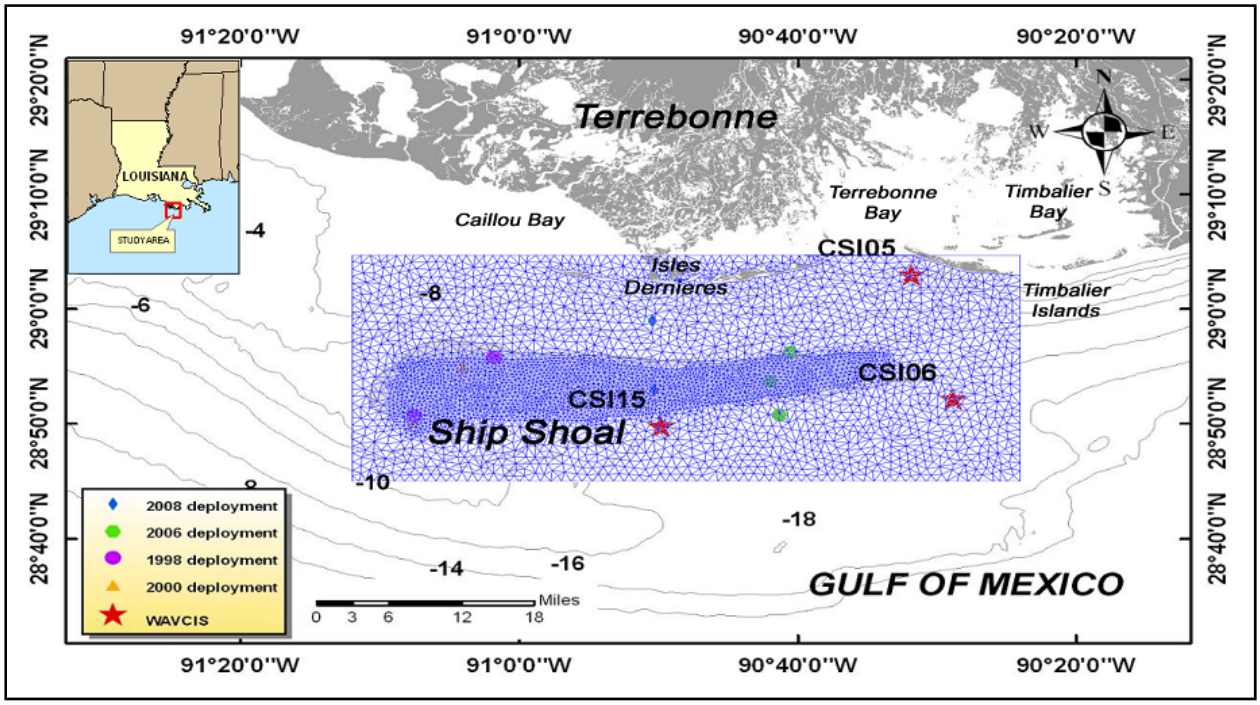

Figure 7.4 Map and computational grids.

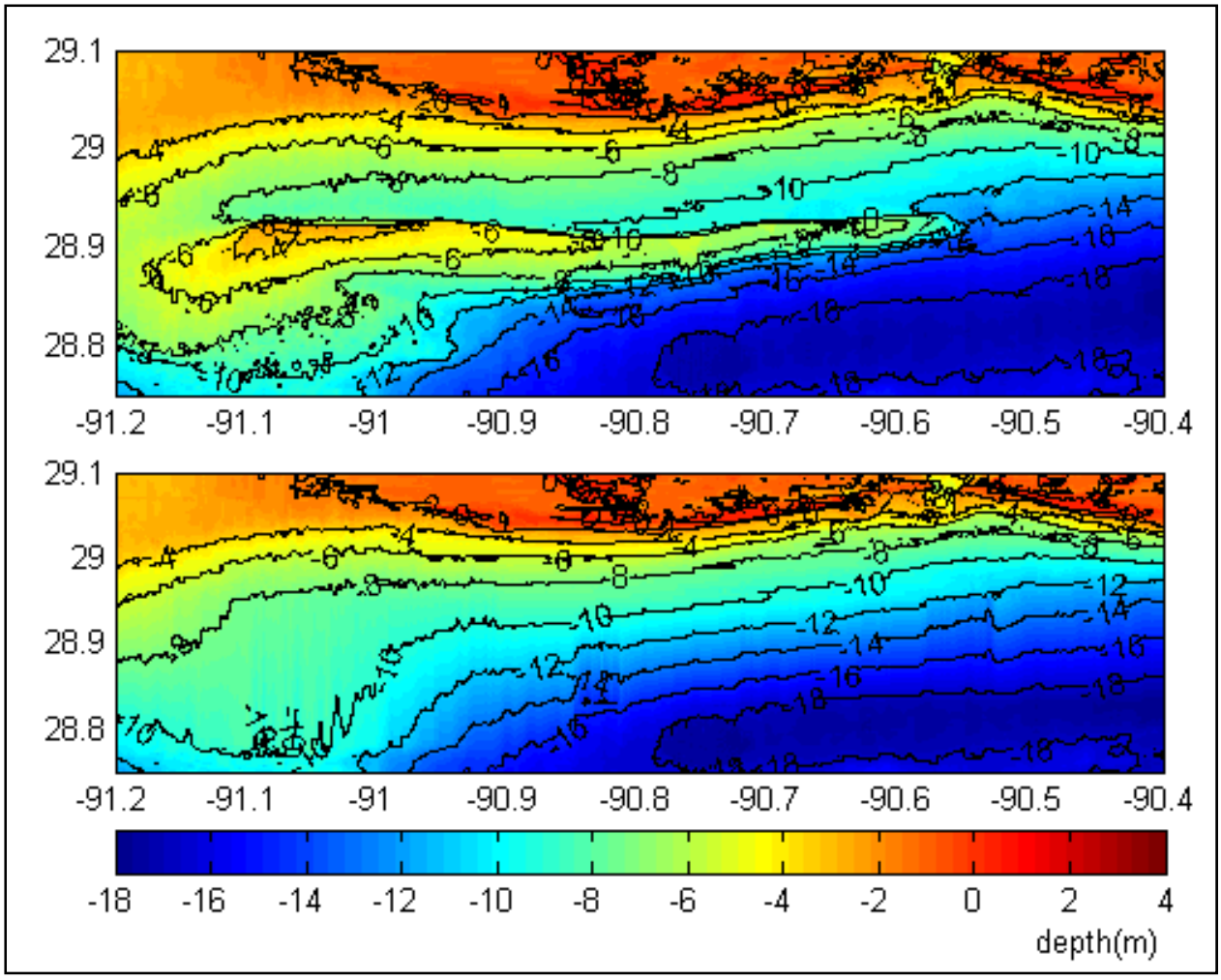


Figure 7.5 Bathymetry of model domain: with shoal (upper) and without shoal (lower).

For the case study A (Table 7.3), deep water boundary conditions were applied along the southern boundary and all three other boundaries (North, East and West) were selected as radiative boundaries for the SW model. The HD model had all four boundaries treated as closed boundaries (Table 7.4). The coastal wave model was nested with the Gulf of Mexico (GOM) regional model for the additional case studies (Case B1-B5 in Table 7.5). A detailed description of the regional wave model is addressed in Jose and Stone (2006). Although all boundaries were assigned as closed, for HD Model, the computational domain for HD model was selected much larger than the wave model (origin: -92.0°W, 28.0°N) in order to avoid vortex effects near the closed boundaries; however, we only used the same area as the wave model domain to discuss current variability over the shoal.

Table 7.3

Case study A: Wind condition (Constant in domain).

| Case | Speed (m/s) | Direction (degree) |
|---|---|---|
| A1 | 20 | NE(45), SE(135), SW(225), NW(315) |
| A2 | 15 | NE(45), SE(135), SW(225), NW(315) |
| A3 | 12 | NE(45), SE(135 ), SW(225), NW(315) |
| A4 | 10 | NE(45), SE(135), SW(225), NW(315) |
| A5 | 5 | NE(45), SE(135), SW(225), NW(315) |

Table 7.4

Case study A: Offshore wave boundary condition (South boundary).

| Case | $H_S$ (m) | $T_P$ (sec) | Direction (degree) |
|---|---|---|---|
| A1 | 6 | 11 | 135 |
| A2 | 4 | 9 | 135 |
| A3 | 3 | 7 | 135 |
| A4 | 2 | 6 | 135 |
| A5 | 1 | 5 | 135 |

Table 7.5

Ship Shoal sand mining scenarios.

| Case | Sand volume (x $10^6$ $m^3$) | Mining area | Excavation depth (m) | Restoration target |
|---|---|---|---|---|
| B-1 | 7.65 | A | 0.24 m | Caminada |
| B-2 | 13.76 | A | 0.43 m | Caminada, Whiskey/Trinity |
| B-3 | 6.12 | B | 0.21 m | Wiskey/Trinity Islands |
| B-4 | 9.18 | B | 0.31 m | Entire Isles Dernieres |
| B-5 | 9.18 | C | 0.37 m | Entire Isles Dernieres |

### 7.3.4. Input Parameters and Initial Conditions

Input parameters were carefully selected from various data sources. For both GOM regional and high resolution coastal models, wind data from a re-analyzed hindcast model by NOAA NCEP (North America Regional Reanalysis: NARR) were used (cf. Mesinger *et al.* 2006). The wind friction coefficient was selected as the constant value of 0.003 rather than linearly varying coefficients based on a calibration study. Bathymetry data from the NGDC (National

Geophysical Data Center) coastal relief model (Divins and Metzger 2008) were initially used; however, the preliminary results indicate that the bathymetry over the domain has significantly changed with the maximum difference is in the order of meters in magnitude with a mean difference of approximately 0.5 m. We corrected the bathymetry by krigging the difference in the bathymetry between the NGDC data and in-situ data from ocean observing stations as well as the bathymetry data obtained from the Louisiana Department of Natural Resources (LDNR); the adjusted NGDC data were used as the offshore bathymetry. For the GOM model, ETOPO2 bathymetry was also used. For keeping initial conditions of all model cases to be consistent, bottom friction for the SW model was estimated from a constant Nikraudse roughness height of 0.04 m rather than that from grain diameters based on Nielsen (1979); results of our preliminary model implementation showed little difference in the result between the two friction factors. For HD, the bottom friction was estimated from quadratic stress law using bottom drag coefficient. Water level was obtained from GOM regional modeling for each boundary (east, west, north, and south). The HD was implemented as a barotropic mode and density changes (e.g. stratification) were not considered (*i.e.*, wind-induced currents). Also, for simplicity, the effects of waves on currents were not included. The time step was selected as 150 seconds for the SW and 10 seconds for the HD. It should be noted that the MIKE 21 SW wave model is not capable of simulating waves over a muddy seabed, which is the case for the Louisiana shelf (e.g., Sheremet and Stone 2003). Therefore, wave dissipation over muddy bottoms is not discussed in this paper.

### 7.3.5. Case Studies

Various wave-climate conditions, mainly following Stone and Xu (1996), were selected to implement the wave and hydrodynamic models for two bathymetric configurations: one with the shoal and one without the shoal in the computational grids. For both models, five wind conditions, namely, severe storms (case A1), strong storms (case A2), moderate storms (case A3), weak storms (case A4), and fair weather (case A5) were selected (see Table 7.3). Stone and Xu (1996) concluded from their case study, which consists of offshore waves propagating from three different directions along the southern boundary, that the waves from the southeast along with predominant southeast winds yielded maximal changes in wave refraction and the highest dissipation rates. In this study, deepwater wave boundary conditions were selected as the southeast waves (*i.e.*, 135 degrees) along the southern boundary (Figure 7.4 and Table 7.4). Constant winds in the domain were incorporated for varying wind speeds and directions listed in Table 7.4. In general, currents over the inner shelf and shoal are highly associated with persistent winds during storms given the fact that tidal currents are generally weak. In this study, four wind directions were selected based on wave climate results as shown in Figures 7.4&7.5 and Table 7.3. Wave model results were further analyzed to estimate sediment re-suspension intensity (RI). In addition, another case study that was based on proposed restoration scenarios (Table 7.5) was implemented. Two representative storms were selected: winter storms (2008/02/25-2008/03/07) and tropical cyclones Isidore and Lili (2002/09/23-2002/10/06). Four scenarios based on different bathymetries were carried out in order to examine impacts of potential sand mining on waves and currents (see Table 7.5).

### 7.3.6. Skill Assessment of the Models

Model validation was conducted using various in-situ data from deployed instruments (SS08_2 in Figure 7.1), and an in-situ observing station, WAVCIS CSI-15 (see the location in Figure 7.1). The validation included visual comparison of both time series data (Figure 7.6) as well as statistical analysis (Table 7.6). It is reported that the widely-used correlation coefficient often cannot evaluate the model well and a small difference between model results and measured data can result in a substantial change in the coefficient (Wilmott 1982). Therefore, instead of the correlation coefficient, the following statistical parameter (Iw in equation 7-1) proposed by Wilmott (1982), and an error function (ε in equation 5-2, see also Johnson *et al.* 2005) in addition to the linear regression coefficient ($r^2$) were used to evaluate the model performance.

$$Iw = 1 - \frac{\sum_{k=1}^{N} (V_{\mathrm{mod}\,el} - V_{measured})^2}{\sum_{k=1}^{N} [\,|\, V_{\mathrm{mod}\,el} - \overline{V}_{measured} \,|\, + |\, V_{measured} - \overline{V}_{measured} \,|\,]^2} \quad \text{..... (7-1)}$$

Where Vmodel, Vmeasured, and  are simulated, measured, and mean values, respectively. N is the number of data. If the two parameters are correlated well, Iw becomes close to 1. The error function was computed based on the following equation. If the values are well correlated, the value approaches 0.

$$\varepsilon = \left[ \frac{\sum_{k=1}^{N} (V_{\mathrm{mod}\,el} - V_{measured})^2}{\sum_{k=1}^{N} (V_{measured})^2} \right] \quad \text{..... (7-2)}$$

Table 7.6

Skill assessment of model results at CSI-15.

| **Parameters** | **Station** | $\mathbf{I_W}$ | **ε** | $\mathbf{r^2}$ |
|---|---|---|---|---|
| Wind speed | CSI-15 | 0.8837 | 0.0697 | 0.7291 |
| Wind direction | CSI-15 | 0.9092 | 0.0917 | 0.7192 |
| Significant wave height | SS08_2 | 0.9343 | 0.0567 | 0.7695 |
| Peak wave period | SS08_2 | 0.7968 | 0.0462 | 0.4638 |
| Wave direction | SS08_2 | 0.6363 | 0.1637 | 0.1168 |
| Surface east current | SS08_2 | 0.7653 | 0.4426 | 0.4154 |
| Surface north current | SS08_2 | 0.7773 | 0.5338 | 0.5225 |
| Bottom east current | SS08_2 | 0.4696 | 4.5675 | 0.1032 |
| Bottom north current | SS08_2 | 0.3283 | 3.3434 | 0.0035 |
| Water level | SS08_2 | 0.8788 | 0.3549 | 0.6650 |
| | CSI-15 | 0.9616 | 0.1504 | 0.8944 |
| Sea surface slope | CSI-6 – CSI-15 | 0.6687 | 0.7195 | 0.2683 |
| | CSI-5 – CSI-6 | 0.7723 | 0.6783 | 0.3843 |

Figures 7.6a and 7.6b show comparisons between the measured and the simulated values of various parameters including wave height, peak period and mean wave direction as well as wind speed, wind direction, water level and surface and bottom currents at the shoal crest (SS08_2) and CSI-15 (see locations in Figure 7.1). Wind data from the in-situ data and the NARR wind data were in good agreement except during storm peaks when the NARR wind speed was often lower than the in-situ data as also reported by Jose *et al.* (2007) (Figure 7.6). The model result provided high IW values (*i.e.*, the values close to 1) and low ε values (*i.e.*, the values close to 0) for wind parameters.

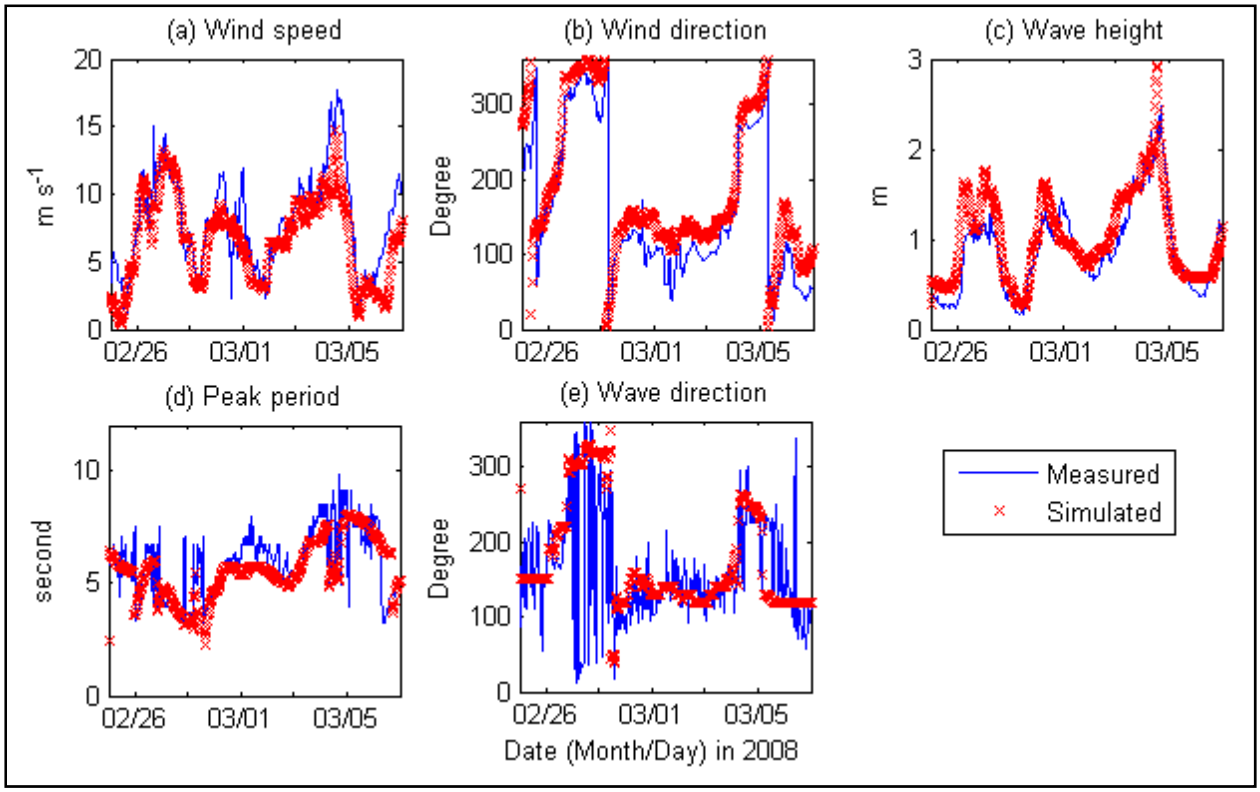


Figure 7.6a Model validation of (a) wind speed, (b) wind direction, (c) wave height, (d) peak wave period, and (e) wave direction (MIKE 21 SW).

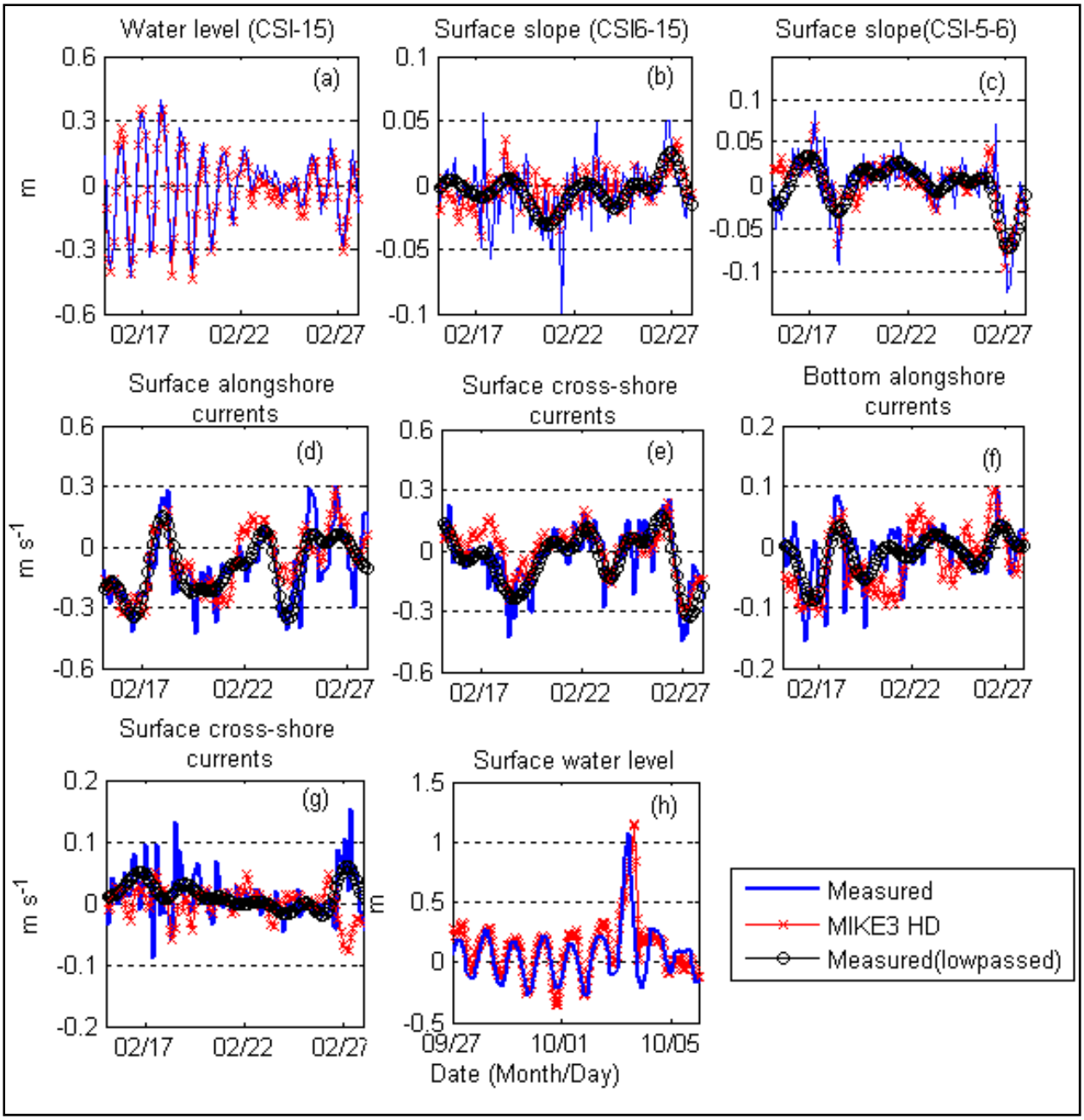


Figure 7.6b Model validation of (a) water level, (b) alongshore surface slope, (c) cross-shore surface slope, (d) alongshore current (surface), (e) cross-shore current (surface), (f)alongshore current (bottom), (g) cross-shore current (bottom), (h) water level during hurricane Lili (MIKE21/3 HD).

For the spectral wave model, all measured and simulated wave parameters agreed reasonably well (Table 7.6). The model result provided high IW values and low ε values for bulk wave parameters. Considering the fact that the model cannot simulate waves over muddy bottoms, it is

reasonable to say that the wave model performs well for the study area. For the HD model, simulated surface current and water level were in general agreement with the measured data (Table 7.6) also supported by high IW values and low ε values; however, simulated bottom cross-shore current showed a low correlation (IW=0.33, ε=3.34, $r^2$=0.0035) with in-situ data probably due to inaccuracy of the bathymetry despite its correction. Simulated sea surface slope for cross-shore and alongshore both agreed well with measured data. Overall, the HD model performed well even if the density changes were not considered.

## 7.4. RESULTS AND DISCUSSION

### 7.4.1. Wave Transformation over the Shoal

Incoming deep water waves significantly transformed as they propagated over complex coastal bathymetry (Figure 7.7). Spatial differences in wave transformation were similar for all cases although having differences in magnitude (Table 7.7). Particular attention was paid to spatially-varying wave dissipation and refraction for different bathymetries. The wave model results provided similar results as given in Stone and Xu (1996). In Figure 7.7, wave height and wave vector distributions with shoal (Figure 7.7 top), and without shoal (Figure 7.7 bottom) were presented. When the wave height was high (Case A1 in Figure 7.7a&b), substantial wave refraction on the western flank of the shoal was clearly evident compared to that without the shoal. As the deep water wave height decreased, the difference became less evident. On the middle and eastern flank of the shoal the difference in the refraction with and without the shoal was minimal (Figure 7.7). The wave height on the western flank of the shoal was significantly smaller than that on the eastern shoal (up to 32 percent difference between the east and west). When the shoal existed, the difference was up to 9 percent higher than the difference without the shoal. The difference decreased as the deep water wave height decreased (Table 7.7). Wave height and wave energy dissipation between south and north of the shoal, as a general trend, decreased from the west toward east except during case 1 for which the dissipation was minimum due to wave dissipation along the seaward boundary of the western shoal, which was significantly shallower than the middle and eastern flank of the shoal. For case A1, the difference in wave height was approximately 34 percent higher on the middle shoal than the eastern flank of the shoal. The dissipation in wave height along the western flank of the shoal was approximately 70 percent higher than that on the eastern flank; while, for the model result without the shoal, the difference in the height was significantly smaller (Table 7.7). Wave energy dissipation showed similar results and maximal difference was 52 percent for the bathymetry with shoal and 9 percent for that without shoal (Table 7.7). The above results indicate that the shoal has significant influence on wave dissipation. The above results further influenced sediment re-suspension on the shoal and which is discussed in the section 7.4.3.

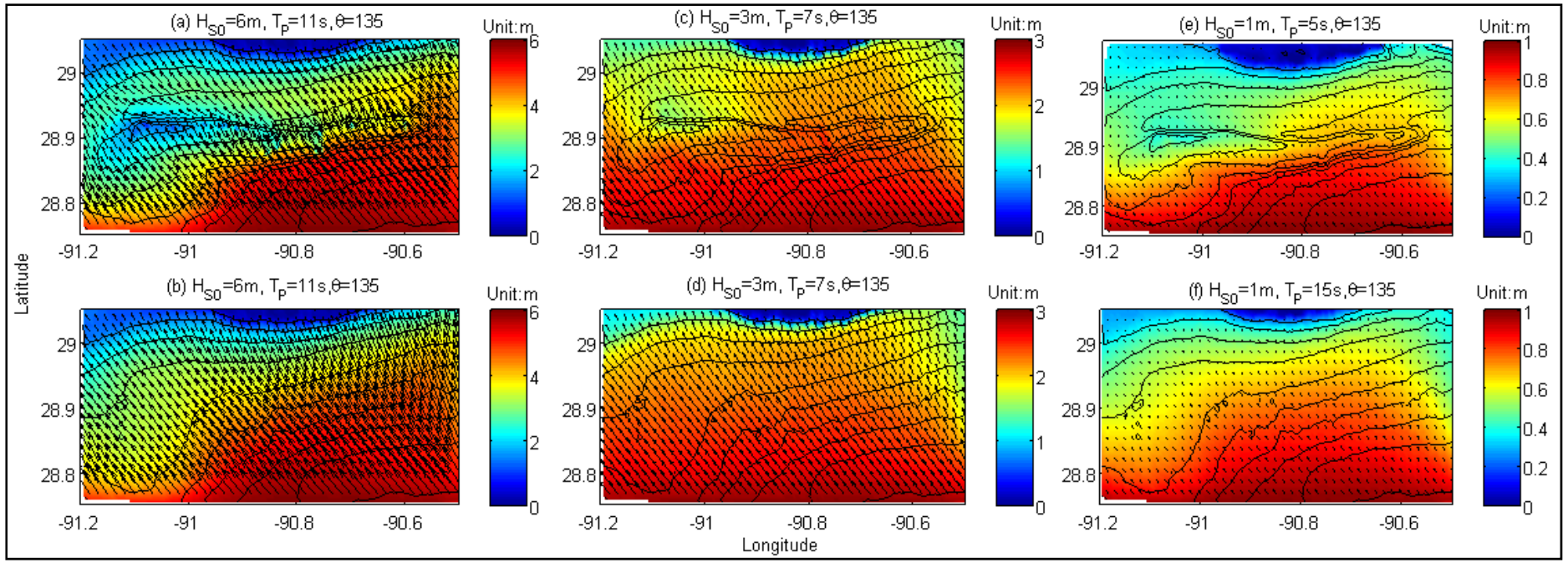


Figure 7.7 Wave height and vector distributions for case A study: (a, b) $H_S$=6m, $T_P$=11 s, Wave direction=135 (degree). (c, d) $H_S$=3 m, $T_P$=7s, Wave direction=135 (degree), (e, f) $H_S$=1m, $T_P$=5 s, Wave direction=135 (degree). Top figures represent the result with shoal and bottom figures the result without shoal.

Table 7.7

MIKE21 SW model result with shoal (left) and without shoal (right).

| Parameter | Case | West | Middle | East | Outside |
|---|---|---|---|---|---|
| $H_S$ (m) | A1 | 1.93 (3.32) | 2.75 (4.46) | 3.85 (4.70) | 5.20 (5.17) |
| | A2 | 2.15 (3.03) | 2.91 (3.41) | 3.23 (3.29) | 3.66 (3.59) |
| | A3 | 2.01 (2.31) | 2.34 (2.35) | 2.21 (2.22) | 2.55 (2.52) |
| | A4 | 1.36 (1.43) | 1.47 (1.41) | 1.38 (1.41) | 1.70 (1.67) |
| | A5 | 0.49 (0.63) | 0.64 (0.77) | 0.70 (0.73) | 0.87 (0.85) |
| PWD (degree) | A1 | 140.0 (140.0) | 150.0 (140.0) | 150.0 (126.3) | 140.0 (130.0) |
| | A2 | 140.4 (140.0) | 150.0 (140.0) | 150.0 (124.2) | 140.0 (130.0) |
| | A3 | 150.0 (130.0) | 150.0 (140.0) | 150.0 (122.1) | 140.0 (130.0) |
| | A4 | 140.7 (140.0) | 140.0 (140.0) | 150 9 (110.8) | 140.0 (138.0) |
| | A5 | 140.0 (140.0) | 140.0 (140.0) | 150.0 (109.1) | 140.0 (139.0) |
| ΔHs<br><br>Upper: ΔHs/Hs,<br><br>Lower: ΔHs (m) | A1 | 0.21 (0.08)<br>0.63 (0.27) | 0.37 (0.32)<br>1.90 (1.64) | 0.25 (0.17)<br>1.26 (0.86) | - |
| | A2 | 0.42 (0.13)<br>1.32 (0.41) | 0.23 (0.13)<br>0.84 (0.46) | 0.12 (0.11)<br>0.41 (0.37) | - |
| | A3 | 0.35 (0.13)<br>0.89 (0.33) | 0.16 (0.13)<br>0.41 (0.32) | 0.14 (0.16)<br>0.33 (0.39) | - |
| | A4 | 0.20 (0.15)<br>0.31 (0.23) | 0.19 (0.22)<br>0.32 (0.36) | 0.24 (0.23)<br>0.40 (0.36) | - |
| | A5 | 0.37 (0.18)<br>0.26 (0.12) | 0.31 (0.23)<br>0.27 (0.20) | 0.23 (0.21)<br>0.19 (0.18) | - |
| RI ($N\ m^{-2}$) | A1 | 0.97 (1.31) | 1.20 (1.42) | 1.50 (1.40) | 1.39 (1.40) |
| | A2 | 1.03 (1.13) | 1.27 (0.95) | 1.18 (0.75) | 0.73 (0.78) |
| | A3 | 0.90 (0.60) | 0.92 (0.27) | 0.45 (0.10) | 0.14 (0.18) |
| | A4 | 0.16 (-0.05) | 0.03 (-0.14) | -0.14 (-0.18) | -0.14 (-0.13) |
| | A5 | -0.11 (-0.11) | -0.15 (-0.15) | -0.19 (-0.19) | -0.15 (-0.15) |

$H_S$: Significant wave height, PWD: peak wave period, $\Delta H_S$: wave dissipation, RI: Re-suspension intensity.

### 7.4.2. Variability of Currents over the Shoal

Simulated current fields varied primarily with wind speeds and directions (Figures 7.8a-d); however the current pattern was more associated with the wind direction than the wind speed. Surface currents generally followed prevailing wind regardless of their speed (Figures 7.8a and 8d). For instance, when northeast winds blew, southwest currents on the eastern flank of the shoal and westward currents on the western flank of the shoal prevailed at the surface (Figure 7.8). The surface currents tend to move toward isobaths; such characteristics were also reported over the northern Gulf coasts, e.g., off the southwest pass (Adams *et al.* 1987), off the Alabama coast (Byrnes *et al.* 2004), and over the western Florida shelf (Marmorino 1983). Bottom

currents were more variable and strongly influenced by the shoal bathymetry particularly on the western shoal. Both surface and bottom currents were stronger over the shallower shoal than the surrounding shoal because of flow acceleration due to the shoal topography, to satisfy continuity despite increases in bottom friction (Table 7.8) (Swift 1985; Snedden and Dalrymple 1999). Data indicate that without the shoal, general spatial patterns of both surface and bottom currents were similar. The surface currents on the western portion of the shoal were higher than those on the eastern flank of the shoal as with the result with the shoal in the computational grid; however, the flow acceleration over the shoal was not evident as seen from the model result with the shoal. Modification of the bottom currents with respect to the inner shelf topography was also not evident.

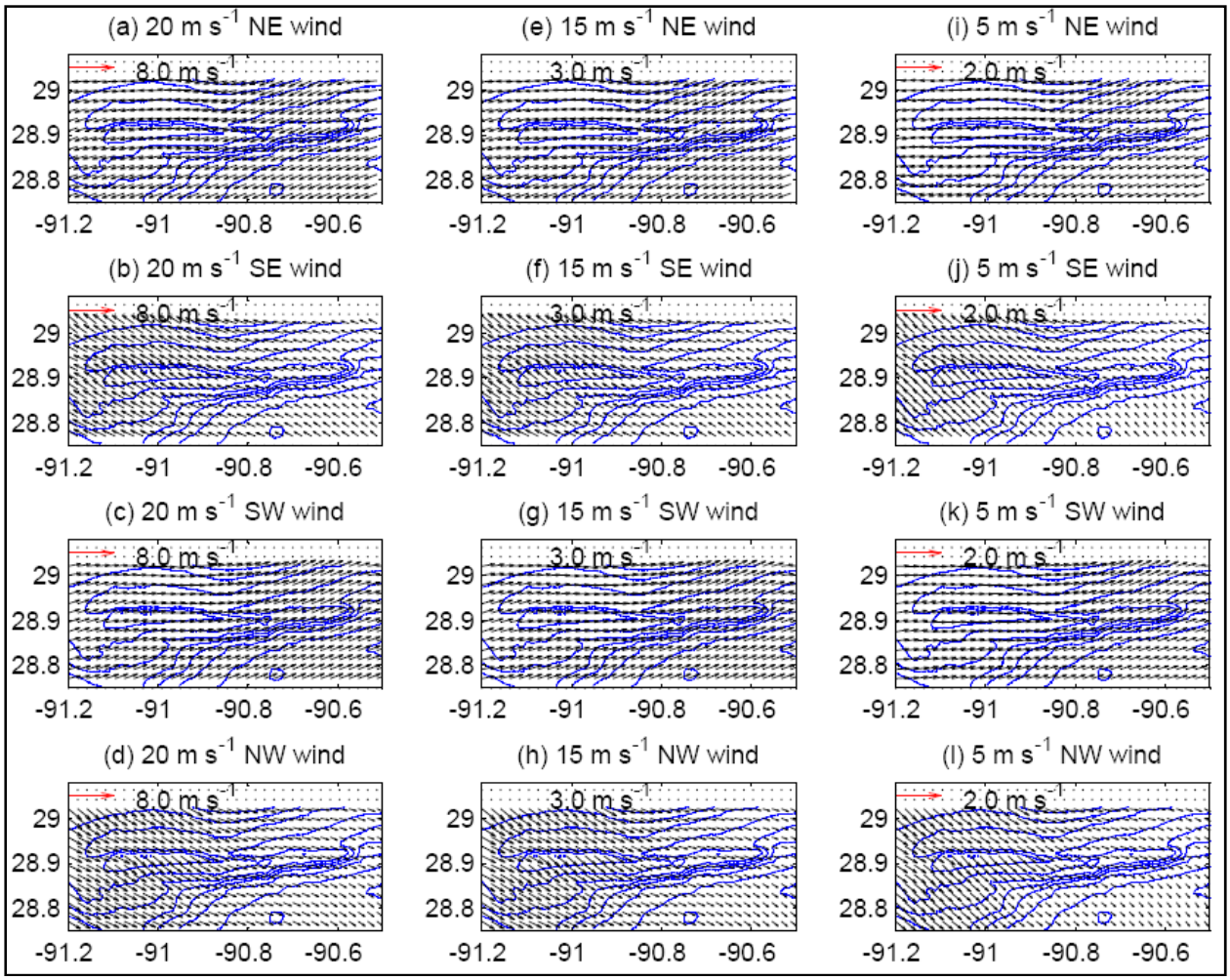

Figure 7.8a Surface currents with shoal for various wind speeds and directions.

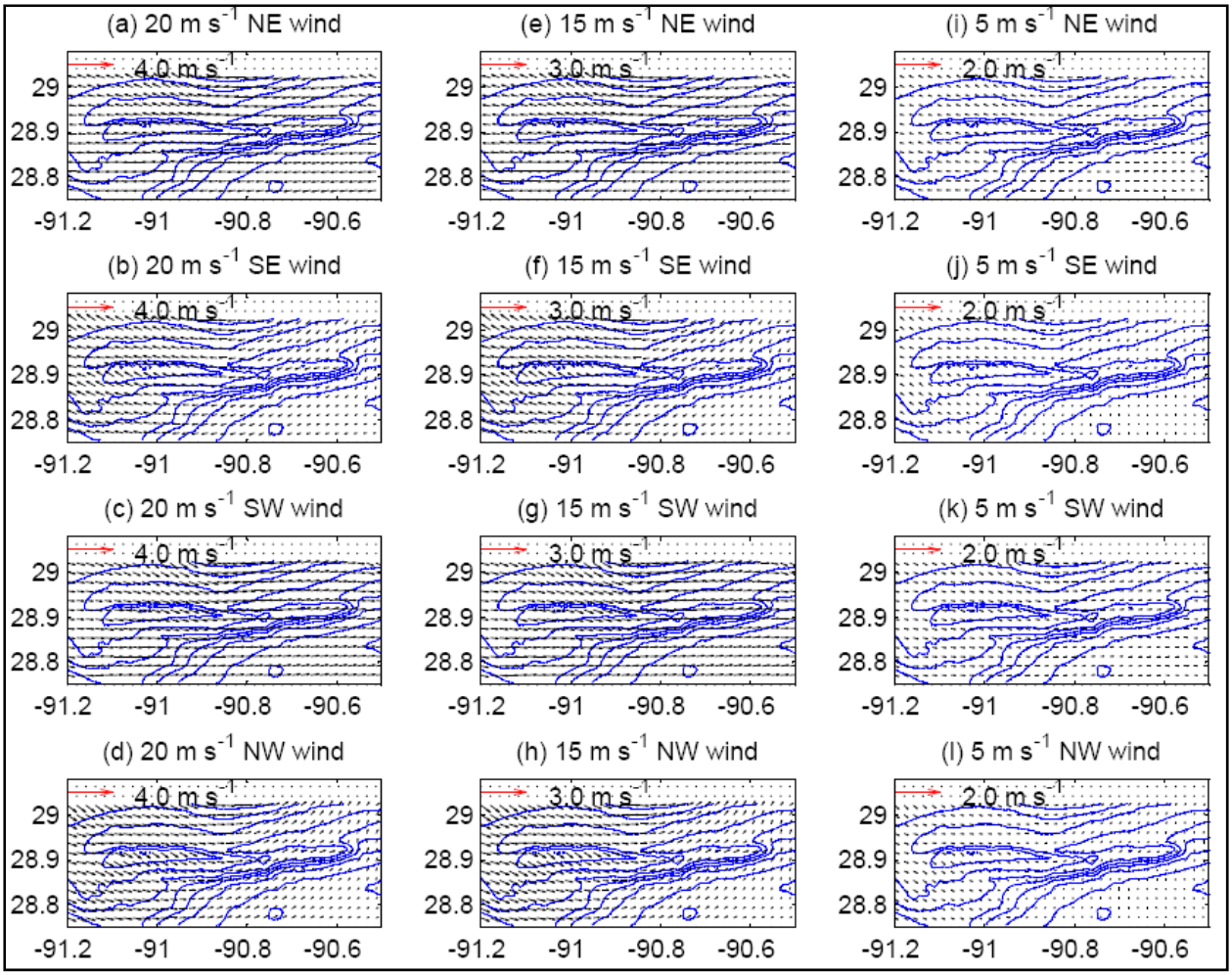


Figure 7.8b Bottom currents with shoal for various wind speeds and directions.

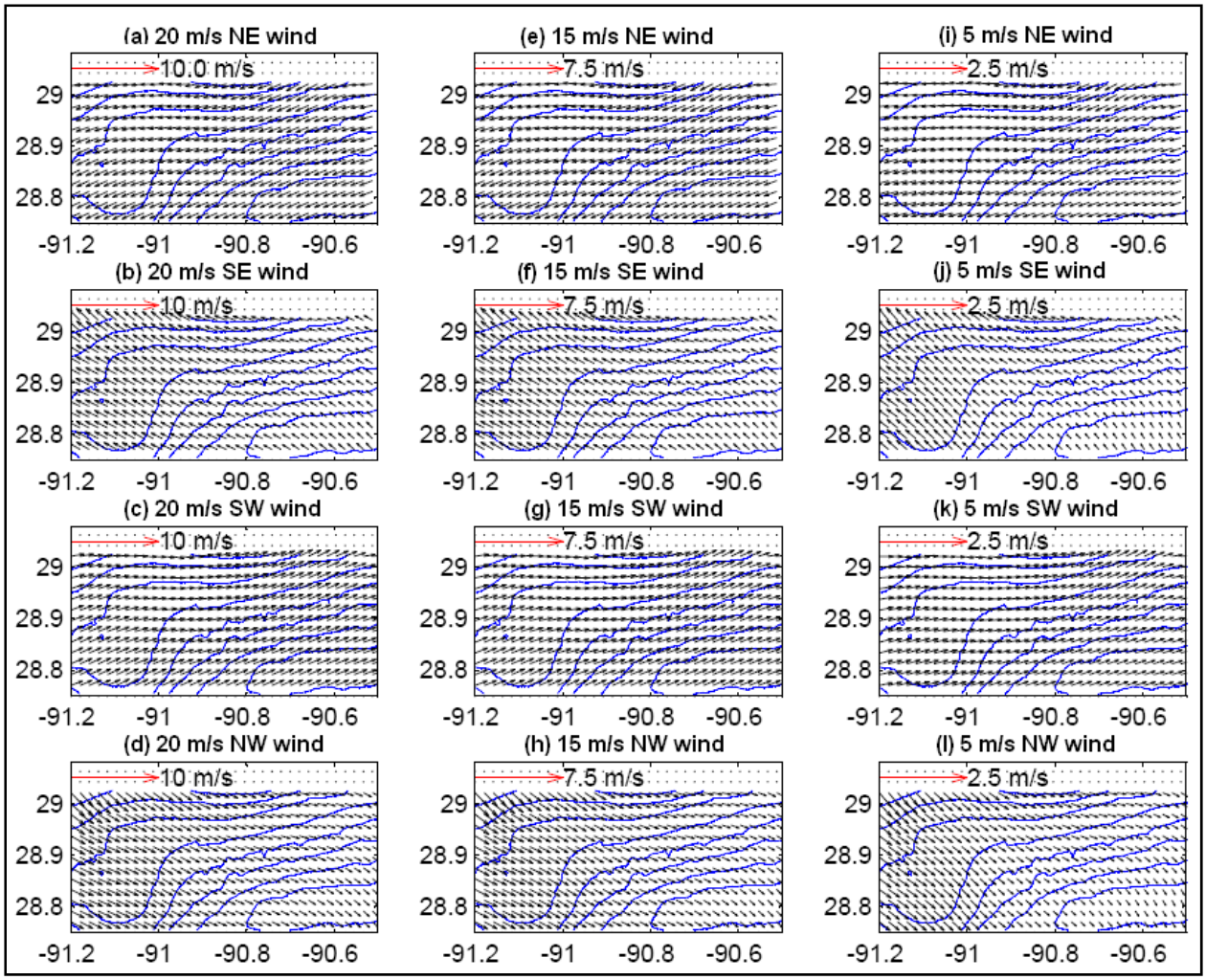


Figure 7.8c Surface currents without shoal for various wind speeds and directions.

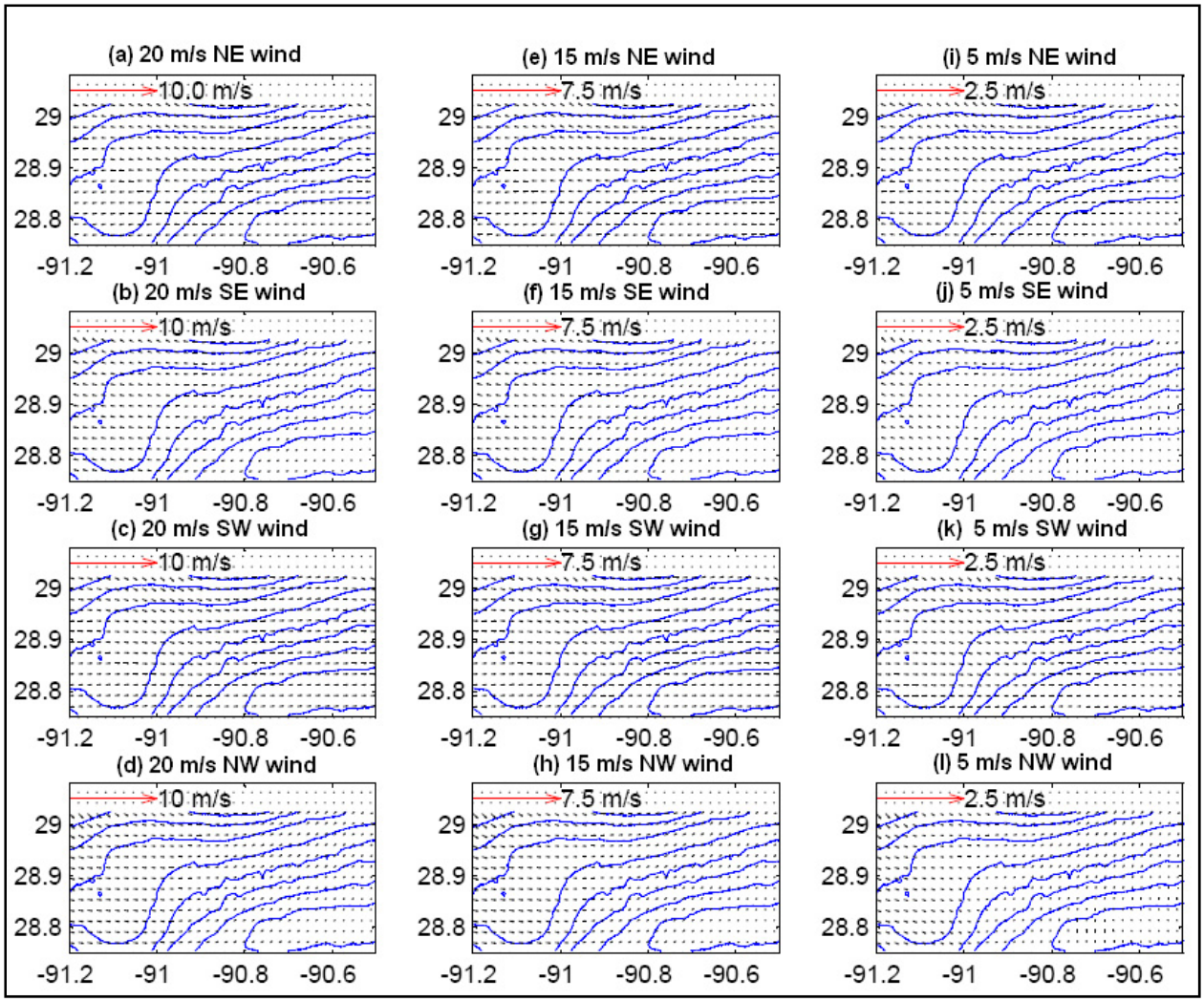


Figure 7.8d Bottom currents without shoal for various wind speeds and directions.

Water fluxes for both u-component (P flux on Table 7.8) and v-component (Q flux on Table 7.8) were high on the western shoal and during high winds; they decreased from the west to east and as the wind speeds decreased (Table 7.8). The alongshore flux was high when the winds blew from the northeast and southwest. In addition, the alongshore flux was significantly higher than cross-shore flux, suggesting the importance of alongshore component of the winds on current variability over the shoal. This can be attributed to the isobaths which trend northeast-southwest, since the currents tend to flow toward the isobaths as a result of geostrophic adjustments (Csanady 1982; Swift 1985; Unoki 1994). Whereas, cross-shore flux was significantly smaller, but much more variable than the alongshore flux (Table 7.8). Overall, the results with and without the shoal had similar variability in terms of the current variations and the fluxes; the difference in the fluxes for two bathymetries was small. The result suggests that neither large-scale nor small-scale sand mining should give rise to abrupt changes in current patterns, but the large-scale sand mining can change the magnitude of the velocity and therefore, fluxes. This current variability has further implications for sediment transport over the shoal.

Table 7.8

M3 HD model result with shoal (left) and without shoal (right)

| Parameter | Wind Speed | Wind direction | Western shoal | Middle shoal | Eastern shoal | Outside (offshore) |
|---|---|---|---|---|---|---|
| P flux (u-component) ($m^2s^{-1}$) | 20 m $s^{-1}$ | NE | -6.36, -6.08 | -3.86, -5.04 | -2.69, -4.53 | -2.12, -3.50 |
| | | SE | -1.81, -2.09 | -2.58, -2.97 | -2.12, -3.06 | -1.90, -3.17 |
| | | SW | 6.44, 6.15 | 4.00, 5.21 | 2.71, 4.71 | 2.17, 3.51 |
| | | NW | 1.85, 2.10 | 2.36, 2.84 | 1.96, 2.79 | 1.75, 3.06 |
| | 15 m $s^{-1}$ | NE | -4.62, -4.44 | -2.89, -3.76 | -2.03, -3.40 | -1.60, -2.65 |
| | | SE | -1.22, -1.43 | -1.86, -2.10 | -1.53, -2.16 | -1.37, -2.29 |
| | | SW | 4.68, 4.49 | 2.97, 3.85 | 2.01, 3.50 | 1.62, 2.65 |
| | | NW | 1.28, 1.46 | 1.72, 2.03 | 1.45, 2.01 | 1.30, 2.26 |
| | 10 m $s^{-1}$ | NE | -2.89, -2.79 | -1.90, -2.45 | -1.34, -2.24 | -1.08, -1.78 |
| | | SE | -0.67, -0.81 | -1.16, -1.25 | -0.96, -1.29 | -0.86, -1.43 |
| | | SW | 2.91, 2.81 | 1.93, 2.49 | 1.32, 2.28 | 1.07, 1.78 |
| | | NW | 0.73, 0.84 | 1.08, 1.23 | 0.92, 1.21 | 0.83, 1.43 |
| | 5 m $s^{-1}$ | NE | -1.18, -1.16 | -0.89, -1.10 | -0.64, -1.03 | -0.52, -0.87 |
| | | SE | -0.20, -0.26 | -0.50, -0.49 | -0.42, -0.47 | -0.34, -0.56 |
| | | SW | 1.18, 1.16 | 0.89, 1.10 | 0.62, 1.03 | 0.52, 0.87 |
| | | NW | 0.23, 0.28 | 0.47, 0.49 | 0.41, 0.44 | 0.34, 0.57 |
| Q flux (v-component) ($m^2s^{-1}$) | 20 m $s^{-1}$ | NE | -0.77, -0.59 | -1.02, -0.96 | -0.33, -0.20 | 0.06, -0.20 |
| | | SE | -0.13, 0.46 | -0.13, -0.18 | 0.55, 0.27 | 1.40, 1.03 |
| | | SW | 0.85, 0.63 | 0.91, 0.93 | 0.25, 0.13 | -0.13, 0.05 |
| | | NW | 0.38, -0.27 | 0.40, 0.29 | -0.56, 0.29 | -1.30, -0.81 |
| | 15 m $s^{-1}$ | NE | -0.50, -0.38 | -0.73, -0.69 | -0.21, -0.12 | 0.11, -0.07 |
| | | SE | -0.14, 0.29 | -0.11, -0.15 | 0.40, 0.18 | 1.05, 0.77 |
| | | SW | 0.57, 0.40 | 0.67, 0.67 | 0.18, 0.09 | -0.13, 0.02 |
| | | NW | 0.29, -0.18 | 0.30, 0.22 | -0.44, -0.23 | -1.01, -0.66 |
| | 10 m $s^{-1}$ | NE | -0.26, -0.18 | -0.45, -0.43 | -0.11, -0.06 | 0.12, 0.01 |
| | | SE | -0.10, 0.17 | -0.09, -0.11 | 0.26, 0.09 | 0.70, 0.52 |
| | | SW | 0.29, 0.20 | 0.43, 0.42 | 0.10, 0.05 | -0.13, -0.01 |
| | | NW | 0.19, -0.12 | 0.21, 0.15 | -0.30, 0.14 | -0.70, -0.48 |
| | 5 m $s^{-1}$ | NE | -0.07, -0.04 | -0.19, -0.18 | -0.03, -0.02 | 0.11, 0.06 |
| | | SE | -0.04, 0.09 | -0.05, -0.06 | 0.11, 0.003 | 0.35, 0.28 |
| | | SW | 0.07, 0.04 | 0.19, 0.18 | 0.02, 0.007 | -0.11, -0.05 |
| | | NW | 0.08, -0.07 | 0.11, 0.08 | -0.13, -0.03 | -0.36, -0.26 |

### 7.4.3. Re-suspension of Bottom Sediments

Changes in sediment re-suspension have strong implications for sediment transport and bed characteristics. We estimated sediment re-suspension (RI) from the computed bulk wave

parameters defined as wave-induced shear stress subtracted by critical shear stress. Wave shear stress was estimated from Madsen (1976) and the critical shear stress for sand bottoms (grain diameter coarser than 63 microns ($63 \times 10^{-6}$ m)) were estimated based on Li *et al.* (1997). The critical stress for sediments finer than 63 microns was chosen as a constant value of 0.15 (N $m^{-2}$) (Kobashi and Stone 2008b). Results are summarized in Table 7.7 and also illustrated in Figure 7.9.

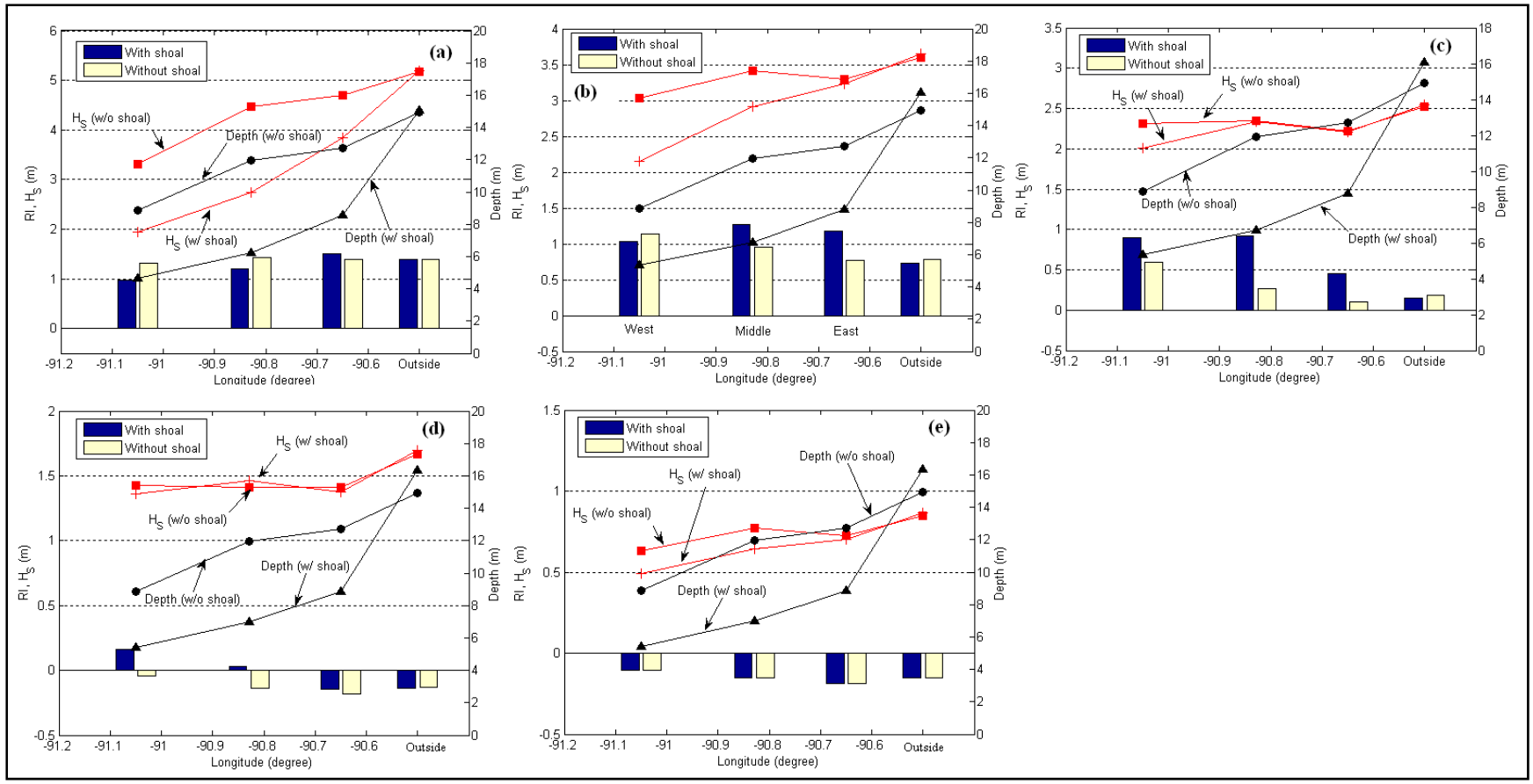


Figure 7.9 Wave re-suspension Intensity (RI) for various cases. (a) Case A1, (b) Case A2, (c) Case A3, (d) Case A4, (e) Case A5.

The RI corresponds to wave height, wave period, and water depth; generally speaking, the higher the wave height and the shallower the depth, the higher the RI. When storms were strong (*i.e.*, case A1 and A2), the RI was high across the domain, but was higher on the middle and eastern shoal than on the western shoal due to wave dissipation on the western shoal. As wave energy decreased, in general trend, the RI on the shoal decreased from the west to east following the change in the shoal bathymetry. For the case A3 (moderate storms), the RI on the western shoal was twice as high as that on the eastern shoal and approximately six times as high as that outside of the shoal. For case A4 (weak storm conditions), the RI was positive on the western and middle shoal and was negative on the eastern flank of the shoal and outside of the shoal. The negative values are in favor of sediment deposition. For the case A5 (fair weather conditions), the RI was negative across the domain, suggesting no sediment re-suspension during fair weather conditions. The results were corroborated by in-situ measurements (Pepper 2000; Kobashi *et al.* 2007b; Kobashi *et al.* 2009a). Recent studies revealed unique sediment dynamics on predominantly a fluid mud bottom on the deeper eastern flank of the shoal during spring 2006 and on predominantly a sandy bottom on shallower middle and western flank of the shoal during winter 1998 and 2008 (Pepper and Stone 2004; Kobashi *et al.* 2007b). Our results suggest that the deeper eastern portion of the shoal, seems to be suitable for the accumulation of fine sediment supplied from the Atchafalaya River during moderate to weak storms, typically during spring. On the western and middle portions of the shoal, re-suspension is prone to outweigh sediment accumulation in spite of its closer location to the Atchafalaya River as in greater detail discussed in Kobashi and Stone (2008a).

Results of the RI without the shoal showed that sediment re-suspension was high on the western flank of the shoal during strong storms because of lower wave dissipation rates despite deeper depth (Table 7.7). However, for most of the model results, the RI without shoal was significantly lower than the re-suspension with shoal, particularly when wave energy was moderate to weak (Figure 7.9). This suggests that a large portion of the shoal sand excavations enhance accumulation of fluid mud on the shoal when sediment is deposited on the shoal (Kobashi *et al.* 2009a). The result has further strong implication for benthic organisms.

### 7.4.4. Impacts of Sand Dredging for Proposed Restoration Scenarios on Waves, Current, and Sediment Suspension

An additional case study was implemented (case B1-B5) to examine changes in physical conditions for various sand mining scenarios from B1 to B5. Two contrasting storms were selected: a winter storm in mid February 2008 (equivalent to moderate storms (case A3)) and a tropical cyclone, Lili (equivalent to severe weather (case A1)). Here results of the cases B2, B4, and B5 were presented (Table 7.9). The results of the cases B2 and B4 were more extensive mining scenarios than B1 and B3 (Table 7.5).

Table 7.9

Maximal difference in magnitude of hydrodynamic parameters between actual bathymetry and hypothetical bathymetry. Top low; Maximal difference in absolute magnitude of each parameter. Bottom low: Maximal values in magnitude of each parameter during model duration.

| Storm | Case | Wave height m | Surface currents m $s^{-1}$ | Bottom currents m $s^{-1}$ | RI N $m^{-2}$ |
|---|---|---|---|---|---|
| Winter storms | B2 | 0.09 | 0.17 | 0.03 | 0.02 |
| | | 1.19 | 0.59 | 0.20 | 0.82 |
| | B4 | 0.04 | 0.11 | 0.06 | 0.02 |
| | | 1.30 | 0.49 | 0.15 | 0.62 |
| | B5 | 0.03 | 0.16 | 0.06 | 0.02 |
| | | 1.67 | 0.10 | 0.10 | 0.60 |
| Hurricane Lili | B2 | 0.07 | 0.09 | 0.04 | 0.01 |
| | | 1.52 | 0.97 | 0.33 | 1.10 |
| | B4 | 0.04 | 0.15 | 0.07 | 0.08 |
| | | 2.06 | 0.75 | 0.22 | 1.16 |
| | B5 | 0.07 | 0.05 | 0.03 | 0.04 |
| | | 3.47 | 0.06 | 0.15 | 1.39 |

During tropical cyclone Lili, the maximum difference in wave height over the mining area A, was 0.07 m for scenario B2, 0.04 m over area B for scenario B4, and 0.07 m over area C for scenario B5, respectively (Table 7.9). The difference in current velocity at the surface and bottom showed less than 0.15 m $s^{-1}$ and 0.07 m $s^{-1}$ for all cases (B2, B4, and B5). RI changed in magnitude of less than 0.08 N $m^{-1}$ for all cases.

During a winter cold front in mid-February, 2008, the difference in wave height on each mining area was 0.09 m for the scenario B2 and 0.04 m for the scenario B4, respectively (Table 7.9). Maximal differences in magnitude of surface currents were 0.17 m $s^{-1}$ over area A during, 0.11 m $s^{-1}$ over area B, and 0.16 m $s^{-1}$ over area C (Table 7.9). RI changed in magnitude of 0.02 N $m^{-2}$ for the cases B2 and B4, and B5 (Table 7.9). Compared to maximal values during model duration as listed in Table 7.9, the above values are significantly small and thus, small-scale sand mining is not expected to have profound impacts on hydrodynamics and sediment transport over the shoal.

# CHAPTER 8
# HIGH BENTHIC MICROALGAL BIOMASS FOUND ON SHIP SHOAL, NORTH-CENTRAL GULF OF MEXICO

## 8.1. INTRODUCTION

Recently, off-shore shoals on the U.S. continental shelf have received greater attention because they have been identified as potentially exploitable sand deposits for use in coastal stabilization and restoration projects. However, the biotic composition and ecological function of these shoals is much less well studied than the surrounding continental shelf environment (Brooks *et al.* 2004). One example is Ship Shoal, a submerged relict barrier island located on the central Louisiana coast ~ 25 km from shore. Ship Shoal alone is considered one of the largest sand sources in the Gulf of Mexico (Drucker *et al.* 2004) with the potential to supply 1.6 billion cubic yards of fine sand (Michel *et al.* 2001). As large, shallow sand deposits surrounded by deeper, muddy sediments, Louisiana shoals are unique local features that may serve important biological functions.

*In situ* primary production and allochthonous riverine inputs of carbon form the base of near-shore marine food webs, including those on shoals. *In situ* primary production may occur in the water column and, under appropriate conditions, on the sediment surface. Historically, benthic microalgae (BMA) have been thought to contribute little to shelf-wide primary production and benthic food webs due to light limitation. However, recent studies have shown that BMA biomass and benthic primary production (BPP) on shelf systems may be high (reviewed in Gattuso *et al.* 2006). For example, working on the North Carolina continental shelf, Cahoon and Laws (1993) found that microalgae collected from sediments in water depths of 14 to 40 m were primarily benthic diatoms rather than settled phytoplankton. Furthermore, they found that sedimentary algal biomass exceeded the integrated water column phytoplankton biomass over much of their study area and gross BPP was sometimes similar to integrated water-column primary production (Cahoon and Cooke 1992). Algal biomass in the sediments off the coast of Georgia and Florida exceeded depth-integrated water column values and gross BPP averaged almost two-thirds of water-column primary production (Nelson *et al.* 1999; Jahnke *et al.* 2000).

Pelagic primary production has been frequently studied on the Louisiana continental shelf (LCS), while studies of BMA are far fewer despite the potentially important role of BMA in nitrogen cycling (Risgaard-Petersen 2003 and references therein) and the observation that BPP may be an important oxygen source below the pycnocline (Bierman *et al.* 1994; Larson and Sundbäck 2008). To our knowledge, no studies of BPP have been conducted on Louisiana's shoals. In the surrounding shelf, Bierman *et al.* (1994) found that BPP in the western LCS is about 30 percent of water column primary production, and Dortch *et al.* (1994) calculated that primary productivity in the bottom water and sediment surface could re-supply 23 percent of daily $O_2$

consumed by near-bottom respiration. However, other researchers have considered BPP to be a minor component of shelf bottom-water oxygen dynamics (Rowe 2001; Quiñones-Rivera *et al.* 2007). Clearly, understanding the role of BMA and BPP on the LCS requires additional investigation.

Conditions on Louisiana's shoals may be conducive to BPP in several ways. First, the shallow depth (~5 to 12 m on Ship Shoal) may facilitate light penetration to the benthos. Similarly, the sandy sediments may be conducive to BPP because they lack a nepheloid layer of light-attenuating fine sediments and light extinction rates are relatively low (Kuhl *et al.* 1994), compared to fine sediments, facilitating primary productivity below the sediment surface. Also, the high permeability of sand may contribute to rapid nutrient flux into pore water (Huettel and Rusch 2000). Thus, Louisiana's shoals may support high BPP compared to off-shoal sediments, which generally have much higher silt and clay content.

Ship Shoal has only recently been inventoried biologically and investigators have found a high population density of spawning blue crabs, *Callinectes sapidus* (C. Gelpi, Louisiana State University, unpublished data) as well as a macrobenthic community with a high species richness and biomass (S. Dubois, French Research Institute for Exploration of the Sea, unpubl. data). Ship Shoal may promote the maintenance of regional diversity by functioning as a hypoxia refuge and as a source for new macroinvertebrate recruits after hypoxia related mortality (S. Dubois, French Research Institute for Exploration of the Sea, unpubl. data). BMA may support these important functions on Ship Shoal in several ways. BMA may be an important oxygen source to bottom water on Ship Shoal, which is particularly relevant given the severe seasonal hypoxia that is characteristic of the northern Gulf of Mexico (Rabalais *et al.* 2007). BMA may also be an important food source not present in deeper, muddy off-shoal areas where detrital phytoplankton, fecal pellets and terrestrial carbon sources are the dominant sedimentary organic matter component (Radziejewska *et al.* 1996; Dortch *et al.* 2000; M. Grippo, Louisiana State University, unpubl. data). Given the potential importance of BMA to ecosystem function on the LCS, we investigated sedimentary algal biomass and composition and the potential for BPP on Ship Shoal including the spatial and temporal distribution of BMA and their relationship to physical and chemical factors.

## 8.2. METHODS

### 8.2.1. Study site and sample collection

Ship Shoal is a shallow relict barrier island approximately 25 km off the coast of Terrebonne Bay, Louisiana (Latitude 28° 54.725` N and Longitude 90° 54.592` W at the center). The shoal is 50 km long and 1 to 12 km in width and is oriented parallel to the shoreline. The bathymetry of the shoal varies along east-west and north-south gradients. The western region is shallow and depth increases toward the east. The northern edge is well defined by a sharp change in slope,

while the southern edge is characterized by a shallow slope. Sampling stations were therefore chosen to capture potential variation along both the east-west and north-south gradients. Over the shoal, three transects were placed in north-south orientation and other stations were located along or around the central spine of the shoal. We sampled a total of 27 stations on Ship Shoal during the spring (June 2005, May 2006), summer (August) and fall (October) of 2005 and 2006 (Figure 8.1). Some stations were not sampled in October 2006 due to severe weather.

Sediment chlorophyll (Chl) *a*, bottom-water dissolved oxygen (DO), sediment grain size, salinity, temperature and water depth were measured at each station. Water samples were collected approximately 1 m from the bottom using a 5-L Niskin bottle. Temperature, salinity and DO were measured with a YSI 85 handheld multimeter. Three boxcores were taken at each station using a Gulf of Mexico (GOMEX) box core. From each box core, we took a 4- and a 2-cm deep subcore for grain size analysis and chl *a* measurement, respectively using a syringe corer (2.5 cm inner diameter). Based on prior work (MacIntyre and Cullen 1995; Radziejewska *et al.* 1996; Light and Beardall 1998; Cartaxana *et al.* 2006), we considered 2 cm sufficient to collect most of the chl *a* in the sediment. Cores for sediment chl *a* were immediately frozen in liquid $N_2$ and stored at -80° C upon return to the laboratory until HPLC analysis.

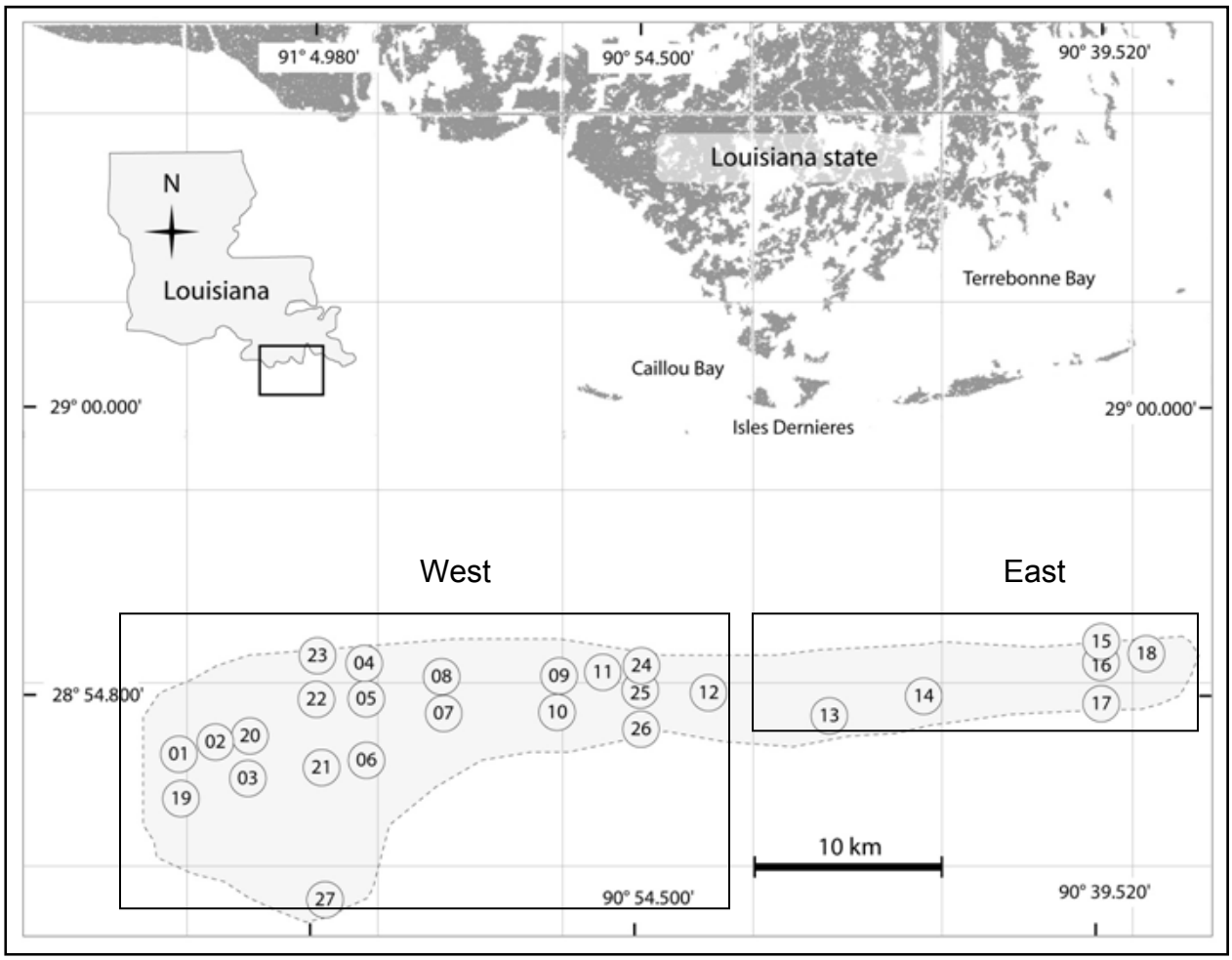

Figure 8.1 Map of Ship Shoal and sampling stations.

Beginning in May 2006, we measured downwelling photosynthetically active radiation (PAR) at 4 stations on the western end of Ship Shoal and 3 stations on the eastern end of Ship Shoal. At the same stations, we also collected surface, mid-depth, and bottom-water samples (in triplicate) for photosynthetic pigment analysis. Seawater was filtered on pre-ashed Whatman GF/F filter paper (47 mm; 0.7 µm nominal pore size) and stored in liquid $N_2$ until analysis. Downwelling photosynthetically active radiation (PAR) was measured at 1-m intervals with a LICOR LI-192SA Underwater Quantum Sensor connected to a LICOR LI-1000 datalogger. The PAR data were corrected for changes in surface irradiance using a ship-board LICOR LI-190SA light sensor. Using PAR data, an extinction coefficient ($K_{PAR}$ ) was calculated for each station and used to determine the percent of surface light reaching sediment surface ($I_z$) using the equation:

$$I_z=I_o(e^{-kz}),$$

Where, $I_o$ is surface irradiance, $k$ is the light attenuation coefficient ($K_{PAR}$) and $z$ is the bottom depth (m).

To assess the relative contribution of settled phytoplankton and BMA to the total sedimentary algal biomass in 2006, we collected additional sediment cores from stations in the eastern and western portions of Ship Shoal (nine stations total). The 2-cm deep sediment cores were taken from box-core samples using a 2.5 cm inner diameter syringe corer.

### 8.2.2. Laboratory Analysis

Average grain size was determined by first washing sediments through a 63-µm aperture sieve to separate the coarse sediments from the silt/clay (< 63 µm) fraction. Both fractions were then dried at 60°C and weighted to determine percent silt/clay. The > 63 µm fraction was dry sieved through 22 stacked sieves ranging from 63 µm to 2 mm and a grain-size profile was calculated using Gradistat software (Blott and Pye 2001). Percent organic carbon was determined for selected sediment samples using a Perkin-Elmer 2400 Elemental Analyzer. Before organic carbon analysis, sediments were weighed into pre-weighed silver tins and exposed to concentrated HCl fumes in a desiccator for 48 h to remove carbonates.

All photosynthetic pigment analyses were conducted using the methods of Buffan-Dubau and Carman (2000). Prior to analysis, whole sediment samples were freeze-dried after which 100 percent acetone was added to each sample. After a 60 second sonication, samples were extracted overnight in the dark at 4°C. After extraction the sample was centrifuged at 2000 rpm for 10 min and the supernatant was filtered and analyzed by High Performance Liquid Chromatography (HPLC). For water-column samples, filters were placed in 100 percent acetone and briefly sonicated then extracted overnight in the dark at 4°C before HPLC analysis. The volume of water-column filtrate varied from 0.5 to 2 L depending on turbidity. HPLC analysis was performed using a Hewlett Packard 1100 liquid chromatograph coupled to a diode array

spectrophotometer and a Hewlett Packard 1046A fluorescence detector. Pigments were separated using reverse –phase liquid chromatography with a C18, 5-µm column. Run time was 25 min.

In addition to chl *a*, several marker pigments were used as indicators of dominant algal groups (Jeffrey and Vesk 1997), and their concentration relative to chl *a* was used to detect spatial and seasonal changes in sediment algal community composition. Pheopigments are chl *a* degradation products formed during consumption of algae (Le Rouzic *et al.* 1995; Jeffrey and Vesk 1997; Buffan-Dubau and Carman 2000) and algal senescence (Head *et al.* 1994; Louda *et al.* 1998). Pheopigment data may therefore provide information on general trends in microalgal grazing and community senescence. Here, we define total pheopigments as the sum of pheophorbide a and pheophytin a. Reference standards were available for 11 pigments: chl *b*, fucoxanthin, violoxanthin, alloxanthin, diatoxanthin, diadinoxanthin, lutien, and zeaxanthin, and β-carotene, pheophorbide a and pheophytin a. Pigments were identified based on retention time and their match to available pigment standards, and pigment concentrations were calculated from peak areas using HPChemstation software.

The relative abundance of pennate and centric diatoms was used as a proxy for the contribution of benthic and pelagic diatoms to benthic chl a. The classification of marine centric and pennate diatoms into planktonic and benthic categories, respectively, is not rigid and one pennate genus, *Pseudo-nitzschia,* is a common phytoplankter in the Gulf of Mexico (Dortch *et al.* 1997). However, most pennate marine diatoms are benthic and therefore this method provides information on the relative contribution of water column and benthic primary producers to the sedimentary algae.

All sediments collected on Ship Shoal were sand with little particulate matter. Therefore, diatom cells could be efficiently extracted from sediment samples for microscopic examination by simply agitating the sediment and pipetting a sub-sample onto a counting dish. Using an inverted microscope (up to 400X magnification), the first 100 diatoms encountered while moving along a transect line were classified as pennate or centric based on cell morphology. This procedure was replicated four times for a total of 400 cell counts. Only fully or partially pigmented diatoms were included in counts. *Pseudo-nitzschia* was rarely encountered and when present was not included in the analysis.

### 8.2.3. Data analysis

As described in the results section, data inspection suggested that variation in water depth and sediment granulometry across Ship Shoal from east to west exceeded variation from north to south. Given the potential importance of these physical conditions to BPP, we grouped the 27 Ship Shoal stations by geographic location into western and eastern areas (Figure 8.1) for further analysis. Geographically, the main body of Ship Shoal is in the west, with a thin strip projecting to the east. Consequently, 21 stations were assigned to the western grouping while 6 stations were assigned to the eastern grouping.

Spatial and temporal differences in sediment chl *a,* fucoxanthin and total pheopigments were tested using a three-way-analysis of variance (ANOVA) with main effects of year (2005-2006), location (east and west) and month (May/June, August, October) as factors. Data were square root transformed to approximate normality and equal variance. When significant a factor effect was significant, pairwise comparisons were made using Holm-Sidak procedure.

For each sampling cruise, a Pearson correlation matrix was constructed to assess the relationship between sediment chl *a*, DO, salinity, temperature and depth, grain size and percent silt/clay. Integrated water-column chl *a* (WCI) and bottom-water chl *a* (BWC) were incorporated into the correlation matrix beginning in May 2006. To determine the relative biomass of sediment and water-column algae, chl *a* was integrated over the water column and converted to $mg/m^2$. The ratio of sediment BMA to phytoplankton biomass was then calculated.

## 8.3. RESULTS

### 8.3.1. Sediment characteristics, water chemistry and light

Spatial gradients in depth and grain size were found on Ship Shoal. Depth across the shoal ranged from 5 to 11 m and generally increased from west (5 to 8 m) to east (9 to 10 m). Sediment on Ship Shoal was well sorted fine- to very-fine sand with a low silt/clay content (usually < 2percent; Table 8.1). Mean grain size generally increased from west to east, a pattern attributable to the higher percentage of shell hash (measured as percent gravel) on the eastern end. Sediment organic carbon values from the June 2005 cruise were generally less than 0.2 percent across all stations. Bottom-water dissolved oxygen (D.O.) concentrations were above hypoxic levels (4 mg/l) at all stations and seasons, with the October D.O. levels higher than May/June and August (Table 8.1). Bottom-water salinity was generally greater than 30 ppt and no spatial patterns across the shoal were evident.

Table 8.1

Summary of seasonal bottom water and sediment data (mean ±std) for the eastern and western portions of Ship Shoal during spring (May/June), summer (August) and fall (October) of 2005-2006.

| Station grouping | Depth (m) | Mean Grain size (μm) | % silt/clay | percent gravel | Dissolved Oxygen (mg/l) | Temp (°C) | Salinity (ppt) |
|---|---|---|---|---|---|---|---|
| Spring | | | | | | | |
| East | 8.8± 1.1 | 182.3±22.3 | 1.1±0.7 | 2.4±2.0 | 4.6±0.8 | 26.4±1.5 | 33.2±2.4 |
| West | 6.4±1.3 | 147.6±13.2 | 1.3±0.7 | 0.6±1.3 | 5.7±0.7 | 27.8±1.4 | 31.6±1.7 |
| Summer | | | | | | | |
| East | 8.4±1.1 | 208.7±57.4 | 1.6±1.4 | 3.9±4.0 | 5.8±0.4 | 30.3±0.5 | 34.8±0.5 |
| West | 6.1±1.2 | 153.5±15.1 | 1.6±1.2 | 0.2±0.1 | 5.0±0.7 | 31.0±0.3 | 32.0±1.2 |
| Fall | | | | | | | |
| East | 9.0±1.2 | 203.3±26.2 | 0.9±0.7 | 2.9±2.6 | 7.6±0.4 | 25.1±1.9 | 33.4±1.1 |
| West | 6.4±1.2 | 142.4±13.6 | 2.6±2.8 | 0.1±0.1 | 7.4±0.3 | 25.4±1.6 | 32.3±0.9 |

Water-column chl *a* concentration had an overall range of 0.4 to 4.6 μg/l at the surface, 0.8 to 5.3 μg/l in mid water, and 1.5 to 14.5 μg/l in bottom waters (Figure 8.2). With the exception of October, chl *a* was higher in bottom-water samples compared to samples from the surface and mid-depth (Figure 8.2). Seasonal trends were present as well, with chl *a* concentration generally lowest in August. Water-column integrated (WCI) phytoplankton biomass was also lowest in August. The WCI values were similar in May and October (Figure 8.3). The WCI chl *a* was consistently higher on the eastern end of Ship Shoal where water depth was greatest (Figure 8.3).

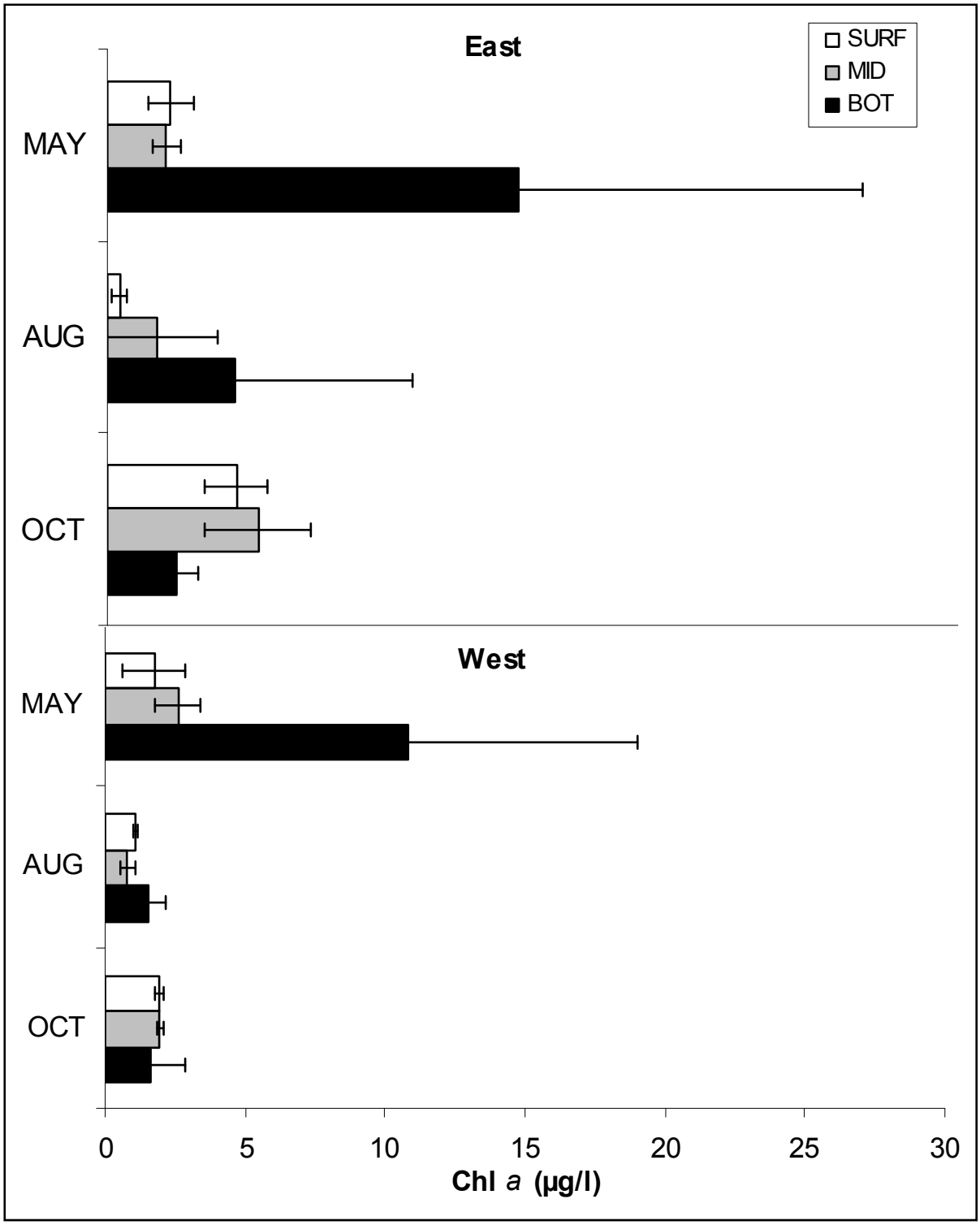


Figure 8.2 Surface, mid-depth and bottom water-column chlorophyll a values (µg/l) on the eastern and western portions of Ship Shoal in 2006. Chl *a* values represent the mean ±std.

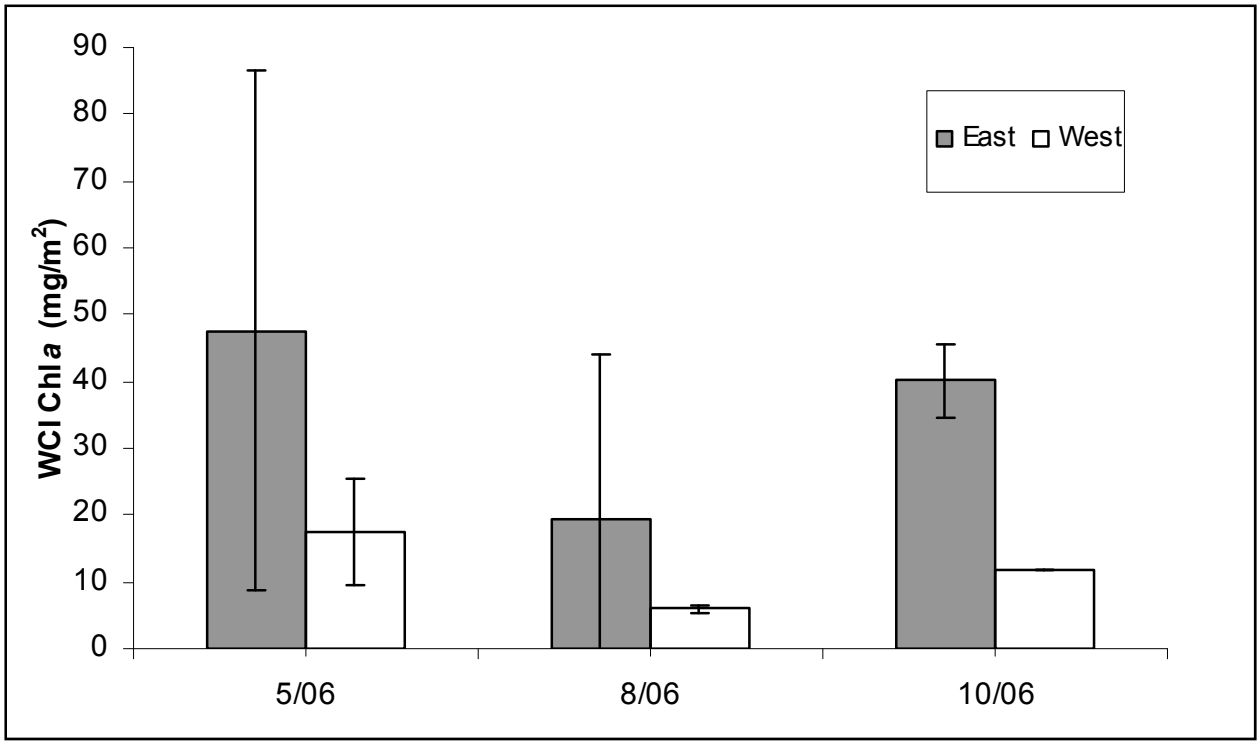


Figure 8.3 Water-column integrated Chl *a* (mean±std) for east (E) and west (W) stations during May, August, and October 2006.

Over all sampling dates, estimated PAR reaching the sediment surface ranged from 2 to 652 µmol photons $s^{-1}m^{-2}$ depending on time of day and cloud cover (Table 8.2). The percentage of surface light reaching the sediment was generally > 1 percent. The percent of surface light reaching the sediment surface was lowest in October (0.03 to 1.3 percent) and highest in August (13-38 percent). May values were intermediate, ranging from 1.5 to 17.5 percent (Table 8.2). The percent of surface PAR reaching the sediment was similar at the east and west station groupings, despite the fact that eastern stations were deeper on average than western stations. Pearson correlations revealed no significant relationship in May, August or October between water depth and the percent of surface irradiance at the sediment. These results may be explained by the higher $K_{PAR}$ values consistently found on the western end of Ship Shoal (Table 8.2).

Table 8.2

Photosynthetically active radiation (PAR), percent surface PAR on the seafloor and extinction coefficient ($K_{PAR}$) for east and west Ship Shoal stations. PAR values are a range for that location/date. Percent surface PAR at sediment and $K_{PAR}$ are mean ± std for each location/date.

| Location | May 2006 | August 2006 | October 2006 |
|---|---|---|---|
| | PAR at sediment surface ($\mu mol\ s^{-1} m^{-2}$) | | |
| East | 38-170 | 269-652 | 2-18 |
| West | 93-500 | 175-435 | 4-31 |
| | % Surface light at the bottom | | |
| East | 6.9 ± 7.4 | 27.6 ± 9.8 | 0.8 ± 0.5 |
| West | 8.7 ± 5.0 | 21.8 ± 2.6 | 1.0[a] |
| | $K_{PAR}$ | | |
| East | 0.36 ± 0.09 | 0.15 ± 0.05 | 0.53 ± 0.05 |
| West | 0.51 ± 0.11 | 0.28 ± 0.07 | 0.62 ± 0.30 |

[a] Only one western station sampled in October due to inclement weather

### 8.3.2. Sediment algae

The Chl *a* concentration in the sediment was highly variable both within and between stations (Figure 8.4). Three-way ANOVA revealed a significant year effect ($p<0.001$) with 2006 sediment chl *a* significantly higher than 2005. Seasonal variability was also high with average chl *a* values for the entire shoal ranging from < 10 to 50 $mg/m^2$ in 2005 and from 21 to 53 $mg/m^2$ in 2006. Sediment chl *a* was significantly lower in October compared to May/June ($p = 0.017$). With the exception of August 2005, sediment chl *a* concentrations were very similar at the eastern and western stations, and no significant differences were detected ($p=0.054$). No significant interactions were found between year, month and location.

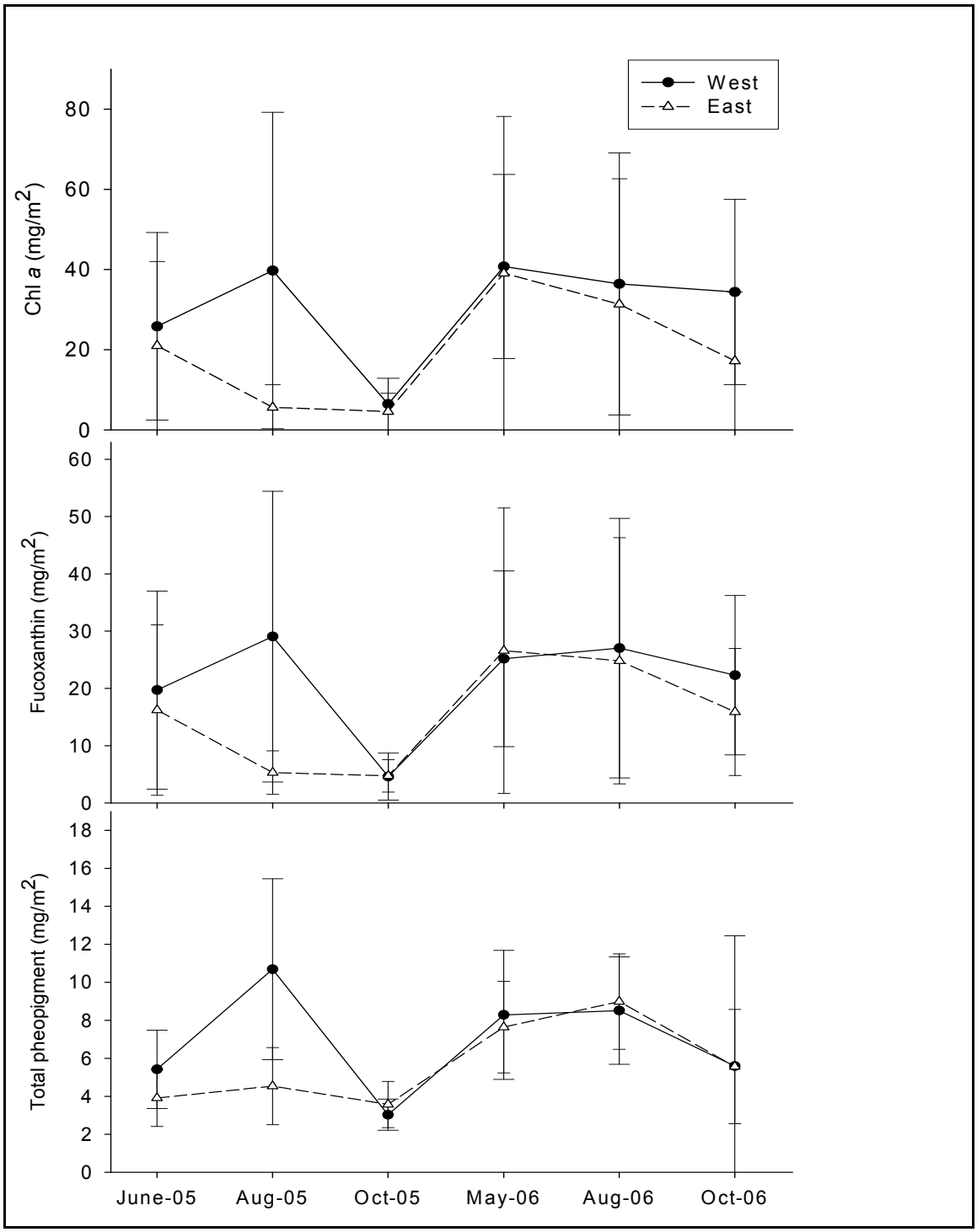


Figure 8.4 Sediment chlorophyll *a*, fucoxanthin, and total pheopigments (mean ± std) for eastern (E) and western (W) station groups for spring, summer, and fall 2005-2006.

Pearson correlations reveal no significant relationships between sediment chl *a* and depth, temperature, salinity, DO, grain size or percent silt/clay in 2005 (Table 8.3). In 2006, the percent of surface light reaching the bottom, integrated water column chl *a*, and bottom water chl *a* were included in the correlation analysis. Sediment chl *a* again showed no significant relationship to any variable except in October 2006 when a significant positive relationship was found with temperature ($r^2$=0.684; *p*=0.007; Table 8.3).

Table 8.3

Pearson correlation coefficients between sediment Chl *a* and physical and water-quality parameters collected in 2005 and 2006. A "*" indicates a significant relationship is (α=0.05). Nd means no data.

| | Depth (m) | Temp (°C) | Salinity (ppt) | Dissolved Oxygen (mg/l) | Percent Silt/clay | Grain Size (μm) | % surface light on seafloor | WCI Chl *a* | BW Chl *a* |
|---|---|---|---|---|---|---|---|---|---|
| 2005 | | | | | | | | | |
| June | -0.304 | 0.100 | -0.310 | 0.260 | -0.263 | 0.002 | nd | nd | nd |
| August | -0.315 | 0.298 | -0.150 | -0.030 | nd | nd | nd | nd | nd |
| October | 0.096 | -0.002 | -0.064 | 0.352 | 0.171 | 0.214 | nd | nd | nd |
| 2006 | | | | | | | | | |
| May | -0.099 | -0.083 | -0.012 | -0.008 | 0.183 | -0.180 | 0.133 | -0.426 | -0.480 |
| August | -0.052 | -0.207 | -0.068 | -0.282 | -0.403 | 0.442 | -0.214 | 0.487 | 0.595 |
| October | 0.361 | 0.684* | 0.244 | -0.018 | 0.750 | -0.239 | 0.555 | -0.472 | -0.586 |

Of the marker pigments present in sediments, fucoxanthin was found in the highest concentration. During the two years of sampling, sediment fucoxanthin concentration ranged from <10 to 40 mg/m$^2$. Seasonal and spatial trends for fucoxanthin were similar to chl *a* (Figure 8.4). Although the effect of location on fucoxanthin values was statistically significant (three way ANOVA; $p$=0.035), sediment fucoxanthin values were similar in east and west groupings on most sampling dates (Figure 8.4). Significant seasonal differences ($p$=0.005) were also present with fucoxanthin concentrations in October significantly lower than May/June ($p$=0.002) and August ($p$=0.012). No significant interactions were found between year, season and location. Sediment fucoxanthin:chl *a* ratios were similar across the shoal. The ratio ranged from 0.33 to 1.36 with most values between 0.6 and 0.8. Fucoxanthin:chl *a* ratios were generally highest in August, although values were variable (Table 8.4). These ratios are similar to those found in pure diatom culture (Lucas and Holligan 1999; Table 8.4). Fucoxanthin is diagnostic for diatoms (Jeffrey and Vesk 1997), and linear regression analysis revealed a strong positive relationship between sediment fucoxanthin and sediment chl *a* (linear regression, $R^2$ values > 0.96 for May/June, August, October), suggesting that diatoms were predominant in the sediment microalgae on all sampling occasions. Although fucoxanthin is present in algal classes other than diatoms, the lack of accessory pigments indicative of other classes suggests fucoxanthin was principally derived from diatoms.

In 2005 and 2006, mean total pheopigments (pheophytin a + pheophorbide a) at individual stations ranged from <1 to approximately 25 mg/m$^2$ (Figure 8.4). Total pheopigments were similar across Ship Shoal during most sampling dates and no significant spatial effects were detected (Three way ANOVA; $p$=0.185). A significant season effect was present ($p$<0.001), with lower total pheopigment values in October compared to May/June ($p$<0.001) and August ($p$<0.001) as well as significant differences between May/June and August ($p$=0.031; Figure 8.4). A significant interaction between season and location was found ($p$=0.039). The effect of season was significant in August ($p$<0.001) and October ($p$=0.034) only. In 2005 and 2006, total sediment pheopigments displayed temporal patterns similar to sediment chl *a* (Figure 8.4), but sediment chl *a* did not explain a significant amount of variation in total pheopigment concentrations in sediment cores except in May/June, and too a lesser degree, August (linear regression, data not shown). Total pheopigment:chl *a* ratios were highly variable and spatial patterns across the shoal were not evident (Table 8.4). In 2005, mean values ranged from 0.24 to 1.37 and from 0.15 to 0.96 in 2006, with the highest ratios generally occurring in August in both 2005 and 2006 (Table 8.4).

Table 8.4

Seasonal ratio of chlorophyll *a* to fucoxanthin and total pheopigments on the western and eastern portions of Ship Shoal in 2005 and 2006. Ratios represent the mean ±std.

| | Fucoxanthin:Chl *a* | | Total pheopigments:Chl *a* | |
|---|---|---|---|---|
| | West | East | West | East |
| 2005 | | | | |
| June | 0.80±0.15 | 0.82±0.13 | 0.60±0.71 | 0.57±0.56 |
| August | 0.81±0.17 | 0.80±0.16 | 0.72±0.51 | 1.40±0.88 |
| October | 0.70±0.19 | 0.76±0.18 | 0.28±0.33 | 0.42±0.33 |
| 2006 | | | | |
| May | 0.66±0.15 | 0.74±0.18 | 0.37±0.40 | 0.38±0.31 |
| August | 0.85±0.11 | 0.89±0.34 | 0.71±0.57 | 0.96±1.27 |
| October | 0.69±0.06 | 0.83±0.28 | 0.16±0.06 | 0.88±1.47 |

Peridinin, an indicator of dinoflagellates, was below detection limits in virtually all sediment samples. The cyanobacterial marker pigment, zeaxanthin, was present in 2005 and some 2006 samples, but was usually less than 2 mg/m$^2$ with a zeaxanthin:chl *a* ratio of <0.1. Other pigments indicative of diatoms such as the photoprotective pigments diadinoxanthin and diatoxanthin were also present in the sediment. Marker pigments for other algae were present in low or undetectable concentrations.

Microscopic examinations revealed that in every month and location sampled on Ship Shoal, > 90 percent of diatom cells in sediment samples were pennate, with centric diatoms generally comprising < 10percent of diatom cells (Table 8.5). Most pennate diatoms were tentatively identified as members of the genera *Nitzschia, Navicula* and *Amphora*. *Diploneis* and *Pleurosigma* were also present but less abundant.

Table 8.5

Percent pennate and centric diatoms in sediment algal samples collected in May, August and October of 2006. Percents are the mean ±std for a location.

| | May | | August | | October | |
|---|---|---|---|---|---|---|
| Location | Pennate (%) | Centric (%) | Pennate (%) | Centric (%) | Pennate (%) | Centric (%) |
| East | 92.2 ± 0.6 | 8.8 ± 0.6 | 94.8± 5.4 | 5.2 ± 2.9 | 98.0 ± 1.5 | 2.0 ± 0.2 |
| West | 94.9 ± 5.3 | 5.1 ± 5.5 | 94.4 ± 3.5 | 5.6 ± 3.6 | 99.5 ± 0.6 | 0.5 ± 0.6 |

### 8.3.3. Sediment and water column comparison

Based on accessory pigment:chl *a* ratios, fucoxanthin was the dominant marker pigment in sediment and bottom water samples (Table 8.6), suggesting diatoms were the most abundant algal group in both locations. Despite the shallow depth of Ship Shoal, changes in bottom-water pigment ratios did not correspond with changes in the sediment ratios. For example, zeaxanthin:chl *a* ratios peaked in August, but remained low in the sediment during all other months sampled. Similarly, peridinin was seasonally present in the bottom water, but was below detection limits in sediment samples overall. Conversely, pheopigments were present in sediment samples throughout the year, while pheopigments were detected in the bottom water only in May (Table 8.6).

Table 8.6

Pigment ratios in bottom water (BW) and sediment samples collected simultaneously from the eastern and western phytoplankton stations in 2006.

| | Peridinin:Chl *a* | | Fucoxanthin:Chl *a* | | Zeaxanthin:Chl *a* | | Total pheopigments:Chl *a* | |
|---|---|---|---|---|---|---|---|---|
| Month | BW | sed | BW | sed | BW | sed | BW | sed |
| | East | | | | | | | |
| May | 0.00 | BDL | 0.47 | 0.62 | 0.01 | 0.01 | 0.06 | 0.16 |
| August | 0.05 | BDL | 0.55 | 0.97 | 0.22 | 0.05 | 0.02 | 1.22 |
| October | 0.07 | BDL | 0.48 | 0.91 | 0.05 | 0.08 | BDL[a] | 1.20 |
| | West | | | | | | | |
| May | BDL | BDL | 0.58 | 0.61 | 0.01 | 0.01 | 0.08 | 0.32 |
| August | BDL | BDL | 0.46 | 0.81 | 0.19 | 0.02 | BDL | 0.65 |
| October | BDL | BDL | 0.61 | 0.68 | 0.05 | 0.02 | BDL | 0.18 |

[a] BDL-below detection limits

Mean chl *a* concentration in the sediment and water column were highly variable and the two were not significantly different from each other in any season (Mann-Whitney Rank Sum test). However, on an areal basis, sediment chl *a* exceeded water column integrated chl *a* at 4 of the 6 Ship Shoal stations in May 2006 and 4 of the 7 stations in August 2006 (Figure 8.5). Much of the spatial differences in the ratio across the shoal were related to water-column integration length, with WCI chl *a*: sediment chl *a* ratios highest at the deeper stations. However, in August 2006 the ratio was near 1 even at the deepest stations. During October 2006, WCI chl *a* was greater than sediment chl *a* at only 2 of the 5 stations (Figure 8.5), because, severe weather prevented sampling the more shallow western stations where sediment chl *a* would be most likely to exceed WCI chl *a*.

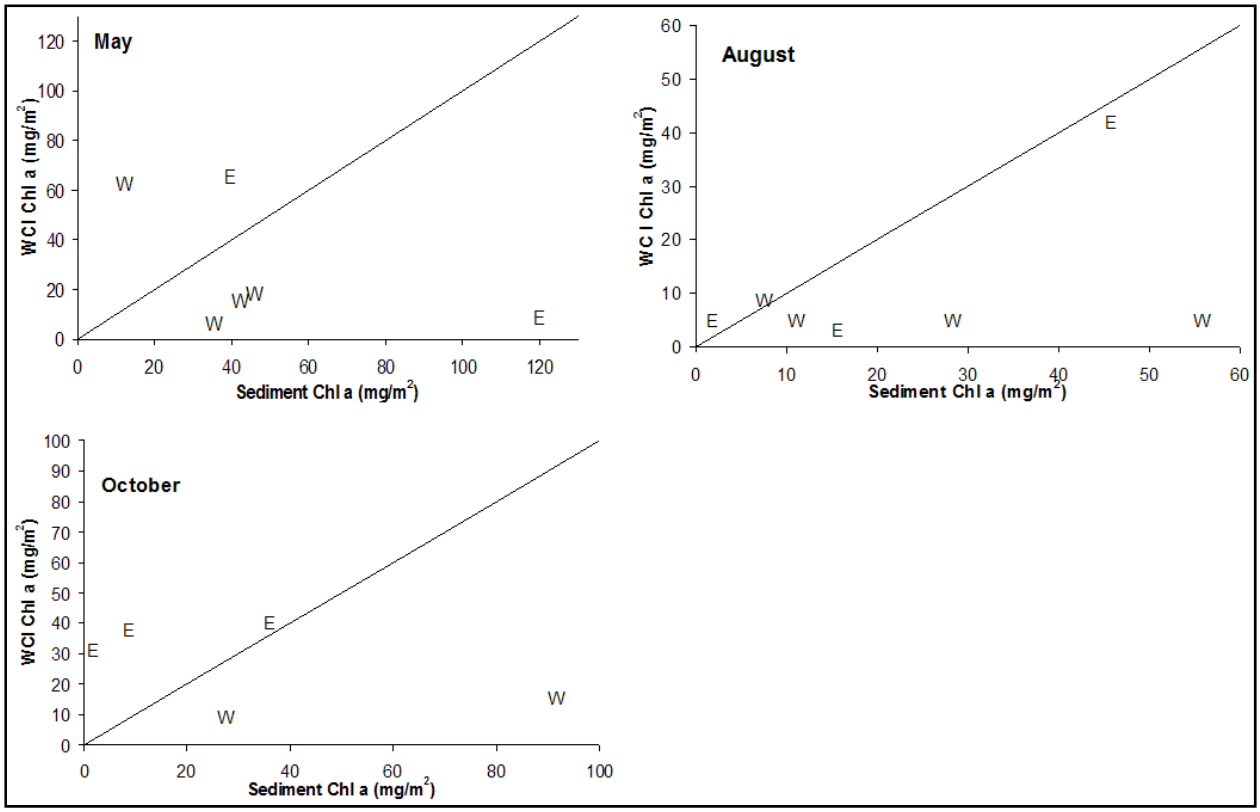


Figure 8.5 Ratio of water column integrated (WCI) Chl *a* to sediment Chl *a* during May, August and October of 2006. The grey line represents 1:1 WCI and sediment Chl *a*. A value to the right of the line indicates sediment Chl a>WCI and a value to the left indicates sediment Chl a<WCI.

## 8.4. DISCUSSION

To appraise the potential for BPP on Ship Shoal we examined the origin and composition of sediment algae and assessed some of the physical factors known to influence BPP. Based on the following observations, we conclude that BMA likely serves as the foundation for unique ecological services provided by Ship Shoal. The PAR profiles indicate sufficient light reaches the seafloor for photosynthesis by BMA, and BPP may be high and seasonally sustained. If so, BPP could contribute to the high dissolved oxygen we observed in Ship Shoal near-bottom water even though surrounding shelf water was hypoxic or near hypoxic in both summers studied (Gulf of Mexico Program 2008). We also found that sediment algal biomass on Ship Shoal was dominated by pennate diatoms, a condition that may be uncommon on the broader LCS where sediment algae is comprised of a large fraction of settled phytoplankton (Turner and Rabalais 1994; Rabalais *et al.* 2004; Wysocki *et al.* 2006; M. Grippo, Louisiana State University, unpubl. data). Finally, the biomass of BMA may periodically rival or exceed water-column integrated phytoplankton biomass. Consequently, BMA rather than phytoplankton may contribute the most to energy flow through the local Ship Shoal food web.

Irradiance levels of 0.1 to 1 percent of surface light are considered the minimum required for photosynthesis, although the actual irradiance required for benthic primary productivity is likely to be even lower (Gattuso *et al.* 2006). Based on these criteria, sufficient light was available for BPP on Ship Shoal throughout the year. Seafloor irradiance was > 5 percent of surface PAR at most stations during May 2006 and > 20 percent at most stations during August. Even during October 2006, when light penetration was lowest, most stations had sediment light levels around 1 percent of surface values. BPP is influenced by substrate composition because light penetration is deeper in sandy compared to muddy sediments (Billerbeck *et al.* 2007). Thus, in addition to its shallow depth, the sedimentary characteristics of Ship Shoal are likely to be more conducive to BPP than the fine, silty sediments typical of the Gulf of Mexico.

Benthic algal chl *a*, on an areal basis, exceeded integrated water column chl *a* at most of the stations during much of the year. The ratio of WCI chl *a* to sediment chl *a* declined with depth as phytoplankton integration length increased. Therefore, sediment algal biomass exceeded phytoplankton biomass most often at the shallow western stations, while the opposite was true at the deeper stations. Algal standing stock are not easily equated to primary production. Also, while our sediment samples went to a depth of 2 cm, only those algal cells in the photic zone of the sediment (1 to 2 mm in sand) are capable of photosynthesis; therefore, it is difficult to know how benthic primary productivity compares to water-column primary productivity on Ship Shoal. Direct measurement of benthic coupled with water-column primary productivity is needed to further evaluate this relationship.

### 8.4.1. Sediment Chl a.

The few measurements of sediment chl *a* reported for the GOM have used contrasting methodologies, units, locations (primarily beneath the Mississippi River Plume) and sediment types, making comparisons with this study tenuous (Radziejewska *et al.* 1996; Chen *et al.* 2003; Rabalais *et al.* 2004; Wysocki *et al.* 2006). Overall, sediment chl *a* concentrations found in this study, i.e., 10 to 50 mg/m$^2$ with individual values often in excess of 100 mg/m$^2$, are similar to other estuarine and marine locations in the Gulf of Mexico (MacIntyre *et al.* 1996), but lower than values reported for the LCS near the Mississippi River Plume where high phytoplankton primary production may contribute to sediment algal biomass (Radziejewska *et al.* 1996).

Both marine and terrestrially derived carbon are found in sediments of the LCS (Trefry *et al.* 1994; Turner and Rabalais 1994) and of the two sources, marine algae are thought to constitute the greater fraction (Eadie *et al.* 1994; Rabalais *et al.* 2004). In turn sedimentary algae may be composed of BMA, settled phytoplankton (as individual cells or zooplankton in fecal pellets) or both. Sedimentary algae from nearby off-shoal locations are mostly phytoplankton or a mix of centric and pennate diatoms suggesting settled phytoplankton are prominent in the fine sediments surrounding Ship Shoal (M. Grippo, Louisiana State University, unpubl. data). In contrast, on Ship Shoal, centric diatoms typically made up less than 10 percent of the benthic diatom community across all sampling locations and seasons suggesting sediment chl *a* is directly

related to BMA biomass rather than phytodetritus. Also, silty sediments on the broader LCS typically have a total pheopigment:chl *a* ratio > 1 indicating algal carbon is in the form of phytodetritus and fecal pellets (Radziejewska *et al.* 1996; Chen *et al.* 2003; Rabalais *et al.* 2004; Wysocki *et al.* 2006). However, for most of Ship Shoal sediment total pheopigment: chl a ratios were generally < 1 indicating new production of high nutritional quality rather than phytodetritus (Tenore 1988; Wieking and Kroncke 2005; Table 8.6). The strong correlations between sediment chl *a* and fucoxanthin also provides persuasive supporting evidence that the high chl *a* concentrations on Ship Shoal are a product of BPP.

The low abundance of settled phytoplankton in Ship Shoal sediments may be depth related. Bottom currents are typically faster on high-relief areas like shoals and there is less overlying water to contribute phytoplankton cells to the sediment. These factors may prevent a significant amount of phytodetritus from accumulating on the sediment surface of Ship Shoal. BMA, on the other hand, are able to use mucilage to minimize resuspension (Miller *et al.* 1996 and references therein). Also, the burial rate of phytodetritus increases with grain size (Ehrenhauss *et al.* 2004; Cartaxana *et al.* 2006 and references therein) so muddy sediments may retain deposited organic matter at the sediment surface for a longer duration than more permeable sediments.

Sedimentary algal biomass was greatest during May/June and August. Similar seasonal patterns have been found in other subtidal locations (Nelson *et al.* 1999; Welker *et al.* 2002) and perhaps reflect seasonal changes in temperature, photoperiod and nutrient availability (Welker *et al.* 2002; Cibic *et al.* 2007) as well as macrofaunal grazing (Hillebrand *et al.* 2000). The interaction between benthic invertebrates and BMA is discussed below. Seasonal differences in sediment chl *a* were most evident in 2005. The large decrease in sediment chl *a* in October of 2005 may also have been related to sediment scour from Hurricanes Katrina (August 29, 2005) and Rita (September 24, 2005), which occurred shortly before our sampling trip.

No consistent, significant relationships were found between sediment chl *a* and any of the measured physical and biological parameters. The fact that depth and sediment light levels were not correlated with benthic algal biomass was unexpected, as most investigators find a relationship between these variables (Cibic *et al.* 2007; Facca and Sfriso 2007). The results are also surprising considering that the sediment PAR levels found in this study, which ranged from 2 to 500 µmol photons $m^{-2}$/s, were generally less than typical saturating light levels derived from *in-situ* primary productivity-irradiance curves for BMA communities, indicating light may limit BPP on Ship Shoal (MacIntyre *et al.* 1996; Dodds *et al.* 1999; Qu *et al.* 2004; Serodio *et al.* 2005). These results may be explained by the high variability/patchiness in sediment chl *a* and the constantly changing light field experienced by BMA as water masses of varying turbidity move over Ship Shoal.

During the passage of winter fronts, the western end of Ship Shoal experiences frequent fluid mud deposition originating from the Atchafalya River system. Fluid muds would impact BMA production by reducing sediment light intensity and by burying the BMA under a layer of fine sediments. The fluid mud appears to be patchy and ephemeral (Kobashi, Chapter 3 of this report) and it was not detected during biological sampling. In addition BMA are motile and are capable of moving through the sediment to more favorable conditions (Wulff *et al.* 1997).

Similarly, the high turnover of microalgae would allow rapid recovery after the passage of the fluid muds.

### 8.4.2. Other sediment pigments

Although Lohrenz *et al.* (1999) found that dinoflagellates were abundant in Louisiana coastal waters during the summer and fall, in this study, dinoflagellate marker pigments were below detection limits in most sediment samples regardless of season. Our results support recent investigations which have demonstrated that phytoplankton collected in settling traps (Dortch *et al.* 2000) and sediments (Rabalais *et al.* 2004; Wysocki *et al.* 2006) on the LCS are primarily diatoms and cynaobacteria. Dinoflagellates may settle to the benthos, but have slower sinking rates than diatoms (Bianchi *et al.* 2002) and may be consumed or decomposed before reaching the seafloor. Although cyanobacteria are common constituents of BMA and zeaxanthin is generally found in high concentrations in the LCS sediments (Rabalais *et al.* 2004), zeaxanthin was present in Ship Shoal sediments at low or undetectable concentrations for much of the sampling period. However, zeaxanthin is a photoprotective pigment produced under high light intensity (Jeffrey and Vesk 1997) and therefore may have low cellular concentrations in shallow habitats like Ship Shoal.

On Ship Shoal, seasonal changes in sediment pheopigment concentrations closely tracked sediment chl *a* suggesting the two are linked (Figure 8.4). Pheopigments have been used as indicators of grazing, microbial decomposition, and to evaluate the seasonal decline of algal communities (Louda *et al.* 1998), such as the post-bloom decay of phytoplankton. Little phytodetritus was observed in Ship Shoal sediment samples, suggesting a lesser contribution of phytoplankton to sediment pheopigments. An increase in pheopigment:chl *a* ratios may also indicate senescing BMA communities (Light and Beardall 1998; Metaxatos and Ignatiades 2002). However, on Ship Shoal, mean pheopigment concentrations and pheopigment: chla ratios were highest in August, when BMA biomass was high. Also, pheopigment:chl *a* ratios did not increase during October when BMA biomass declined. Another source of pheopigments is grazing, and the increase in pheopigment:chl *a* ratios in the summer may have been a product of increased grazing pressure on BMA. In 2006, benthic infauna on Ship Shoal maintained a high average biomass (37.3 g wet weight/ $m^2$) and a significant positive relationship between the abundance of suspension feeding infauna and sediment chl *a* was found in August (S. Dubois, French Research Institute for Exploration of the Sea, unpubl. data). Like macrofauna, meiofauna can consume a large fraction of BMA standing stock (Pinckney *et al.* 2003). Total pheopigment concentration in Ship Shoal sediment samples were significantly related to meiofauna abundance (typically > $10^6$ individuals/$m^2$) in August 2005 (linear regression, $R^2 = 0.297$; $p$=0.003) but not in August 2006 (M. Grippo, Louisiana State University, unpubl. data). Although the abundance of benthic infauna was not a seasonally consistent predictor of sediment pheopigment concentrations, our data are consistent with the hypothesis that the infaunal community on Ship Shoal grazes BMA, and that BMA may influence benthic invertebrate community structure and biomass.

### 8.4.3. Sediment-water column interaction

Shallow water depth and tidal flow may facilitate a tight coupling between the benthos and the overlying water column. For sediment algae this could mean a downward flux of phytodetritus and/or an upward flux of algae from high-bed turbulence. Such a benthic-pelagic exchange is thought to be common in the shallow intertidal zones of estuaries (MacIntyre *et al.* 1996). However, upward flux of BMA may be less prominent in off-shore habitats like Ship Shoal, where multiple lines of evidence from this study suggest limited benthic-pelagic exchange. First, bottom water chl *a* was not correlated with sediment chl *a*. Second, pigment analysis indicated the presence of dinoflagellates and cyanobacteria in bottom-water samples, but marker pigments for both of these taxonomic groups were either absent or present in low concentrations in sediments. Third, pheopigment data suggested little resuspension, as pheopigments were below detectable limits in most bottom water samples but were present in sediment samples collected at the same time period. Finally, sediment transport modeling indicates that during calm weather bottom shear stress on Ship Shoal is less than the threshold required for sediment resuspension (Kobashi *et al.* 2007b). Although the benthic and pelagic phytoplankton components of Ship Shoal appear to interact weakly during calm conditions, periodic resuspension occurs during severe weather which would facilitate algal exchange (Kobashi *et al.* 2007b). Similar results were reported by Nelson *et al.* (1999) who found that extensive sediment mobilization on the South Atlantic Bight typically occurred only during storms.

# CHAPTER 9
# THE MEIOFAUNA COMMUNITY OF SHIP SHOAL

## 9.1. INTRODUCTION

Meiofauna are benthic metazoans large enough to be retained on a 45 μm sieve but small enough to pass through a 0.5 mm sieve. Although small in individual body size (ranging from ~ 0.1-1 μg individual$^{-1}$), meiofauna play important roles in the marine benthos because of their large contribution to energy flow (associated with a high population density and high metabolic rate), by serving as prey for juvenile fish and crustaceans, and by interacting with microbial communities and juvenile macrofauna (Coull 1999). Meiofauna are also considered excellent monitoring tools with which to quantify anthropogenic effects on the environmental health of marine ecosystems (Somerfield and Warwick 1996; Fleeger *et al.* 2008) because they (1) have an intimate association with sediments and lack a larval dispersal stage, (2) simplify sample processing at sea, (3) have short generation times, and (4) have a large information content in terms of abundance and taxonomic composition (Kennedy and Jacoby 1999). Meiofauna may provide information about the severity of effects even at the phylum or class level of taxonomic discrimination (Warwick 1988; Lee and Correa 2005; Somerfield *et al.* 2006) or by using criteria based on body size spectra and functional groupings (Vanaverbeke *et al.* 2003; Fleeger *et al.* 2006; Schratzberger *et al.* 2007).

Relatively few studies of the meiofauna of shallow continental shelf in the northern Gulf of Mexico have been performed. Recent studies have examined the effects of oil and gas platforms on abundance and genetic diversity (Montagna and Harper 1996; Street and Montagna 1996), faunal responses to hypoxia (Murrell and Fleeger 1989; Wetzel *et al.* 2001), the relationships between meiofauna and photosynthetic pigments (Radziejewska *et al.* 1996) and water depth (Baguley *et al.* 2004; Baguley *et al.* 2006a; Baguley *et al.* 2006b), sediment depth profile (Fleeger *et al.* 1995; Radziejewska *et al.* 1996), and the effect of winter storms on emergence into the water column (Thistle *et al.* 1995a; Thistle *et al.* 1995b; Thistle 2003). Most of these studies (except those by Thistle and colleagues) have examined the meiofauna of muddy bottoms. No previous research has been conducted on the meiofauna of sandy shallow subtidal sediments in Louisiana, although the gastrotrich fauna of sand beaches in the Gulf of Mexico has been examined (Todaro *et al.* 1995).

Sandy sediments (with mean particle size > 125 μm and low silt-clay content) typically accommodate an interstitial meiofauna community while muddy bottoms are populated by burrowing meiofauna that push sediment particles aside as they move through the sediment (Wieser 1959). Interstitial meiofauna live in and move through the capillary-water filled spaces between sand grains. Some taxa (e.g., Gastrotricha and Turbellaria) are largely restricted to interstitial environments serving as indicators, while other taxa (e.g., Nematoda and Harpacticoida) express both interstitial (in sandy sediments) and burrowing (in muddy sediments) lifestyles. Interstitial meiofauna are greatly influenced by sediment characteristics.

For example, the highest diversity and abundance of interstitial meiofauna is expected in sediments with mean grains sizes > 200 μm which provides large spaces for movement between sediment particles (Giere 1993). The body shape of interstitial meiofauna is constrained by sediment particle size and/or resulting chemical gradients (Levy and Coull 1977; Tita *et al.* 1999; Soetaert *et al.* 2002), and interstitial meiofauna are typically smaller in body size, more vermiform in body shape with reduced complexity of body form compared to non-interstitial taxa (Swedmark 1964). Life history characteristics of interstitial fauna differ from burrowing species in that brooding is more common and reproductive rates are lower (Swedmark 1964). Ecologically, interstitial meiofauna appear to be less sensitive to physical disturbance (Schratzberger and Warwick 1998) but are generally slower to recolonize sediment after disturbance events (Colangelo *et al.* 1996) compared to burrowing meiofauna (Chandler and Fleeger 1983).

Vanaverbeke & Vincx (Vanaverbeke and Vincx 2008) suggest that meiofauna responses to sand mining may differ from that of macroinfauna because their life histories differ. The purpose of this report is to describe a survey of the meiofauna of Ship Shoal and to consider the potential impact of sand mining on Ship Shoal on the extant meiofauna community.

## 9.2. METHODS

### 9.2.1. Field collections

Meiofauna were collected on Ship Shoal on three cruises (in May/June, August and October) in 2005 and 2006. Samples for meiofauna were taken simultaneously with macroinfauna collections (see Chapter 10 for site details). To summarize, 26 stations were sampled for meiofauna on each cruise. Meiofauna samples at each station were taken from three replicate GOMEX box cores. Two meiofaunal samples were collected with a 2.6 cm inner diameter subcorer to a depth of 4 cm from each box core and pooled. One additional subcore from each station (from one of three box cores) was taken and vertically sectioned on board ship with the use of a precision core extruder following Fuller & Butman (1988). We sectioned samples at 0-5, 5-10, 10-20, 20-30, and 30-40 mm and immediately preserved all samples using 5% formalin.

### 9.2.2. Laboratory analysis

Average grain size for each sampling station was determined by first washing sediments through a 63 μm-aperture sieve to separate coarse sediments from the silt-clay (< 63 μm) fraction. Both fractions were then dried at 60°C and weighted to determine the percent silt-clay. The > 63 μm fraction was dry sieved through 22 stacked sieves ranging from 63 μm to 2 mm, and a grain size profile was calculated using Gradistat software (Blott and Pye 2001). Percent organic carbon was determined for selected sediment samples using a Perkin-Elmer 2400 Elemental Analyzer.

Before analysis, samples were weighed into pre-weighed silver pans and exposed to concentrated HCl fumes in a desiccator for 48 h to remove carbonates.

Meiofauna samples were processed at Louisiana State University. After staining with Rose Bengal, a swirl and decant procedure was used to separate meiofauna from sediments. After swirling, water, but not sand particles, was decanted onto a 45 μm sieve and retained material was rinsed into a beaker. We tested this procedure for extraction efficiency by sequential extraction. Based on the results we estimate that over 98% of the meiofauna were extracted after six decantations, and we adopted this procedure as a standard for all Ship Shoal samples.

Nematodes, crustaceans (including harpacticoid copepods, ostracods, amphipods and cumaceans), annelids, turbellarians and gastrotrichs were identified to major taxon and quantified by microscopic examination. For 2005 collections, a density estimate for each box core was derived by enumerating the number of meiofauna per subcore and then by averaging counts across the number of subcores per box core. Abundance was converted to a standardized area (individuals 10 $cm^{-2}$), and averaged across the three box cores to estimate abundance for a given station. In 2006, only vertical-profile subcores were analyzed (1 per station) and abundance for each taxon was calculated by summing the number of individuals in each layer and converting to a standardized area (individuals 10 $cm^{-2}$).

Sorting quality control was achieved in two ways. Specimens were photographed and photographs were used to train graduate students and student workers participating in sample sorting and identification procedures. Additionally, Dr. Antonio Todaro of the Università di Modena & Reggio Emilia, Italy examined specimens labeled as gastrotrichs from our June 2005 collections and his examination confirmed our identification. Dr. Todaro also examined species composition of these specimens and found that gastrotrich species diversity was low (≤ 3 species); species identifications of gastrotrichs were, therefore, not continued.

Following macrofaunal analysis (see Chapter 10), we grouped the 26 Ship Shoal stations into east (E), middle (M), and west (W) locations to examine the spatial distribution of meiofauna. The east grouping includes stations 14 through 18 (n=5), the middle grouping includes stations 7 to 13 and 24 to 26 (n=10), and the west grouping includes stations 1 to 6 and 19 to 23 (n=11).

A three-way-analysis of variance (ANOVA) was used to test for significant differences in the abundance of meiofauna between years, seasons, and locations. Harpacticoid copepods, nematodes, gastrotrichs and turbellarians were tested because they were consistently found in meiofauna samples; rare taxa such as ostracods, cumaceans and larval polychaetes were not analyzed. For each sample collection, the relationship between the abundance of each major taxon with sediment chlorophyll (Chl) *a*, bottom water dissolved oxygen, water depth, average grain size, and percent silt-clay was examined using scatterplots. Visually evident relationships were tested for statistical significance using linear regression.

To determine the effect of sediment depth layer and season on the vertical depth distribution of meiofauna major taxa, a two-way ANOVA was performed separately for nematode, harpacticoid copepod, turbellarian and gastrotrich abundance data with season (May/June, August, and

October) and core layer in mm (0-5, 5-10, 10-20, 20-30, 30-40) as main effects. A significant interaction between season and core layer was considered indicative of a seasonal effect on sediment depth distribution. To compare differences in sediment depth distribution between the major taxa, we calculated weighted mean sediment depth (see Fleeger *et al.* 1995) of nematodes, harpacticoid copepods, turbellarians and gastrotrichs from for each location and season and compared them using a three-way ANOVA with species, location (E,M,W) and season (May/June, August, October) as factors. Data from 2005 and 2006 were combined for analysis. The vertical distribution of meiofauna in the sediment may be influenced by physical conditions associated with physical-chemical gradients such as oxygen concentration and grain size. Therefore we examined scatterplots of mean weighted depth and bottom water dissolved oxygen, sediment grain size and percent silt-clay content. Visually evident relationships were tested for statistical significance using linear regression.

## 9.3. RESULTS

### 9.3.1. Physical-Chemical Gradients

Spatial gradients in water depth and grain size were found across Ship Shoal. Water depth ranged from 5 to 11 m. Depth generally increased from west (5 to 8 m) to east (9 to 10 m). Sediments on Ship Shoal were well sorted fine to very fine sand with low silt-clay content (Table 9.1). Grain size generally increased from west to east, a pattern attributable to a greater occurrence of gravel-sized shell hash on the eastern shoal. Sediment carbon from the June 2005 cruise was analyzed and values were generally less than 0.2% across Ship Shoal. Hypoxia (D.O. < 2 mg/l) was rarely observed on Ship Shoal even in summer (Table 9.1). Bottom water salinity was generally greater than 30‰ and spatial patterns across Ship Shoal were not evident.

Table 9.1

Summary of seasonal bottom water and sediment data (mean ±std) for the eastern and western portions of Ship Shoal during spring, summer and fall of 2005-2006.

| Station grouping | Depth (m) | Mean Grain size (μm) | silt/clay (%) | Gravel (%) | Dissolved Oxygen (mg/l) | Temp (°C) | Salinity (ppt) |
|---|---|---|---|---|---|---|---|
| **Spring** | | | | | | | |
| East | 8.8± 1.1 | 182.3±22.3 | 1.1±0.7 | 2.4±2.0 | 4.6±0.8 | 26.4±1.5 | 33.2±2.4 |
| West | 6.4±1.3 | 147.6±13.2 | 1.3±0.7 | 0.6±1.3 | 5.7±0.7 | 27.8±1.4 | 31.6±1.7 |
| **Summer** | | | | | | | |
| East | 8.4±1.1 | 208.7±57.4 | 1.6±1.4 | 3.9±4.0 | 5.8±0.4 | 30.3±0.5 | 34.8±0.5 |
| West | 6.1±1.2 | 153.5±15.1 | 1.6±1.2 | 0.2±0.1 | 5.0±0.7 | 31.0±0.3 | 32.0±1.2 |
| **Fall** | | | | | | | |
| East | 9.0±1.2 | 203.3±26.2 | 0.9±0.7 | 2.9±2.6 | 7.6±0.4 | 25.1±1.9 | 33.4±1.1 |
| West | 6.4±1.2 | 142.4±13.6 | 2.6±2.8 | 0.1±0.1 | 7.4±0.3 | 25.4±1.6 | 32.3±0.9 |

### 9.3.2. Meiofauna

At all stations and sampling dates, nematodes were the numerically dominant taxon, generally comprising > 94% of all individuals (Table 9.2). Harpacticoid copepods, gastrotrichs and turbellarians were also common, but in much lower densities than nematodes (Table 9.2). Consequently, major taxon diversity was low at many sites. Total meiofauna density did not differ significantly between locations or among seasons on Ship Shoal. However, there was a significant effect of year ($p < 0.001$), with meiofauna densities in 2005 significantly lower than in 2006 (Figure 9.1). At the level of major taxon, nematode ($p < 0.001$), harpacticoid copepod ($p < 0.001$), and turbellarian ($p < 0.001$) densities were higher in 2006 compared to 2005 (Table 9.2; Figure 9.2 a to f). Within years, mean densities of the major taxa were generally highest in May/June and August and lowest in October. These seasonal differences in density were significant for harpacticoid copepods ($p = 0.003$) and turbellarians ($p < 0.001$), but not gastrotrichs and nematodes (Figure 9.2 a to f). Significant spatial differences in meiofaunal density between the east, middle and west station groups were found only for turbellarians ($p = 0.002$), which were significantly higher in the central compared to the eastern end of Ship Shoal (Figure 9.2 a to f).

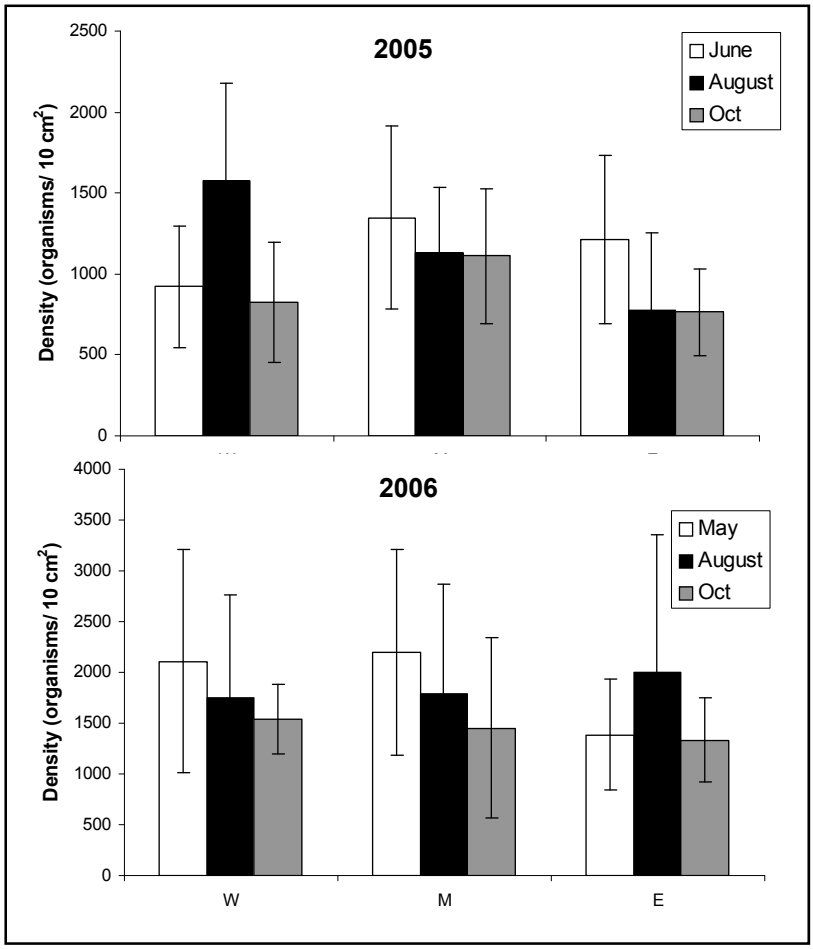


Figure 9.1 Total meiofaunal density (mean individuals 10 cm-2 ± stdev) at the west (W), middle (M) and east (E) stations during June, August and October 2005 sampling.

Table 9.2

Total mean meiofauna density (mean individuals 10 $cm^{-2}$ ± std) for all 2005-2006 box-core samples on Ship Shoal.

| | 2005 | | | 2006 | | |
|---|---|---|---|---|---|---|
| | June | August | October | May | August | October |
| Nematoda | 1079.6 ±452.8 | 1199.4 ±568.0 | 855.1± 390.7 | 1746.5 ±943.3 | 1638.7 ±1029.4 | 1226.6 ±387.9 |
| Gastrotricha | 25.4 ±7.3 | 23.8 ±23.5 | 17.4 ±21.4 | 169.7 ±314.8 | 61.3 ±84.3 | 29.1 ±28.8 |
| Turbellaria | 24.5 ±10.9 | 20.7 ±12.3 | 14.8 ±10.2 | 46.4 ±24.6 | 53.9 ±28.0 | 44.4 ±82.5 |
| Copepoda | 9.4 ±8.8 | 9.7 ±7.4 | 2.3 ±3.4 | 7.3 ±7.0 | 20.2 ±16.9 | 23.2 ±23.5 |
| Nauplii | 7.2 ±6.5 | 14.3 ±14.2 | 1.6 ±1.7 | 19.8 ±23.4 | 27.5 ±35.0 | 116.4 ±249.2 |
| Unknown Annelida | 1.8 ±2.0 | 5.6 ±4.4 | 1.7 ±2.5 | 5.5 ±6.1 | 2.4 ±4.2 | 0.8 ±1.7 |
| Polychaeta | 2.5 ±2.3 | 2.3 ±2.8 | 0.3 ±0.3 | 4.7 ±5.8 | 2.6 ±3.2 | 0.8 ±1.4 |
| Ostracoda | 0.9 ±1.0 | 1.7 ±2.7 | 0.7 ±1.0 | 1.0 ±1.5 | 1.7 ±2.8 | 0.2 ±0.6 |
| Amphipoda | 0.4 ±0.4 | 0.4 ±0.5 | 0.1 ±0.2 | 1.6 ±3.3 | 0.1 ±0.4 | 0.1 ±0.5 |
| Bivalvia | 0.9 ±1.4 | 0.8 ±1.2 | 0.7 ±1.7 | 1.3 ±2.7 | 1.1 ±2.0 | 0.0 |
| Gastropoda | 0.1 ±0.1 | 0.0 | 0.0 | 0.0 | 0.1 ±0.7 | 0.0 |
| Cumacea | 0.1 ±0.2 | 0.0 | 0.0 | 0.0 | 5.0 ±0.0 | 0.0 |
| Isopoda | 0.0 | 0.2 ±0.3 | 0.0 | 0.0 | 0.0 | 0.0 |
| Unknown | 0.4 ±1.2 | 0.3 ±1.1 | 0.0 | 0.0 | 0.0 | 0.0 |

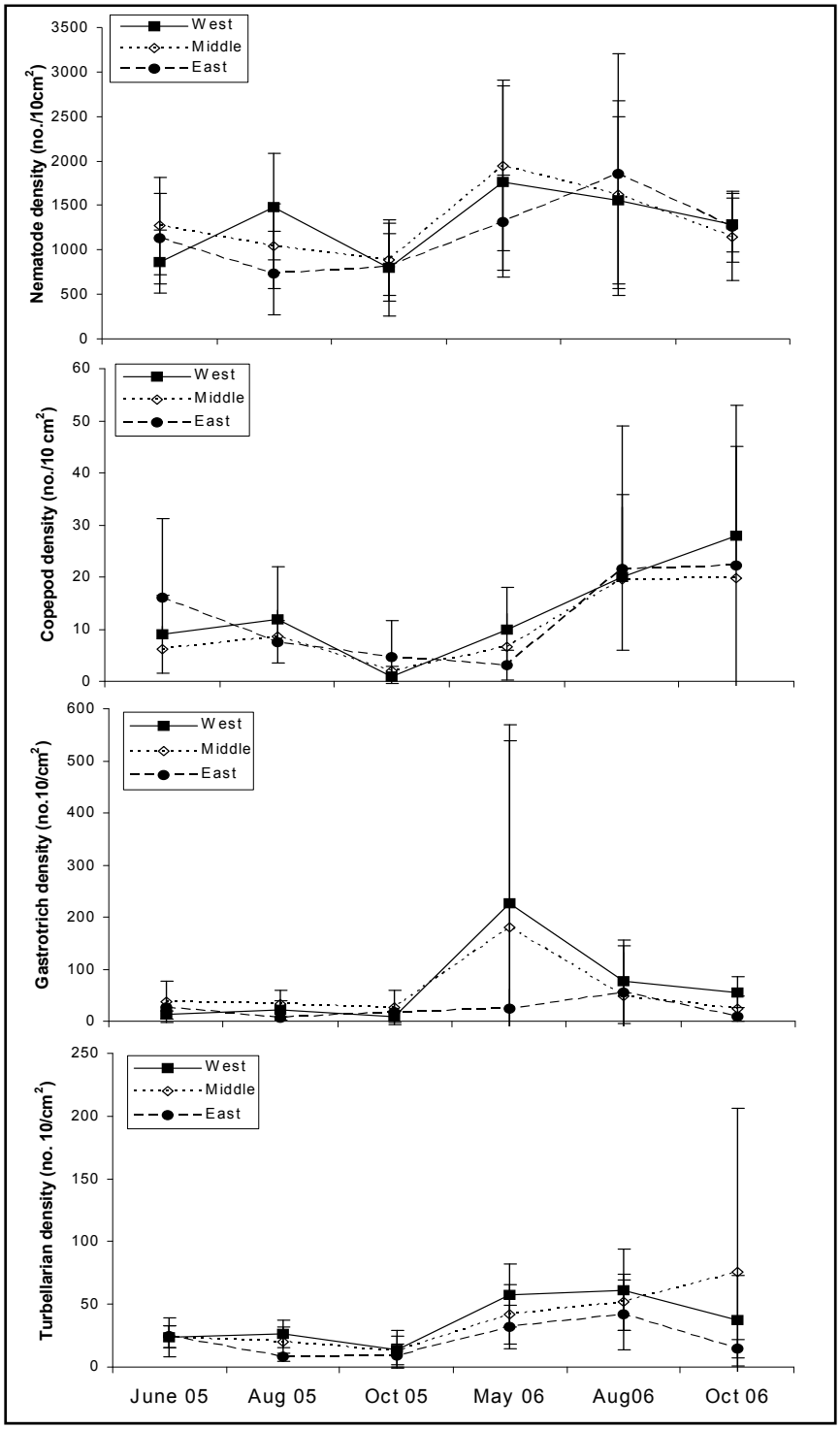


Figure 9.2 (a through f). Density of the most common meiofaunal taxa (mean individuals 10 $cm^{-2}$ ± stdev) at the west (W), middle (M) and east (E) stations during June, August and October 2005 sampling.

Environmental factors did not explain significant amounts of variation in the abundance of total meiofauna or individual major taxa. Visual examination of scatterplots did not suggest relationships between the densities of harpacticoid copepods, nauplii, nematodes, turbellarians, and gastrotrichs and the environmental factors including sediment Chl *a*, bottom-water dissolved oxygen, mean grain size and percent silt-clay. Low dissolved oxygen may decrease infaunal abundance, especially for sensitive groups such as copepods (Wetzel *et al.* 2001). However, hypoxic levels of dissolved oxygen were generally not found in 2005-2006; consequently, a strong relationship between dissolved oxygen and meiofaunal abundance may not consistently occur on Ship Shoal. Water depth appeared to be related to the abundance of some taxa in August 2005. Linear regression revealed a significant negative relationship between water depth and the abundance of nematodes ($p = 0.046$), nauplii ($p = 0.005$), gastrotrichs ($p = 0.003$), and turbellarians ($p < 0.001$). However, similar relationships between water depth and abundance were not found for other sampling dates.

Vertical profiles suggest that meiofaunal abundance was highest in the upper 2 cm of sediment and generally decreased between 3 and 4 cm (Figure 9.3). Only harpacticoid copepods were most abundant in the uppermost cm (Figure 9.3). In 2005, the numerical abundance of nematodes ($p < 0.001$), copepods ($p < 0.0031$), and gastrotrichs ($p < 0.001$), but not turbellarians was significantly different among the five core layers (Figure 9.3). Similarly, the abundance of all four taxa differed significantly between core layers in 2006 ($p < 0.001$ to 0.002). The depth distribution of these major taxa did not appear to change seasonally as there was no significant interaction between season and sediment depth distribution ($p > 0.05$) for any taxon analyzed in 2005 or 2006.

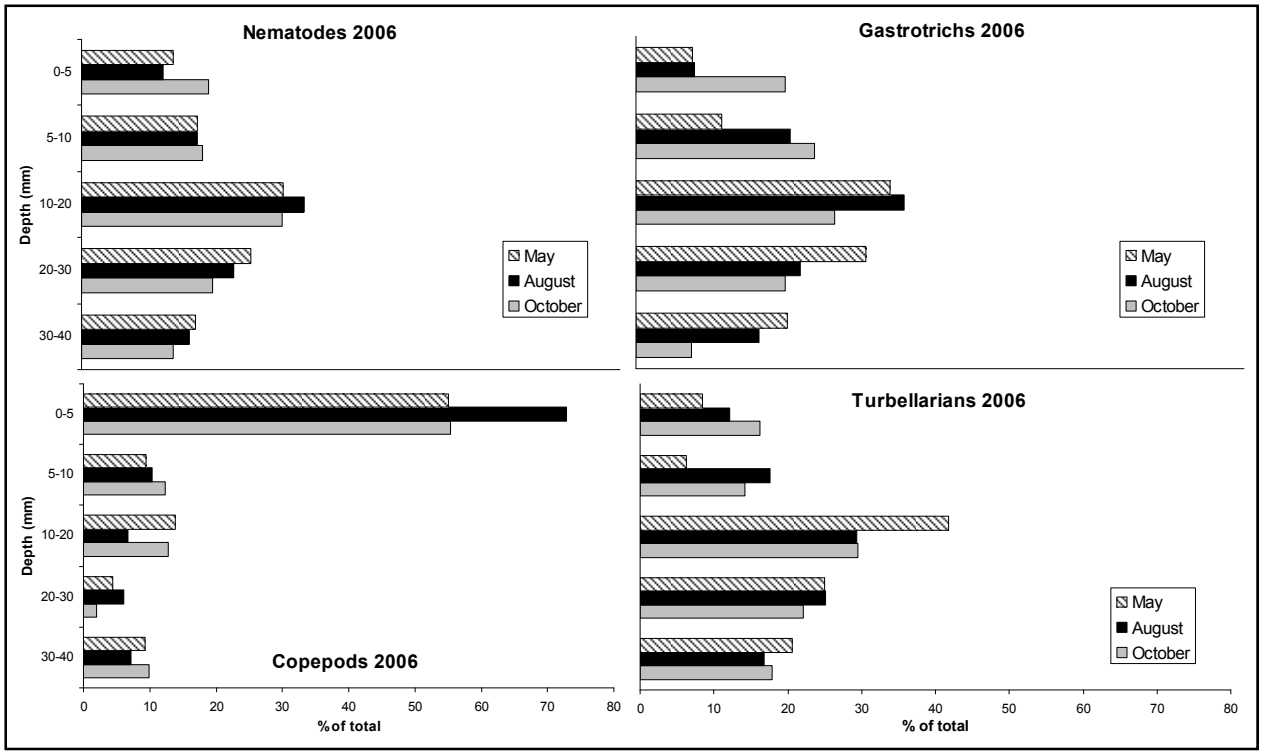


Figure 9.3 (a through f). Vertical profile for meiofauna (mean percent of total core at each depth layer) collected in May/June, August and October 2005 and 2006. Note that the first two bars represent half-centimeter sections, while the other bars are one-centimeter sections.

Season and taxon ($p < 0.001$ for both), but not location, had significant effects on mean weighted depth. Meiofauna depth in the sediment was significantly deeper in October compared to May/June and August. Harpacticoid copepods were significantly nearer to the sediment surface in profiles compared to turbellarians, nematodes and gastrotrichs in all collections. There was no interaction between season and major taxon suggesting that seasonal effects did not differ between major taxa. There was an interaction between location and some taxa. Copepods had a significantly deeper mean weighted depth at W compared to E and M. Gastrotrichs displayed the opposite trend, having a significantly greater depth at M compared to Wand E. Visual analysis of scatterplots did not suggest relationships between near-bottom dissolved oxygen, mean grain size, and percent silt-clay and the mean weighted depth of harpacticoid copepods, nematodes, gastrotrichs and turbellarians in any season or year.

## 9.4. DISCUSSION

Our research suggests that Ship Shoal meiofauna are interstitial in lifestyle compared to the burrowing meiofauna of surrounding sediments high in silt-clay content. Not only does the presence of indicator taxa (e.g., gastrotrichs) differ on and around Ship Shoal, but Ship Shoal nematodes are significantly more slender in body form than from surrounding muddy sediments

(Fleeger unpublished). This decreased diameter facilitates sliding in interstitial spaces between sand grains and is associated with interstitial lifestyle (Tita *et al.* 1999). Sediments with a mean grain size from 125-200 μm and low silt-clay content such as Ship Shoal's are expected to house an interstitial meiofauna but with low diversity compared to coarser sands (Wieser 1959). As predicted, Ship Shoal appears to have a low major taxon and species diversity of interstitial meiofauna, including gastrotrichs (Todaro, unpublished) and harpacticoid copepods (Fleeger, unpublished). Interstitial meiofauna have different ecological relationships and life histories compared to burrowing meiofauna and macrofauna (Vanaverbeke and Vincx 2008), and below we discuss how these differences may affect the fauna and their response to sand mining.

Several lines of evidence from our survey suggest that Ship Shoal meiofaunal major taxon and species composition differs substantially from that found on surrounding muddy bottoms on the Louisiana continental shelf. Nematodes dominated meiofaunal collections on Ship Shoal (as is expected for most of the seafloor, Coull 1988) but the occurrence of less abundant taxa differed considerably from the surrounding muddy seafloor. For example, gastrotrichs and turbellarians are characteristic of sandy sediments and were common and always present on Ship Shoal. Kinorhynchs (which are usually restricted to sediments with high silt-clay content) did not occur on Ship Shoal even though they are common in surrounding sediments (Murrell and Fleeger 1989; Radziejewska *et al.* 1996). Size spectrum and tail type analysis suggest that nematode communities differ on Ship Shoal compared to the surrounding seafloor (Fleeger unpublished). Sediment composition is generally recognized as a principal determinant of meiofauna species composition, including on sandbanks (Vanaverbeke *et al.* 2002). Macrofauna species composition on Ship Shoal also differs from the surrounding Louisiana shelf (Dubois et al., Chapter 10). Dubois et al. further speculate that Ship Shoal may be an important biodiversity "hotspot" in the northern Gulf of Mexico for macrofaunal invertebrates and that recruits from Ship Shoal may contribute to large-scale patterns of dispersal in the Gulf; Ship Shoal may play a similar role for meiofaunal populations.

Meiofaunal densities on Ship Shoal ranged from about 900-1800 individuals 10 $cm^{-2}$ across all seasons and collections while densities from the surrounding Louisiana continental shelf typically range from ~1000-4000 individuals 10 $cm^{-2}$ (Murrell and Fleeger 1989; Radziejewska *et al.* 1996). Lower abundances in sandy sediments in the same geographic region are commonly reported for meiofauna (Giere 1993). Studies of sandbanks in the North Sea (Vanaverbeke *et al.* 2000) have found average abundances to be about 500 individuals 10 $cm^{-2}$. Depth profiles for meiofauna on Ship Shoal peaked in the second cm for all taxa except harpacticoid copepods which were most abundant in the surface cm. Similar patterns have been reported at muddy sediment sites in the northern Gulf of Mexico (Fleeger *et al.* 1995; Radziejewska *et al.* 1996). The causes of lower abundances of interstitial meiofauna are not understood but may be a function of reproduction and dispersal. Interstitial meiofauna commonly brood offspring and have low reproductive output and/or a low intrinsic rate of natural increase (Swedmark 1964). Interstitial meiofauna are known to disperse from sandy habitats through association with the water column (Hagerman and Rieger 1981; Service and Bell 1987) but most studies suggest their colonization of azoic sediment is slower than that of burrowing meiofauna (Chandler and Fleeger 1983; Colangelo *et al.* 1996).

Meiofaunal abundance was not correlated with specific physical/chemical conditions on Ship Shoal. This was so even though variations in sediment type, water depth and light levels were documented across Ship Shoal. Most compellingly, we could find no evidence that hypoxia affects meiofauna on Ship Shoal. Neither abundances nor vertical profiles were related to oxygen concentration over seasonal time scales, and our dissolved oxygen data suggest that Ship Shoal does not typically experience seasonal hypoxia, although short-term hypoxia may occur. Meiofaunal abundance on Ship Shoal was significantly higher in 2006 than 2005. There were large hurricanes (e.g., Katrina, Rita) in the Gulf of Mexico in 2005 but none occurred in 2006. Interstitial fauna do not burrow deep enough to avoid erosion during winter storms in the northern Gulf of Mexico (Thistle *et al.* 1995a) suggesting that hurricanes may erode and suspend meiofauna leading to reduced abundance. On the other hand, some environmental factors (e.g., Chl *a*) varied as much over small spatial scales as over Ship Shoal as a whole. Interstitial meiofauna may rely on *in situ* benthic primary production (e.g., benthic diatoms) for the base of their food web (Blanchard 1991). Grippo et al. (Chapter 8) suggest that benthic primary production is high on Ship Shoal. If so, changes in meiofaunal abundance that accompany phytoplankton sedimentation events in other locations (Vanaverbeke *et al.* 2004; Franco *et al.* 2008) may not occur on Ship Shoal. In addition, critical environmental variation may occur at times we have not sampled. For example, Kobashi et al. (Chapters 6 & 7) suggest that a thick deposition of fine-grained sediment sometimes occurs on Ship Shoal in association with winter storms and high riverine outflow (potentially from November – April). This fine-grained material may clog interstitial spaces (and inhibit interstitial meiofauna) and restrict light to benthic microalgae. We have not collected meiofauna during such events and cannot be sure how deposition of fine sediments may affect meiofaunal abundance or diversity. However, the entry of fine-grained material into the sediment matrix may produce long-term effects on meiofauna by clogging interstitial spaces. Such effects on sediment may explain the lack of correlation of meiofauna with other physical factors, because the effect on the sediment may override other environmental factors. Generally however, interstitial meiofauna appear to be more resilient than burrowing fauna to physical disturbance (Schratzberger and Warwick 1998), and this resilience may also contribute to the lack of correlations with physical-chemical data. Macrofaunal abundance and diversity did vary seasonally and with physical gradients on Ship Shoal (see Chapter 10).

The responses of meiofauna to sand mining have been reported in peer-reviewed journals (by using before-after collection designs to examine changes following sand mining or by examining recovery after cessation of mining) only from sandbanks in the North Sea. Vanaverbeke *et al.* (2007) found that sand extraction favored predatory nematodes and that longer nematodes (which are more susceptible to disturbance) became rare as a result of sand mining. Vanaverbeke & Vincx (2008) found that although nematode density, diversity and biomass did not change two years after cessation of sand exploitation, nematode community composition did change and was more stable than in a recently extracted site. These studies were conducted in much coarser sand than is found in Ship Shoal and the ability to draw conclusions relevant to Ship Shoal from this work is uncertain, especially without before and after collections from a sand removal site in the Gulf of Mexico.

Responses to sand mining by meiofauna will likely differ from that of macrofauna because of differences in life history and dispersal ecology (Vanaverbeke and Vincx 2008). An initial reduction in the abundance of meiofauna is expected after sand removal because meiofauna are unlikely to be able to avoid removal by burrowing to a deeper sediment profile (Thistle *et al.* 1995a). Meiofauna densities are typically highest in the upper 4-6 cm of sediment depth, and Ship Shoal vertical profiles show most meiofauna peak in the second cm. However, the recovery rate of interstitial meiofauna is difficult to predict and will, in part, depend on the physical perturbations associated with the methods of mining (e.g., because meiofauna are influenced by the variation in sediment conditions, the frequency with which dredge furrows are created or filled will likely influence meiofauna communities). Interstitial meiofauna appear to be more resilient to sublethal physical disturbance than macrofauna, as meiofauna are well adapted to disturbance associated with storms and frontal passages, while sedentary and tubiculous macroinfauna may be sensitive to mechanical disturbances (Austen *et al.* 1989; Hall and Harding 1997). Comparisons between interstitial meiofauna and macrofauna suggest differences in reproductive and dispersal rates will affect recovery. For example, most meiofauna lack dispersing larval stages but adults and juveniles both re-colonize through the overlying water, which facilitate rapid recovery of areas affected by small-scale disturbances (Chandler and Fleeger 1983). In contrast, large areas of disturbance may be more rapidly colonized by macrofauna larvae because they are better adapted to long-distance dispersal. Meiofauna probably have high annual rates of reproduction compared to macrofauna because of their high number of generations per year (often $\geq$ 9, Fleeger and Palmer 1982) even though brood size is low. Studies suggest that macrofauna recovery following sand disturbance may take many months to years (Palmer *et al.* 2008). Similarly, studies with meiofauna also suggest a slow trajectory to return to pre-mining conditions (Vanaverbeke *et al.* 2002; Vanaverbeke and Vincx 2008). We suggest that monitoring studies of both macrofauna and meiofauna, however, will have value to evaluate the effects and recovery from sand extraction.

# CHAPTER 10
# DIVERSITY AND COMPOSITION OF MACROBENTHIC COMMUNITY ASSOCIATED WITH SANDY SHOALS OF THE LOUISIANA CONTINENTAL SHELF

## 10.1. INTRODUCTION

Recently, sandy shoals of the US continental shelf have received increased attention because they have been identified as potential exploitable sand deposits (Drucker *et al.* 2004). This is especially true for the Louisiana coast where a single shoal (Ship Shoal) is considered one of the largest sand sources in the Gulf of Mexico (Drucker *et al.* 2004), containing 1.6 billion cubic yards of fine sand intended for beach reinforcement and coastal stabilization projects designed to prevent coastal erosion due to storm damages and prevent wetland loss due to anthropogenic disturbances that induce sea-level rise (Michel *et al.* 2001). This increased interest in shoals highlights the observation that the benthic and nektonic composition of shoals is less well studied than other continental shelf environments (Brooks *et al.* 2006). Faunal composition may be important to predicting recovery after sand-mining and to understanding ecological relationships on shoals. For example, benthic invertebrates are directly related to the sediment they inhabit (Gray 1974; Snelgrove and Butman 1994), and any sand-mining activity or associated human-related change in sediment features may negatively affect the resident community and consequently impact trophic relationships within these communities. It is thus of primary importance to identify and characterize macroinfaunal benthic assemblages associated with potential sand-mining sites.

The macrobenthos of some Louisiana – Texas shoals (i.e. Sabine and Healds Shoals) have been recently investigated (Cheung *et al.* 2006) but these studies and a recent macrobenthic survey of Louisiana in-shore and off-shore waters (Baustian 2005) did not include Ship Shoal, partly because its shallow depth has discouraged access by larger research vessels. Ship Shoal's benthic species assemblages might be used as a food source for numerous fishes or large crustaceans that permanently or temporarily forage on this shoal. In addition, because of its location in the north central Gulf of Mexico, and unlike the west Florida shelf, Ship Shoal is surrounded by muddy soft-bottoms affected by seasonally hypoxia events that causes drastic decreases in abundances of benthic species inhabiting this "dead zone" (Rabalais *et al.* 1994; Justic *et al.* 1996). It is unknown whether benthic populations living on Ship Shoal are affected by hypoxic events. It is possible that Ship Shoal may serve as an hypoxia refuge for benthic populations or as a seed-bank to disperse and recolonize the surrounding hypoxic area when normoxia returns.

The overall objectives for this study are thus to better understand the potential role Ship Shoal is likely to play in the Louisiana's coastal ecosystem, and to address the potential effects of sand-mining on the benthic community. Our approach was to describe spatial and seasonal variations in diversity and structure of macrobenthic assemblages associated with Ship Shoal over a

relatively fine-scale latitudinal and longitudinal gradient and to link community patterns with variation in environmental parameters.

## 10.2. MATERIAL AND METHODS

### 10.2.1. Study site

Samples were taken from 21 stations on Ship Shoal, located in the north central part of the Gulf of Mexico approximately 20 km off-shore from Terrebonne Bay and Isles Dernieres, Louisiana (28°54.092N , 91°00.989 W). The shape of this shoal is elongated, parallel to the shore. It spans a 50 km distance along the east-west dimension and 1 to 10 km along the north-south dimension (Figure 10.1). Based on depth contours available on existing sea charts, stations were chosen according to an east-west distribution with three main north-south transects, one in the east (stations 15-16-17), one in the west (stations 23-22-21), and one in the middle (stations 24-25-26). Other stations were distributed along the spine of this sandy shoal in three main groups: east stations from station 18 to station 13, central stations from station 12 to station 09 and 10, and west stations from stations 07 and 08 to station 01 and 19. The general bathymetry of the shoal is related to east-west and north-south gradients: the western region is the shallowest (ca. 4 m) and the depth increase toward the east (ca. 10 m). A north-south transect across the shoal shows that the northern edge is well-defined with sharp slope while the slope of the southern edge is more gentle with depth increasing slightly from the spine – i.e. middle – of the shoal toward the south, making the definition of the southern edge difficult to discern.

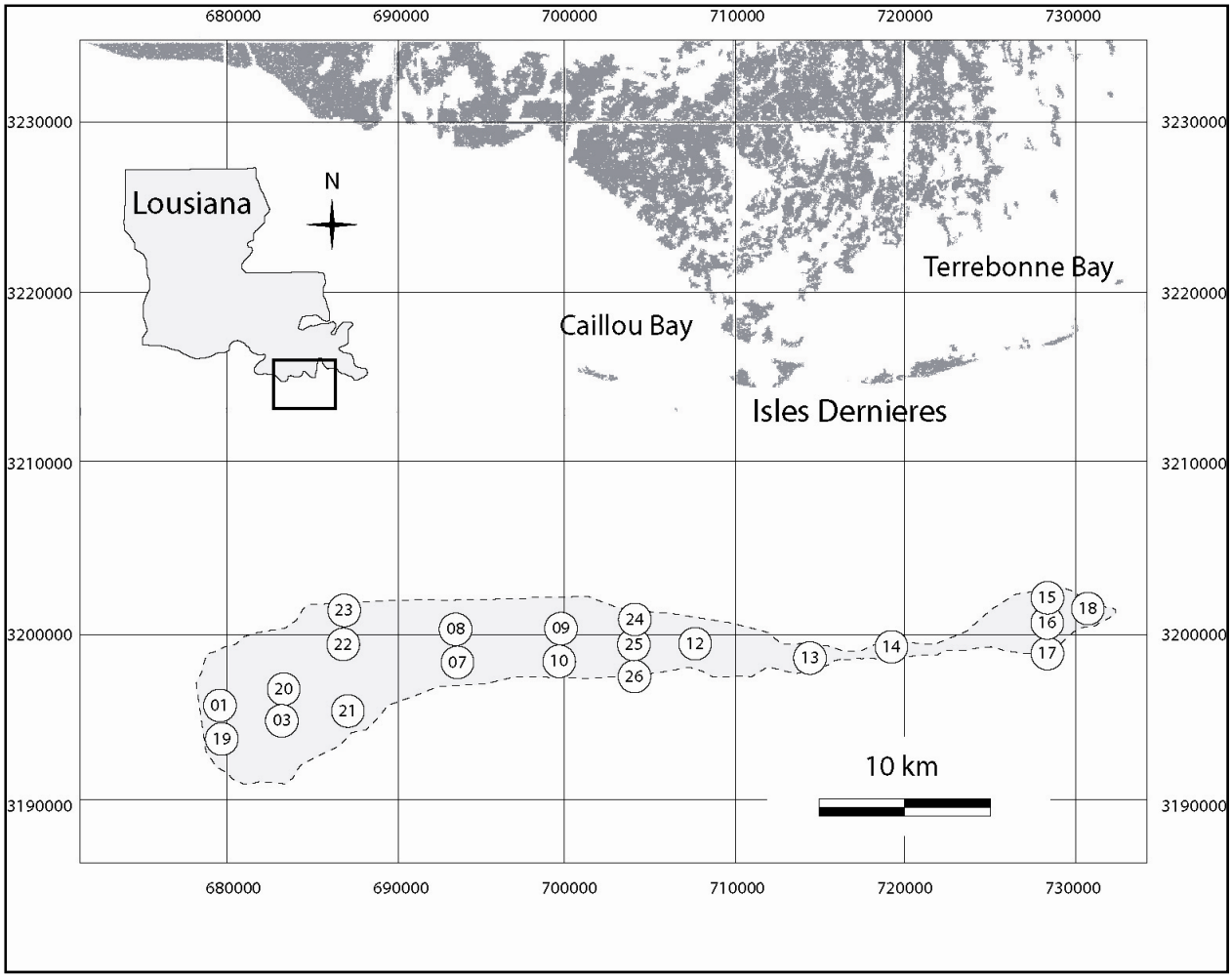


Figure 10.1 Geographic position of the 21 sampling stations on Ship Shoal, off Louisiana. General contour of Ship Shoal (dotted lines) has been established based on sea chart depth contours and field observations.

### 10.2.2. Field sampling

Samples were collected during three cruises in 2006 using the Louisiana Universities Marine Consortium (LUMCON) Research Vessel "ACADIANA": May (21$^{st}$ to 24$^{th}$; Spring), August (19$^{th}$ to 21$^{st}$; Summer) and October the 30$^{th}$ and November the 1$^{st}$ (Autumn). Because of inclement weather, only 16 stations were sampled in October. Macrofauna was collected using a GOMEX box corer which has been shown to efficiently sample muddy and very fine to fine sandy sediments (Boland and Rowe 1991). Three replicates of 900 cm$^2$ (30 × 30 cm) were taken at each station. Subsamples for sediment analysis and chlorophyll *a* sediment content were extracted from each box core with a 3 cm diameter cylinder over ca. 5 cm depth. Sediment samples were frozen until ready for analysis. Water characteristics (temperature, salinity, dissolved oxygen = DO) were monitored ca. 1 m above the bottom.

Box core samples were sieved at sea on a 500 μm sieve using seawater. Retained organisms, including sediment, was fixed and preserved in 5 percent buffered formalin and returned to the laboratory.

### 10.2.3. Laboratory analysis

In the laboratory, macroinvertebrates were sorted to major taxon (i.e. polychaetes, mollusks and others) and transferred to 70 percent ethanol. Wet weight of each group (shells included for mollusks) was taken before all individuals were sorted, identified to the species level (or the lowest taxonomic level possible) and enumerated. Species were classified into five feeding-guilds: (1) suspension-feeders, (2) surface deposit-feeders, (3) interface feeders (i.e. species which can switch from suspension-feeding to surface deposit-feeding), (4) sub-surface deposit-feeders and/or psammivors, (5) predators or scavengers/detritivores, based on taxonomic affiliation of families after Fauchald and Jumars (1979) for polychaetes, Yonge and Thompson (1976) for mollusks and Pechenik (2005) for other taxonomic groups. Some nematodes and planktonic copepods were retained but were excluded from analysis following Rzeznik-Orignac *et al.* (2004).

Sediment particle size analysis was conducted for each station. Sediment samples were washed with distilled water through a 63 μm sieve to separate sand from silt and clay and to dissolve NaCl particles that may agglomerate smaller particles. The fraction <63 μm was collected in a bowl with water and allowed to settle for 72 hours. The water was then siphoned and the silt/clay fraction dried to constant weight in an oven at 60°C, then weighed. The sand fraction was dried to constant weight in an oven at 60°C, and placed on a Ro-Tap sieve shaker for 3 min (21 sieves from 2 mm to 63 μm mesh size with ½ Φ intervals). The fraction retained on a 2 mm mesh size is the gravel fraction (consisting mostly of shell debris). The average particle size and the sorting index σ were determined using the Folk and Ward (1957) method. Results were processed by the Gradistat software (Blott and Pye 2001).

### 10.2.4. Statistical analysis

Data were analyzed using univariate and multivariate methods. Macrofauna species diversity was estimated using species richness and Hill's (1973) heterogeneity of diversity indices: N1 = exp(H'), where H' is Shannon-Wiener diversity ($\log_e$ - Shannon 1948); and N2 = 1/SI, where SI is Simpson's index (Simpson 1949); N1 is sensitive to the number of medium-density species whereas N2 is sensitive to the number of very abundant species (Whittaker 1972). Species richness – i.e. the number of different species – is also called N0, consistently with N1 and N2 indices. These indices are well suited to the analysis of diversity of benthic macrofauna communities and, together with the equitability index J' (Sheldon 1969), are recommended by Gray (2000) to measure heterogeneity of marine coastal diversity.

One-way ANOVA was used to test for geographic and seasonal trends in species richness, diversity indices, and species abundances. Cochran's test was used to determine homogeneity of variances and, if necessary, data were $\log_e$ (x+1) transformed. When parametric ANOVA testing was acceptable, the Student-Newman-Keuls (SNK) test was used for multiple comparisons. Post-hoc comparisons were performed using Tukey HSD tests. A significance level of $p < 0.05$ was used in all tests.

Differences in the composition of the macrofaunal assemblages between sites were determined using non-metric multidimentional scaling (nMDS) and cluster analysis (group average mode), followed methods of Clarke and Warwick (1994), using the Primer package (Clarke and Gorley 2001). Unstandardized multivariate data were $\log_e$ (1+x) transformed to down-weight the importance of the very abundant species, and similarity matrices were calculated with the Bray-Curtis similarity index. The statistical significance of differences among sites was assessed using analysis of similarities (ANOSIM), a non-metric method based on randomization of rank-similarities among all samples (Clarke 1993), as well as multiple pair-wise comparisons. To build the matrix, species occurring in less than 5 percent of the samples, with only one individual, were excluded. To identify within two different sample groups in which species primarily accounted for the observed assemblage differences, SIMPER (similarity percentage) routines were performed using a decomposition of Bray-Curtis dissimilarity on $\log_e$ (x+1) transformed abundance data. Species were listed in decreasing order of their importance in discriminating the two sets of samples (Clarke and Gorley 2001).

Two approaches were use to link environmental parameters - i.e. depth (m), sediment grain size (mean grain-size, sorting index), silt/clay and gravel (%) content, bottom DO (mg $L^{-1}$) and chlorophyll *a* (mg Chl *a* g sediment$^{-1}$) sediment content - with the Ship Shoal macrobenthic community: (1) pair-wise regressions were used between environmental parameters and descriptors of benthic community (*i.e.* N0, N1, N2, taxonomic biomass or mean species abundances) to explore if the variation in one environmental parameter followed the variation in species richness and (2) multivariate BIOENV procedures (see Clarke and Ainsworth 1993 for details) were used to determine how spatial patterns in multivariate invertebrate community structure were related to spatial patterns in multivariate environmental structure, i.e. to what extent observed biological patterns fits with variations environmental parameters.

## 10.3. RESULTS

### 10.3.1. General description

A total of 29331 macrofaunal individuals in 161 species were collected from Ship Shoal during the three cruises (see Appendix A). Polychaetes represented 45 percent (72 species) of the total species number, following by crustaceans (28 percent, 46 species) and mollusks (17 percent, 27 species). Other taxa (nemerteans, sipunculids, anthozoans etc.) represented 10 percent (16 species). Global species richness exhibited a sharp decrease from spring to autumn, together

with the mean species richness ($p < 10^{-5}$). Except for a significant difference between N1 in autumn and N1 in spring or summer ($p < 0.003$), heterogeneity indices and equitability did not exhibit seasonal variation (Table 10.1). In terms of abundances, polychaetes and crustaceans predominated the Ship Shoal community with mean abundances between 1500 and 2000 individuals $m^{-2}$ in spring (Figure 10.2). Within these two taxonomic groups, spionids and amphipods were respectively the largest component, representing more than 50 percent of individual polychaetes and 80 percent of the crustaceans. Amphioxus *Branchistoma floridae* (Cephalochordata) abundance peaked in summer. Community mean biomass (wet weight) followed the same pattern, from 40.55 g $m^{-2}$ (SE = 5.24) in spring to 21.77 g $m^{-2}$ (SE = 2.88) in summer and 15.44 g $m^{-2}$ (SE = 3.22) in autumn (Figure 10.3). While this decrease in biomass occurred throughout the year for polychaetes, it was not significant between summer and autumn for mollusks or between spring and summer for other taxa.

Table 10.1

Species richness and heterogeneity of diversity and equitability (mean ± SE) for each season. Core cross-sectional area = 0.09 $m^2$. Results of one-way ANOVA for each measurement, where same letters indicate non-significant differences at *p*-level = 0.05.

| | Seasonal global species richness | Species Richness | Heterogeneity of diversity N1 = exp (H') | Heterogeneity of diversity N2 = 1/SI | Equitability J' |
|---|---|---|---|---|---|
| Spring | 134 | 33.19 ± 1.53 [a] | 13.90 ± 1.15 [a] | 8.67 ± 0.86 | 0.72 ± 0.10 |
| Summer | 118 | 23.71 ± 1.05 [b] | 12.40 ± 0.96 [a] | 8.19 ± 0.73 | 0.77 ± 0.08 |
| Autumn | 91 | 13.54 ± 1.01 [c] | 8.38 ± 0.80 [b] | 6.08 ± 0.58 | 0.78 ± 0.11 |

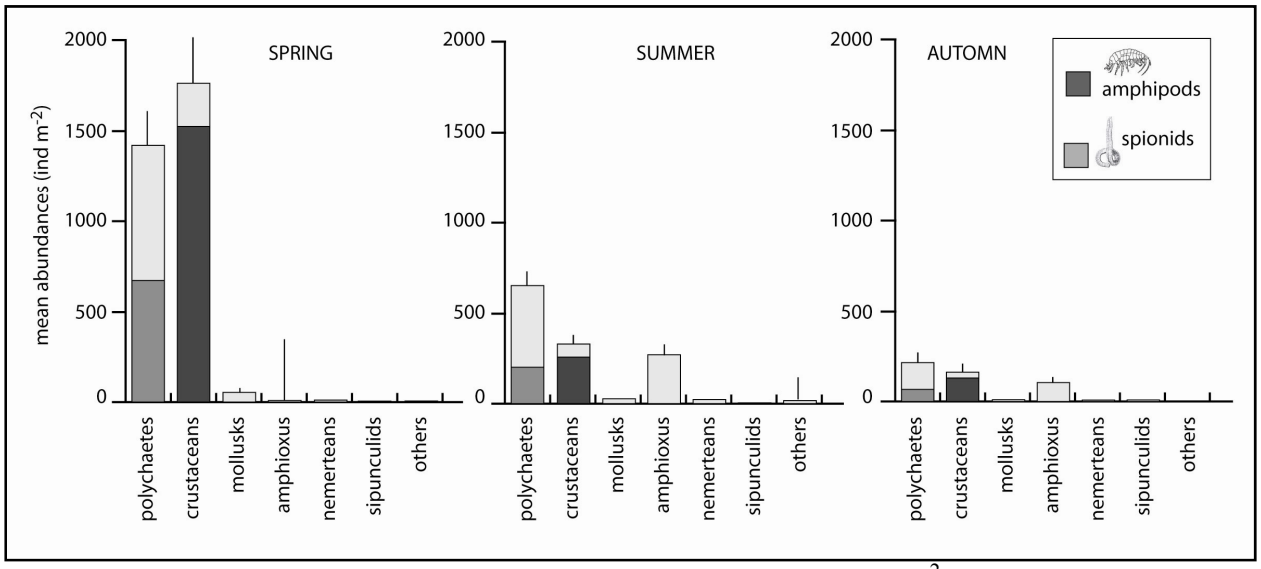


Figure 10.2 Seasonal variations in abundances (individuals $m^{-2}$; mean ± SE) of main taxonomic groups, with emphasis on spionids and amphipods. Core cross-sectional area = 0.09 $m^2$.

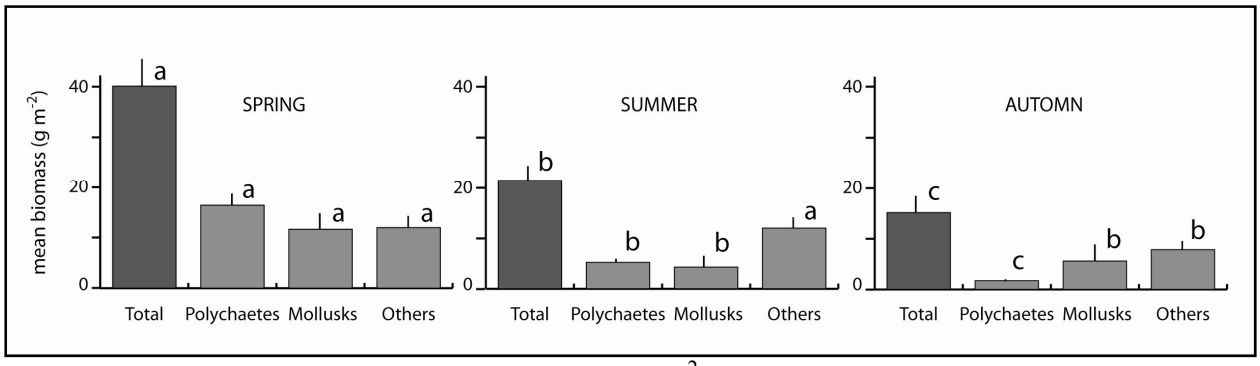


Figure 10.3 Mean biomass (wet weight; g $m^{-2}$; mean ± SE) of polychaetes, mollusks (including shells) and other taxonomic groups according to seasonality. Core cross-sectional area = 0.09 $m^2$. Letters a, b and c refers to statistical differences between the 3 seasons for total biomass, polychaetes, mollusks and others.

Significant differences in diversity and abundances between west, middle and east stations of Ship Shoal, as well as between north and south stations (ANOVA; Table 10.2) were observed. More precisely, species richness was significantly higher in the southernmost stations of the shoal in spring ($p = 0.032$), summer ($p = 0.002$) and autumn ($p = 0.030$) than in the middle or in the northernmost stations. The Figure 10.4 illustrated spring variations of global species richness (i.e. all different species for one station) and mean species richness within the three transects across the shoal and showed that both global and mean species richness exhibited southernmost stations (i.e. 17, 26 and 21) with higher species richness. We noticed the same pattern in summer and autumn. Mean species abundances were significantly higher in the southern edge in spring ($p = 0.018$), summer ($p < 10^{-6}$) and autumn ($p < 1.16\ 10^{-4}$) but were also significantly higher in the western region in spring ($p = 0.004$), summer ($p < 10^{-6}$) and autumn ($p = 1.13\ 10^{-4}$) than in the central or in the eastern region of the shoal. The N1 and N2 indices exhibited more seasonal differences; in spring, both indices were significantly higher toward the west (N1, $p = 7.2\ 10^{-5}$ ; N2, $p = 4.0\ 10^{-4}$) and the southern edge (N1, $p = 0.012$ ; N2, $p = 0.029$) but both indices only exhibited a significant north-south gradient in summer (N1, $p = 6\ 10^{-4}$ ; N2, $p = 4.4\ 10^{-6}$) and no significant variation in autumn. While total biomass showed no significant variation, polychaete biomass was significantly higher in the west and south in spring ($p = 0.013$ and $p < 10^{-7}$, respectively) and in summer ($p = 0.026$ and $p = 3\ 10^{-4}$, respectively).

Table 10.2

Results of ANOVA tests showing east-west gradient and north-south gradient within Ship Shoal area according to diversity indices, species abundance and biomass for each season. SR = species richness (N0), N1 and N2 = heterogeneity of diversity. Post-hoc columns indicated results of post-hoc comparisons between E (east), M (middle) and W (west) or between N (north), M (middle) and S (south), with " = " indicating non-significant difference and " < " indicating significant difference at *p*-level = 0.05.

| Spring | east - west gradient | | | north - south gradient | | |
|---|---|---|---|---|---|---|
| | F | p-level | post-hoc | F | p-level | post-hoc |
| SR | 2.91 | NS | - | 4.27 | 0.032 | N = M < S |
| N1 | 18.35 | $7.2\ 10^{-5}$ | E < M < W | 5.91 | 0.012 | N < M < S |
| N2 | 13.05 | $4.0\ 10^{-4}$ | E < M < W | 4.41 | 0.029 | N < M = S |
| abundances | 13.06 | $4.0\ 10^{-3}$ | E = M < W | 5.19 | 0.018 | N < M = S |
| total biomass | 1.07 | NS | - | 2.09 | NS | - |
| polychaete biomass | 5.77 | 0.013 | E < M = W | 39.29 | $1.0\ 10^{-7}$ | N = M < S |

| Summer | east - west gradient | | | north - south gradient | | |
|---|---|---|---|---|---|---|
| | F | p-level | post-hoc | F | p-level | post-hoc |
| SR | 2.85 | NS | - | 8.83 | 0.002 | N < M < S |
| N1 | 1.52 | NS | - | 11.40 | $6\ 10^{-4}$ | N = M < S |
| N2 | 3.17 | NS | - | 15.04 | $4.4\ 10^{-6}$ | N = M < S |
| abundances | 58.82 | $1\ 10^{-6}$ | E< M < W | 37.42 | $1\ 10^{-6}$ | N < M < S |
| total biomass | 2.13 | NS | - | 0.15 | NS | - |
| polychaete biomass | 4.47 | 0.026 | E = M < W | 13.15 | $3\ 10^{-4}$ | N = M < S |

| Autumn | east - west gradient | | | north - south gradient | | |
|---|---|---|---|---|---|---|
| | F | p-level | post-hoc | F | p-level | post-hoc |
| SR | 11.32 | $6.54\ 10^{-4}$ | E = M < W | 4.26 | 0.030 | N = M < S |
| N1 | 2.80 | NS | - | 1.93 | NS | - |
| N2 | 1.11 | NS | - | 1.16 | NS | - |
| abundances | 15.71 | $1.13\ 10^{-4}$ | E< M < W | 9.39 | $1.16\ 10^{-4}$ | N < M < S |
| total biomass | 0.47 | NS | - | 1.15 | NS | - |
| polychaete biomass | 0.06 | NS | - | 0.06 | NS | - |

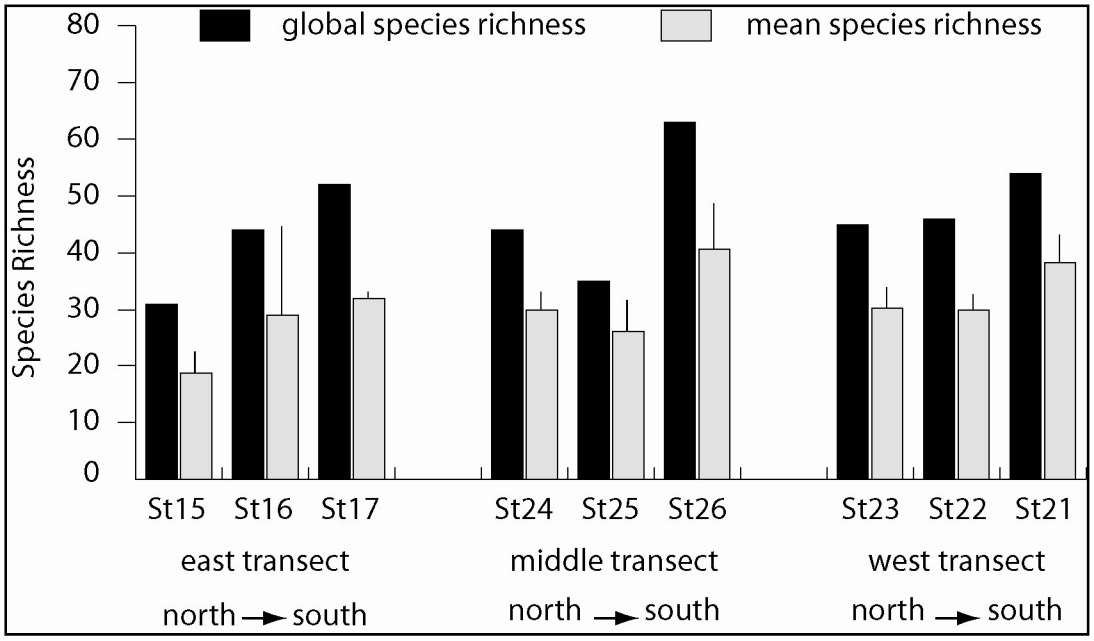


Figure 10.4 Global and mean (± SE) species richness in spring on Ship Shoal within the east, middle and west transects on the Ship Shoal. Core cross-sectional area = 0.09 $m^2$. See Figure 10.1 for precise location of the stations.

In terms of the measured environmental parameters, Ship Shoal constituted a relatively homogenous sandy habitat (Table 10.3). Sediment analysis revealed that all 21 stations were well or very well sorted unimodal and typified as sand or slightly gravelly sand for the most eastern stations (stations 14 to 18). Silt/clay (i.e. particles < 63 µm) and gravel (i.e. particles > 2 mm - primarily shell fragments) were very low at each station. Mean grain size, smaller in the west part of the shoal and larger in the east, was significantly inversely correlated in spring with N0 ($r = 0.722$; $p < 0.001$), N1 ($r = 0.477$; $p < 0.05$), N2 ($r = 0.421$; $p < 0.05$) and species abundances ($r = 0.601$; $p < 0.01$). The DO at the sediment surface was also correlated with N0 ($r = 0.596$; $p < 0.01$) and species abundances ($r = 0.670$; $p < 0.01$) in spring. Dissolved oxygen and sediment grain size were autocorrelated ($r = 0.569$; $p < 0.01$). No significant relation was found between environmental parameters and any diversity indices in summer or autumn.

Table 10.3

Seasonal variations in monitored environmental parameters over Ship Shoal.

| | Spring | | Summer | | Autumn | |
|---|---|---|---|---|---|---|
| | min - max | mean ± sd | min - max | mean ± sd | min - max | mean ± sd |
| Depth (m) | 4.2 - 10.2 | 6.9 ± 1.6 | 4.2 - 9.4 | 6.4 ± 1.5 | 4.9 - 10.5 | 7.2 ± 1.7 |
| Mean grain size (µm) | 127.7 - 198.1 | 159.9 ± 20.6 | 118.1 - 323.3 | 170.0 ± 39.5 | 115.6 - 320.6 | 174.3 ± 46.2 |
| Silt/clay content (%) | 0.3 - 3.4 | 1.4 ± 1.0 | 0.3 - 4.5 | 1.4 ± 1.1 | 0.3 - 18.1 | 1.9 ± 4.2 |
| Gravel content (%) | 0.0 - 3.7 | 0.5 ± 1.0 | 0.1 - 11 | 1.2 ± 2.6 | 0.1 - 11.8 | 1.4 ± 3.1 |
| Sorting index | 1.2 - 1.7 | 1.2 ± 0.1 | 1.2 - 2.5 | 1.3 ± 0.3 | 1.3 - 2.4 | 1.3 ± 0.3 |
| Chlorophyl *a* (mg $m^{-2}$) | 12.0 - 120.1 | 41.8 ± 27.4 | 2.7 - 122.0 | 37.0 ± 31.5 | 1.8 - 94.0 | 30.2 ± 21.8 |
| Dissolved oxygen (mg $L^{-1}$) | 2.0 - 8.4 | 6.1 ± 1.5 | 4.5 - 8.3 | 6.3 ± 1.1 | 6.3 - 7.2 | 6.9 ± 0.3 |

## 10.3.2. Macrofaunal benthic assemblages

### *10.3.2.1. Annual variability*

Cluster analysis of the macrofauna abundance data showed a strong seasonal effect in sample composition (Figure 10.5), supported by ANOSIM results (global R = 0.684; $p < 0.001$; Table 10.4). The SIMPER results (Table 10.4) comparing seasons showed that a small number of species contributed most to the dissimilarity among seasons: the amphipods *Acanthohaustorius* sp.A and *Protohaustorius bousfieldi*, the polychaetes *Spiophanes bombyx* and *Dispio uncinata*, and the amphioxus *Branchiostoma floridae*. These species had a very high frequency of occurrence in samples each season but exhibited strong decreases in abundances, especially between spring and summer, with the exception of the amphioxus *B. floridae* which was more abundant in summer. Many species contributed to a smaller extent to the discrimination between spring and other seasons because they had low abundances and high frequency of occurrence in spring but occurred only in a few stations in summer and autumn. This was mainly the case for polychaetes such as *Scolelepis texana*, *S. squamata*, *Paraprionospio pinnata*, *Spiochaetopterus costarum*, *Phyllodoce mucosa*. In addition to *B. floridae*, a few species with a high frequency of occurrence were more abundant in summer, such as the polychaetes *Thalenessa spinosa* and *Eupolymnia nebulosa* or the nemertean *Micrura leidyi*. The polychaete *Paramphimone* sp.B and the shrimp *Acetes americanus* almost only occurred in autumn. A few species are equally found in spring, summer or autumn with a high frequency of occurrence, such as the polychaetes *Neanthes micromma* and *Nepthys simoni*, the gastropod *Oliva sayana*, the hermit crab *Pagurus annulipes* or the mole crab *Albunea paretti*.

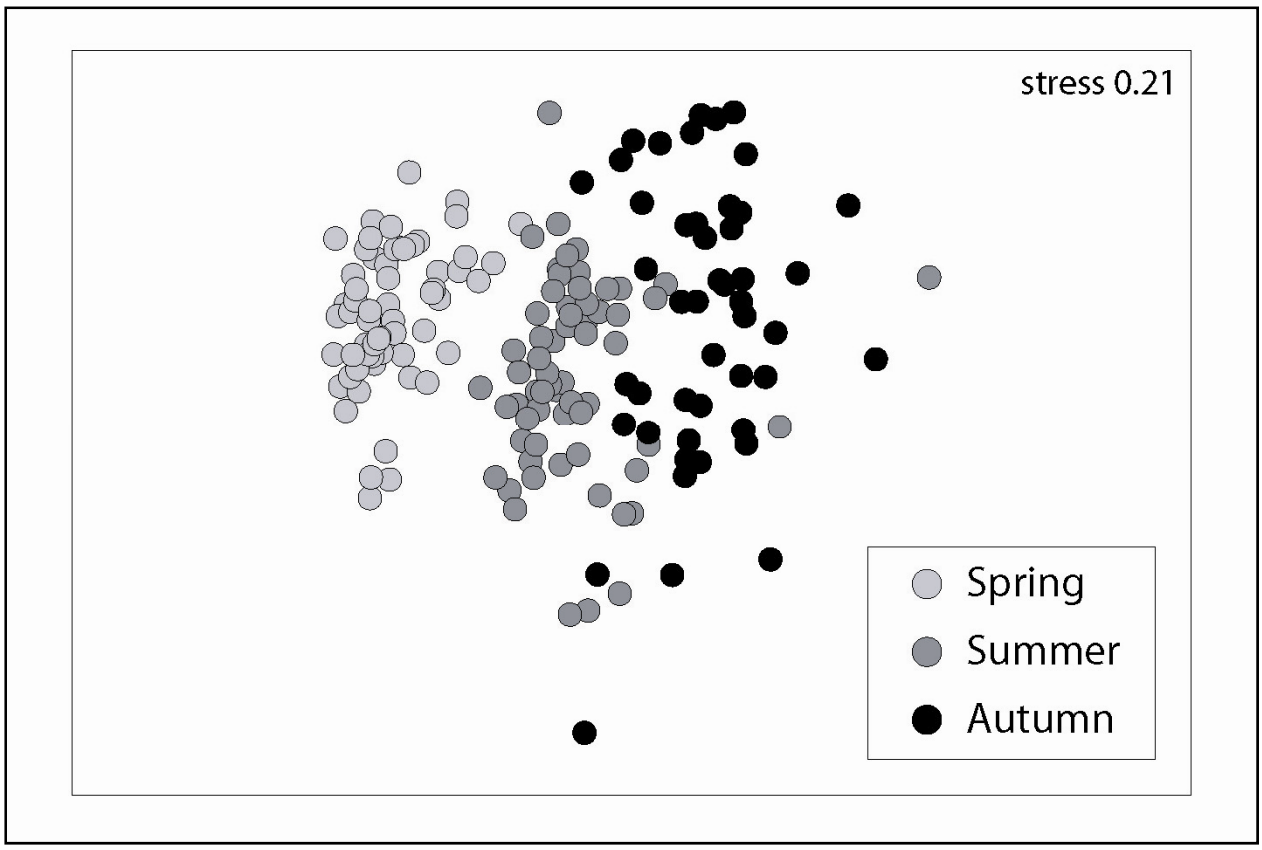


Figure 10.5 Multi-dimensional scaling ordination diagram of all samples of all stations showing seasonal changes in species composition and assemblages. Ordination was based on unstandardized log-transformed abundances matrix.

Table 10.4

ANOSIM and SIMPER results comparing species composition according to seasons. Core cross-sectional area = 0.09 $m^2$. SIMPER cumulative dissimilarity cut-off = 50%. See Figure 10.6 for nMDS plots.

| | Spring | Summer | Spring | Autumn |
|---|---|---|---|---|
| R statistic | 0.733 | | 0.861 | |
| p-value | 0.001 | | 0.001 | |
| Similarity (%) | 38.34 | 33.97 | 33.97 | 28.55 |
| Bray-Curtis dissimilarity (%) | 81.38 | | 88.35 | |
| Contribution to dissimilarity (%) | *Acanthohaustorius* sp. A | 14.85 | *Acanthohaustorius* sp. A | 18.69 |
| | *Protohaustorius bousfieldi* | 8.41 | *Spiophanes bombyx* | 8.83 |
| | *Branchiostoma floridae* | 7.66 | *Protohaustorius bousfieldi* | 8.26 |
| | *Spiophanes bombyx* | 7.04 | *Dispio uncinata* | 4.44 |
| | *Dispio uncinata* | 3.84 | *Microprotopus raneyi* | 3.83 |
| | *Prionospio pygmaea* | 3.74 | *Ampelisca* sp. C | 3.70 |
| | *Microprotopus raneyi* | 3.41 | *Branchiostoma floridae* | 3.41 |
| | *Ampelisca* sp. C | 3.34 | | |

| | Summer | Autumn |
|---|---|---|
| R statistic | 0.459 | |
| p-value | 0.001 | |
| Similarity (%) | 33.97 | 28.55 |
| Bray-Curtis dissimilarity (%) | 76.70 | |
| Contribution to dissimilarity (%) | *Branchiostoma floridae* | 16.12 |
| | *Acanthohaustorius* sp. A | 10.51 |
| | *Prionospio pygmaea* | 9.18 |
| | *Protohaustorius bousfieldi* | 6.37 |
| | *Scoloplos* sp.B | 3.82 |
| | *Mediomastus californiensis* | 2.86 |
| | *Magelona* sp.A | 2.64 |

### *10.3.2.2. Spatial distribution in spring, summer and autumn*

Cluster analyses also showed a clear difference in species assemblages between samples from the same season (Figure 10.6). The SIMPER analyses revealed that in spring (global $R = 0.564$; $p < 0.001$) and summer (global $R = 0.323$; $p < 0.001$), samples from east, middle and west Ship Shoal region differed from each other mainly because of changes in species abundances. The SIMPER also showed that discrepancies in species composition were predominately found between the east and the rest of the shoal, as the middle and west regions were similar in species composition.

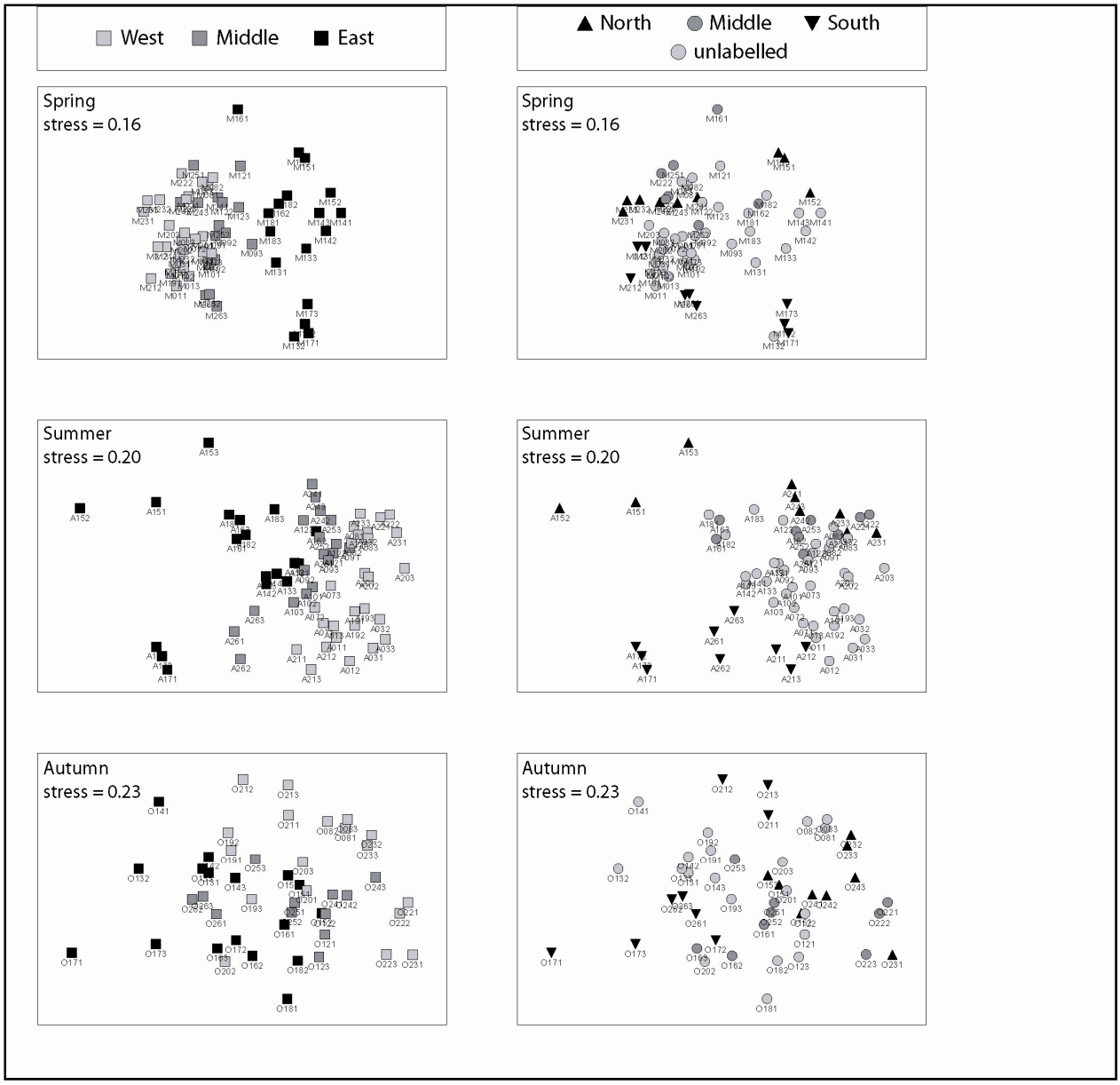


Figure 10.6 Multi-dimensional scaling ordination diagrams based showing, for spring (top), summer (middle) and autumn (bottom) samples east-west variations (left panels) or north-south variations (right panels). A schematic of the shoal is provided to illustrate the position of the stations on the east-west and north-south transects (see Figure 10.1 and description of study site for details). Ordination was based on unstandardized log-transformed abundances matrix.

In spring, the amphipod *Acanthohautorius* sp.A and spionids *Spiophanes bombyx* and *Dispio uncinata* contributed most to the dissimilarity between regions but also most to the similarity within each region. Amphipod species contributed the most to changes in species composition across the whole of the study area: *Protohaustorius bousfieldi* occurred almost only in the west

stations, while *Hartmanodes ranyei*, *Microprotopus ranyei* and *Ampelisca* sp.C were more abundant in the middle and western stations.

In summer, the lancelet *Branchiostoma floridae*, the amphipod *Acanthohautorius* sp.A and the polychaete *Prionospio (Apoprionospio) pygmaea* contributed mostly to the dissimilarity between regions but also mostly to the similarity within each region. Polychaete species contributed most to the discrimination between groups: *Euplolymnia nebulosa*, *Scoloplos* sp.B, *Tharyx annulosus* dominated abundances in the west stations, *Thalenessa cf. spinosa* was more abundant in the middle region and *Nereis falsa*, *Neanthes micromma* and *Travisia hobsonae* in the east region.

In autumn, similarity indices decreased, as revealed by higher dispersion of samples plots (Figure 10.6), because of larger discrepancies between sample composition and species abundances. The lancelet *B. floridae* and the amphipod *Acanthohautorius* sp.A were the two structuring species in that season, again with *P. bousfieldi* occurring mostly in the west stations and polychaetes *Magelona* sp.A and *Magelona* sp.H.

In addition to the east-west changes in benthic assemblages, Figure 10.6 also revealed in spring and summer that stations from the north of the three transects shared a high similarity threshold (i.e. 46.33 percent and 36.77 percent for north and south stations and in spring, respectively and 29.84 percent and 34.14 percent for north and south stations and in summer, respectively). This result was mainly due to species that exhibited higher abundances in the southern stations, such as the polychaetes *Owenia fusiformis*, *Mediomastus californiensis*, *Tharyx annulosus*, *Magelona* sp.H, *Spiophanes bombyx*, *Scoloplos* sp.B., *Paraprionospio pinnata* or higher abundances in the north stations such as the polychaetes *Nepthys simoni* and *Magelona* sp.A or the cumaceans *Oxyurostylis smithi* and *Cyclaspis varians*.

The BIOENV procedures showed that variations in macrobenthic assemblages were best matched by a combination of three or four environmental variables in spring, that were depth / grain size / percent gravel (Spearman correlation = 0.687) or depth / grain size / percent gravel / DO (Spearman correlation = 0.682). In summer, depth provided the best match (Spearman correlation = 0.505). No significant correlations were found in autumn.

### 10.3.3. Feeding guilds

Species that are able to switch between suspension-feeding and surface deposit-feeding dominated the trophic guild in spring (47 percent), and exhibited a decrease in summer (31percent) and autumn (30 percent) (Figure 10.7). True suspension-feeders almost disappeared in autumn while the dominance of species relying on deposit-feeding varied but did not decrease. Only the dominance of predators/scavengers increased with seasons, from 8 percent in spring to 30 percent in autumn. In spring, abundance in sub-surface deposit-feeders / psammivorous species was positively correlated with water depth ($r = 0.545$; $p < 0.01$) and percent silt/clay ($r = 0.524$; $p < 0.01$) but negatively correlated with sediment mean grain size ($r = 0.471$; $p < 0.05$). On the contrary, abundance of surface deposit-feeders was negatively correlated with water

depth ($r = 0.747$; $p < 0.001$) and percent silt/clay ($r = 0.538$; $p < 0.01$). In summer, abundance in sub-surface deposit-feeders was positively correlated with water depth ($r = 0.451$; $p < 0.05$) and abundance in surface deposit-feeders was negatively correlated with depth ($r = 0.427$; $p < 0.05$). Abundance in suspension-feeders or interface-feeders was positively correlated with chlorophyll *a* sediment content ($r = 0.523$; $p < 0.05$).

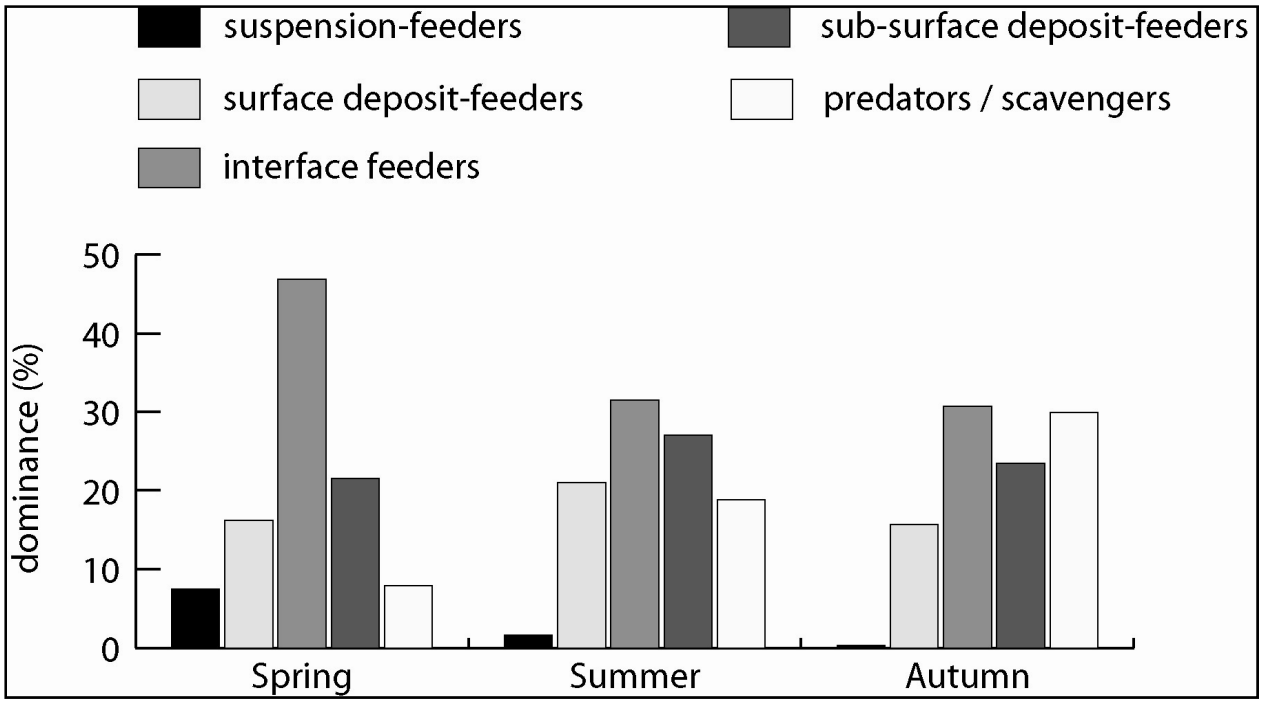


Figure 10.7 Seasonal variations in dominance (%) of the five feeding guilds. Interface feeders are species which can switch between suspension-feeding and surface deposit-feeding.

## 10.4. DISCUSSION

### 10.4.1. The Ship Shoal macrobenthic assemblage

Ship Shoal is a large, discrete formation composed of fine to very fine sand (ca. 150 µm diameter) about 25 km offshore from the Louisiana coast. Environmental gradients of water depth (increasing depth toward the east) and granulometry (increasing mean grain size toward the east) characterize the Shoal. In terms of benthic macroinvertebrates, our results suggest that Ship Shoal represents a faunally distinct habitat type in a transition between in-shore and off-shore habitats. Species composition revealed differences between east and west areas, along with differences between northern and southern edges of the shoal. Ship Shoal hosted a unique combination of macroinfauna composed of species commonly found typically among the swash zone of sandy beach communities associated with the Mississippi and northwest Florida seashore

(e.g. *Leitoscoloplos fragilis*, *Scolelepis squamata*, *Dispio uncinata*) (Rakocinski *et al.* 1998), or abundant in shallow enclosed bays of the northern Gulf of Mexico (e.g. *Paraprionospio pinnata*, *Gyptis vittata*, *Notomastus latericeus*, *Mulinia lateralis*) (Mannino and Montagna 1997; Montagna and Ritter 2006), as well as species typically found in muddy off-shore environments (e.g. *Armandia maculata*, *Magelona* sp.H, *Tellina versicolor*, *Nassarius acutus*) (Baustian 2005).

A significant number of species not reported previously for the Louisiana continental shelf were found on Ship Shoal. Uebelacker and Johnson (1984) provided a distribution range of polychaete species occurring on a large portion of the outer continental shelf of the northern Gulf of Mexico, e.g. south Texas (Texas), central Louisiana (Louisiana) and Mississippi-Alabama-west Florida (Florida) outer shelves. Based on that comprehensive work, we discerned that 50 percent of polychaete species found on Ship Shoal (35 species) were reported either from Florida continental shelf only (23 species) or from both Texas and Florida continental shelves (12 species). While most of these polychaete species occurred sporadically on Ship Shoal (e.g. *Streptosyllis pettiboneae*, *Myriowenia* sp.A, *Anaitides groenlandica*), a few species (*Phyllodoce mucosa*, *Thalenessa cf spinosa*, *Nereis falsa* or *Nepthys simoni)* exhibited high frequency of occurrence with low density (ca. 10 individual $m^{-2}$). The sediment characteristics of Ship Shoal are similar to that of the Florida shelf (Posey *et al.* 1998). In addition, a recent large-scale study of current circulation in the northern Gulf of Mexico (Ohlmann and Niiler 2005) found a strong connectivity between the shelves, especially during passage of tropical storms that allowed particles to cross the Florida-Louisiana shelf-break and the Mississippi river outflow. Along the Louisiana coast, Ship Shoal represents a suitable area for larvae to settle and for a diverse group of species adapted to life in fine sand to survive and develop. The findings presented here strongly suggest that Ship Shoal in particular and Louisiana sandy shoals in general could play an important role in the dispersal and gene flow of benthic species over large spatial scales in the continental shelf of the Gulf of Mexico. More locally, Ship Shoal may serve as a source pool for recruitment of benthic invertebrates to surrounding areas affected by seasonal hypoxia; abundances of benthic invertebrates increase after hypoxia ends (Rabalais *et al.* 2001). Molecular tools would be of primary interest in testing such hypotheses.

The Ship Shoal community appears to be a melange of species from several origins. Among species found throughout the year, with a high frequency of occurrence, mole crabs *Albunea paretti* and amphioxus *Branchiostoma floridae* best typified the very fine-sand shoal community and comprised most of the biomass. In that so-called *Albunea-Brachiostoma* community, we typically found the polychaetes *Nephtys simoni*, *Neanthes micromma*, *Dispio uncinata* and *Magelona* sp.A, the amphipod *Acanthohautorius* sp.A and the burrowing shrimp *Ogyrides alphaerostris*. They constituted the basis of the sandy shoal community, which exhibits variation according to seasons or according to on-shore or off-shore influences.

Among species that make Ship Shoal benthic assemblages unique was the lancelet (= amphioxus) *Branchiostoma floridae*. The occurrence of amphioxus has been reported in sandy-shore macrobenthic community of barrier islands to the west of the Mississippi river (Hefley and Shoemaker 1952; Rakocinski *et al.* 1998), but this is the first report of large abundances of amphioxus (up to 760 ind $m^{-2}$) off the Louisiana coast. Mainly large individuals were found carrying eggs in spring samples and a large number of juveniles were found along with adults in

summer samples, leading to the hypothesis that Ship Shoal might be an important sandy habitat for reproduction and recruitment of amphioxus *B. floridae*.

Contrary to the commonly observed pattern of an overall decrease in species number and total density with increasing water depth (e.g., Thouzeau *et al.* 1991), it appeared that the diversity indices and species abundance did not vary within the relatively narrow depth ranges found on Ship Shoal. But BIOENV procedures showed that water depth and mean grain size were the two main environmental parameters that coincided with changes in composition of species assemblages over Ship Shoal.

### 10.4.2. Is Ship Shoal a diversity hotspot?

The overall species richness of macrobenthos on Ship Shoal totaled 118 species (with a mean per sample of 23.71 ± 1.05). Benthic assemblages over a large sampling area off the central coast of Louisiana affected by hypoxia were studied by Baustian (2005) and Rabalais *et al.* (2001). Mean species richness (19.1 ± 2.3) was reported for the same season (summer) by Baustian (2005). Since this study covered a much broader area (ca. 4000 $km^2$) than the present study (ca. 200 $km^2$), and encountered a greater habitat variety (muddy substrata through gravelly soft-bottoms) one would expect the species richness to be comparatively much higher than Ship Shoal for a similar number of stations (Rosenzweig 1995). Baustian (2005) also studied seasonal variations in macrobenthic community at one particular site that typifies muddy soft-bottom environments surrounding Ship Shoal (ca. 10 km off Ship Shoal). This survey showed a similar decrease in species richness and abundances from spring to autumn: mean species richness ranged 4 to 14 species in May and October. Species number ranged from 13 to 33 species for the same months in Ship Shoal sediments. Thus, Ship Shoal appears to maintain a higher number of species than nearby locations on the Louisiana shelf. Biodiversity in benthic communities is often linked with many environmental factors, of which sediment characteristic is of primary importance (Gray 1974). Traditionally, infaunal species richness is lower in muddy communities than in sandy community but heterogeneous sands have typically more species than well-sorted mobile sands, which are characterized by dominance of polychaetes and amphipods, as found in Ship Shoal (e.g., Van Hoey *et al.* 2004).

A significant difference in diversity indices was found between the northern and southern edges of Ship Shoal (biodiversity in southern stations was higher), showing that variations may also occur over small latitudinal gradients (less than 10 km). This north-south gradient may be explained by the higher abundances of large tube-building polychaete species at stations close to the southern edge, and contributes to the high diversity on Ship Shoal compared to nearby non-shoal habitats. Onuphidae *Diopatra cuprea* and *Onuphis emerita occulata* or Oweniidae *Owenia fusiformis* build tubes that protrude several cm above the sediment surface, increasing surface heterogeneity and providing habitat for other small invertebrates (Zühlke 2001; Dubois *et al.* 2002), as well as settlement surface for larval and postlarval benthic organisms (Qian and Chia 1991). This last hypothesis was supported by high densities of spionid and oweniid juveniles in southern samples.

Baustian's (2005) seasonal study of the area around Ship Shoal showed that, while polychaetes dominated (ca. 50 percent) throughout the year, mollusks were the second most important taxonomic group (24 percent in May, 45 percent in August and 38 percent in October). *Nuculana acuta*, *Natica pusilla* and *Abra aequalis* were particularly abundant in Baustian's study but were found on Ship Shoal in very low abundances (less than 3 ind. $m^{-2}$). We found that mollusks represented < 3 percent of the macroinfauna on Ship Shoal, but that crustaceans, and especially amphipods, were almost as abundant as polychaetes (even more abundant in spring), while it is traditionally assumed that polychaetes are the most diverse and dominant taxonomic group in most marine and estuarine environments (e.g. Hutchings 1998).

### 10.4.3. Is Ship Shoal a local refuge from seasonal hypoxia?

Mid-summer surveys from 1993 to 2000 have revealed a severe and persistent hypoxia phenomenon (i.e. DO < 2 mg $L^{-1}$) on the inner- to mid-Louisiana continental shelf (Rabalais *et al.* 2001). While Ship Shoal is situated in this area prone to hypoxia, our estimates of bottom DO concentrations over the entire shoal were fairly high and constant in spring (6.1 ± 1.5 mg $L^{-1}$), summer (6.3 ± 1.1 mg $L^{-1}$) and autumn (6.9 ± 0.3 mg $L^{-1}$), with only one spring sample reaching 2.0 mg $L^{-1}$. Ship Shoal might therefore be considered a hypoxia refuge for benthic invertebrate sensitive to low DO concentrations. Amphipods occurred in very high abundances over the Ship Shoal and species *Acanthohaustorius* sp.A, *Protohaustorius bousfieldi*, *Ampelisca* sp.C and *Hartmanodes nyei* were highly-ranked among the benthic assemblages throughout the year. In contrast, the Baustian (2005) investigation confirmed that crustaceans in general and amphipods in particular are absent from muddy areas surrounding Ship Shoal in summer and autumn. As amphipods are known to be affected by low oxygen values (Gaston 1985; Wu and Or 2005), together these results support the hypothesis that Ship Shoal is a hypoxia refuge for benthic species. Shallow depths, wave action and biogenic activity all probably contributed to Ship Shoals higher DO concentrations. The high density of tubiculous polychaetes (e.g. spionids, representing between 30 percent and 50 percent of polychaete density, as well as *Owenia fusiformis*, or *Onuphis emerita occulata*) may enhance oxygen flux in sediment surface layer (Jorgensen *et al.* 2005).

Species abundances exhibited a steady but large rate of decline between spring, summer and autumn, affecting amphipods as well as all other taxonomic groups (except amphioxus). Although its possible that the springtime macrofauna abundances in 2006 may have been below average due to a long-term disturbance effect generated by Hurricane Katrina (August 2005), the seasonal declines found in 2006 should still be representative of trends in macrofauna abundance on Ship Shoal even if the absolute numbers may be lower than normal. The magnitude and extent of these declines suggest an increase in the rate of mortality. If we exclude a hypoxia event as the cause (as suggested by observations of oxygen and surface-sediment conditions in 2006), possible reasons for such an increase include ephemeral fluiditic flood layer sedimentation (e.g. Wheatcroft and Sommerfield 2005) and a seasonal influx of benthic predators (e.g. Langlois *et al.* 2005). A several-centimeter-thick sediment layer deposited by

summer and autumn flooding of Atchafalaya and Mississippi Rivers on the adjacent Louisiana continental shelf is possible but very unlikely based on data collected by US Army Corps of Engineers in 2006 (data available at www.mvn.usace.army.mil/eng/edhd/watercon). Flooding events are most likely to affect Ship Shoal in the winter and spring when continental cold fronts occur and when river flow is high (Allison *et al.* 2005; Kobashi *et al.* 2007b) and fluidic layers were not observed during our summer and fall collections. A large influx of predators may therefore be the more likely hypothesis. Gelpi et al. (in prep.) found expectedly high concentrations of spawning/hatching blue crabs *Callinectes sapidus* in summer 2006 in Ship Shoal, but not in spring trawls. These blue crabs *C. sapidus* actively fed on Ship Shoal and are known to be important benthic predators which may have a strong influence on polychaete and bivalve populations (Bell *et al.* 2003). We suggest here that seasonal blue crab predation (perhaps supplemented by other predators such as white, brown shrimp and croaker) on Ship Shoal maybe contribute to the observed seasonal decline in the macroinfaunal community.

### 10.4.4. Is Ship Shoal macrofauna sensitive to sand-mining disturbance?

Ship Shoal has been identified as perhaps the most significant sand resource (ca. 1.6 billion cubic yards of fine sand) in the northern Gulf of Mexico (Brooks *et al.* 2006). Sand from the shoal may be used to supply beach reinforcement and coastal stabilization projects and mitigate Louisiana coastal erosion and wetland loss (Michel *et al.* 2001). Dredging and mining activities would inevitably negatively affect, at least temporarily, the Ship Shoal benthic community (see review by Newell *et al.* 1998). Our study provides baseline information that may help understand how the Ship Shoal community functions and its sensitivity to human disturbances in general and sand-mining disturbances in particular. Given the size of Ship Shoal, it is likely that mining would remove only a fraction of the available sand but localized effects may be strong.

Newell et al. (1998) estimated that the rate of recovery for sandy environments after dredging or mining activities is much longer (2 to 3 years) than the rate for muddy environments (6 to 8 months), and may be even longer depending on the proportion of sand removed, the proportion of slow-growing species and the intensity of environmental disturbance. Palmer *et al.* (2008) found that effects of a dredge excavation pit on macrofauna off the western coast of Louisiana was slow and did not recover over three years after excavation. Ship Shoal community exhibits an equilibrated and species-rich community, as indicated by diversity indices and equitability index, suggesting it is controlled by biological interactions rather than extreme changes in environmental parameters. Numerous species (including *Branchisotoma floridae*, *Scoloplos* sp., *Sabellides* sp., *Terebellides* sp. and *Dosinia* sp., *Tellina* sp., *Ensis* sp.) found on Ship Shoal have been designated "equilibrium species" (K-strategists) (Newell *et al.* 1998) as these species are relatively large in body size, have a slow reproduction rate and a long life-cycle. These species, and the amphipod fauna as a whole, and are considered sensitive species (Gesteira and Dauvin 2000) and will probably be strongly affected over long-term by mining effects. Large species are abundant on Ship Shoal and accounted for most of the biomass; the mean biomass (25.9 g wet weight $m^{-2}$) on Ship Shoal is high compared to other areas of similar water depth (Thouzeau *et al.* 1991; Pinn and Robertson 2003). A shift to dominance of the sand-mined area by small-

rapid-growing species will reduce the community biomass and may elicit indirect effects at higher trophic levels, for example on fishes and crustaceans using Ship Shoal as a feeding ground. Spionid polychaetes are known to be "disturbance specialists" or "opportunistic species" (r-selected species, Pianka 1970). They generally have a rapid rate of reproduction and growth and readily colonize disturbed habitats (e.g. Dubois *et al.* 2002; Palmer *et al.* 2008). These "disturbances specialists" will be less sensitive to sand-mining than "equilibrium species".

Excavation of sand will undoubtedly increase water depth and local turbidity due to the overflow of fine particles and hence reduce benthic primary production occurring in this shallow area. Sand removal may also modify hydrodynamic patterns and wave action. Grippo et al. (unpublished) found that benthic microalgae may have higher biomass than phytoplankton integrated through the water column on Ship Shoal, suggesting benthic algae are important to the shoal's food web. The high benthic biomass we observe may be related to high levels of *in situ* primary production (e.g., our observed correlation between chl *a* and benthic interface feeders). Thus, changes in primary production will likely influence the benthic community, again reducing community biomass and further altering community composition. Changes in water depth may therefore lead to long-term alterations in ecosystem function in higher trophic levels as well. Further studies (that focus on recovery or the scale of sand removal) are necessary to fully understand consequences of human disturbances on Ship Shoal macrofaunal community.

# CHAPTER 11
# SEASONAL HABITAT USE OF SHIP SHOAL BY PENAEID SHRIMP AND CROAKER

## 11.1. INTRODUCTION

In this chapter, we focus on penaeid shrimp species-- brown shrimp (*Farfantepenaeus aztecus)* and white shrimp (*Litopenaeus seiferus*), as well as Atlantic croaker (*Micropogonias undulates*) collected in trawl samples taken on Ship Shoal. These species constitute some of the most important commercial fisheries in Louisiana. Penaeid shrimp have supported one of the nation's most valuable fisheries since the 1930's (Lindner and Anderson 1956; Condrey 1980) (Muncy 1984). According to Louisiana Department of Wildlife and Fisheries (LDWF) trip ticket report data, 110.9 million pounds of shrimp valued at $139.8 million were landed in Louisiana in 2007. White shrimp landings valued at $95.5 million accounted for approximately 64.5 million pounds or 58 percent of total shrimp landings (http://www.wlf.louisiana.gov/news/). Croaker (one of the most common members of the family Sciaenidae on the Louisiana shelf) have several food, bait and industrial uses. However, much of the croaker caught each year are trawl by-catch associated with shrimping.

The feeding ecologies of white and brown shrimp are similar. Both are dominant, epibenthic deposit-feeding invertebrates known to burrow and swim. Though little has been published on predator-prey relationships of white or brown shrimp in the Gulf's offshore waters, they are believed to occupy a central position in the coastal food chain. They are variously described as omnivores/opportunistic carnivores (Muncy 1984). Some studies have suggested that juvenile brown shrimp are more carnivorous than white shrimp (McTigue and Zimmerman 1991), but it is unknown whether this applies to adults or to individuals on the continental shelf. In turn, they are major food items for a variety of carnivores including spotted seatrout, red drum, Atlantic croaker, black drum, flounders, catfish, seabirds, and marine mammals (Condrey 1980; Louisiana Department of Wildlife and Fisheries (LDWF) 1992).

Intense, direct competition (by exploitation of interference) between brown and white shrimp appears to be reduced by seasonal and spatial differences in habitat use. Most juvenile brown shrimp are recruited to Louisiana estuaries in the spring and begin an offshore migration in May to open waters of the Gulf of Mexico > 120 m where they complete their life cycle. In contrast, juvenile white shrimp are primarily recruited to Louisiana's estuarine waters in summer and fall, migrate to Gulf waters of less than 55 m, and may reenter estuarine waters before completing their life cycle (Muncy 1984). Because of these overlapping life history features, white and brown shrimp are expected to seasonally compete for food and space in the Ship Shoal region during the late spring and summer months.

Atlantic croaker are estuarine dependant and spawn near the mouths of inlets or off-shore during an extended spawning season lasting from October to March. After spawning, larvae enter estuaries and spend their post-larval and juvenile stages in the salt marsh feeding first on

zooplankton followed by small benthic invertebrates. First-year recruits leave the estuary in summer and fall for over wintering grounds on the continental shelf. As adults, croaker are strongly demersal, feeding primarily on benthic macroinvertebrates and small fishes. Croaker begin spawning in their second or third year. Spawning has been reported to occur at a wide range of depths, from inlets to deep mid-shelf waters. Off-shore spawning and wintering grounds in Louisiana have not been identified and to our knowledge do not include Ship Shoal.

The pressures of overfishing, habitat loss and the increasing size and frequency of hypoxia along the Louisiana-Texas continental shelf have given conservation of fisheries an increased urgency. To many species, sand mining represents another potentially adverse impact to fisheries resources. However, it is difficult to asses the potential effects of sand mining on the fauna of Ship Shoal because there are few data available on Ship Shoal as fishery habitat. For example, although the Southeast Area Monitoring and Assessment Program (SEAMAP, Rester *et al.* 2007) has been conducting trawl surveys off Louisiana for over two decades, Ship Shoal was not surveyed. Fishery dependent and independent catch statistics suggest a historical affinity of white shrimp for the inshore area west of Ship Shoal and surveys conducted by the LDWF from 1969 to 1974 revealed that numbers of overwintering white shrimp between Ship Shoal and Trinity Shoal were correlated with inshore commercial landings in Terrebonne Parish (Gaidry and White 1973). However, Brooks *et al.* (2004) summarizing SEAMAP trawls conducted on and around Tiger Shoal, Trinity Shoal, Sabine Bank and Heald Bank from 1982 to 2000, concluded that: 1) there was no distinct shoal fish community; 2) in winter, fish abundance and biomass were generally lower on shoals compared to off-shoal areas, but the relationship was variable in summer; 3) there were comparatively fewer commercially exploited species on or near the shoals compared to off-shoal areas. However, only a few of the trawl samples were actually taken on the interior of the shoals; consequently, few data are available for the shoals themselves and (as previously noted) no data were reported for Ship Shoal.

With this study, we surveyed the distribution and abundance of croaker and penaeid shrimp on Ship Shoal during spring, summer and fall in order to determine the seasonality and duration of their residency. Using gut content analysis, we also examined whether penaeid shrimp and croaker use Ship Shoal food resources as well as what resources were most important. By determining which food items were commonly consumed, we draw some conclusions about how sand mining may impact the resources.
Methods

## 11.2. FIELD COLLECTIONS & ANALYSIS

### 11.2.1. Trawl collections

After conducting exploratory trawls in June 2005, nine trawl stations were established across Ship Shoal in August 2005. Three stations were established on the eastern flank, three on the western flank and three in the middle of the shoal. The three stations were positioned to sample

edge and interior shoal habitat based on existing bathymetry. Thirty-minute nighttime trawls were conducted using a 25 foot otter trawl in as compatible a fashion with SEAMAP trawling protocols as possible. Latitude and longitude for each sampling station is given in Table 11.1. All shrimp, blue crabs, and croaker were frozen and returned to LSU for gut content analysis and assessment of reproductive condition. Blue crabs were prominent in the catch and are discussed in Chapter 12. Some additional physical and biological data were collected at each station and include sediment chl a, bottom water dissolved oxygen, PAR profiles and water depth (see Chapter 8).

Table 11.1

Approximate latitude and longitude of 30 minute trawling stations.

| Station | Latitude | Longitude |
|---|---|---|
| 15 | 28º 55.668 | 90º 39.551 |
| 16 | 28º 55.268 | 90º 39.543 |
| 17 | 28º 53.999 | 90º 39.508 |
| 20 | 28º 53.568 | 91º 07.246 |
| 21 | 28º 52.527 | 91º 04.01 |
| 22 | 28º 55.082 | 91º 04.985 |
| 24 | 28º 55.296 | 90º 54.496 |
| 25 | 28º 54.793 | 90º 54.487 |
| 26 | 28º 53.59 | 90º 54.514 |

### 11.2.2. Laboratory analysis

The stomach contents of brown shrimp, white shrimp and croaker were removed and examined under a dissecting microscope. For shrimp, potential food resources were recorded as present or absent and a percent frequency of occurrence was calculated for each food type. For croaker, the percentage of each prey type comprising the entire stomach contents was visually estimated for each fish using a gridded plate. A large number of shrimp and croaker contained no stomach contents. The number of individuals with empty stomachs are reported, but were not included in the dietary analysis.

### 11.2.3. Data analysis

The number of shrimp and croaker collected was generally low; therefore intra-shoal statistical comparisons of abundance were considered inappropriate. No trawls were conducted in the off-shoal waters surrounding Ship Shoal in 2006. Therefore, to compare the use of nearby off-shoal and Ship Shoal habitat by shrimp and croaker we analyzed SEAMAP catch data from Statistical Zone 14 which includes the waters around Ship Shoal. We used SEAMAP trawl data from the

time periods that most closely corresponded to our own Ship Shoal trawls (usually less than 1 month apart). Although SEAMAP trawls and our Ship Shoal trawls were generally 30 minutes, the SEAMAP trawl was 40 feet, while the trawl we used on Ship Shoal was 25 ft. Consequently, the SEAMAP trawls may have collected more individuals per unit time than our Ship Shoal trawls.

Because few brown shrimp were caught, individuals collected in 2005 and 2006 were pooled by season (spring, summer, fall) and a chi square test was used to compare stomach contents of brown shrimp between seasons. The analysis only included the more frequently recorded food items including crustacean parts, amphipods, polychaetes and unidentified material. Few white shrimp and croaker were collected on Ship Shoal during 2005 and 2006; therefore, their diets were not analyzed statistically.

## 11.3. RESULTS AND DISCUSSION

### 11.3.1. Physical description.

Spatial gradients in depth and grain size were found on Ship Shoal. Depth across the shoal ranged from 5 to 11 m. Depth generally increased from west (5 to 8 m) to east (9 to 10 m). Sediment on Ship Shoal was well sorted fine to very fine sand with low silt/clay content. Grain size generally increased from west to east, a pattern attributable to the higher percentage of shell hash on the eastern shoal. Sediment carbon from the June 2005 cruise was analyzed and values were generally less than 0.2 percent across Ship Shoal. Bottom water salinity was generally greater than 30 ppt and no spatial patterns across the shoal were evident. Hypoxia (D.O. < 2 mg/l) was rarely observed on Ship Shoal even in summer cruises. Consequently, it is unlikely the distribution and abundance of nekton on Ship Shoal was affected by hypoxia.

### 11.3.2. Trawl collections

The catch of brown shrimp, white shrimp and croaker are presented in Figure 11.1. Overall, the catch for all three species was very low. Consequently, no spatial trends, if present, could be detected across Ship Shoal. Throughout the sampling period, brown shrimp dominated shrimp catch, with large, spawning white shrimp found in comparatively low numbers. Brown shrimp catch averaged less than 10 individuals per trawl except in May 2006 when a mean of 159± 50 individuals per trawl were collected on the eastern end of Ship Shoal. With the exception of May 2006, the mean white shrimp catch was generally less than one individual per trawl. Croaker numbers were also generally low (< 1 individual per trawl) except during August 2005 and October 2006 when large numbers were caught at the eastern and central stations. These dates correspond to the peak off-shore migration by croaker that occurs in the fall as juveniles move to off-shore spawning and wintering grounds (Lassuy 1983).

For croaker and penaeid shrimp, SEAMAP catch per trawl of croaker and penaeid shrimp in waters around Ship Shoal was highly variable, but was on average much higher than the mean catch for on Ship Shoal (Table 11.2). This was true for all trawling dates, suggesting that the abundance of these species was lower on Ship Shoal than in surrounding waters. The limited available studies suggest that white shrimp prefer organically rich, silty substrate (Muncy 1984). Similarly, prior trawl assessments of brown shrimp abundance indicate higher numbers are found on muddy substrate, and laboratory studies confirm a preference for loose peat and sandy mud (Lassuy 1983). Thus, the substrate preferences of penaeid shrimp may account the difference in catch between the sandy shoal and more silty off-shoal areas.

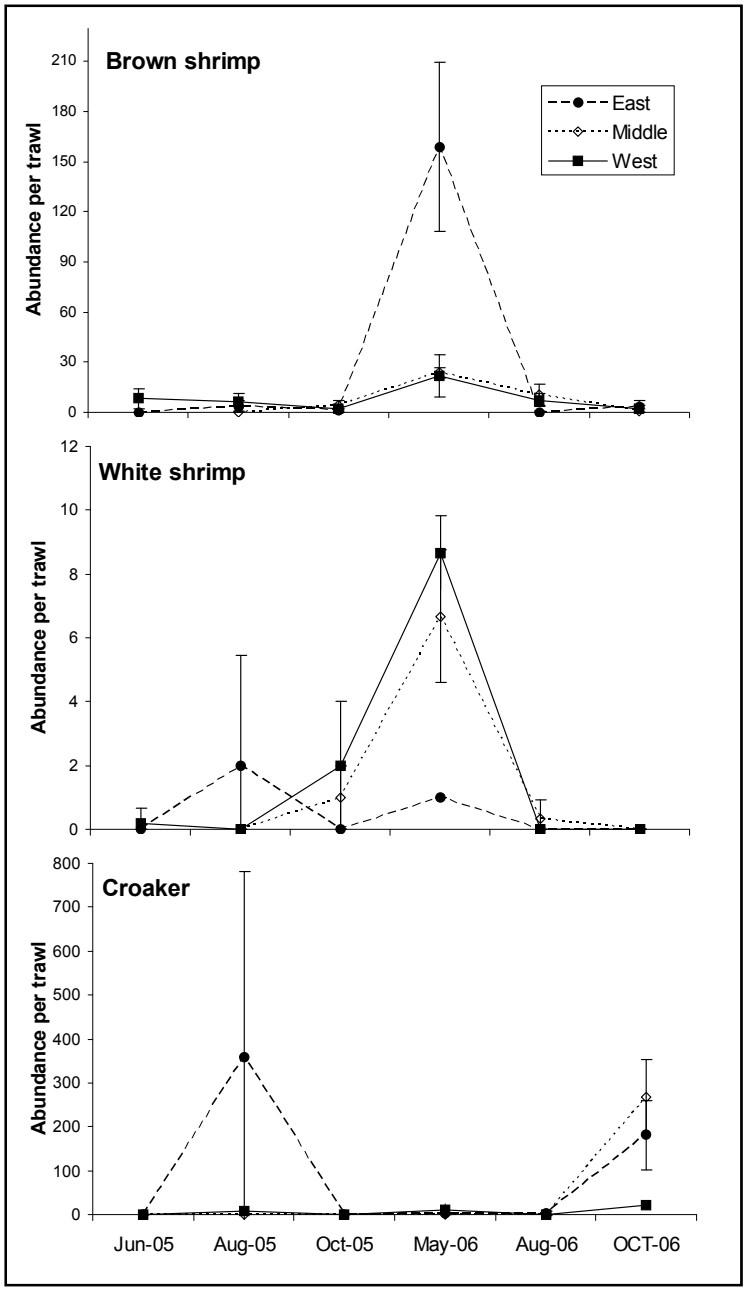


Figure 11.1 Brown shrimp, white shrimp and croaker catch on Ship Shoal from June 2005 to August 2006.

The mean length of brown shrimp was similar throughout the year, while the average length of white shrimp decreased (Table 11.3). These data suggest that differing populations of penaeid shrimp were sampled on Ship Shoal during spring, summer, and fall as different age cohorts moved from the estuaries to/or across Ship Shoal and surrounding areas and, ultimately, in the case of brown shrimp, to deeper off-shore spawning grounds.

Table 11.2

Comparison of brown shrimp, white shrimp and croaker catch (mean abundance per trawl) on Ship Shoal and off-shoal SEAMAP trawls in the spring, summer and fall of 2005 and 2006.

| | June/July 05 | October 05 | November 05 | May/June 06 | July/August 06 | Oct/Nov 06 |
|---|---|---|---|---|---|---|
| | **Croaker** | | | | | |
| **Off-Shoal SEAMAP** | 1093.1 ±1224.7 | 384.4 ±557.7 | 902.7 ±898.7 | 65.7±94.1 | 480.3 ±643.8 | 675.0 ±655.1 |
| **Ship Shoal** | 0.0 | 0.0 | No data | 4.8 ±9.0 | 1.2 ±3.3 | 31.7 ±8.7 |
| | **Brown shrimp** | | | | | |
| **Off-Shoal SEAMAP** | 60.6±52.5 | 89.9±94.5 | 100.2±152.4 | 116.3±112.7 | 41.0 ±72.7 | 108.7 ±142.4 |
| **Ship Shoal** | 7.0±6.4 | 2.6±2.5 | No data | 56.1±64.7 | 5.9 ±5.7 | 1.7 ±2.3 |
| | **White shrimp** | | | | | |
| **Off-Shoal SEAMAP** | 13.5 ±17.6 | 26.0 ±28.9 | 58.1±51.0 | 21.9 ±17.7 | 0.0 ±0.0 | 60.4 ±41.7 |
| **Ship Shoal** | 2.8 ±6.9 | 1.0 ±1.4 | No data | 5.9 ±5.4 | 0.1 ±0.3 | 0.0 |

The mean length of brown shrimp was similar throughout the year, while the average length of white shrimp decreased (Table 11.3). These data suggest that differing populations of penaeid shrimp were sampled on Ship Shoal during spring, summer, and fall as different age cohorts moved from the estuaries to/or across Ship Shoal and surrounding areas and, ultimately, in the case of brown shrimp, to deeper off-shore spawning grounds. White and brown shrimp may reach sexually maturity at >120 mm but maturity typically occurs at > 140 mm especially for females. White shrimp collected on Ship Shoal were substantially larger than brown shrimp, with mean length ranging from 127 mm in the fall to 175.4 mm in the spring, compared to brown shrimp which had a mean length <97 mm on all sampling occasions. Thus, based on size, the white shrimp collected in spring and summer were likely sexually mature, but only immature brown shrimp were likely collected on Ship Shoal. These findings support earlier studies which found that white shrimp migrate from estuaries at a larger size (100-140 mm) than brown shrimp (90-100 mm; Lassuy 1983; Muncy 1984 and references therein) and that brown shrimp spawn in deeper water than white shrimp (Lassuy 1983; Muncy 1984 and references therein).

Croaker reach sexual maturity at 140 to 170 mm (Waggy *et al.* 2006). Croaker collected on Ship Shoal ranged from 129 to 166 mm indicating a mix of adults and juveniles. In contrast to shrimp, the size and weight of individual croaker increased throughout the year suggesting the population may not have been transient on Ship Shoal and was sampled on each cruise. Adult and juvenile croakers are reported to overwinter off-shore and return to the estuaries during the spring where they reside until late summer and fall (Lassuy 1983). However, the observation that length increased from our spring to fall collections suggests that some croaker remain off-shore and reside on and around Ship Shoal. Estuarine migrants are an additional, and perhaps primary, off-shore population source in the summer and especially the fall when off-shore migration peaks (Lassuy 1983).

Table 11.3

Average length and weight ( ±std) of brown shimp, white shrimp and croaker collected on Ship Shoal in May/June, August, and October (2005 and 2006 combined).

| | Brown shrimp | | White shrimp | | Croaker |
|---|---|---|---|---|---|
| | Female | Male | Female | Male | |
| **Length (mm)** | | | | | |
| **May/June** | 89.8±12.3 (n= 257) | 89.3±8.1 (n= 176) | 171.5±14.7(n=13 ) | 170.1±8.4 (n=17) | 129 ±49.5 |
| **August** | 97.3±14.0 (n=29 ) | 89.7±8.4 (n= 39) | 165.7±8.2 (n= 6) | none collected | 143.3 ±18.6 |
| **October** | 90.9±11.1 (n=21) | 75.0±12.6 (n=11) | 127.8±24.8 (n=4 ) | 126.4±3.4 (n=5 ) | 166.3 ±14.5 |
| **Weight (g)** | | | | | |
| **May/June** | 5.7±3.2 | 5.3±1.6 | 40.8±10.8 | 39.6±7.1 | 30.6 ±15.4 |
| **August** | 7.8±3.2 | 5.8±1.7 | 38.4±7.5 | none collected | 31.5 ±15.9 |
| **October** | 6.1±2.8 | 3.6±1.0 | 15.5±7.1 | 15.3±1.5 | 48.9 ±14.9 |

### 11.3.3. Gut content analysis

A total of 64 white shrimp, 322 brown shrimp and 287 croaker gut contents were examined. For croaker and white shrimp, the number of specimens available for analysis varied greatly by sampling cruise. Less than 10 individuals were collected on three of the six sampling trips for croaker five of the six trips for white shrimp.The percentage of empty stomachs was higher in shrimp than croaker. Overall, 44.4 percent of brown shrimp and 35.5 percent of white shrimp contained empty stomachs, compared to 18.5 percent of croaker. Empty stomachs may have resulted from regurgitation during the 30-minute trawl, and does not necessarily indicate that specimens were not foraging pre-capture.

Unidentified crustacean parts were the most frequently found recognizable food item in the stomachs of brown shrimp and white shrimp. Amphipods and polychaetes were also common in the stomach contents (Table 11.4 and 11.5). Bivalves, copepods, cumaceans, and tanaids were also found, but with much lower frequency of occurrence. Throughout the sampling period unidentified material was found in 20 to 46 percent of stomachs examined.

The diets of white and brown shrimp appeared to be similar. There was a significant seasonal change in the proportion of dietary components ($p < 0.001$), with polychaetes most frequently found in stomach contents during the summer and crustaceans most frequently found in the spring and fall (Table 11.4 and 11.5). The change in the relative dietary importance of polychaetes and crustaceans corresponds somewhat to seasonal changes in their relative abundance, suggesting shrimp are feeding on Ship Shoal. For example, in 2006, crustaceans were numerically dominant on Ship Shoal during May but decreased in abundance relative to polychaetes in August (Dubois et al., Chapter 10). During the same time period, polychaetes displayed a corresponding increased frequency in the stomach contents of brown shrimp relative to crustaceans food sources (Table 11.4). Dubois suggests that blue crabs are important

predators of macrofauna on Ship Shoal that may contribute to seasonal declines. However, based on their relatively low abundance, penaid shrimp do not likely exert a similar control over macrofauna density.

Table 11.4

Frequency of occurrence of food types found in the stomach contents of brown shrimp collected on Ship Shoal in 2005 and 2006.

| | **2005** | | | **2006** | | |
|---|---|---|---|---|---|---|
| **Stomachs** | **June** | **August** | **October** | **May** | **August** | **October** |
| **Examined** | 42 | 27 | 23 | 178 | 47 | 5 |
| **Empty** | 28 | 10 | 12 | 62 | 30 | 1 |
| | | | % Frequency | | | |
| Unid crustaceans | 46.5 | 20.7 | 45.8 | 35.2 | 19.2 | 66.7 |
| Polychaetes | 10.7 | 17.2 | 12.5 | 8.3 | 23.1 | 0.0 |
| Amphipods | 14.3 | 3.4 | 12.5 | 16.2 | 0.0 | 0.0 |
| Bivalve | 3.6 | 10.3 | 0.0 | 0.8 | 0.0 | 0.0 |
| Copepods | 3.6 | 3.4 | 0.0 | 2.0 | 0.0 | 0.0 |
| Cumacean | 0.0 | 0.0 | 0.0 | 5.1 | 0.0 | 0.0 |
| Tanaid | 0.0 | 0.0 | 0.0 | 2.8 | 0.0 | 0.0 |
| Other | 0.0 | 0.0 | 0.0 | 2.4 | 11.5 | 0.0 |
| Unidentified | 21.4 | 44.8 | 29.2 | 27.3 | 46.2 | 33.3 |

Table 11.5

Frequency of occurrence of food types found in the stomach contents of white shrimp collected on Ship Shoal in 2005 and 2006.

| | **2005** | | | **2006** | | |
|---|---|---|---|---|---|---|
| **Stomachs** | **June** | **August** | **October** | **May** | **August** | **October** |
| **Examined** | **1** | **6** | **9** | **47** | **1** | **0** |
| **Empty** | **1** | **3** | **4** | **15** | **0** | **0** |
| | | | % Frequency | | | |
| Unid crustaceans | na | 42.9 | 30.0 | 29.2 | 33.3 | na |
| Polychaetes | na | 42.9 | 20.0 | 6.2 | 33.3 | na |
| Amphipods | na | 0.0 | 10.0 | 18.5 | 33.3 | na |
| Bivalve | na | 0.0 | 0.0 | 0.0 | 0.0 | na |
| Copepods | na | 0.0 | 0.0 | 1.5 | 0.0 | na |
| Cumacean | na | 0.0 | 0.0 | 4.6 | 0.0 | na |
| Tanaid | na | 0.0 | 0.0 | 1.5 | 0.0 | na |
| Other | na | 0.0 | 0.0 | 1.5 | 0.0 | na |
| Unidentified | na | 14.3 | 40.0 | 36.9 | 0.0 | na |

Table 11.6

Percent (mean ± std) of each food type (as a percentage of total stomach contents) found in the stomach contents of croaker collected in 2005 and 2006 on Ship Shoal.

| | 2005 | | | 2006 | | |
|---|---|---|---|---|---|---|
| **Stomachs** | **June** | **August** | **October** | **May** | **August** | **October** |
| **Examined** | **0** | **72** | **0** | **37** | **9** | **169** |
| **Empty** | **0** | **39** | **0** | **12** | **1** | **1** |
| | | | % Frequency | | | |
| Amphipods | na | 21.4 | na | 17.6 | 0.0 | 1.1 |
| Unid. crustaceans | na | 30.8 | na | 5.6 | 7.1 | 7.7 |
| Burrowing shrimp | na | 19.2 | na | 9.6 | 5.0 | 9.0 |
| Polychaetes | na | 24.0 | na | 12.3 | 45.7 | 5.4 |
| Copepods | na | 0.0 | na | 0.0 | 0.0 | 1.9 |
| Crab | na | 1.0 | na | 0.2 | 0.2 | 0.2 |
| Tanaid | na | 0.0 | na | 0.0 | 0.0 | 0.0 |
| Cumaceans | na | 0.0 | na | 0.8 | 0.0 | 0.0 |
| Bivalve | na | 1.0 | na | 0.0 | 0.0 | 0.0 |
| Amphioxis | na | 0.0 | na | 0.6 | 5.2 | 17.9 |
| Other | na | 0.0 | na | 5.0 | 0.0 | 3.5 |
| Unidentified | na | 76.3 | na | 44.1 | 37.8 | 44.4 |

Amphipods, burrowing shrimp, unidentified crustaceans, and polychaetes comprised most of the recognizable croaker stomach contents in 2005 and 2006 (Table 11.6). Unidentified material made up an average of 76.3 percent of the diet of croaker collected in August 2005 and ranged from 37.8 to 44.4 percent of the diet in 2006. In 2005, croaker were only collected in August, so a seasonal dietary comparison is not possible for that year. In 2006, amphipods made up 17.6 percent of the diet in May but their dietary contribution was much lower on subsequent sampling dates. The contribution of the cephalochordate amphioxus to the diet of croaker increased from May to October 2006, and the contribution of polychaetes was higher in the summer of 2006 compared to May and October (Table 11.6). Seasonal changes in diet appear to reflect changes in infaunal communities. For example, amphioxus was most abundant in August and October of 2006 (Dubois et al., Chapter 10), which is also the time period in which their contribution to croaker stomach contents was greatest (Table 11.6). Also, in August 2006, the abundance of polychaetes increased relative to other infauna (Dubois et al., manuscript in prep), which corresponds to the increase in the dietary contribution of polychaetes to croaker stomach contents. However, the dietary contribution of polychaetes decreased substantially in October 2006 even though polychaetes remained numerically dominant relative to other infauna (Dubois et al., Chapter 10).

## 11.4. CONCLUSION

One goal of this study was to determine the distribution and abundance of croaker and penaeid shrimp on Ship Shoal during spring, summer and fall in order to determine the seasonal use and duration of their residency. We did not find evidence of strong habitat use or residency by shrimp or croaker on Ship Shoal as these species were typically found in low numbers compared to off-shoal SEAMAP stations. Also, although our temporal sampling frequency was low, it appears that different populations were sampled during each season suggesting shrimp are not resident on Ship Shoal for more than a few months, but rather move across or over the shoal. With brown shrimp this likely reflects a movement to deeper, off-shoal spawning sites. With white shrimp, this may reflect the 'grazing-like' movements noted by Lindner and Anderson (1956). However, because these species have significant off-shore overwintering and spawning populations, winter sampling is likely necessary to accurately determine the use of Ship Shoal by shrimp and croaker.

Given the historic link between white shrimp production and Ship Shoal area, the potential for sand mining related impacts exists. However, the results of our investigation do not suggest the extensive use of Ship Shoal by white shrimp. Similarly, negative impacts of sand mining on brown shrimp production are difficult to envision, given its transitory use of the Ship Shoal. The effects of sand mining on nekton are expected to be less severe than for infauna, as infauna have comparatively limited mobility. For example, several studies have found that dredging did not substantially change fish communities, and have even found a post-mining increase in fish abundance at dredged sites (Saloman 1974; Courtenay *et al.* 1980; Nelson and Collins 1987; USACE 2001). At minimum, during dredging operations, nekton would be displaced by turbidity and noise, although the displacement would be temporary. Additional impacts would result from localized turbidity associated with sand extraction, which could potentially clog the feeding and respiratory structures of nekton unable to avoid the mine area. However, given that few shrimp were collected on Ship Shoal, direct mortality to these nekton resulting from sand mining is likely to be minimal.

While direct shrimp and croaker mortality may be low, if food resources are slow to recover or recover inadequately, long-term adverse impacts to these nekton may result. The effect of offshore dredging on marine benthos has been studied extensively and most studies show large initial changes in macrofauna abundance, diversity, and species composition following dredging (Diaz *et al.* 2004). Thus, a second objective was to examine whether penaeid shrimp and croaker use Ship Shoal food resources as well as what resources were most important. Our data indicate that shrimp and croaker feed primarily on polychaete worms and haustoriid amphipods, both abundant on Ship Shoal. It is therefore likely that Ship Shoal provides valuable foraging habitat when shrimp and croaker are present on the shoal. The short and long-term effects of sand mining on benthic invertebrates depends in part on species life-history and the extent of the mining operation. Offshore dredging effects are often temporary, but recovery times are variable, with most studies reporting rapid recovery (<1 year) depending on species, local physical conditions, and the season in which mining occurs (reviewed in USACE 2001; Greene 2002; Hobbs 2002; Jutte *et al.* 2002; Posey and Alphin 2002; Diaz *et al.* 2004). Recovery of

abundance and diversity can take three years or longer, and pre- and post-dredge species composition may display long-term differences (Byrnes *et al.* 2004). Stone and Webster Environmental Services (1991) examined offshore borrow areas near Ocean City, New Jersey and found a community dominated by surf clams, the gastropods, haustoriid amphipods, and magelonid polychaetes, all of which are organisms commonly found on Ship Shoal. However, Van Dolah et al. (1994) tracked invertebrates in a mining site off Folly Beach, South Carolina, and found a decrease in haustoriid amphipods, but an increase in other taxa commonly found on Ship Shoal including nepthtyd polychaetes and the clam *Mulina lateralis*. These observations suggest mining will likely change the invertebrate species composition on Ship Shoal in the short-term, but many common species can be expected to recover in time. For example, the opportunistic species of polychaetes such as capitellids will likely recolonize the mine site quickly. While these polychaetes will likely provide food for nekton, recovery of the existing diversity of food resources on Ship Shoal may take longer, and it is unkown whether this change in resources will affect the diet quality of generalist feeders like penaeid shrimp and croaker.

Penaeid shrimp and croaker avoid severely hypoxic conditions by concentrating in near-shore and off-shore waters oxic waters along the edge of the hypoxic zone (Craig and Crowder 2005). Hypoxia was rarely detected on Ship Shoal even in the summer, which suggests the possibility that Ship Shoal could serve as a hypoxia refuge. Hypoxia in the waters to the south of Ship Shoal was extensive in 2005 and 2006. Although the inshore waters north of Ship Shoal may be a larger refuge (Craig and Crowder 2005), Ship Shoal has abundant food resources and could serve as suitable habitat.

# CHAPTER 12
# BLUE CRAB (*CALLINECTES SAPIDUS*) USE OF THE SHIP/TRINITY/TIGER SHOAL COMPLEX AS A NATIONALLY IMPORTANT SPAWNING/HATCHING/FORAGING GROUND: DISCOVERY, EVALUATION, AND SAND MINING RECOMMENDATIONS BASED ON BLUE CRAB, SHRIMP AND SPOTTED SEATROUT FINDINGS.

## 12.1. INTRODUCTION

### 12.1.1. Overview

The Minerals Management Service (MMS) is addressing the recent demand for long-term use of U.S. continental shelf sand resources for coastal erosion management, a critical challenge to Louisiana's ecosystems and economies (e.g. Minerals Management Service (MMS) 2008). Louisiana considers barrier island restoration as a promising way to combat wetland loss with sand mined from Ship Shoal, located off the central Louisiana coast (Figure 12.1), as the most feasible sediment source. Additional resources on the nearby Trinity and Tiger Shoals (Figure 12.1) are also being considered.

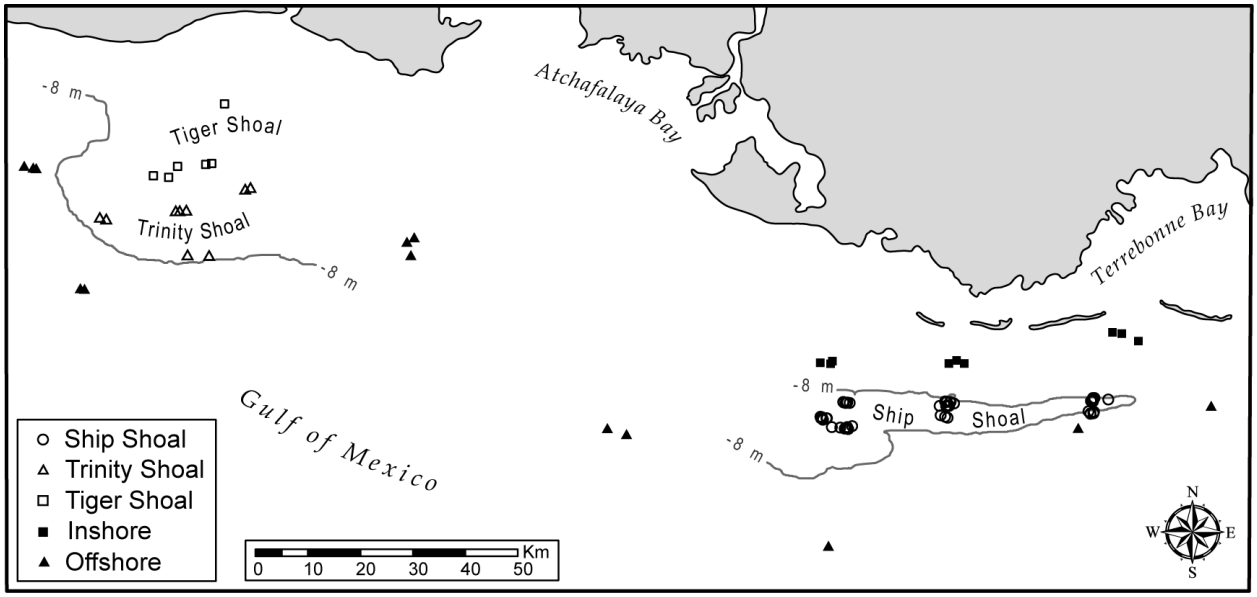


Figure 12.1 Ship/Trinity/Tiger Shoal Complex (STTSC) and trawl station locations for 2005-07. Areas within the STTSC are divided into five groups (see key). Ship, Trinity, and Tiger Shoals are partly outlined by the 8 m contour associated with each shoal (based on Braud 1999).

Together Ship, Trinity, and Tiger Shoal and the surrounding waters can be considered the Ship/Trinity/Tiger Shoal Complex (STTSC, Figure 12.1). The STTSC supports major demersal fisheries on white and brown shrimp (Litopenaeus setiferus and Farfantepenaeus aztecus), species which are major components of the STTSC ecosystem. Given the national importance of these fisheries and the constraints in which they operate, negative impacts of sand mining on these directed fisheries would have far reaching implications. The present study (Chapter 12) was conducted as part of a larger effort to understand the sand-mining ecology of Ship Shoal (Stone *et al.* 2004b) and the STTSC (Stone *et al.* 2006). Since these larger projects contained funds for shrimp-directed, fishery independent trawls of the study areas, the present study was closely coupled with the two larger studies.

During our shrimp-directed trawling efforts, we found unexpected and persistent concentrations of spawning, hatching, and foraging female blue crabs (Callinectes sapidus) in the STTSC, first on Ship Shoal in 2005 and 2006 and then on the STTSC in 2007 when MMS funding allowed a broadening of our study area. Almost all of our crabs were healthy, mature females involved in foraging and brood production/care (Figure 12.2). One mature female was soft-shelled and had recently mated, and two other mature females showed signs of recent mating. At the same time, we found little evidence that white or brown shrimp, or their economically and ecologically important predator spotted seatrout (Cynoscion nebulosus), were abundant on the surface of Ship, Trinity, or Tiger Shoal.

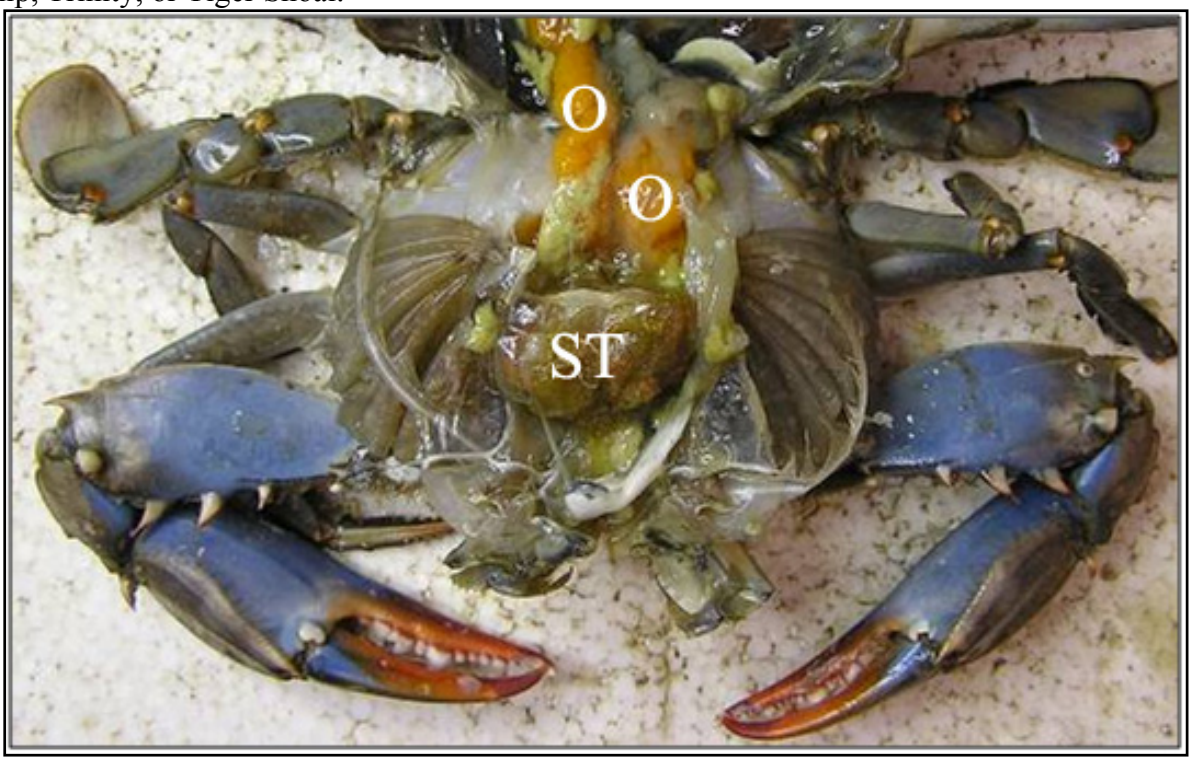


Figure 12.2 Interior view of a nonovigerous blue crab, which had hatched empty egg casings, from the Ship/Trinity/Tiger Shoal Complex. The full stomach (ST), full ovary (O), and egg casings (not shown) suggest that this crab was actively foraging while preparing to spawn again.

Given these dual findings, the focus of the present study shifted from an analysis of the potential impacts of sand mining on the abundance and condition factor/fecundity of shrimp to spawning blue crabs. Blue crabs are an ecologically important crustacean which supports the world's most valuable crab fishery, despite recent reports of regional overfishing. Louisiana currently leads all other U.S. states in blue crab landings.

Our study represents at least five blue crab firsts. It is the first time analysis of covariance (ANCOVA) and multiple regression analyses have been used to assess multiple indicators of condition factor and reproductive vigor of mature female blue crabs within and across spawning areas; the first documentation of an extensive blue crab spawning/hatching/foraging ground in offshore waters; the first indication that mating of blue crabs is not limited to estuarine conditions; the first indication that the nemertean Carcinonemertes carcinophila may have an observable effect on blue crab health or weight; and the first statistical suggestion that prey reduction through crab predation has resulted in a decline in crab fecundity. In addition we present evidence that the STTSC crabs are in a continuous spawning cycle from at least April through October and that the currently used index of blue crab size (width of the carapace across the lateral spines) should be replaced with better indicators of overall size and volume.

For the purpose of evaluating the potential impacts of sand mining, we develop and test a series of regression, multiple regression, ANCOVA, and analysis of variance (ANOVA) approaches which can be used in a BACI to monitor the impact of sand mining on the abundance, condition factor, and reproductive vigor of mature female blue crabs. While all of our approaches proved meaningful, our density-related results are the least sensitive, though our fishery-independent catch statistics are comparable to other studies of blue crab abundance across the U.S. Our results are most sensitive to changes in blue crab condition factor and reproductive vigor, making us confident that this portion of our overall approach would detect any meaningful adverse impacts of the limited sand mining currently being considered by MMS for Ship Shoal. We recommend an enhancement of both approaches for use in an ecologically-based monitoring of the potential impacts of sand mining operations on this newly discovered, and nationally important, blue crab spawning/hatching/foraging ground.

### 12.1.2. Original project scope and reasons for project revision

Our original intention for this project was to study how the population dynamics of three recreationally, commercially, and ecologically important species – white shrimp, spotted seatrout, and brown shrimp--on Ship Shoal might be affected by sand mining. Particular emphasis was to be paid to white shrimp, given their historic use of the area and importance as a spotted seatrout prey. Shrimp were to be collected by participating in the onshoal cruises conducted under Stone *et al.* (2004b) and offshoal cruises conducted by the Louisiana Department of Wildlife and Fisheries (e.g., Hanifen 2008)**.** Samples of seatrout were to be collected from recreational fishers who frequented Ship Shoal and its surrounding waters. Multiple regression and ANCOVA models relating relevant life history features to

environmental conditions were to be developed and used in a BACI analysis of the impacts of sand mining on the three species of concern.

The six questions we were to address were:

1. Are white and/or brown shrimp populations more concentrated at Ship Shoal as compared to non-shoal areas?
2. Are spotted seatrout and Atlantic croaker populations more concentrated at Ship Shoal as compared to non-shoal areas?
3. Does the sex ratio, stage of maturation, mean size, and/or condition factor of these fishery resources differ between Ship Shoal and non-shoal areas independent of the effects of season, water depth, and/or year?
4. What are the dominant prey species found in the guts of these organisms?
5. Are the gut content patterns of these four fishery resources different between Ship Shoal and non-shoal areas? If so, do these differences reflect known prey preferences for sandy substrate?
6. Are non-shoal areas likely to serve as alternative foraging and maturing habitats for these four fishery resources during periods of sand removal from Ship Shoal and/or during recolonization of and removal sites?

During the initial phase of this project, we found little evidence for direct, persistent use of Ship Shoal by white or brown shrimp or regular recreational use of Ship Shoal by recreational fishers. At the same time, under separate MMS funding (Stone *et al.* 2004b) we found unexpected concentrations of female blue crabs apparently using Ship Shoal as a spawning, hatching, and foraging ground. As time progressed, it became apparent that the surface of Ship Shoal is not currently an important white shrimp habitat in terms of fishery independent catch or commercial fishing effort. At the same time, it became equally apparent that not only Ship Shoal, but Trinity Shoal and (to a lesser extent) the entire STTSC, are important spawning, hatching, and foraging grounds for blue crabs. Therefore, we began applying and expanding the types of measurements we had intended for our shrimp-related BACI to our catches of blue crabs.

### 12.1.3. Review of the relevant blue crab literature

This review relies heavily on the current synthesis provided in Kennedy and Cronin (2007). Additional references are included as appropriate.

Blue crabs are an ecologically and economically important crustacean, historically common along the U.S. Atlantic and Gulf of Mexico coasts. Blue crab supports the most valuable crab fishery in the world (Eggleston *et al.* 2008). The U.S. fishery dominates the world catch of blue crabs (UN 2008). Within the United States, Louisiana leads all other states in recent (1997-2006) hard-shelled landings (26% of the U.S. total), followed by North Carolina (22%), the Chesapeake Bay states of Maryland and Virginia (31%, combined) and the remaining thirteen blue-crab producing states (Rhode Island to Texas, 21%, combined) (NOAA 2007).

Louisiana's recent dominance in U.S. blue crab landings is largely attributable to 1) increases in Louisiana's yield and 2) recent declines in the blue crab fisheries of Chesapeake Bay ,Maryland and Virginia), North Carolina, and other states (statistics in NOAA 2007). The Chesapeake and North Carolina declines are attributed to overfising and habitat degradation. As a result, management in these areas are considering/implementing methods of increasing spawning stock biomass through regulations (i.e., migration corridors and spawning sanctuaries) augmented by an experimental release of hatchery-raised juveniles (Aguilar *et al.* 2008; Eggleston *et al.* 2008) .

Major features of the blue crab life cycle include 1) a single, life-time mating event for the female; 2) a salinity-associated separation of the sexes following mating; 3) post- fertilization care of young by the ovigerous (in-berry) female; 4) hatching in continental-shelf associated waters; and 5) estuarine development of juveniles (Churchill 1919; Van Engel 1958).

Mating is expected to occur when the female is undergoing her terminal molt (Churchill 1919) and involves a soft-shelled female and hard-shelled male. A hard-shelled adult female is not expected to mate. Until the present study, mating has only been reported from estuarine systems. A female may mate with more than one male during her terminal molt, however a single-partner mating is expected for most females. Sperm are transferred in spermatophores and stored in the female's spermathecae. The spermathecae of newly mated females are filled with a hardened seminal fluid, which begins to soften and disappear over a period of perhaps two months (Hard 1945; Wolcott *et al.* 2005).

After the terminal molt, the ovary begins to develop mature eggs. During spawning, eggs are released into the female's spermathecae and fertilized with a portion of the stored sperm. It is expected that the sperm to egg ratio required for fertilization is greater than 1:1. The possibility that the concentration/viability of stored sperm may artificially limit fertilization is of concern in areas where males are intensely harvested (Hines *et al.* 2003; Carver *et al.* 2005).

Once released from the female's body cavity, the eggs attach to the females' swimmerets (Churchill 1919). The presence of sediment may be necessary for egg attachment (Schaffner and Diaz 1988). The attached egg mass is commonly referred to as a 'sponge'. As the fertile eggs develop, proliferation of pigments in the embryo change the color of the sponge from bright orange (newly released) to black (ready to hatch) within a period of about fifteen days.

Tagging and tracking studies suggest that spawning along the U.S. Atlantic and central/western Gulf occurs within the lower estuary or just outside the estuary (Tagatz 1968; More 1969; Carr *et al.* 2004). Since egg development and hatching success are apparently enhanced by salinities of at least 20 ppt (Sandoz and Rogers 1944; Davis 1965), seaward movement of estuarine-based, pre-hatching females is expected to enhance larval success, though parasitism, disease, and fouling of adult females is expected to increase with salinity (Shields and Overstreet 2007). There is evidence suggesting that some females will migrate back into less saline estuarine waters between hatchings to forage (Daugherty 1952; Tankersley *et al.* 1998), while others may continue to move seaward for successive spawns (Hench *et al.* 2004; Forward *et al.* 2005). Published gut content and stable isotope studies of spawning/hatching crabs are lacking.

Tagging studies on the west coast of Florida suggest an interesting variation on the movement of post-mating/pre-spawning females (i.e., Steele 1991). Here some females may spawn near their mating estuary while other females migrate long distances along the coast before spawning.

Mature females may have more than seven broods per spawning season (Dickinson *et al.* 2006) and live to spawn in multiple seasons. After hatching, remnants of old, empty egg cases remain attached to the swimmerets of the mother crab for an unknown period (Churchill 1919).

There are a limited number of equations describing various aspects of the population dynamics of mature female blue crabs. These include width-weight equations for nonovigerous female blue crabs (Newcombe *et al.* 1949; Pullen and Trent 1970; Hines 1982; Olmi and Bishop 1983; Rothschild *et al.* 1992; modified from H. Perry in Guillory *et al.* 2001, Figure 3.5; Lipcius and Stockhausen 2002). The statistical similarities of these equations have not been tested. In addition there are two published studies relating fecundity to either dry body weight or size (Hines 1982; Prager *et al.* 1990). The statistical similarities of these equations have not been tested. Dickinson et al. (2006) provides four, clutch-specific equations relating sponge volume to width which suggest a decline in sponge volume with clutch number. Reasons for this decline were not explored, but may relate to crab culture in minnow traps.

### 12.1.4. Development of revised project hypotheses

#### *12.1.4.1. Blue crab observations*

We found unexpected and persistent concentrations of spawning, hatching, and foraging female blue crabs off the Louisiana coast in 2005 to 2007, first on Ship Shoal in 2005 and 2006 and then on the STTSC in 2007 when MMS funding allowed a broadening of our study area. Of the 516 crabs, 511 were mature females, four were mature males, and one was an immature male. The vast majority of mature females (90%) were either in-berry (Figure 12.3) or/and contained full gonads (Figure 12.4c). The majority of nonovigerous females had hatched egg casings on their abdomens (Figure 12.5) and full ovaries (C in Figure 12.4) suggesting that they were preparing for an additional spawn. While many of our crabs contained acorn barnacles (*Chelonibia patula* Ranzani and Balanus spp.; Shields and Overstreet 2007) on the exoskeleton, the gooseneck barnacle *Octolasmis muelleri* (Coker; Shields and Overstreet 2007) on their gills, and/or the nemertean *Carcinonemertes carcinophila* (Kölliker; Shields and Overstreet 2007) in their gills and/or sponges, almost all appeared healthy (Figure 12.6).

We also found the first reported evidence of the offshore mating of blue crabs. One mature female was undergoing her terminal molt (adult abdomen, incompletely calcified exoskeleton, top and middle panels of Figure 12.7) and had enlarged spermathecae which were consistent with Jivoff *et al.* (2007)'s description of a female blue crab which had just copulated (bottom panel of Figure 12.7).

In addition to the female in Figure 12.7, we found two other female blue crabs within the STTSC which had evidence of recent mating but hardened exoskeletons (Figure 12.8). Virtually all of the remainder of our female blue crabs examined had resorbed spermathecae (Figure 12.9), characteristic of post-mating ovarian development in preparation for spawning.

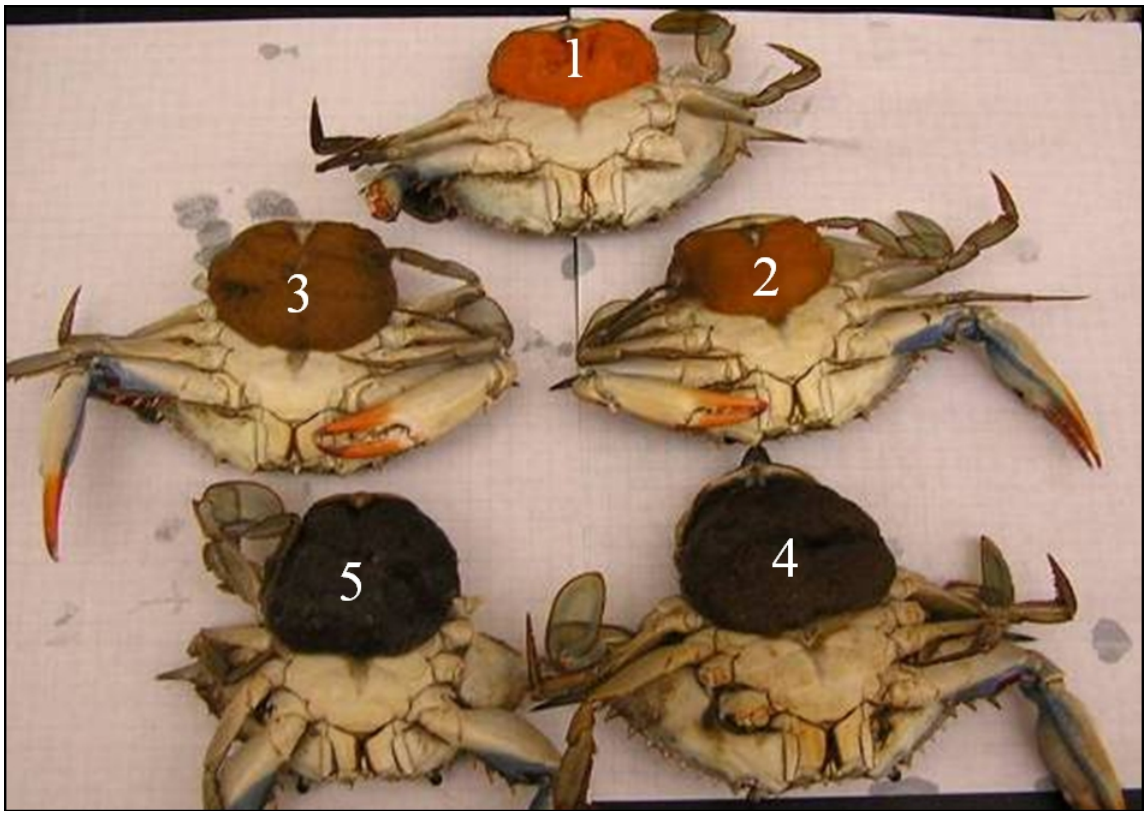


Figure 12.3 Ventral view of five female blue crabs of the Ship /Trinity/Tiger Shoal Complex with extruded sponges ranked according to developmental stage (1-5) of the sponge. The color change of the sponge is associated with the proliferation of pigments by the embryos as they develop. According to Jivoff et al., 2007, brood development takes approximately two weeks.


Figure 12.4 Interior view of mature female blue crabs of the Ship/Trinity/Tiger Shoal Complex displaying our three, Hard (1945)-based assessments of ovarian condition. (A) Light is consistent with both Hard's stage I where the ovary is described as "small, inconspicuous, white in color" and Hard's stage V where the ovary is described as "collapsed, grey or brownish in color." (B) Medium is consistent with Hard's stage II for ovaries of an intermediate size. (C) Full is consistent with Hard's stage III where the ovary is "preceding first ovulation…bright orange and of large size" or stage IV where the ovary is "between ovulations…orange in color and of large size.

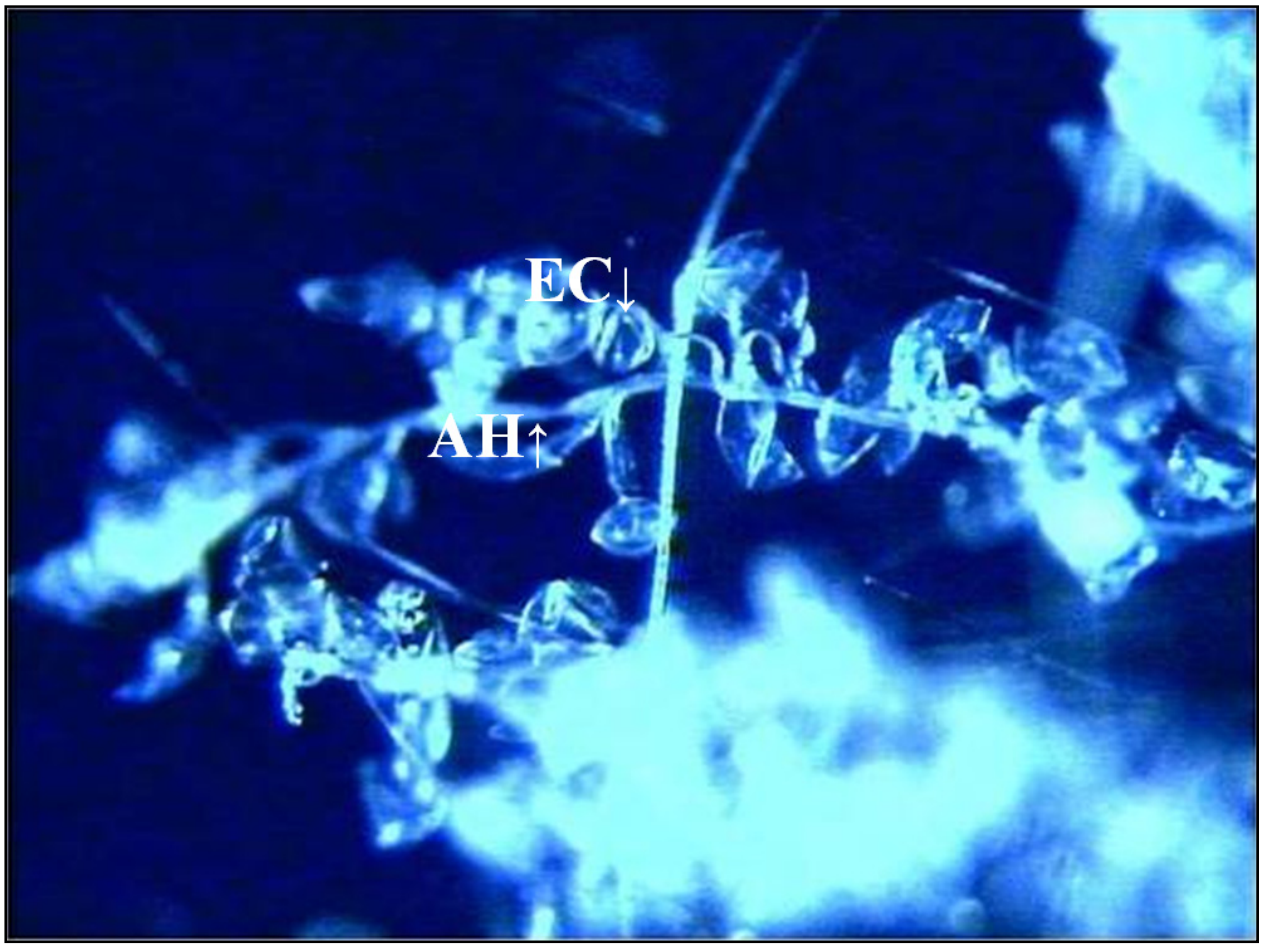


Figure 12.5 Microscopic image of hatched egg casings (EC) on individual abdominal hairs (AH) located on the pleopods of a female blue crab from the Ship/Trinity/Tiger Shoal Complex. These remnants are evidence that the female has spawned and hatched at least one previous sponge (Churchill, 1919).

Figure 12.6 Examples of the most common symbionts of the Ship/Trinity/Tiger Shoal Complex blue crabs. Top left: Dorsal view of gills showing a high infestation of the nemertean *Carcinonemertes carcinophila* (light colored, encapsulated structures indicated by the probe). Top right: Ventral view of gills with high (> 200 individuals) infestation of the gooseneck barnacle *Octolasmis muelleri* . Bottom left: Dorsal view of a female blue crab with acorn barnacles attached to the carapace. Bottom right: Ventral view of a sponge infected with *C. carcinophila* which are particularly evident as thread-like structures inside the white box.

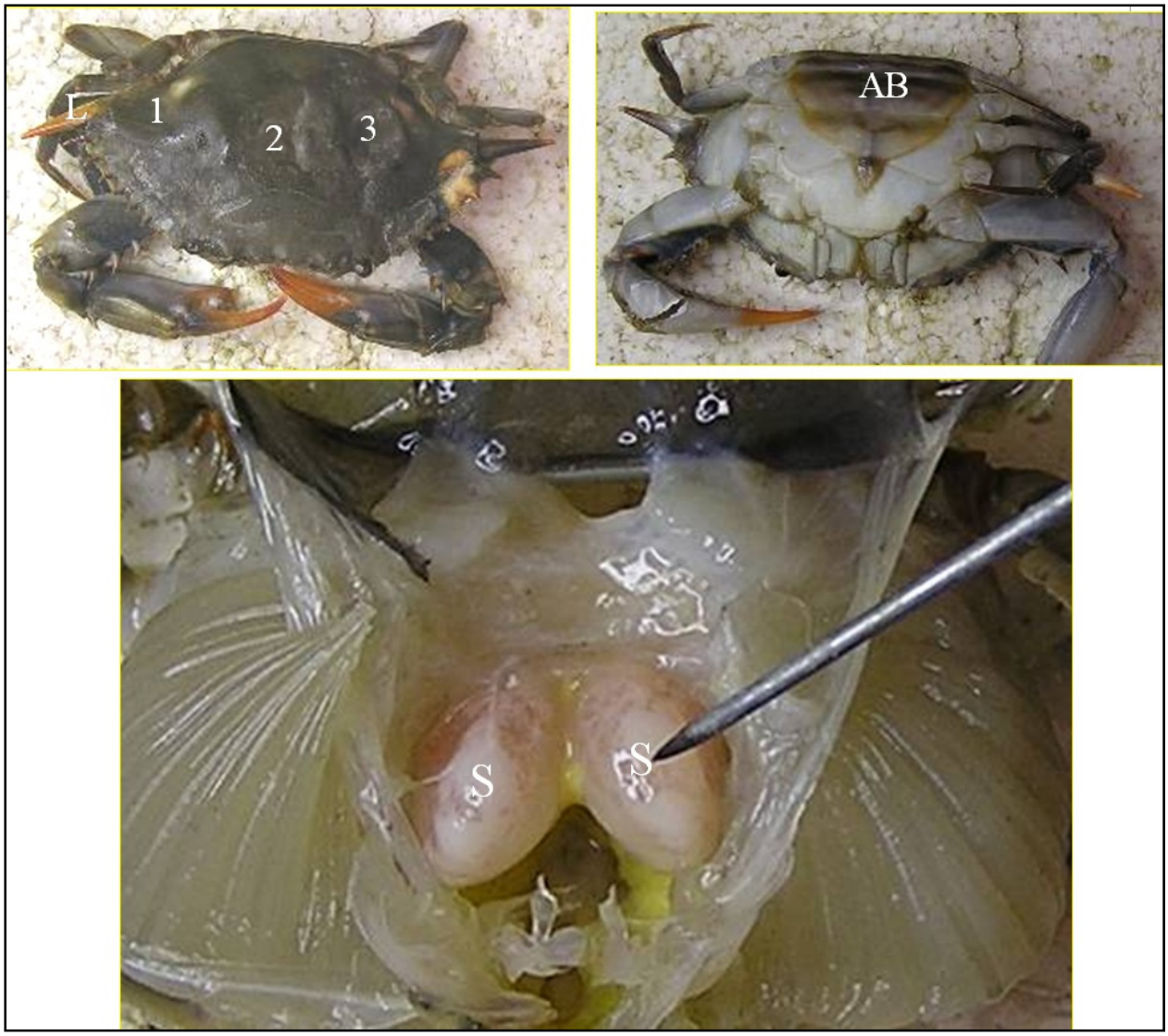


Figure 12.7 Three views of a female blue crab showing evidence of mating on the Ship/Trinity/Tiger Shoal Complex. Top left: Dorsal view showing signs of soft-shelled condition -- pliable dents in the carapace (1, 2, and 3) and downward bend of lateral spine (L). Top right: Ventral view showing rounded abdomen of mature female (AB). Bottom: Internal view showing two spermathecae engorged with ejaculate (S, tip of pointer). The condition of these spermathecae are entirely comparable to the description Jivoff et al. (2007, p. 261) provides of a female blue crab which has just copulated: "the easily visible pink seminal fluid, capped with a dense accumulation of white spermatophores".Mechanical manipulation of these spermathecae revealed that they are also consistent with Wolcott *et al.*'s (2005), Scale 1, "hard plug" spermathecae for crabs which have mated within the past two weeks. The crab is also consistent with Hard's (1945) stage I as the ovary is not readily visible, a condition Hard expects for female crabs which have recently mated during their terminal molt.

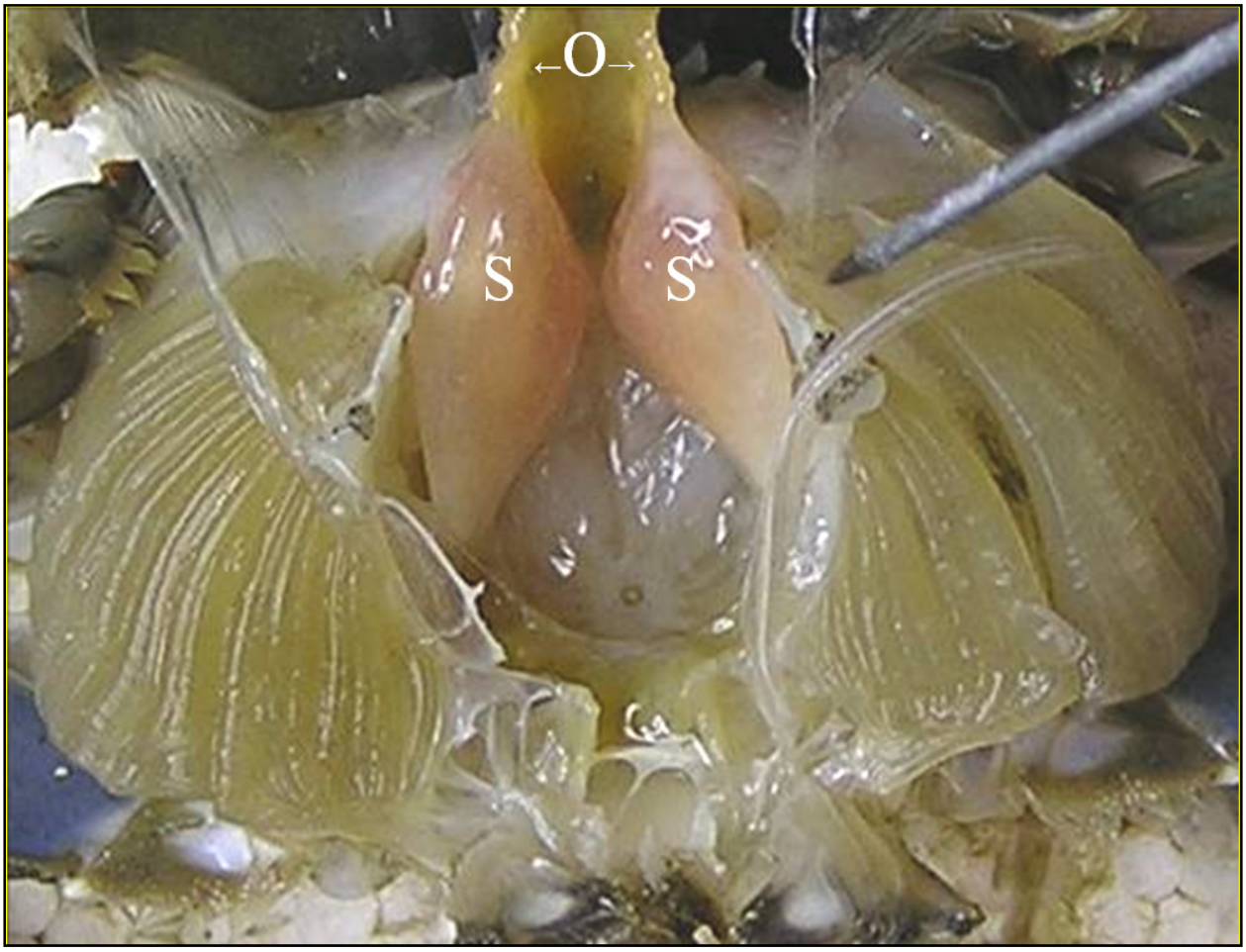


Figure 12.8 Interior view of a recently mated female blue crab from the Ship/Trinity/Tiger Shoal Complex with a hardened exoskeleton. The spermathecae (S) are beginning to soften and resorb. This crab is consistent with Wolcott et al.'s (2005), scale 2 in which a spermatheca appears as a "soft plug, in which the seminal fluid is softening." The developing ovary (O) is consistent with Hard's (1945), stage 2, which describes the "growth period of the ovary, from the time of copulation to the time of ovulation" with a concurrent decrease in the size of the spermathecae.

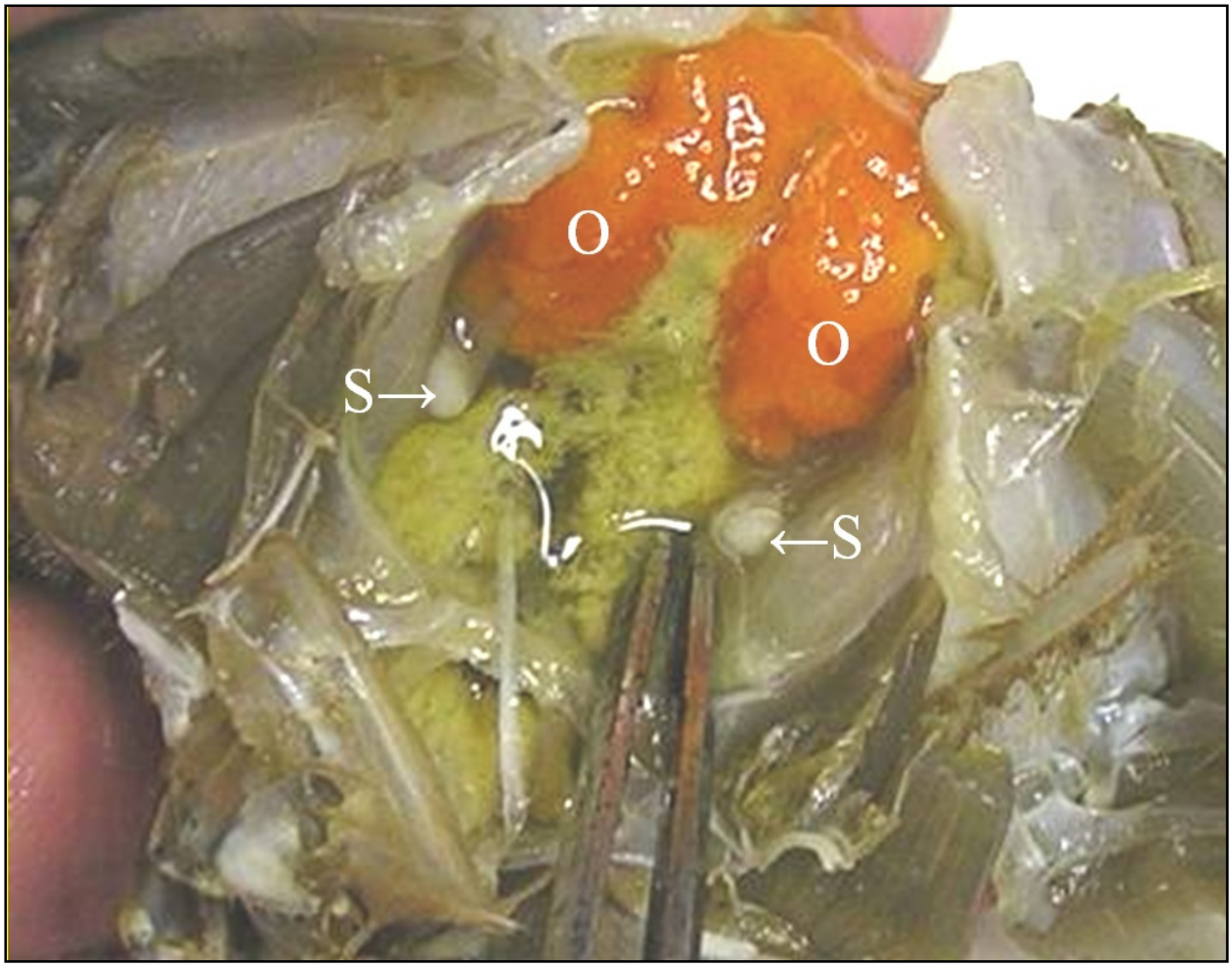


Figure 12.9 Interior image of a mature female blue crab from the Ship/Trinity/Tiger Shoal Complex whose spermathecae (S) have decreased in size due to absorption of the seminal fluid. This particular female had evidence of a previous spawn in the form of hatched egg casings on her pleopods. As such she is consistent with of Wolcott et al.'s (2005) scale 5 which describes the spermathecae of a brooded female. Her full ovarian condition (O) indicates she is preparing to extrude another sponge and is consistent with Hard's (1945) stage 4, which describes the ovarian state between broods.

### *12.1.4.2. Blue crab hypotheses*

As our project developed, we began to realize that the STTSC complex was an important spawning/hatching/foraging ground for female blue crabs and that we could develop useful statistical tools to detect adverse impacts of limited sand mining within the STTSC on its blue crab population(s). Our specific, testable hypotheses are:

1. There is no statistical difference in condition factor of the STTSC crabs and those from recognized blue crab spawning, hatching, and/or foraging grounds.

2. There is no statistical difference in size/fecundity relationship of blue crabs on STTSC crabs and those from recognized blue crab spawning grounds.
3. Mature female blue crabs on STTSC are in a continuous spawning/hatching cycle during at least April-October.
4. The conventional measure of blue crab size provides the best statistical tool to describe the dependence of blue crab weight on volume.
5. Condition factor and fecundity of blue crabs on the STTSC will not be affected by month, area, ovigery, parasitism by nemerteans in the gills or sponge, parasitism by goose neck barnacles in the gills, and fouling by acorn barnacles on the exoskeleton.
6. There are no temporal or spatial differences in the use of the STTSC as a blue crab spawning/hatching/foraging ground.
7. There is no statistical difference in mature female crab abundance between the STTSC and conventionally recognized blue crab spawning grounds.

## 12.2. MATERIALS AND METHODS

To test four hypotheses we used a combination of regression, stepwise multiple regression and ANCOVA analyses and took the following measurements of STTSC blue crabs obtained in Stone *et al.* (2004b; 2006) during spring, summer, and fall of 2006, and 2007:

TT – carapace width between the lateral spines,
BB – carapace width at the base of lateral spines,
L -- carapace length,
H -- carapace height,
W – crab weight without acorn barnacles,
T – tail weight
C – body weight without tail (W – T),
P – ovigerous/nonovigerous (presence/absence of a sponge),
SC – sponge color on a five-point scale, of bright orange (1) to black (5) (Figure 12.3),
SN – nemertean intensity (*C. carcinophila*) on sponge (four-point scale, Figure 12.6),
E – number of eggs (in millions) in a sponge
BC -- acorn barnacle (*C. patula*, Balanus spp.) exoskeleton coverage (10 point scale, Figure 12.6),
BW -- acorn barnacle weight,
D -- largest acorn barnacle diameter,
O – ovary fullness on a three-point scale (Figure 12.4),
G -- gooseneck barnacle (*O. muelleri*) intensity on gills (six-point scale, Figure 12.6),
GN -- presence/absence of the nemertean *C. carcinophila* on gills; gill nemerteans (Figure 12.6).

The available literature allowed us to test hypotheses 1 and 2 with other areas, but required that we make a decision between using either wet weights and dry weights of our whole crabs. We chose to use wet weights of whole crabs as this allowed us to make the most comparisons.

All statistical analyses were done using version 9.1.3 of SAS (SAS Institute Inc. 2004). With the exception of the ANOVA used to test hypothesis 6, all of our results are significant at $p > 0.01$. For our test of hypothesis 6, we accepted differences at $p = 0.1$, as we did not wish our limited trawling effort to inadvertently discount the importance of an area/month within the STTSC as an important spawning/hatching/foraging ground. We used the "stepwise" procedure in our multiple regression analysis, allowing the default settings to regulate model selection.

To test hypothesis 6, we used ANOVA to compare temporal and spatial trends in our STTSC data obtained in Stone et al. (Stone *et al.* 2006) for the spring, summer, and fall of 2007. To test hypothesis 7, we used the regression analysis to compare the peak catch rates we obtained in the STTSC in Stone et al. (2004b; 2006) for 2005, 2006, and 2007 with those reported in the literature for recognized blue crab spawning grounds.

The specific literature used to test hypotheses 1, 2, and 7 are briefly reviewed at the beginning of each of these sections in the section 12.3 entitled **Test of the hypotheses**. The tests of hypotheses 1 and 4 required us to use the conventional measure of crab width found in the literature (TT). In testing hypothesis 4, we found TT to be statistically less predictive of weight than the other size measurements we took. We therefore included a brief review of relevant theory at the beginning of the section 12.3.1 entitled **Test of hypothesis 1**.

All linear measurements were made in mm; all weights, in g wet weight. All statistical analyses were conducted using SAS (Statistical Analysis System, Cary, NC). We did not transform our catch statistics as we used distribution free techniques available in SAS to analyze our STTSC catch data and because the aggregate data available in the literature was untransformed. Measurements made on Ship Shoal crabs in 2005 are consistent with those obtained for the STTSC in 2006 and 2007, but did not encompass the entire range of parameters we eventually measured, and are therefore not included in our condition factor analyses. A description of our sampling trips and computerized listings of our STTSC measurements is being included in the respective final reports for Stone et al. (2004b; 2006).

## 12.3. TEST OF HYPOTHESES

### 12.3.1. Test of hypothesis 1 (condition factor, national comparison)

The condition factor is the ratio of a fish's weight (W) to a linear estimate (X) of its volume (V). Usually length (L) is used as the measure of X. Condition factors are commonly used to compare the health of fish between differing populations, under the assumption that the heavier fish (per unit of length) are healthier (e.g., Ricker 1975). When W and X are measured over a range of sizes in at least two different populations, differences in the condition factor are normally tested using a form of the general size/weight relationship:

$$W = aX^b, \qquad (12\text{-}1)$$

where a and b are constants (e.g., Newcombe *et al.* 1949). If the specific gravity is 1, X=V, and W and X are in g and $cm^3$, respectively, then the constants 'a' and 'b' both equal one. When L is used to estimate volume, Equation 12-1 is called a length-weight relationship and has the form:

$$W = aL^b. \qquad (12\text{-}2)$$

Equation 12-1 and Equation 12-2 can be fit directly to a data set using nonlinear statistics. Or the equations can be linearized:

$$\log W = \log a + b(\log X) \qquad (12\text{-}1a)$$
$$\log W = \log a + b(\log L) \qquad (12\text{-}2a)$$

and fit to the log transformed data using parametric statistical techniques. Since both procedures have their advantages and disadvantages (e.g., Ricker 1975), researchers normally examine the behavior of their data in both the transformed and untransformed state.

Statistical comparisons of condition factors between differing populations can be conducted using ANCOVA if the raw data are available or there are sufficient replicate equations per treatment. When an ANCOVA cannot be run because the raw data are unavailable or because there are insufficient replicate equations, regression analysis can be used to compare equations between differing populations. In the latter case, a regression of loga versus b should generate a single straight line with a negative slope and a random scatter of the residuals, unless the condition factor varies among the populations being considered. Though common in the literature, comparisons of slopes (b) without a consideration of the corresponding intercepts (a) is not an appropriate comparison of condition factors, since b is not independent of a. For example, a seasonal decline in specific gravity (as would occur with an increase in energy reserves stored as lipids) would theoretically depress b and increase a if the relationship between L and V remains constant.

With blue crab, it has become common to use the width of the carapace instead of length and to measure width (in mm) as the distance between the lateral spines on the carapace (TT) (Table 12.1). The desirability of this convention has been questioned since the lateral spines are often damaged and different spine morphologies within the same population have been shown to have different predictive capacities (Olmi and Bishop 1983). Regardless, the conventional measurement (TT) has not been tested against other linear measures of size.

Table 12.1

Published female blue crab width-weight equations, $W = aTT^b$, where W is either in wet weight (g) or dry weight (g) and TT is carapace width between the lateral spines (in mm).

| Weight | Area | a | b | Source |
|---|---|---|---|---|
| Wet | Chesapeake Bay, VA/MD | 0.000343 | 2.575 | Newcombe et al., 1949 |
| | | 0.003487 | 2.1165 | Rothschild and Ault, 1992 |
| | | 0.000631 | 2.47 | Lipcius, 2002 |
| | Ashley River, SC | 0.004185 | 2.1083 | Olmi and Bishop, 1983 |
| | Mississippi | 0.0001810 | 2.7814 | Perry in Guillory et al., 2001 |
| | Galveston Bay, TX | 0.0002874 | 2.6395 | Pullen and Trent, 1970 |
| Dry | Delaware | 8.9125 | 0.005 | Hines, 1982 |

To compare the condition factor of our STTSC crabs with those in Table 12.1 which used wet weight, we first fit our STTSC nonovigerous crab data to Equation 12-1a using TT as an estimate of X, and obtained:

$$\log W = -3.0739 + 2.3964 * \log TT \qquad (12\text{-}3)$$

(residual sum of squares [$R^2$] = 0.80). Then we compared the published wet weight equations in Table 12.1 with Equation 12-2 by plotting the respective log(a) values against the respective values of b. We found a striking inverse relationship between loga and b:

$$\log(a) = 1.9065 - 2.0602 * b \qquad (12\text{-}4)$$

($R^2$ = 0.99), Figure 12.10. These results suggest that all the individual length-weight equations considered conform to a single relationship for nonovigerous female blue crabs. As such our analysis finds no statistical difference in the condition factors for these populations of nonovigerous female blue crabs which range from Chesapeake Bay in the 1940s to the STTSC in 2006-2007. Based on this overall similarity in condition factors from all known blue crab studies, we are unable to reject hypothesis 1 and conclude that the STTSC currently supports a healthy habitat for spawning/hatching/foraging female blue crabs.

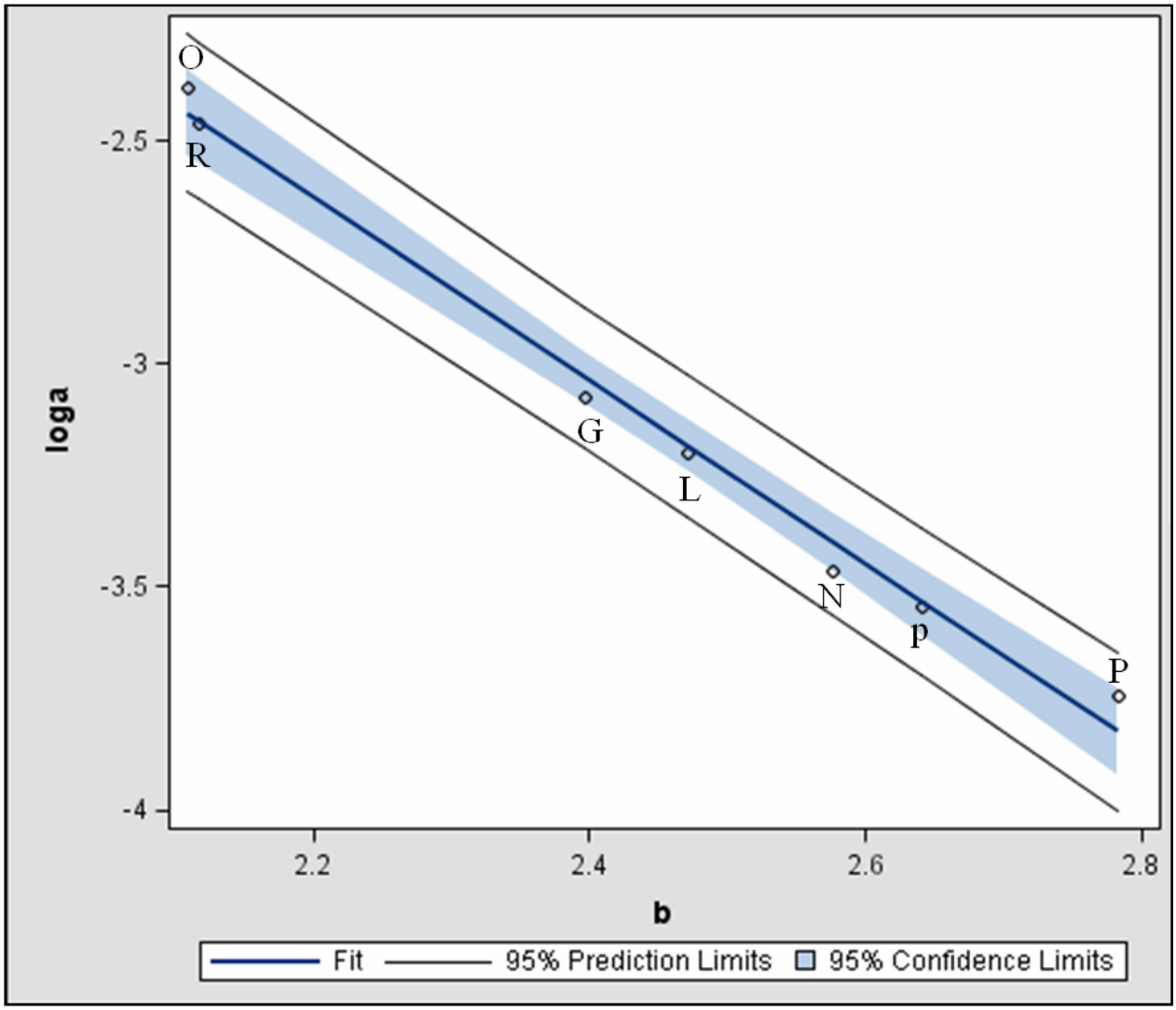


Figure 12.10 Results of a regression analysis run to test the hypothesis that the available width-weight equations (logW = loga + b(logTT), where W is g wet weight and TT is carapace width in mm between the lateral spines) for nonovigerous female blue crabs conform to a single family of curves. Open circles are the intercepts (loga) and slopes (b) of width–weight relationships for Chesapeake Bay, VA/MD (N, Newcombe *et al.* 1949; R, Rothschild *et al.* 1992; and L, Lipcius and Stockhausen 2002), Ashely River, NC (O, Olmi and Bishop 1983), Mississippi (P, modified from Perry in Guillory *et al.* 2001), Ship/Trinity/Tiger Shoal Complex, LA (G, this report); and Galveston Bay, TX (p, Pullen and Trent 1970). The regression fit is loga = 1.9065 - 2.0602 * b ($R^2$ = 0.99).

### 12.3.2. Test of hypothesis 2 (fecundity, national comparison)

We used an ANCOVA to compare the fecundity of our SSTTC crabs with that reported for Chesapeake Bay by Prager *et al.* (1990) with their dry weight procedure. We found no effect of area (Chesapeake Bay, STTSC) in the ANCOVA we ran of E on TT with area as a class variable. The single regression fit to the data,

$$\text{logE} = -4.8453 + 2.1151*\text{logTT}, \qquad (12\text{-}5)$$

($R^2$ =0.31), Figure 12.11, predicts a linear increase in fecundity (measured in number of eggs/sponge) with increasing size of the mature female. The analysis finds no difference in the fecundity/size relationship of ovigerous crabs between the STTSC and Chesapeake Bay. We are unable to reject hypothesis 2 and conclude that the STTSC supports as fecund a population of spawning blue crabs as Chesapeake Bay did before its apparent decline in crab abundance.

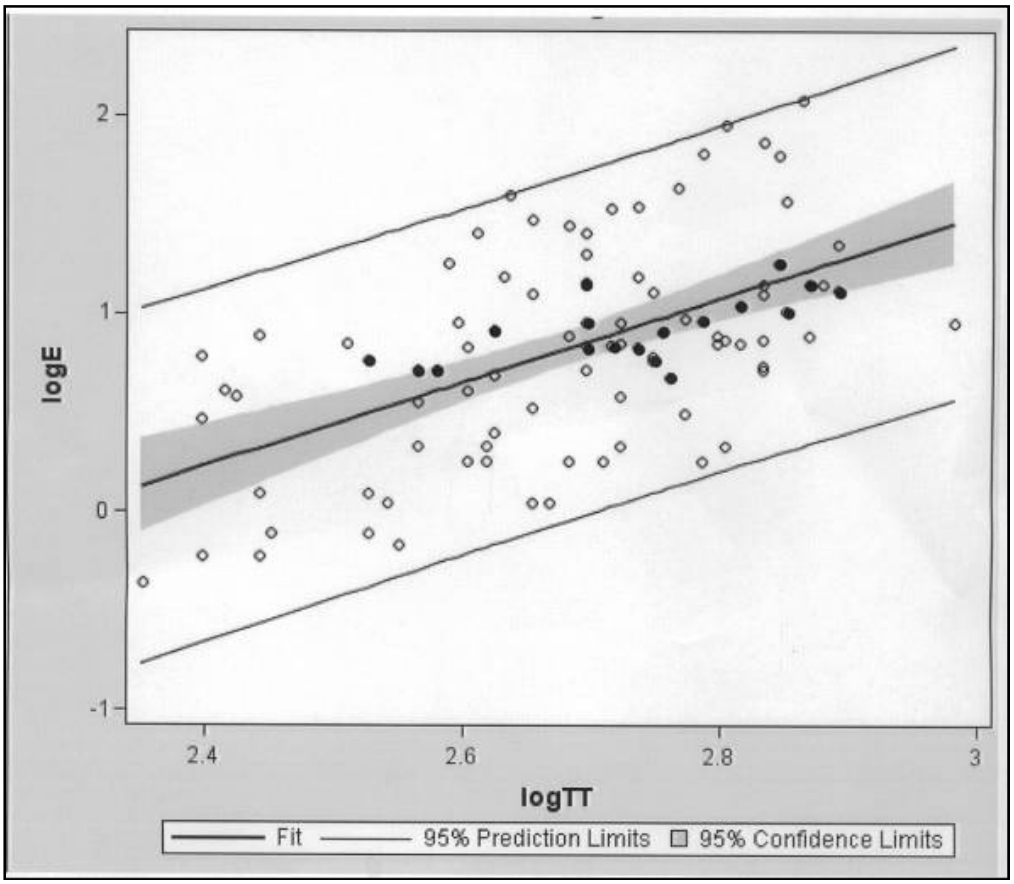


Figure 12.11 Results of an ANCOVA run to test the hypothesis that there is no difference in the fecundity-size relationships for mature female blue crabs from the Chesapeake Bay, VA/MD (open circles, Prager *et al.* 1990) and the Ship/Trinity/Tiger Shoal Complex, LA (closed circles, this report). The regression fit is logE = -4.8453 + 2.1151*logTT ($R^2$ =0.31), where E is millions of eggs/female and TT is width (cm) between the tips of the lateral spines of the carapace.

### 12.3.3. Test of hypothesis 3 (continuous spawning/hatching cycle during study)

During our dissections, we noticed a general relationship between ovarian condition (Figure 12.4), the presence or absence of a sponge, and the color of the eggs on a sponge (Figure 3) when present. Generally we came to expect that nonovigerous crabs would have comparatively full ovaries and that the ovarian fullness of ovigerous crabs would increase as embryo development increased (and the sponge changed from bright orange to black). The general impression was that ovarian recovery began immediately after spawning and continued at a constant rate through brooding so that a new brood would be spawned shortly after the present brood had hatched.

Based on these observations, we hypothesized that our female blue crabs were in a continuous spawning/hatching cycle on STTSC during at least April through October, and that they would undergo another spawn as soon as the ovary had recovered from the present spawn. Under this hypothesis, the ovarian condition of our nonovigerous females could be predicted by the rate of ovarian development exhibited by our ovigerous females. The simplest test we could develop for this hypothesis is: There was a linear increase in ovarian fullness, O, of our STTSC females from O = 1 (light ovary) after an existing brood had been spawned (time T = O) to O = 3 (full ovary) just before the next brood was spawned. In this simplest test, the average ovarian fullness of our nonovigerous females should occur at the predicted midpoint of the inter-sponge period.

To test this possibility, we first computed the average ovarian fullness by sponge color ($O_{SC)}$; assumed (based on Jivoff *et al.* 2007) that each of our five sponge colors represented three days of embryo development time; and regressed $O_{SC}$ against the respective estimate of average embryo age in days (t, where t = 0 at spawning). The result:

$$O_{SC} = 0.9908 + 0.0971 * t \qquad (12\text{-}6)$$

($R^2$ =0.97) describes a linear recovery in ovarian fullness between spawning and hatching of an existing brood and predicts that full ovarian recovery (O = 3) will occur 6d after hatching (T = 21) and that the average $O_{SC}$ of our nonovigerous crabs will be attained at t = 18d. Then we reran the regression, but included our measure of average ovarian fullness as occurring at 18d. The results (Figure 12.12) strongly suggest that the STTSC crabs were in a continuous spawning cycle, producing successive spawns every 21 d. As a result we cannot reject hypothesis 3.

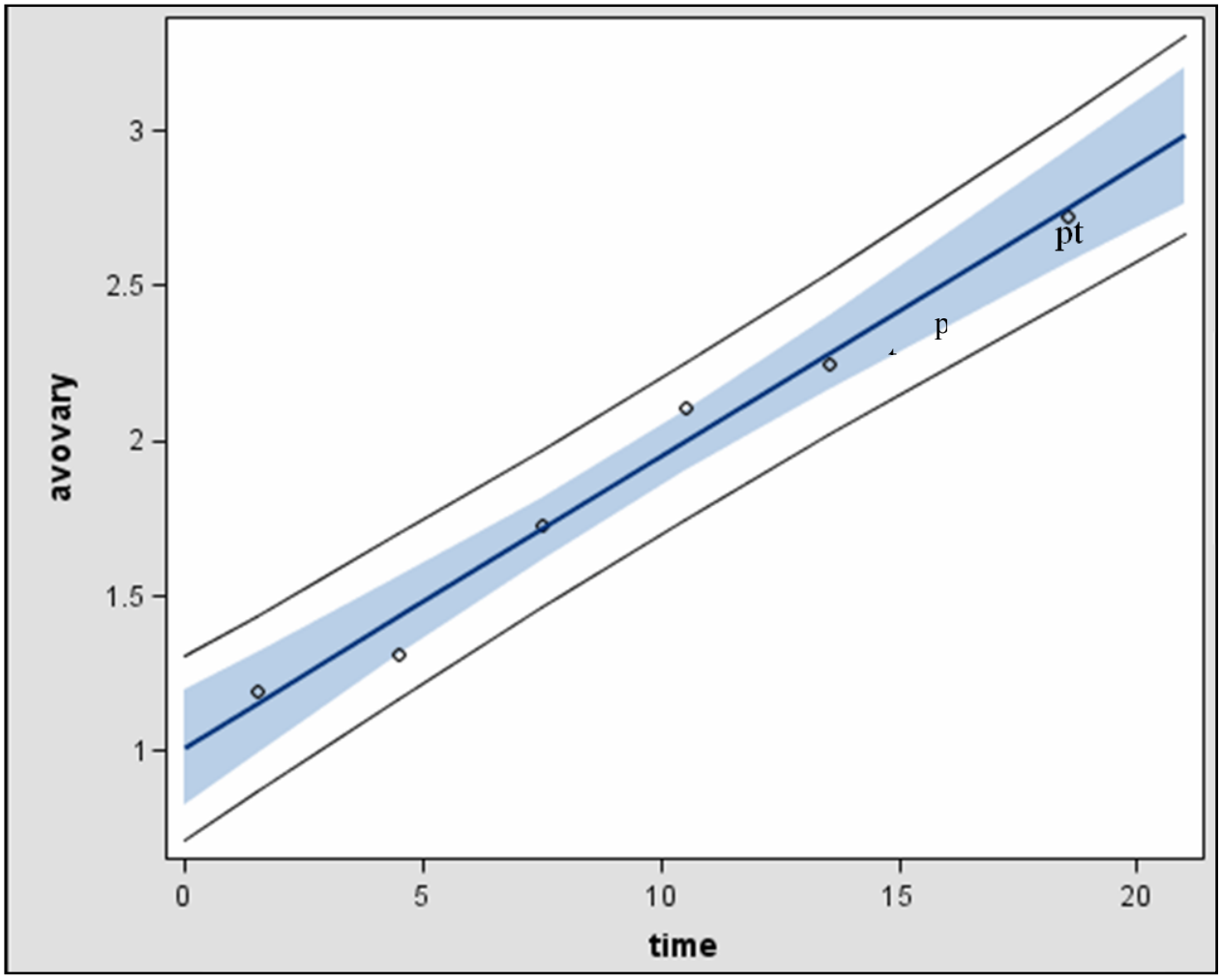


Figure 12.12 Testing the hypothesis that female blue crabs on the Ship/Trinity/Tiger Shoal Complex in April through October are in a continuous spawning/hatching cycle. In the test, the average ovarian development for crabs of differing sponge colors ($O_{SC,}$ avovary, open circles) is first regressed against an estimate of embryo development time (t, time) derived using sponge color and Jivoff *et al.* (2007). The regression (not shown), $O_{SC} = 0.9908 + 0.0971 * t$, ($R^2 = 0.97$) is then used to predict the inter-brood period (t-21d). The "regression" shown is fit both to our data and to the prediction (pt) that the observed average ovarian condition of our nonovigerous crabs occurred at the midpoint (t=18 d) of the predicted inter-brood period.

### 12.3.4. Test of hypothesis 4 (traditional estimate of size)

We ran a stepwise multiple regression analysis to find the most predictive linear measurement of body weight for female STTSC crabs by area and month. Here we tested the effect on W of TT,

BB, L, H, P, month (M), and area (A for our five STTSC areas, Figure 12.1). The procedure selected a six parameter model of the form:

$$\log W = -3.2247 + 0.8071*\log BB + 0.0843*P + 1.5973*\log L + 0.5918*\log H - 0.0025*M + 0.0023*A \quad (12\text{-}7)$$

($R^2 = 0.968$) which uses three linear measures of size and ovigery, month, and area to predict weight. The procedure also revealed that a two-parameter model of the form:

$$\log W = -3.1743 + 0.0854*P + 3.0017*\log L, \quad (12\text{-}8)$$

($R^2 = 0.960$) provides as realistically good a fit as the six parameter model based on a comparison of model complexity and the minimal difference in $R^2$'s (0.008).

Both Equations 12-7 and 12-8 clearly indicate that the historically used TT is a poorer linear indicator of V than is L, H, or BB and that we should reject hypothesis 4. However, given the ubiquitous and long use of TT, we decided to examine the issue further through a series of ANCOVAs with P as a class variable and seven differing linear estimators of V in Equation 12-1a (L, H, TT, BB, L*H*BB, $L^2$*BB, and $L^2$*H).

The results are presented in Table 12.2. Based on a comparison of $R^2$ 's, the three volume estimators, L*H*BB, $L^2$*BB, and $L^2$*H, provided slightly better predictors of weight than all single linear measurements. With single linear estimators, L was the most predictive estimator of weight ($R^2 = 0.961$), though followed closely by BB and H. The traditionally used TT was the least predictive ($R^2 = 0.806$).

Table 12.2

Comparison of size (X, mm) – weight (W, g) relationships for mature female blue crabs (n=388) from the Ship/Tiger/Trinity Shoal Complex, Louisiana, 2006-2007. Measurements of length (L), height (H), and width across the lateral spines (TT) follow Newcombe et al. (1949). BB is the carapace's width between the bases of the lateral spines. Solutions are provided for the results of ANCOVAs testing the effect of ovigery on the relationship logW = loga + b(logX), where X is varied as in column one, below. For each estimate of X, the base equation given is for ovigerous females. The corresponding equation predicting the weight of the nonovigerous females is obtained by adding c to log(a), and d to b. When d = 0, the ANCOVA's interaction term is not significant and the equation reflects parallel slopes. Note that TT has the lowest $R^2$, and is therefore least useful in predicting weight.

| X estimator | $R^2$ | log(a) | b | c | d |
|---|---|---|---|---|---|
| Length (L) | 0.961 | -2.8452 | 2.8651 | -0.5165 | 0.2424 |
| Height (H) | 0.925 | -1.977 | 2.7446 | -0.4573 | 0.2445 |
| Width at base (BB) | 0.942 | -3.7103 | 2.9111 | -0.0887 | 0 |
| Width at tips (TT) | 0.806 | -2.3349 | 2.1025 | -0.7394 | 0.2942 |
| L*H*BB | 0.966 | -2.9455 | 0.9682 | -0.4627 | 0.0706 |
| $L^2$*BB | 0.965 | -3.1503 | 0.9636 | -0.4846 | 0.0711 |
| $L^2$*H | 0.964 | -2.6440 | 0.9601 | -0.5105 | 0.0839 |

The comparatively poorer behavior of TT as an indicator of crab weight is graphically demonstrated in Figure 12.13, where we examine the fits obtained in Table 12.2 for BB and TT. Note the clearer separation of ovigerous and nonovigerous females when BB is used instead of TT to measure width. Varied lateral spine morphologies (Figure 12.14, Olmi and Bishop 1983) likely account for the poor predictive ability of TT as measure of carapace width and of volume.

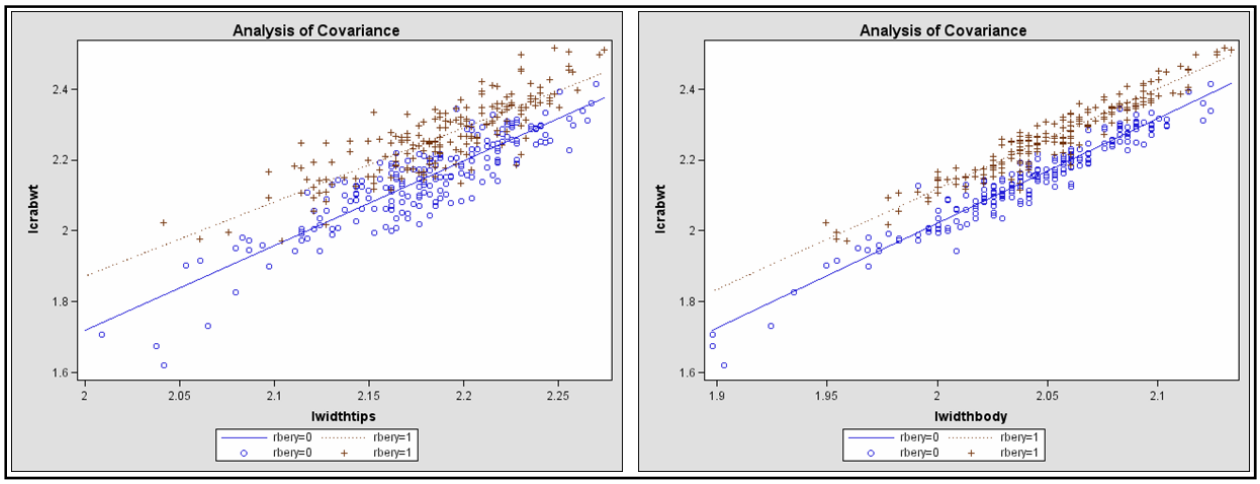


Figure 12.13 Graphical comparison of the ability of two measurements of carapace width to predict the weights (lcrabwt) of ovigerous (rbery = 1) and nonovigerous (rbery = 0) female blue crabs. In the top graph, width (lwidthtips) is measured as the distance between the tips of the lateral spines on the carapace. In the bottom graph, width (lwidthbody) is measured as the distance across the carapace between the bases of the lateral spines. Solutions to the regressions fitted to the data are included in Table 2. Note the much broader scatter of the data in the top graph, reflecting the much poorer ability of this measurement of size to predict weight.

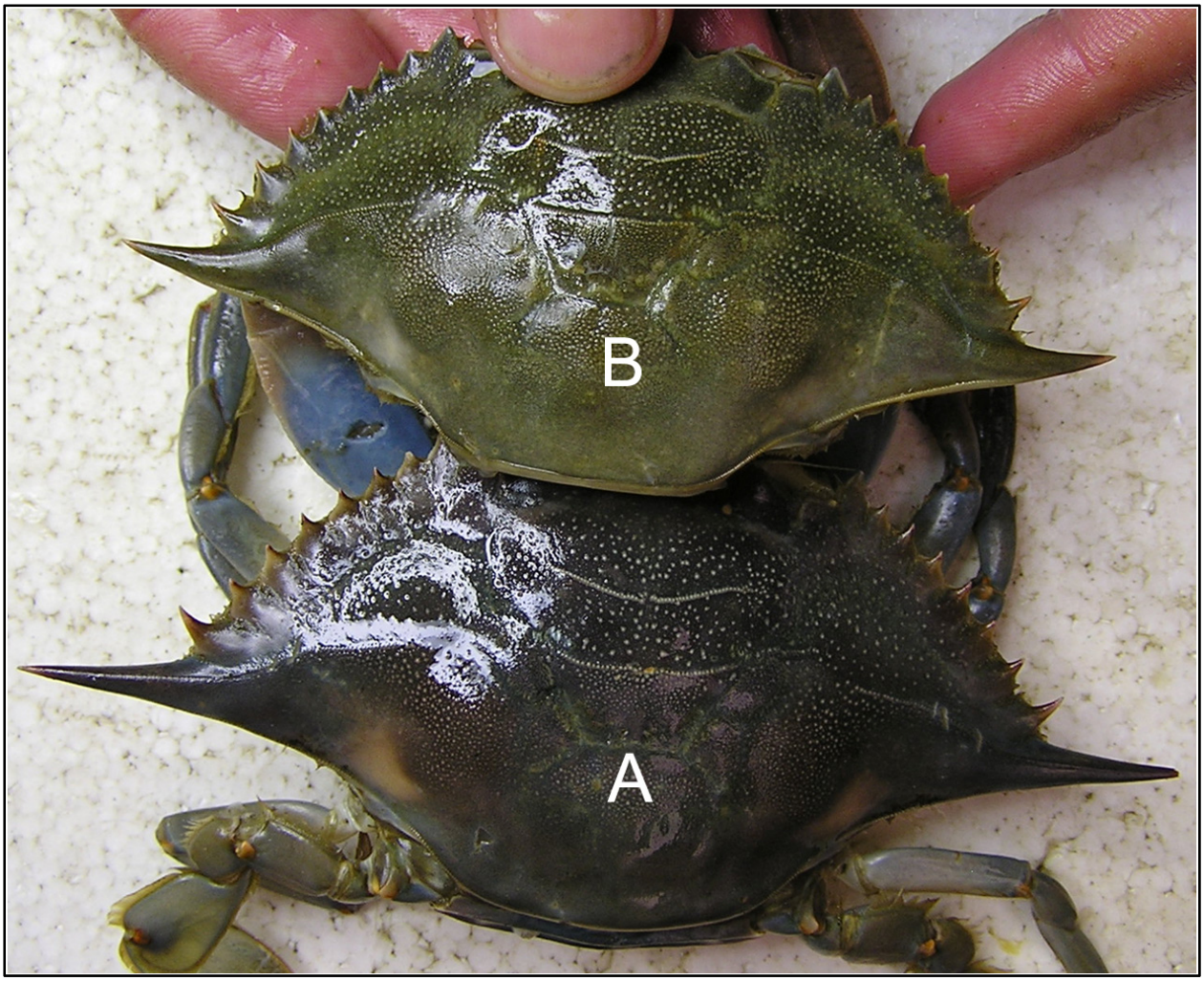


Figure 12.14 Dorsal view of the carapace of two similar size mature female blue crabs (A and B) from the Ship/Trinity/Tiger Shoal Complex displaying striking morphological differences of the lateral spines. The long-spined "acutidens" carapace form of Olmi and Bishop (1983) is represented by crab A, while their short-spined "typica" carapace form is represented by crab B.

Our results strongly suggest that TT should not be used as the primary measure of linear size in studies which wish to examine condition factors of blue crabs from differing environments/populations and that blue crab researchers begin replacing TT as the preferred index of blue crab size with some combination of L, BB, and H or a mathematical representation of V. As a result, we reject hypothesis 4.

### 12.3.5. Test of hypothesis 5 (factors affecting condition factor/fecundity during study)

As an overall test of hypothesis 5 we reran the stepwise regression procedure used to generated Equation12-7, but also included SC, O, BC, BW, D, G, SN, and GN to examine the possible impacts on condition factor and fecundity of fouling, parasitism, ovarian condition, and embryo development stage. The stepwise procedure resulted in a eight parameter model in which TT was included as the final parameter with a partial increase in $R^2$ of 0.0003. Since we saw no compelling theoretical reason to suggest that V should be described by four linear estimates of size, we chose the seven parameter model for discussion:

$$\begin{aligned} \log W = {} & -3.1557 + 0.7472*\log BB + 0.0974*P + \\ & 1.6066*\log L + 0.5904*\log H + \\ & 0.0107*O + 0.0094*GN - 0.0016(M) \end{aligned} \qquad (12\text{-}9)$$

($R^2 = 0.972$). With an $R^2 = 0.972$, Equation 12-9 provides slightly more explanation of the data than Equation 12-7, ($R^2 = 0.968$), though the complexity of Equation 12-9 makes it difficult to assign meaning to those parameters which have little predictability. As with Equation 12-7, L and P account for most of the variation in the data, $R^2 = 0.960$. Ovarian fullness, O, is entered as the forth parameter generating Equation 12-9, and increases the $R^2$ by 0.0039. G precedes M in parameter selection, though the contribution of each is minimal (0.0012 and 0.0003 respective increases in $R^2$).

By excluding SC, BC, BW, D, G, and SN from the final model, the selection procedure suggests that these parameters were not as predictive of weight as those selected. There are a number of possible reasons for these exclusions. On one hand, SC is associated with P and O. Therefore, the main impact of SC could be explained by the presence of P and O in Equation 12-9. And in a somewhat similar fashion, A (a minor factor in Equation 12-7) is not included in Equation 12-9, suggesting that its effect is explained by one or more of the physiological variables which were included. On the other, BC, BW, D, and G are not included in Equation 12-9, suggesting that the level of acorn barnacle fouling and gooseneck barnacle infestation we observed did not affect the condition factor our STTSC crabs.

By including O, GN, and M in Equation 12-9, the selection procedure suggests that these parameters have a predictive effect on weight. We used ANCOVAs to investigate each of these possibilities below.

Since ovarian fullness varied with ovigery (Equation 12-6, Figure 12.12), we used the weight of the carapace (C) instead of the W in an ANCOVA run with O as a class variable in a regression of logL on logC. The results:

$$\begin{aligned} \log C = {} & a + 3.0511 * \log L, \\ & \text{where } a = -3.3054 \text{ when } O = 1, \\ & \quad = -3.3060 \text{ when } O = 2, \text{ and} \\ & \quad = -3.2913 \text{ when } O = 3 \end{aligned} \qquad (12\text{-}10)$$

($R^2 = 0.93$), suggests that an average "full" ovary increased the carapace weight by about 3.3% over a "light" ovary, Figure 12.15.

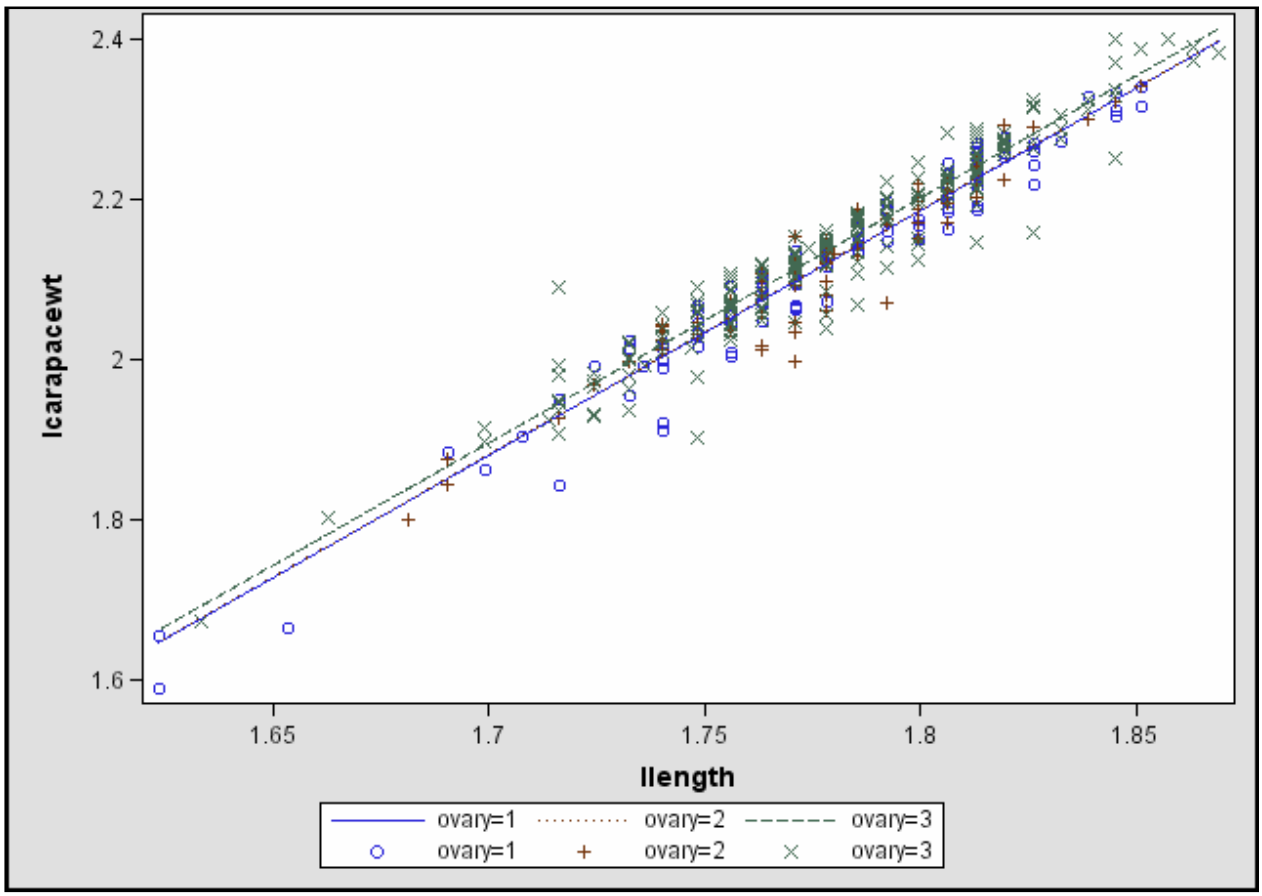


Figure 12.15 Results of an ANCOVA testing the effect of ovarian fullness (O, ovary) on the logarithmic relationship between carapace weight (logC, lcarapacewt) and length (logL, llength) for Ship/Trinity/Tiger Shoal Complex female blue crabs. The results predict that carapace weight will increase as O increases from 1 (light) to 3 (full). Lines fit to the data are the solution to: LogC = a + 3.0511 * logL, where a = -3.3054 when O = 1, a = -3.3060 when O = 2, and a = -3.2913 when O = 3 ($R^2$ = 0.93).

A similar ANCOVA run with GN as a class variable in a regression of logW on logL found a significant impact of nemerteans in the gills on the length-weight relationship of the form,

$$\log W = a + 3.2069 * \log L$$

$$\text{where } a = -3.4903 \text{ when GN} = 0$$

$$= -3.5065 \text{ when GN} = 1 \qquad (12\text{-}11)$$

($R^2$ = .86). Equation 12-11 predicts that the presence of nemerteans in the gills will decrease the body weight by about 3.7%, Figure 12.16.

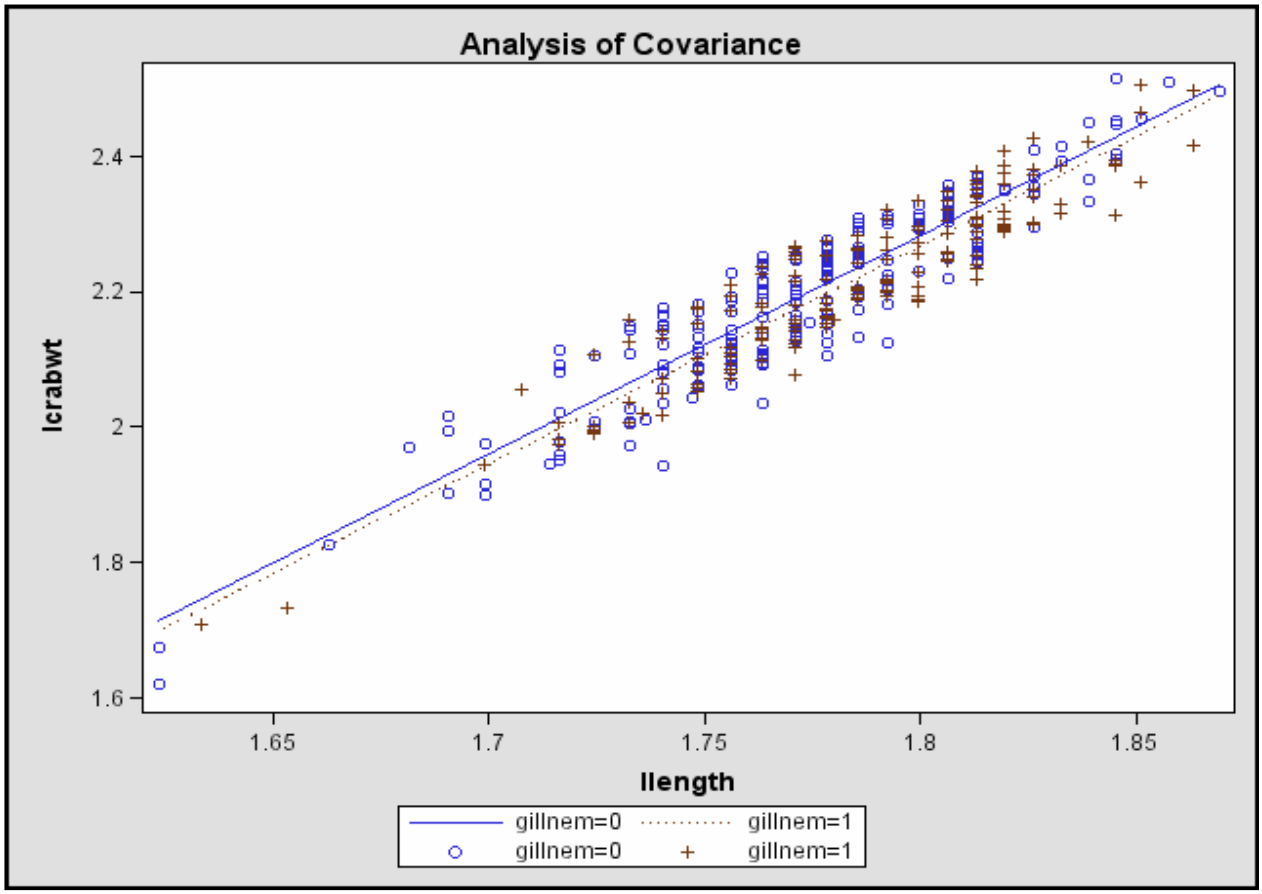


Figure 12.16 Results of an ANCOVA testing the effect of the presence/absence of the nemertean Carcinonemertes carcinophila (GN, gillnem) on the logarithmic relationship between crab weight (logW, lcrabwt) and length (logL, llength) for Ship/Trinity/Tiger Shoal Complex female blue crabs. The results predict that the presence of C. carcinophila in the gills will decrease body weight. Lines fit to the data are the solution to: log W = a + 3.2069 * logL where a = -3.4903 when GN = 0 and a = -3.5065 when GN = 1 (R2 = .86).

To examine our data for a possible minor effect of month on weight, we hypothesized that the monthly decline in prey abundance we are observing in the infauna samples we have collected under Stone et al. (Stone *et al.* 2004b; Stone *et al.* 2006; Dubois *et al.* In Review) would have a negative impact on the weight of the sponge due to ingestion-limited growth. To test this possibility, we regressed logT on logL with month as a class variable. Here our data limited us to a consideration of ovigerous crabs with well developed embryos (SC > 3, brown and black sponges). The ANCOVA revealed a significant main effect of month. The predicted regression,

logT = a + 2.1014 * logL,
where a= -2.0596 for April,
= -2.0949 for May,
= -2.1284 for August, and

= -2.1388 for October (12-12)

($R^2 = 0.60$), suggests that the observed weight of black/brown sponges for a given length interval of STTSC crab will decline at a fairly constant monthly rate (Figure 12.17). As a result of this decline, the sponge of a given length interval of crab will be approximately 20% lighter in October than expected in April. The result is consistent with the hypothesis that a seasonal decline in crab prey abundance limited crab egg production and suggests that the effect of month on crab weight may be due to ingestion-limited growth.

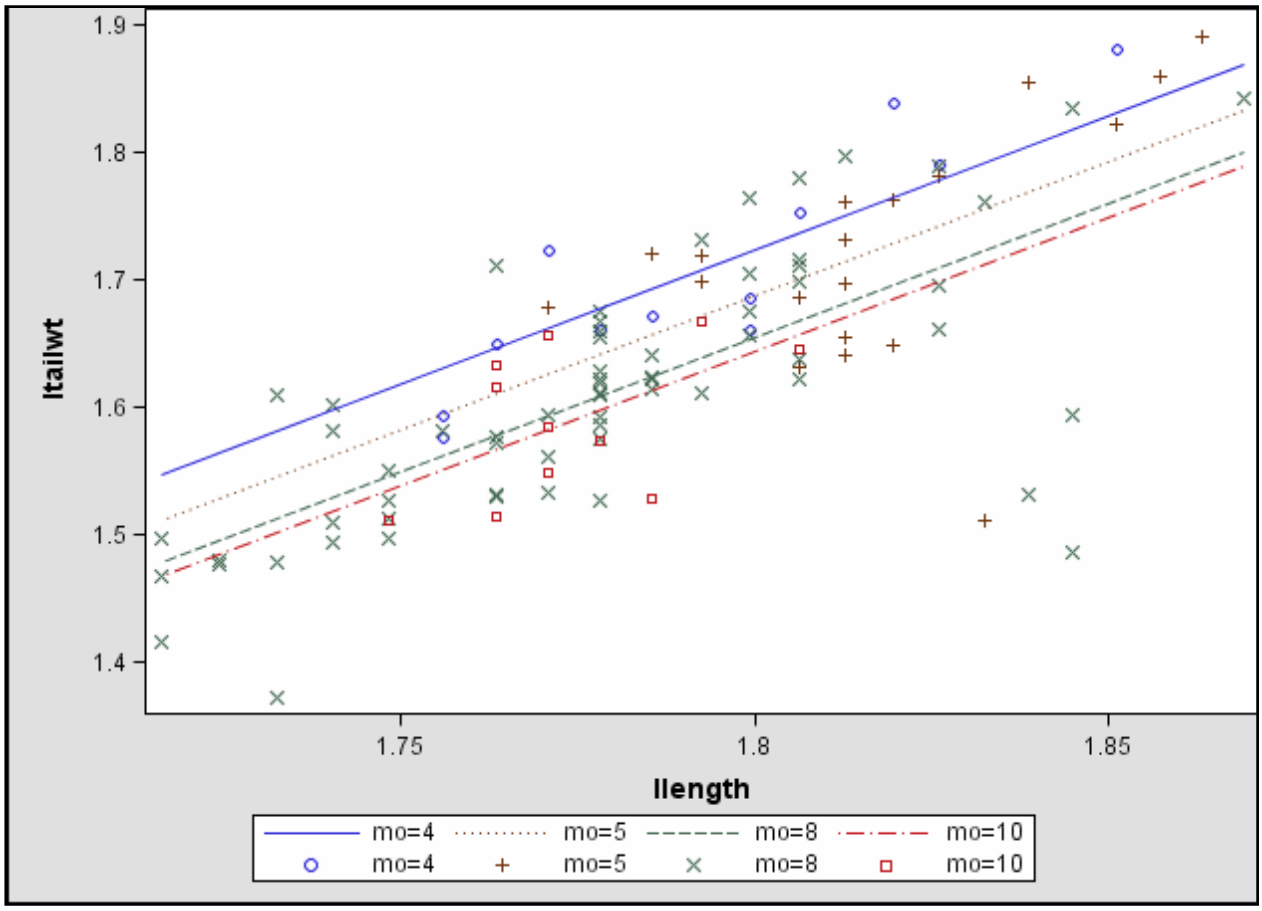


Figure 12.17 Results of an ANCOVA testing the effect of the month (M) on the logarithmic relationship between tail weight (log T, ltailwt) of ovigerous crabs with well developed embryos and length (logL, llength) for Ship/Trinity/Tiger Shoal Complex blue crabs. Lines fit to the data are the solution to: logT = a + 2.1014 * logL, where a = -2.0596 for April, a=-2.0949 for May 5, a = -2.1284 for August, and a = -2.1388 for October ($R^2 = 0.60$).

While the results of our ANCOVAs suggested that the effects of O, GN, and M we noted in Eq. 9 could be real, we remained interested in the effect of SC on weight for two reasons. First, we expected that dry weight of the embryos would decline with development stage due to metabolism of the yolk. Second (and conversely), we expected wet weight of the embryos

would increase with hydration as the embryos approached hatching (e.g, Davis 1965). To test for an effect of development stage on the weight of our embryos, we ran an ANCOVA in which we regressed logT for ovigerous crabs on logL with sponge color, SC, as a class variable. We obtained:

$$\begin{aligned} \log T = {} & a + 2.2808 * \log L, \\ & \text{where: } a = -2.4842 \text{ when SC} = 1, \\ & \qquad = -2.4759 \text{ when SC} = 2, \\ & \qquad = -2.4510 \text{ when SC} = 3, \\ & \qquad = -2.4310 \text{ when SC} = 4, \text{ and} \\ & \qquad = -2.4391 \text{ when SC} = 5, \end{aligned} \qquad (12\text{-}13)$$

($R^2$=0.59) which suggests a fairly sudden increase in the wet weight of the tail as SC increases above 2 (Figure 12.18). Equation 12-13 suggests an approximate 10% increase in wet weight of the eggs as they mature, probably reflecting hydration.

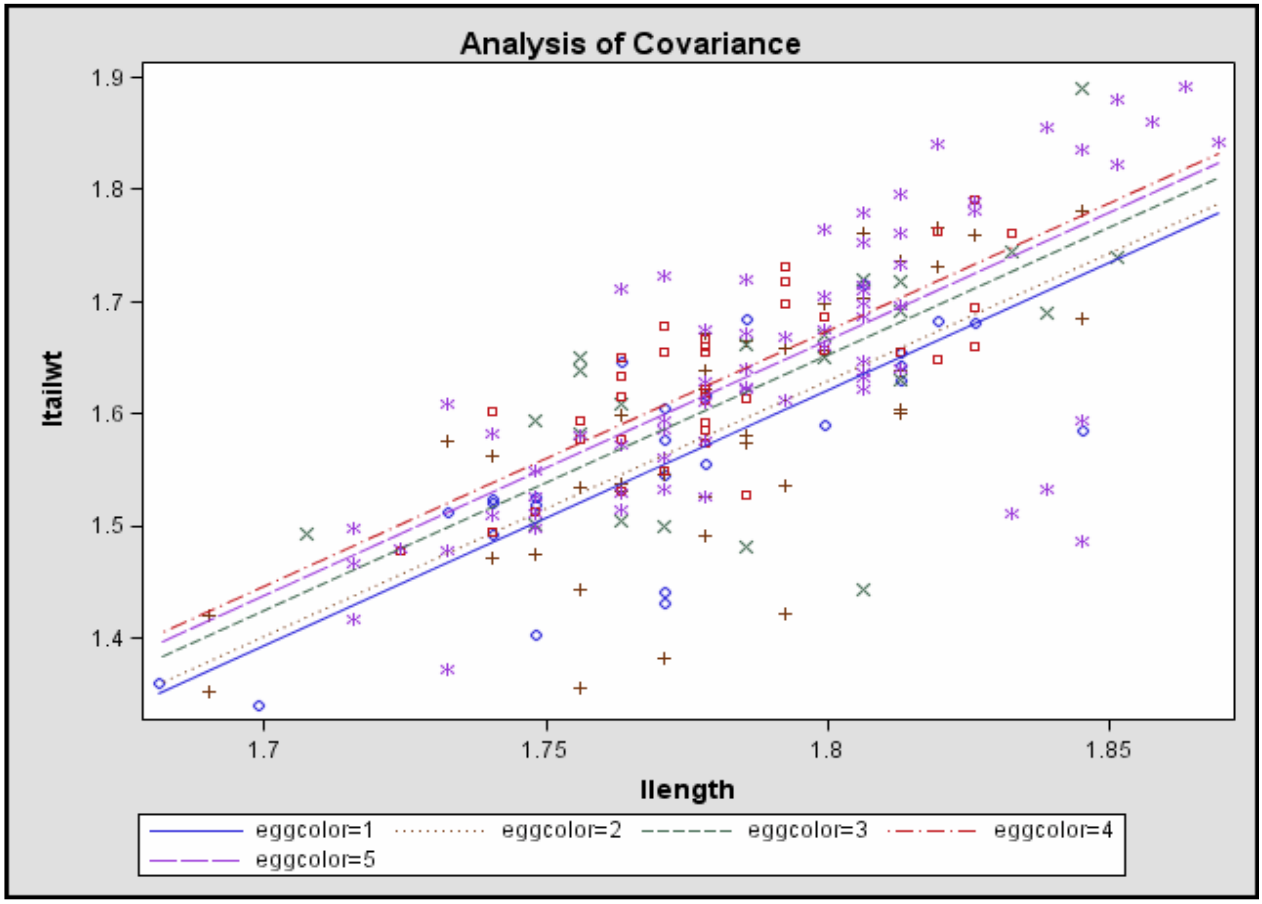


Figure 12.18 Results of an ANCOVA testing the effect of the embryo development stage represented by sponge color (SC, eggcolor) on the logarithmic relationship between tail weight (log T, ltailwt) of ovigerous crabs and length (logL, llength) for Ship/Trinity/Tiger Shoal Complex blue crabs. Lines fit to the data are the solution to: logT = a + 2.2808 * logL, where: a = -2.4842 when SC = 1, a = -2.4759 when SC = 2, a = -2.4510 when SC = 3, a = -2.4310 when SC = 4, and a = -2.4391 when SC = 5 (R2=.59).

Based on these analyses we reject hypothesis 5. We accept the likelihood that O, GN, and prey availability have a meaningful effect on crab weight in our study and conclude that our overall approach provides a meaningful technique to monitor the impact of sand mining on the condition factor and reproductive vigor of STTSC crabs.

### 12.3.6. Test of hypothesis 6 (temporal/spatial abundance patterns during study)

We ran an ANOVA on our 2007 STTSC data comparing mean catch rates as a function of month (April, August, and October) and area (Ship Shoal, Trinity Shoal, Tiger Shoal, Offshore area,

and inshore area (Figure 12.1). The results, Figure 12.19, suggests that mature female crab abundance 1) peaks on Ship and Trinity Shoals in August, 2) is substantial on Ship and Trinity Shoals from at least April through October and on the STTSC Inshore area in April through August, and 3) occurs throughout the remainder of the STTSC study area at a reduced level in April through October. Mean area catch rates across all months and mean monthly catch rates across all areas were significantly different from zero. Across all months, both Ship Shoal and Trinity Shoal had significantly greater mean monthly-area catch rates than the offshore area and Tiger Shoal. Mean monthly catch rates across all areas in August were significantly higher than April and October. Mean August catch rates for Ship and Trinity Shoals were significantly greater than those from the offshore area and Tiger Shoal for all months and from the Inshore area in October.

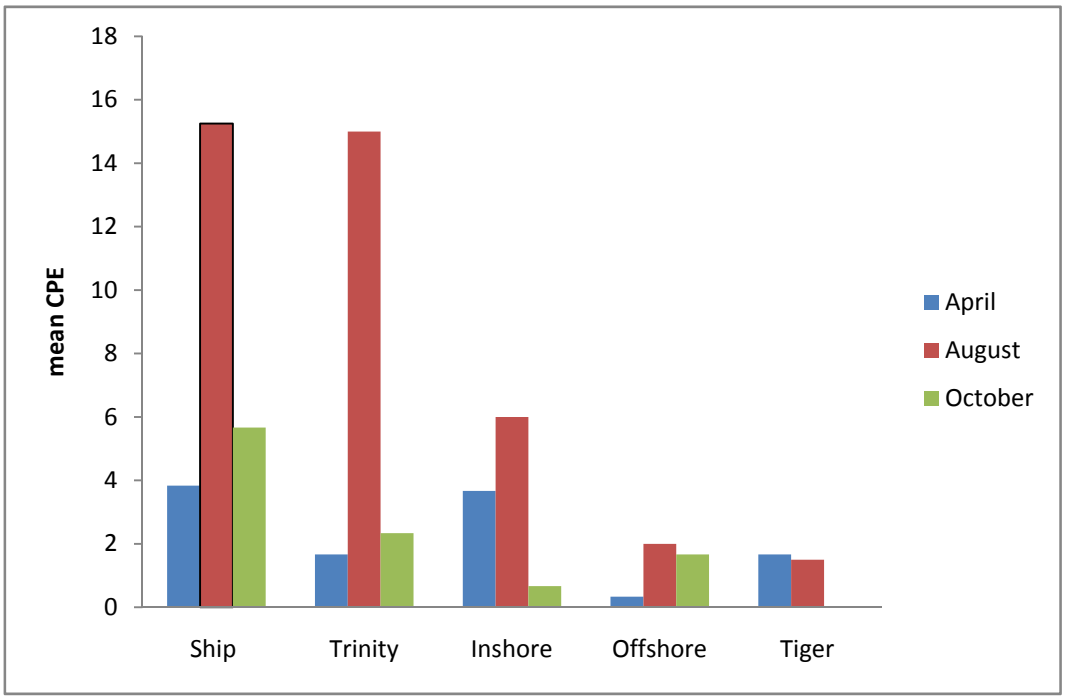


Figure 12.19 Comparison of mean catch rates of mature female blue crabs by area and month for the Ship/Trinity/Tiger/Shoal Complex in 2007. The August means for Ship and Trinity Shoals are significantly different ($\alpha$=0.1) from those of the Offshore area and Tiger Shoal for all months as well as for the Inshore area in October.

Given the results of our ANOVA (Figure 12.19), we reject hypothesis 6 and suggest that the abundance of spawning/hatching/foraging female blue crabs in the STTSC will peak on Ship and Trinity Shoals in August.

### 12.3.7. Test of hypothesis 7 (spawning grounds, national comparison)

Fishery independent catch rates of mature female blue crabs in areas recognized as blue crab spawning grounds are reported by More (1969) for Galveston Bay, TX; Adkins (1972) for Terrebonne Bay, LA; Archambault *et al.* (1990) for Charleston Harbor, SC; Lipcius and Stockhausen (2002) for Chesapeake Bay, VI/MD; and Eggleston *et al.* (In Review) for Pamlico Sound, NC. Size and duration of the trawl effort vary across these studies, as do number of areas sampled, duration and timing of study, and temporal aggregation of the published data. Most of the published studies represent at least two years of sampling and report their data in monthly averages by area. Lipcius divides his catches into two periods: one of high abundance, and one of low. None statistically compare their catch rates with other, geographically-different studies.

We calculated the average peak catch rates of mature female blue crabs by area/month/gear on a catch per month basis for each of the above studies and for our study, adjusting all average catch rates to 30 minutes of trawl time. We regressed the adjusted average peak catch rates (PC) against the width of the trawl (TW). The result:

$$PC = 44.5221 - 2.9142 * TW \qquad (12\text{-}14)$$

($R2 = .47$; Figure 12.20) suggests that peak catch rates of mature female blue crabs on these known or suspected spawning grounds are fairly consistent with a simple, single linear relationship which predicts that catch rates will decline with an increase in the size of the trawl used to sample the population. This decline, if real, may be more a function of vessel size than trawl efficiency, since most studies of blue crab spawning grounds have been conducted in 'shallow' waters. Given these results, we cannot reject hypothesis 7, and conclude that the available abundance data support the concept that STTSC is an important blue crab spawning ground.

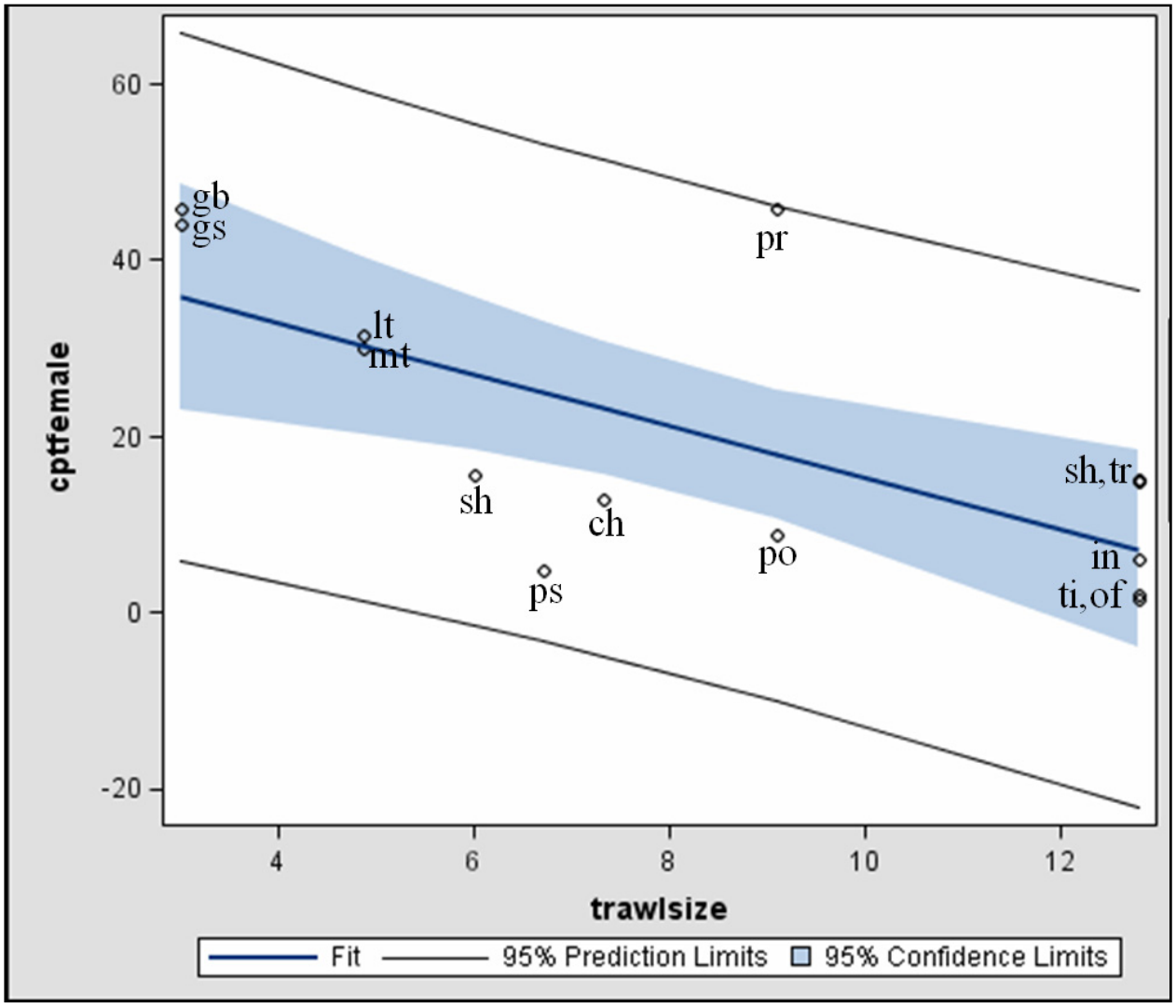


Figure 12.20 Results of a regression comparing average peak catch rates of mature female blue crabs by area/month/gear (PC, number/30 min) with width of trawl (TW, trawlsize, m) from recognized blue crab spawning grounds and our study areas. Points plotted are from More (1969, Galveston Bay=gb and Gulf surf=gs), Adkins (1972, mt=middle Terrebonne Bay and lt=lower Terrebonne Bay, LA), Archambault *et al.* (1990, ch=Charleston Harbor, SC), Lipcius and Stockhausen (2002, pr=pre-phase shift and po=post-phase shift Chesapeake Bay, VI/MD), Eggleston *et al.* (In Review, ps=Pamlico Sound, NC), and this study (sh=Ship Shoal, tr=Trinity Shoal, ti=Tiger Shoal, in=Inshore, and of=Offshore). The regression fit to the data is PC = 44.5221 -2.9142*TW ($R^2$ = 0.47).

## 12.4. SUMMARY OF FINDINGS AND FISHERY-RELATED RECOMMENDATIONS

The STTSC is a nationally important, though unprotected, offshore blue-crab spawning/hatching/foraging ground from at least April through October, and an offshore blue crab mating site. During April-October, mature female crabs appear to be in a continuous spawning cycle, producing new broods approximately every 21 days while actively foraging to supply the necessary energy for this continuous reproductive activity. Egg production apparently declines slightly as the season progresses, perhaps reflecting some ingestion-limited growth of the ovary as infaunal prey densities decline. Condition factor appears to be positively associated with increases in ovarian condition and the presence of nemerteans (*C. carcinophila*) on the gills and negatively affected by a seasonal decline in prey abundance, but does not appear to be negatively impacted by acorn barnacles (*C. patula* and Balanus spp.) on the exoskeleton, gooseneck barnacles (*O muelleri*) on the gills, or nemerteans (*C. carcinophila*) in the sponge (all conditions normally associated with higher salinity waters). Within the STTSC, Ship and Trinity Shoals appear to be the most important spawning/hatching/foraging grounds, especially in August.

During our sampling, we did not notice any apparent relationship between blue crab condition factor and any of the physical/chemical parameters we measured. In our 2005 and 2006 sampling on Ship Shoal, we did begin to see the possibility of a positive relationship between blue crab abundances and oxygen. We are currently exploring the relationship between blue crab abundance and oxygen concentration under separate MMS funding of our current STTSC project. However, when viewed in light of our national comparisons of blue crab condition factor, fecundity, and abundance, we believe that the overall environmental conditions we encountered on Ship Shoal in 2005 and 2006 and on the STTSC in 2007 are favorable for a continuous and highly successful blue crab spawning/hatching cycle during at least April through October, provided environmental conditions and fishing pressure do not change.

A comparison of our results with the available literature suggests that the techniques employed here could enhance our understanding of other blue crab populations.

Finally, there does not appear to be a directed fishery currently operating on the female blue crabs in the STTSC and the current social norm in Louisiana, the Gulf, and Nation seems to favor a protection of spawning crabs. This lack of a directed fishery on the reproductively active STTSC crabs likely enhances the stability of Louisiana's traditional inshore blue crab fishery. A conservative management strategy would assure the stability of the current inshore blue crab fishery by protecting STTSC blue crabs from a directed harvest until their contribution to the health of the current inshore fishery can be assessed. National efforts to restore the Chesapeake Bay and North Carolina populations have found no inexpensive "quick fixes". For example, Chesapeake Bay stock enhancement scientists "expect the production cost of blue crab juveniles will be ... in the range of U.S.$0.15—30/juvenile" and that there will be a "10% survival of cultured females until spawning in the sanctuary" (Zohar *et al.* 2008, p31). Under this scenario, the hatchery costs associated with the arrival of mature ("hatchery") female blue crabs on the spawning grounds would be $18 to $36/dozen, or approximately the current retail price of blue crabs in the Louisiana market.

# CHAPTER 13
# SYNTHESIS, CONCLUSIONS AND RECOMMENDATIONS FOR FUTURE SAND DREDGING ON SHIP SHOAL OFF THE LOUISIANA COAST

In order to examine morpho-hydrodynamics (i.e. waves, currents, bottom boundary layer physics and sediment transport) and biological characteristics (i.e., indicators of benthic primary productivity and meiofaunal, macrofaunal and nekton communities) associated with Ship Shoal, a transgressive sand shoal off the Louisiana coast, extensive field surveys (geo-physical and oceanographic) and numerical modeling were conducted. Our detailed efforts allowed for the following synthesis of the conclusions from each task. Recommendations are also included for the proposed sand dredging from the shoal which may mitigate the environmental damages associated with large scale dredging (millions of cubic yards/meters).

## 13.1. SAND PROSPECTING

Sand resources along the southern Louisiana coast are relatively scarce given the large volumes of sand required for restoration of the rapidly degrading barrier and coastal systems. During this investigation, twenty vibracores were obtained from Ship Shoal, a well-known sand source offshore of the Isles Dernieres. The study area along the eastern end of Ship Shoal, commonly known as South Pelto, mainly contained very clean sand (less than 5% silt in the upper shoal units) that ranged in thickness from 4 to 6 m (13 – 19.7 ft) and generally ranged in grain size from 0.15 to 0.2 mm (2.32 - 2.73$\phi$). Approximately 21.6 x $10^6$ $m^3$ of clean sand has been estimated to occur in three borrow areas. Buffers around oil and gas infra-structure and other magnetic anomalies occurring in and around the study area were avoided during borrow area design to ensure quality of the borrow sediments and to enhance the safety of dredging operations. Sand deposits identified along South Pelto in this study have significant potential to support large-scale coastal restoration along coastal regions within the vicinity of Ship Shoal. Sand from this borrow area is proposed to be used for restoration of the Caminada-Moreau headland restoration project which is approximately 48 km in the alongshore direction. This source is one of the very few viable sources given its geographical juxtaposition to the spoil site and volume of material necessitated.

## 13.2. HYDRODYNAMIC MODELING AND *IN SITU* MEASUREMENTS

### 13.2.1. Preliminary modeling of fluvial sediment dispersal and its influence on Ship Shoal

Given the complexities of deltaic environments, both along the coast and on the inner shelf, a detailed evaluation of bottom boundary layer (BBL) physics and sediment transport was undertaken with a state-of-the art model, MIKE 21 and MIKE 3, within the context of potential future dredging on Ship Shoal. The following synthesis of the data and interpretations can be noted:

(1) Strong wind speed and directionality of tropical and extra-tropical storms ostensibly influenced the fluvial sediment dispersal and transport on the inner shelf off the Louisiana coast and hence, its shallow shoals, viz., Ship Shoal. The excess debouchments of sediment from the Atchafalaya River occasionally coincided with post-frontal events so that material being transported and deposited onto the inner shelf and also onto the shoals, farther south, generally occurred during the waning phase of the storm.
(2) A prevailing westward dispersal pattern during the winter-spring season shifted to the southeast following strong post-frontal northwesterly winds, which in turn generated southeastward currents and further transport fluvially-derived fine sediments from both the Atchafalaya River and Atchafalaya Bay to the southeast. According to the model and analysis of satellite imagery, these eventually settled, at least ephemerally, on Ship Shoal, located approximately 50 km southeast from the river mouth. Data indicated sediment transport events occurred in pulses and in tandem with high fluvial sediment discharge during spring floods and/or when local sediment re-suspension peaked. While, during tropical cyclones, fluvially-derived sediment transport occurred based on strong local sediment re-suspension and mixing, and was possibly in part based on high SSC from both the lower Atchafalaya River and the Wax Lake Outlet, being redistributed onto the Atchafalaya Shelf and the adjacent shoals, viz., Tiger and Trinity shoals.
(3) Our preliminary modeling efforts to link the Atchafalaya River sediment plume structure to storm winds and its consequent effects on Ship Shoal corroborated the results of *in-situ* measurements by demonstrating a strong response of the dispersal to various wind conditions, illustrating conspicuous shifts in sediment dispersal patterns during post-frontal wind conditions. For the model case with northwest winds, illustrated in C*hapter 3*, sediment plumes transported southeastward did not reach Ship Shoal after 20 days of the model duration under all storm wind conditions; while, the case with combined no wind and northwest wind provided that sediment plumes transported further southeastward and reached Ship Shoal within 3 days of post-frontal winds.
(4) Results from numerical model studies, detailed in *Chapter 7* suggest that sediment supply from offshore to Ship Shoal may not be significant except during strong storms, (Hurricanes), given the fact that sediment re-suspension off the shoal is much lower than that on the shoal (on average 70-80 percent less);
(5) Frequencies of the dispersal shifts (approximately once every 8 days) and the sediment plume that reached Ship Shoal (approximately once every 19 days) had no correlation *with mo*nthly mean river discharge; however the latter was strongly correlated with monthly mean wind stress, suggesting the importance of storm winds vis-à-vis the dispersal shifts rather than river discharge, although increased river discharge likely cont*ributes* high fluvial sediment supply into the Atchafalaya Bay and farther offshore to the inner shelf;

### 13.2.2. Wave-current-fluid mud-sand interaction

The upper 2.5 cm of the surface of Ship Shoal is characterized by a heterogeneous suite of sediments including fine-grained sands, coarser-grained sediments (i.e., shell hash) and fluid mud. These findings have important hydrodynamic and biological implications and were therefore investigated throughout the remainder of this report. The following hydrodynamic conclusions are based on the data and interpretations derived from this study:

(1) The numerical model outputs and OBS observations denote an occasional sediment plume shift from the Atchafalaya River/Bay to the southeast results in accumulation of a thin fluid mud layer on a portion or portions of the shoal. Ponar grab samples collected on Ship Shoal in the spring of 2007 suggest that the maximal thickness of such a fluid mud layer would be approximately 2 - 4cm and that it would be spatially patchy in nature. On the other hand, during the 2006 deployment, a thickness of 15 cm and 30 cm for unconsolidated and partially consolidated fluid mud respectively, in the waning phase of storms, were measured from a location along the eastern flank of the shoal.

(2) The accumulated fluid mud layer strongly interacted with bottom sediment through the process of sediment re-suspension, vertical mixing, hindered settling, and re-distribution, resulting in a maximum of 20 cm of erosion followed by 30 cm of accumulation at the deployment site. Ship Shoal, although comprised primarily of sediment in the sand range, may undergo short-lived but substantial changes in sediment type in the bottom boundary layer with surficial sediments being comprised of predominantly fine silts and clays during portions of the spring flood season. The temporal and spatial extent of these changes should be explored, as biological measurements strongly suggest that the nature of these events do not 'unduly' disrupt the stability of the biological system.

(3) Data collected during the 2008 deployment showed that the bottom sediments were comprised primarily in the sandy range and hence the bottom boundary layer dynamics followed conventional approaches.

(4) Wave ripples (based on underwater camera imagery taken from Ship Shoal during the spring 2007 biological cruise), were formed when the shoal crest was exposed to sand, and the ripples were likely washed out during severe storms when wave orbital velocities exceeded approximately 0.6 m $s^{-1}$. The washed-out ripples were likely re-established in the wake of the storms.

(5) The rate of transport for cohesive sediment was more than an order of magnitude higher than those numerically derived non-cohesive sediment transport as calculated for fine sand sampled during the retrieval cruise in 2006, suggesting the importance of fluid mud transport.

(6) The accumulation of fluid mud may be ephemeral and non-uniform on the shoal given the frequencies of the dispersal shifts (once every 19 days) and more frequent sediment re-suspension events associated with winter storms (once every 6.0 days).

### 13.2.3. Numerical modeling

Numerical modeling was undertaken to establish pre- and post-patterns of the hydrodynamics in accord to various dredging scenarios. State-of-the-art numerical models were utilized and compared to *in-situ* observation for skill-assessment purposes. Syntheses of the model results are presented below:

(1) Results obtained from numerical modeling of waves, currents and sediment transport, were in general agreement with *in-situ* observational data and satellite images except during peak storm conditions. Simulated currents also agreed with *in-situ* currents; however, bottom cross-shore currents were poorly correlated with *in-situ* bottom currents and are probably due to the inaccuracy of shoal bathymetry despite depth corrections.
(2) From the seaward to the landward flank of the shoal, significant wave height attenuation of 22% was computed for southerly waves and 28% for northerly waves. The dissipation of wave energy over the shoal resulted in re-suspension and transport of shoal sediment during storm events. This level of wave energy attenuation also points to the effectiveness of the shoal in shielding the already vulnerable coast against frequent cold fronts and occasional hurricanes; The evolution of the energy spectra, when the cold front crosses the study area, was abrupt and the dominant direction shifted from southwest to north across the shoal. This shift is attributed to wave refraction due to the shoal as well as the veering of the wind direction.
(3) In spite of the influences of freshwater and fluvial sediments from the Atchafalaya River, a barotropic hydrodynamic model performed reasonably well on examining currents over the shoal and the surrounding inner shelf.
(4) Waves and wave-induced sediment re-suspension significantly changed between the two extreme scenarios, viz., with and without the shoal. While, for the case of partial removal of the shoal, more realistic in terms of the scope of the proposed mining projects, the variability in the waves and wave-induced sediment re-suspension were computed as insignificant.
(5) Although there are differences in magnitudes for the model results with and without the shoal, large-scale targeted sand mining did not result in abrupt changes in current patterns.
(6) Sediment re-suspension intensity (RI) was high across the inner shelf and the shoal during severe and strong storms; in general, it was spatially different and dependent upon physical forcing (i.e. wind and deep water waves). The RI decreased from the shallowest western portion of the shoal to the deepest eastern flank of the shoal; the RI off the shoal was significantly lower than that on the shoal. The results suggest that the deeper eastern flank of the shoal is in favor of fluid mud accumulation. This suggestion was supported by *in-situ* measurements.

The data presented here demonstrated that Ship Shoal, recently recognized as having a unique physical and biological environment, is exposed to recurring sandy and muddy bottoms and provided conspicuously different bottom boundary layer dynamics (BBLD) for the 2006 deployment on the eastern shoal and the 2008 deployment on the middle shoal. This uniqueness

was caused by fluvial sediment supply from the Atchafalaya River and sediment re-suspension and settling associated with winter storms on the shoal. The distribution of fluid mud, based on the repeated sediment sampling and *in-situ* measurements, may be considered as patchy and ephemeral. The patchiness of the fluid mud distribution is extremely difficult to resolve within the scope of this study, given the unavailability of seasonal sediment data from the entire shoal environment. The data also suggest that as storm intensity varies, strongest in January and decreases toward Spring, the eastern portion of the shoal tends to be more susceptible to the accumulation of fluid mud than the middle and western portions of the shoal; moreover, sediment re-suspension and re-distribution tend to outweigh sediment supply during Spring and results in the formation of a sandy surface layer on the shoal by the end of the winter storm season, in May.

### 13.2.4. Sand mining recommendations resulting from the physical studies

The results of the numerical modeling studies reviewed above suggest that large-scale sand dredging would have spatially profound impacts on waves and sediment suspension on the shoal, however, no abrupt changes to current patterns. The changes in wave transformation and sediment suspension suggest that large-scale sand dredging may enhance fluid mud accumulation on the shoal.

The above findings have further important implications for benthic biological communities on the shoal which was recently found to be a biological "hotspot" and an oxygen refuge compared to the surrounding inner shelf. Shoal macrofauna are abundant, have a high biomass and require access to the sediment surface for feeding. Long and persistent burial by muddy sediments will likely reduce abundance and biomass and would be expected to limit species diversity. There is an information gap regarding the possibility of a seasonal change in the bed characteristics of Ship Shoal and our collaborative biological study results although the shoal bottom sediments likely influence the shoal benthic communities. For example, meiofauna communities do not seem to be as diverse as macrofauna. Interstitial meiofauna may be impacted by fine grained sediments that enter the interstitial pore spaces between sands during burial with fluvially derived sediment, limiting populations in ways that may not influence macrofauna. However, physical and biological studies both agreed that large-scale sand mining would have profound impacts on both shoal physical and biological environments and thus, is not recommended. Targeted small-scale mining should have minimal impacts and the impacts are expected to be mitigated through natural processes within several years after the termination of sand extraction.

## 13.3. ECOLOGICAL MEASUREMENTS

Based on Louisiana's and MMS's concerns regarding dredging of Ship Shoal borrow sites especially in relationship to Louisiana's nationally important shrimp fishery, the following questions were addressed: 1. What is the abundance, taxonomic composition and community structure of Ship Shoal's meiofaunal community? 2. What are the abundance, taxonomic

composition and community structure of Ship Shoal's macrofaunal community? 3. How are Ship Shoal's meio/macrofaunal communities affected by physical parameters (e.g. substrate composition, water depth, currents, position on the shoal), and water chemistry (e.g. temperature, salinity, oxygen concentration, turbidity)? 4. What is the relationship between the dominant members of Ship Shoal's benthic communities and the gut contents/fullness of its white and brown shrimp? 5. What are the potential impacts of sand mining on the taxonomic composition and community structure of Ship Shoal communities? (How rapidly will these communities recover and how will the taxonomic composition of the recolonized areas compare with pre-impact conditions). Our original research plan called for sampling areas before and after sand mining to directly measure mining impacts on biological communities and the rates of meiofaunal, macrofauna and nekton recovery. However, planned sand mining of Ship Shoal was unexpectedly delayed (partly due to Hurricanes Katrina and Rita) and was not initiated during the project period.

As described in more detail below, we found Ship Shoal had several features that make it unique compared to surrounding muddy sediments. For example, we found a high biomass of benthic microalgae on Ship Shoal in contrast to the surrounding muddy sediments where benthic production is considered minor and sediments are dominated by settled phytoplankton (i.e., phytodetritus). Ship Shoal also had an unexpectedly high diversity and biomass of benthic macroinfauna, with many of the species restricted to sand shoals only. Also unexpected was the apparently low abundance of penaeid shrimp and croaker on the shoal. However, large, reproductively active populations of blue crabs were discovered, which is particularly notable because female blue crabs were previously not known to migrate and/or aggregate in high densities far off-shore. Our findings suggest that Ship Shoal is an unexpected but significant feeding and spawning ground for blue crabs that recruit to Louisiana's estuarine population. Overall, the unique physical features of Ship Shoal have enabled a distinctive biological community to develop.

### 13.3.1. Ship Shoal grain size and water chemistry

The sedimentology of bottom sediments in addition to water chemistry where evaluated during this project and the following conclusions derived:

(1) Spatial gradients in depth and grain size were found on Ship Shoal. Depth across the shoal ranged from approximately 5 to 11 m and generally increased from west (5 to 8 m) to east (9 to 11 m).
(2) Sediment on Ship Shoal was well sorted fine- to very-fine sand (mean grain size ranged from 120 to 200 μm) with low silt/clay content (usually < 2%). Mean grain size generally increased from west to east, a pattern attributable to the higher percentage of shell hash (measured as percent gravel) on the eastern end. Sediment organic carbon values were generally less than 0.2% across all stations.
(3) Bottom-water dissolved oxygen (D.O.) concentrations on Ship Shoal were above hypoxic levels (2 mg/l) at all stations and seasons.

### 13.3.2. Benthic Primary Producers

(1) We examined the origin, composition, and spatial and temporal distribution of sediment algae on Ship Shoal, which because of its depth and sediment characteristics, is potentially favorable to benthic primary production (BPP) by benthic microalgae. Light levels at the shoal bottom ranged from < 1 to 30% of surface photosynthetically active radiation (PAR), and were judged sufficient for benthic photosynthesis throughout the year
(2) Average algal biomass values for Ship Shoal displayed high seasonal variability, ranging from < 10 to 50 $mg/m^2$ in 2005 and from 21 to 53 $mg/m^2$ in 2006. Sediment algal biomass was highest in the spring and summer and was not consistently correlated with any of the physical parameters recorded including sediment light levels and water depth. Photosynthetic pigment analysis indicated sedimentary algae were predominately diatoms across all stations and sampling seasons, and microscopic analysis of sediment samples revealed that the diatoms were primarily benthic with only a minor fraction of settled phytoplankton present. Comparison of pigments from the sediment and bottom water suggested weak exchange of benthic and pelagic algae between the two compartments. Algal biomass in the sediment exceeded that of the overlying water column over much of Ship Shoal during the spring and summer.
(3) The high benthic algal biomass (equivalent to values typical of estuaries) strongly suggests that BPP may contribute to the food web on Ship Shoal.

### 13.3.3. Meiofauna

(1) The meiofauna community of Ship Shoal is composed of an interstitial assemblage numerically dominated by nematodes but with the common occurrence of harpacticoid copepods, gastrotrichs and turbellarians. Total meiofauna density ranged from 900-1800 individuals $10cm^{-2}$ across all seasons and was low compared to surrounding sediments. The density of meiofauna did not differ significantly between locations or among seasons on Ship Shoal; however, meiofauna densities in 2005 were lower than in 2006. Collections in 2005 and 2006 showed that meiofaunal abundance was highest in the upper 2 cm of sediment and decreased between 3 and 4 cm.
(2) Environmental factors (e.g., sediment chl a, bottom-water dissolved oxygen, mean grain size and percent silt-clay) did not explain significant amounts of variation in the abundance of total meiofauna or individual major taxa.
(3) Although not highly diverse in terms of major taxa or species diversity, the presence of a unique interstitial fauna on Ship Shoal suggests that shoals may contribute substantially to the overall biodiversity of benthic invertebrates of the north-central Gulf of Mexico.

### 13.3.4. Macrobenthos

(1) For macroinvertebrates, Ship Shoal represents a faunally distinct habitat type in a transition between in-shore and off-shore habitats. Ship Shoal hosts a unique combination of macroinfauna composed of species common 1) among the swash zone of sandy beach communities associated with the Mississippi and northwest Florida seashore, 2) in shallow enclosed bays of the northern Gulf of Mexico, and/or 3) in muddy off-shore environments. A significant number of macroinvertebrates species not reported previously for the Louisiana continental shelf were found on Ship Shoal. Fifty percent of polychaete species we found on Ship Shoal were previously only reported from either the Florida continental shelf only or from both Texas and Florida continental shelves. Our findings, in conjunction with our current understanding of the sediments and current of the northern GOM strongly suggest that Ship Shoal in particular and Louisiana sandy shoals in general could play an important role in the dispersal and gene flow of benthic species over large spatial scales in the continental shelf of the GOM. More locally, Ship Shoal may serve as a source pool for recruitment of benthic invertebrates to surrounding areas affected by seasonal hypoxia.

(2) Among species that make Ship Shoal benthic assemblages unique was the lancelet (= amphioxus) *Branchiostoma floridae*. This is the first report of large abundances of amphioxus (up to 760 ind $m^{-2}$) off the Louisiana coast. Our findings of large, egg carrying individuals in the spring and numerous juveniles in the summer suggests that Ship Shoal is an important sandy habitat for reproduction and recruitment of amphioxus *B. floridae*.

(3) Ship Shoal harbors a high-biomass (averaging 25.9 g $m^{-2}$) and high-diversity (161 species) assemblage of macroinfauna. Ship Shoal appears to maintain a higher number of species than nearby locations on the Louisiana shelf and may be considered a diversity hotspot. Biodiversity increased from north to south on Ship Shoal. This may due to the higher abundance of large tube-building polychaetes on the southern edge as these tubes protrude above the surface, increasing habitat and settlement opportunities. Water depth and mean grain size were the two main environmental parameters that coincided with changes in composition of species assemblages over Ship Shoal.

(4) Based on our macroinfauna sampling/analyses (and our findings of a likely Ship Shoal BMA/macroinfauna/blue crab food web), it appears to us that Ship Shoal is an important hypoxia refuge for macroinfauna sensitive to low DO concentrations reported for the surrounding area (e.g. Rabalais et al., 2001). For example, amphipods--known to be affected by low oxygen-- occurred in very high abundances over the Ship Shoal and were highly ranked among the benthic assemblages throughout the year. Shallow depths, wave action and biogenic activity all probably contributed to Ship Shoals higher DO concentrations. The high density of tubiculous polychaetes we found may enhance oxygen flux in sediment surface layer.

(5) Species abundances exhibited a steady but large rate of decline between spring, summer and autumn, most likely in response to predation by high concentrations of spawning/hatching blue crabs *Callinectes sapidus*.

### 13.3.5. Nekton other than blue crabs

(1) We evaluated the distribution and abundance of croaker and penaeid shrimp on Ship Shoal during spring, summer and fall in order to determine the seasonal use and duration of their residency. We did not find evidence of strong habitat use or residency by shrimp or croaker on Ship Shoal as these species were typically found in low numbers compared to off-shoal SEAMAP stations. Also, although our temporal sampling frequency was low, it appears that different populations were sampled during each season suggesting shrimp are not resident on Ship Shoal for more than a few months, but rather move across or over the shoal. Length data suggested croaker were a mix of adults and juveniles with an extended residency on and around Ship Shoal. However, because these species have significant off-shore overwintering and spawning populations, winter sampling is likely necessary to accurately determine the use of Ship Shoal by shrimp and croaker. Crustaceans were the most frequently found recognizable food item in the stomachs of brown shrimp and white shrimp, although polychaetes were also common, especially in the summer. Amphipods, burrowing shrimp, unidentified crustaceans, and polychaetes comprised most of the recognizable croaker stomach contents. The data suggest nekton feed on Ship Shoal, although temporal changes in the gut contents of shrimp and croaker did not always correspond with seasonal changes in infaunal communities.

### 13.3.6. Blue crab

(1) We find that Ship Shoal is a nationally important, though unprotected, offshore blue-crab spawning/hatching/foraging ground from at least April through October, and an offshore blue crab mating site.
(2) During April-October, mature female crabs appear to be in a continuous spawning cycle, producing new broods approximately every 21 days while actively foraging to supply the necessary energy for this continuous reproductive activity.
(3) Blue crab egg production apparently declines slightly as the season progresses, perhaps reflecting some ingestion-limited growth of the ovary as infaunal prey densities decline.
(4) Blue crab condition factor on Ship Shoal is comparable to that reported for other, nationally recognized inshore spawning ground. Condition factor on Ship Shoal appears to be positively affected by ovarian condition and negatively affected by a seasonal decline in prey abundance and the presence of nemerteans (*C. carcinophila*) on the gills, but does not appear to be negatively impacted by acorn barnacles (*C. patula* and Balanus spp.) on the exoskeleton, gooseneck barnacles (*O muelleri*) on the gills, or nemerteans (*C. carcinophila*) in the sponge (all conditions normally associated with higher salinity waters).
(5) The lack of a directed blue crab fishery on Ship Shoal crabs likely enhances the stability of Louisiana's traditional inshore blue crab fishery. Since there is no 'quick and inexpensive fix' to the dramatic declines in the blue crab fisheries of Chesapeake Bay and North Carolina, conservative management will seek to maintain the stability of

Louisiana's inshore fishery by protecting Ship Shoal's population of spawning blue crabs.

### 13.3.7. Potential biological effects of large-scale sand mining

The unique biological communities of Ship Shoal compared to the surrounding area results from the shoal's distinctive physical features including shallow depth, sandy sediment and normoxic bottom water. Thus any mining related changes in physical habitat may result in extensive biological changes. These changes will be long-term but not necessarily permanent, as physical conditions at the mining site will eventually return to the pre-mining state through natural processes. Numerical modeling suggests that large-scale sand dredging would have spatially profound impacts on waves and sediment suspension on the shoal, which may enhance fluid mud accumulation on the shoal particularly in the deeper eastern portion of Ship Shoal. Although there was little evidence of a biological impact from post-frontal sediment deposition on Ship Shoal, an extended residence of muds along the bottom boundary layer would likely increase the mortality of sedentary biota. The accumulation of fine sediments would also increase sediment respiration and, consequently, the potential for hypoxia especially on the deeper portions of Ship Shoal. Large-scale sand mining would also increase the accumulation of fine sediments which would also likely decrease or eliminate sensitive (mostly large-bodied) macrobenthic species. The impacts described above would be greatly reduced under a small scale sand removal scenario, because modeling suggest changes on sediment resuspension and wave dynamics would be minimal. Based on these physical changes we can make the following assumptions about the impacts of sand mining on Ship Shoal biota.

(1) Large-scale sand mining will directly reduce BMA productivity by removing sediment and temporarily decreasing sediment light levels. Recovery of BMA is dependent on the depth of sand mining and potentially, changes in grain size after completion of mining, as any mining related increase in water depth will decrease sediment light and an increase in fine sediments may alter the BMA community and productivity.
(2) Responses to large-scale sand mining by meiofauna will likely differ from that of macrofauna because of differences in life history and dispersal ecology. An initial reduction in the abundance of meiofauna is expected after sand removal because meiofauna are unlikely to be able to avoid removal by burrowing to a deeper sediment profile. The recovery rate of interstitial meiofauna is difficult to predict without empirical data but will, in part, depend on the physical characteristics associated with mining.
(3) Dredging and mining activities would inevitably negatively affect, at least temporarily, the Ship Shoal benthic community. Given the size of Ship Shoal, it is likely that mining would remove only a fraction of the available sand but localized effects may be strong. Ship Shoal community exhibits an equilibrated and species-rich community, as indicated by diversity indices and equitability index, suggesting it is controlled by biological interactions rather than extreme changes in environmental parameters. Numerous species found on Ship Shoal have been designated "equilibrium species": relatively large in body

size, slow reproduction rate, and a long life-cycle. These species and the amphipods are considered sensitive species and will probably be strongly affected over the long-term by mining effects. A shift to dominance of the sand-mined area by small-rapid-growing species is predicted to follow sand mining, reducing community biomass and eliciting indirect effects at higher trophic levels, for example on fishes and crustaceans using Ship Shoal as a feeding ground. On the other hand, Ship Shoal's spionid polychaetes are known to be "disturbance specialists" or "opportunistic species": rapid rate of reproduction and growth and readily colonize disturbed habitats. These "disturbances specialists" will be less sensitive to sand-mining than "equilibrium species". This reduction in benthic biomass may elicit indirect effects at higher trophic levels using Ship Shoal.

(4) Excavation of sand will undoubtedly increase water depth and local turbidity due to the overflow of fine particles and hence reduce benthic primary production occurring in this shallow area. Sand removal may also modify hydrodynamic patterns and wave action. Grippo et al. (in press) found that benthic microalgae may have higher biomass than phytoplankton integrated through the water column on Ship Shoal, suggesting benthic algae are important to the shoal's food web. The high benthic biomass we observe may be related to high levels of *in situ* primary production (e.g., our observed correlation between chl *a* and benthic interface feeders). Thus, changes in primary production will likely influence the benthic community, again reducing community biomass and further altering community composition. Changes in water depth may therefore lead to long-term alterations in ecosystem function in higher trophic levels as well. Further studies (that focus on recovery or the scale of sand removal) are necessary to fully understand consequences of human disturbances on Ship Shoal macrofaunal community.

(5) Large-scale mining may have regional as well as local impacts on macrofauna. For example, another unique attribute of Ship Shoal is that it may serve as a larval "stepping stone" connecting populations of sandy sediment communities from the eastern to western end of the northern Gulf of Mexico that disperse using currents. Although sand-mining is not anticipated to change currents around Ship Shoal, the change in sediment type may reduce the amount of suitable habitat for colonizing sand sediment species. Large scale sand mining may also reduce the capacity of Ship Shoal to act as a seed bank for recolonization of surrounding areas affected by seasonal hypoxia.

(6) At minimum, during dredging operations, nekton would be displaced by turbidity and noise, although the displacement would be temporary. Additional impacts would result from localized turbidity associated with sand extraction, which could potentially clog the feeding and respiratory structures of nekton unable to avoid the mining area and of blue crab larvae released over the Shoal. Direct mortality to nekton resulting from sand mining on Ship Shoal is likely to be minimal. Given their transitory and/or limited use of Ship Shoal, negative impacts of sand mining on groundfish and penaeid shrimp production are unlikely, unless infaunal food resources undergo permanent or long-term changes after mining. On the other hand, female blue crabs use the Shoal as a foraging and spawning ground from at least April to October and are therefore more likely to be negatively impacted by any disruption in their food resources on the Shoal. Mining will likely change the benthic invertebrate species composition on Ship Shoal in the short-term and the possibility to elicit bottom-up effects (especially on species like blue crab), but many

common infauna species can be expected to recover in time. For example, the opportunistic but small-bodied species of polychaetes will likely recolonize the mine site quickly. While these polychaetes will likely provide food for nekton, recovery of the existing diversity of food resources on Ship Shoal may take longer, and it is unknown whether this change in resources will affect the diet quality of generalist feeders like penaeid shrimp and croaker.

(7) Our statistical analyses suggest that Ship Shoal blue crabs are healthy and fecund and that the indices and techniques developed and used in this report can be successfully used to monitor the impact of limited sand mining on these crabs. We recommend that at a minimum this monitoring program use box cores and either trawls or crab traps and be designed to test for changes in infaunal abundance and composition, as well as blue crab abundance, reproductive and body weight condition factors. Appropriate morphometric and condition-factor indices include: multiple measures of body volume, extent of parasitism and fouling, presence/viability/development stage of sponge, stage of ovarian development, concentration/viability of stored sperm, and lipofuscion concentration (for ageing).

(8) Additional studies are required to suggest how limited sand mining operations currently proposed for Ship Shoal may affect blue-crab larval survival and recruitment to Louisiana's estuaries and whether the presence of blue crabs makes Ship Shoal an important seaturtle foraging ground (i.e., Seney and Musick 2007).

(9) A continuance of the cautious approach to sand mining being exhibited by MMS for the STTSC is recommended, given the possibility that fecundity of blue crab on the STTSC becomes seasonally limited by prey abundance under prevailing natural conditions. In addition, recent studies within coastal Louisiana (Palmer et al., 2008) showed significant sand mining related declines in macrofaunal abundance, biomass, and diversity.

# REFERENCES


Adams, C.E., D.J. Swift and J.M. Coleman. 1987. Bottom currents and fluviomarine sedimentation on the Mississippi prodelta shelf: February-May 1984. Journal of Geophysical Research 92(C.13):14595-14609.

Adkins, G. 1972. A study of the blue crab fishery in Louisiana. A study of the blue crab fishery in Louisiana. Technical Bulletin. Louisiana Wildlife and Fisheries Commission, Baton Rouge, Louisiana 3:31-57.

Aguilar, R., E.G. Johnson, A.H. Hines, M.A. Kramer and M.R. Goodison. 2008. Importance of blue crab life history for stock enhancement and spatial management of the fishery in Chesapeake Bay. Reviews in Fisheries Science 16(1-3):117-124.

Allison, M.A., A. Sheremet, M.A. Goñi and G.W. Stone. 2005. Storm layer deposition on the Mississippi-Atchafalaya subaqueous delta generated by Hurricane LILI. Continental Shelf Research 25:2213-2232.

Archambault, J.A., E.L. Wenner and J.D. Whitaker. 1990. Life-History and Abundance of Blue-Crab, Callinectes-Sapidus Rathbun, at Charleston Harbor, South-Carolina. Bulletin of Marine Science 46(1):145-158.

ASTM. 1987. Standard method for particle-size analysis of soils, designation D422-63. 1987 Annual Book of ASTM Standards, Volume 04.08 Soil and Rock; Building Stones; Geotextiles. Philadelphia: American Society for Testing Materials.

Austen, M.C., R.M. Warwick and M.C. Rosado. 1989. Meiobenthic and macrobenthic community structure along a putative pollution gradient in southern Portugal. Marine Pollution Bulletin 20:398-404.

Baguley, J.G., L.J. Hyde and P.A. Montagna. 2004. A semi-automated digital microphotographic approach to measure biomass. Limnology and Oceanography: Methods 2:181-190.

Baguley, J.G., P.A. Montagna, L.J. Hyde, R.D. Kalke and G.T. Rowe. 2006a. Metazoan meiofauna abundance in relation to environmental variables in the northern Gulf of Mexico deep sea. Deep-Sea Research 53:1344-1362.

Baguley, J.G., P.A. Montagna, W. Lee, L.J. Hyde and G.T. Rowe. 2006b. Spatial and bathymetric trends in Harpacticoida (Copepoda) community structure in the Northern Gulf of Mexico deep-sea. Journal of Experimental Marine Biology and Ecology 330:307-326.

Baumann, T., B.B. Goree, W.M. Lovelace, P.A. Montgomery, G.B. Ross, D.J. Walter and A.N. Ward. 2006. Water Resource Data Louisiana Water Year 2005. Water Data Report USGS-WDR-LA-05-1. 913 pp.

Baustian, M.M. 2005. Benthic communities in the northern Gulf of Mexico hypoxic area: potential prey for demersal fish. master thesis. Louisiana State University, Baton Rouge. 61 pp.

Bell, G.W., D.B. Eggleston and T.G. Wolcott. 2003. Behavioral responses of free-ranging blue crabs to episodic hypoxia. II. Feeding. Marine Ecology-Progress Series 259:227-235.

Bianchi, T.S., C. Rolff, B. Widbom and R. Elmgren. 2002. Phytoplankon pigments in Baltic Sea seston and sediments: Seasonal variablility, fluxes, and Transformations. Estuarine, Coastal and Shelf Science 55:369-383.

Bierman, V.J., Jr., S.C. Hinz, D.W. Zhu, W.J. Wiseman, Jr., N.N. Rabalais and R.E. Turner. 1994. A preliminary mass balance model of primary primary productivity and dissolved oxygen in the Mississippi River plume/inner gulf shelf region. Estuaries 17:886-899.

Billerbeck, M., H. Røy, K. Bosselmann and M. Huettel. 2007. Benthic photosynthesis in submerged Wadden Sea intertidal flats. Estuarine Coastal and Shelf Science 71:704-716.

Blanchard, G.F. 1991. Measurement of Meiofauna Grazing Rates on Microphytobenthos - Is Primary Production a Limiting Factor. Journal of Experimental Marine Biology and Ecology 147:37-46.

Blott, S.J. and K. Pye. 2001. GRADISTAT: a grain size distribution and statistics package for the analysis of unconsolidated sediments. Earth Surface Processes and Landforms 26:1237-1248.

Boland, G.S. and G.T. Rowe. 1991. Deep-Sea Benthic Sampling with the Gomex Box Corer. Limnology and Oceanography 36(5):1015-1020.

Braud, D. 1999. Louisiana GIS CD: a digital map of the state. Version 2.0. Louisiana State University. Department of Geography and Anthropology. Baton Rouge, LA.

Brooks, R.A., S.C. Keitzer and K.J. Sulak. 2004. Taxonomic composition and relative frequency of the benthic fish community found on natural sand banks and shoals in the northwestern Gulf of Mexico. (A synthesis of the Southeast Area Monitoring and Assessment Program's Groundfish Survey Database, 1982–2000). US Geological Survey, Coastal Ecology and Consevation Research Group, USGS–Florida Integraed Science Center, CARS, Gainesville, FL. 47 pp.

Brooks, R.A., C.N. Purdy, S.S. Bell and K.J. Sulak. 2006. The benthic community of the eastern US continental shelf: A literature synopsis of benthic faunal resources. Continental Shelf Research 26(6):804-818.

Buffan-Dubau, E. and K.R. Carman. 2000. Extraction of benthic microalgal pigments for HPLC analyses. Marine Ecology Progress Series 204:293-297.

Byrnes, M.R., R.M. Hammer, B.A. Vittor, S.W. Kelley, D.B. Snyder, J.M. Cote , J.S. Ramsey, T.D. Thibaut, N.W. Phillips and J.D. Wood. 2003. Collection of Environmental Data Within Sand Resource Areas Offshore North Carolina and the Implications of Sand Removal for Coastal and Beach Restoration. U.S. Department of the Interior, Minerals Management Service, Leasing Division, Sand and Gravel Unit, Herndon, VA. OCS Report MMS 2000-056. Volume I: Main Text 257 pp, Volume II: Appendices 70 pp.

Byrnes, M.R., R.M. Hammer, B.A. Vittor, J.S. Ramsey, D.B. Snyder, K.F. Bosma, J.D. Wood, T.D. Thibaut and N.W. Phillips. 1999. Environmental Survey of Identified Sand Resource Areas Offshore Alabama: Volume I: Main Text, Volume II: Appendices. U.S. Department of Interior, Minerals Management Service, International Activities and Marine Minerals Division (INTERMAR), Herndon, VA. OCS Report MMS 99-0052. 326 pp. + 132 pp. appendices pp.

Byrnes, R., M. Hammer, T.D. Thibaut and D.B. Snyder. 2004. Physical and Biological effects of Sand Mining Offshore Alabama, U.S.A. Journal of Coastal Research 20(1):6-24.

Cacchione, D.A. and D.E. Drake. 1982. Measurements of storm-generated bottom stresses on the continental shelf. Journal of Geophysical Research 87(C3):1952-1960.

Cacchione, D.A. and D.E. Drake. 1990. Shelf seidment transport: an overview with applications to the northern California continental shelf. In: Le Mehaute, B. and D.M. Hanes, eds. The Sea. New York: Wiley. Pp 729-773.

Cacchoine, D.A., R.W. Sternberg and A.S. Ogston. 2006. Bottom instrumented tripods: History, Application and Impacts. Continental Shelf Research 26:2319-2334.

Cahoon, L.B. and J.E. Cooke. 1992. Benthic microalgal primary production in Onslow Bay North Carolina, USA. Marine Ecology Progress Series 84:185-196.

Cahoon, L.B. and R.A. Laws. 1993. Benthic diatoms from the North Carolina continental shelf: Inner and mid shelf. Journal of Phycology 29:257-263.

Campbell, T., L. Benedet and C.W. Finkl. 2005. Regional Strategies for Coastal Restoration in Louisiana. Journal of Coastal Research SI 44:245-268.

Carr, S.D., R.A. Tankersley, J.L. Hench, R.B. Forward and R.A. Luettich. 2004. Movement patterns and trajectories of ovigerous blue crabs Callinectes sapidus during the spawning migration. Estuarine Coastal and Shelf Science 60(4):567-579.

Cartaxana, P., C.R. Mendes and M.A. van Leuwe. 2006. Comparative study on microphytobenthic pigments of muddy and sandy intertidal sedimets of the Tagus estuary. Estuarine Coastal and Shelf Science 66:225-230.

Carver, A.M., T.G. Wolcott, D.L. Wolcott and A.H. Hines. 2005. Unnatural selection: Effects of a male-focused size-selective fishery on reproductive potential of a blue crab population. Journal of Experimental Marine Biology and Ecology 319(1-2):29-41.

Chandler, G.T. and J.W. Fleeger. 1983. Meiofaunal colonization of azoic estuarine sediment in Louisiana: mechanisms of dispersal. Journal of Experimental Marine Biology and Ecology 69:175-188.

Chao, S.-Y. 1987. River-forced estuarine plumes. Journal of Physical Oceanography 18:72-88.

Chen, N., T.S. Bianchi and J.M. Bland. 2003. Implications for the role of pre- versus post-depositional transformation of chlorophyll-a in the Lower Mississippi River and Louisiana shelf. Marine Chemistry 81:37-55.

Cheung, M.M., R.A. Brooks and K.J. Sulak. 2006. Benthic polychaete assemblages on Sabine and Heald sand banks, northern Gulf of Mexico: a pre-disturbance study on a sand extraction site. USGS Outer Continental Shelf Ecosystem Studies Program Report, Gainesville, FL. 47 pp.

Chuang, W.-S. and W.J. Wiseman, Jr. 1983. Coastal Sea Level Response to Frontal Passages on the Louisiana-Texas Shelf. Journal of Geophysical Research 88(C4):2615–2620.

Churchill, E.P., Jr. 1919. Life history of the blue crab. Bulletin of the U.S. Bureau of Fisheries 36:91-128.

Cibic, T., O. Blasutto, C. Falconi and S.F. Umani. 2007. Microphytobenthic biomas species composition and nutrient availability in sublittoral sediments of the Gulf of Trieste (northern Adriatic Sea). Estuarine Coastal and Shelf Science 75:50-62.

Cipriani, L.E. and G.W. Stone. 2001. Net longshore sediment transport and textural changes in beach sediments along the southwest Alabama and Mississippi barrier islands, U.S.A. Journal of Coastal Research 17(2):443-458.

Clarke, K.R. 1993. Nonparametric Multivariate Analyses of Changes in Community Structure. Australian Journal of Ecology 18(1):117-143.

Clarke, K.R. and M. Ainsworth. 1993. A Method of Linking Multivariate Community Structure to Environmental Variables. Marine Ecology-Progress Series 92(3):205-219.

Clarke, K.R. and R.N. Gorley. 2001. PRIMER v5 : User Manual/Tutorial. PRRIMER-E Ltd. Plymouth.

Clarke, K.R. and R.M. Warwick. 1994. Change in marine communities: an approach to statistical analysis and interpretation. Plymouth Marine Laboratory, Plymouth.

Coast 2050. 1998. Coast 2050: Toward a Sustainable Coastal Louisiana. Louisiana Coastal Wetlands Conservation and Restoration Task Force and the Wetlands and Conservation Authority. Louisiana Department of Natural Resources, Baton Rouge, LA. 173 pp.

Coastal Environment Incorporated (CEI). 2003a. New Cut Dune/Marsh Restoration Project Using Ship Shoal Sediment Coastal Terrebonne Parish, Louisiana: High Resolution Geophysical and Archaeological Survey of the South Pelto Area Block 13 Vicinity of Ship Shoal. C&C Technologies, Lafayette, LA, 43 pp.

Coastal Environment Incorporated (CEI). 2003b. Whiskey Island West Flank Restoration Project Using Ship Shoal Sediment Coastal Terrebonne Parish, Louisiana: High Resolution Geophysical and Archaeological Survey of the Portions of Blocks 87, 88, 89,94 & 95 Ship Shoal Area. C&C Technologies, Lafayette, LA, 43 pp.

Cochrane, J.D. and F.J. Kelly. 1986. Low-Frequency Circulation on the Texas-Louisiana Continental-Shelf. Journal of Geophysical Research 91(C9):10645-10659.

Colangelo, M.A., T. Macri and V.U. Ceccherelli. 1996. A field experiment on the effect of two types of sediment disturbance on the rate of recovery of a meiobenthic community in a eutrophicated lagoon. Hydrobiologia 329:57-67.

Coleman, J.M. and S.M. Gagliano. 1964. Cyclic sedimentation in the Mississippi River delta plain. Transactions of Gulf Coast Association of Geological Societies 14:67-80.

Coleman, J.M., H.H. Roberts and G.W. Stone. 1998. Mississippi River Delta: an Overview. Journal of Coastal Research 14(3):698-716.

Condrey, R. and C. Gelpi. 2008. Blue crab use of the Ship/Trinity/Tiger shoal complex as a nationally important spawning/hatching/foraging ground: Discovery, evaluation, and sand mining recommendations. Final report submitted to U.S. Minerals Management Service. 34 pp.

Condrey, R.E. 1980. Fishery management plan for the shrimp fishery of the Gulf of Mexico U.S. waters. Federal Register 45(218):74178-74308.

Coull, B.C. 1988. Ecology of the marine meiofauna. In: Higgins, R.P. and H. Thiel, eds. Introduction to the Study of Meiofauna. Washington D.C.: Smithsonian Institution Press. Pp 18-38.

Coull, B.C. 1999. Role of meiofauna in estuarine soft-bottom habitats. Austrailan Journal of Ecology 24:327-343.

Courtenay, W.R., Jr., B.C. Hartig and G.R. Loisel. 1980. Ecological Evaluation of Beach Nourishment Project at Hallandale (Broward County), Florida: Evaluation of fish populations adjacent to borrow areas of beach nourishment project. Hallandale (Broward

County), Florida, Vol. I. Miscellaneous Report 80-1 (I). Fort Belvoir, VA. Coastal Engineering Research Center, U. S. Army Corps of Engineers, 23 pp.

Cragg, J., G. Mitchum and W. Sturges. 1983. Wind-induced sea surface slopes on the west Florida shelf. Journal of Physical Oceanography 13:2201-2212.

Craig, J.K. and L.B. Crowder. 2005. Hypoxia-induced habitat shifts and energetic consequences in Atlantic croaker and brown shrimp on the Gulf of Mexico shelf. Marine Ecology Progress Series 294:79-94.

Csanady, G.T. 1982. Circulation in the coastal ocean. Dordrecht: D. Reidel Pub. 279 pp.

Daugherty, F.M., Jr. 1952. The blue crab investigation. The Texas Journal of Science 1:77-84.

Davis, C.C. 1965. A study of the hatching process in aquatic invertebrates: XX. The blue crab, Callinectes sapidus, Rathbun, XXI. The nemertean, Carcinonemertes carcinophilia (Kolliker). Chesapeake Science 6(4):201-208.

Davis, R. and D. Fitzgerald. 2004. Beaches and coasts. Blackwell Publishing. 419 pp.

DHI. 2005. MIKE21&3 Flow Model FM. Hydrodynamics and Transport Module, Scientific Documentation. 42 pp.

Diaz, R.J., J. G.R. Cutter and I. C. H. Hobbs. 2004. Potential impacts of sand mining offshore of Maryland and Delaware: Part 2-Biological considerations. Journal of Coastal Research 20(1):61-69.

Dickinson, G.H., D. Rittschof and C. Latanich. 2006. Spawning biology of the blue crab, Callinectes sapidus, in North Carolina. Bulletin of Marine Science 79(2):273-285.

DiMego, G.J., L.F. Bosart and G.W. Endersen. 1976. An examination of the frequency and mean conditions surrounding frontal incursions into the Gulf of Mexico and Caribbean Sea. Monthly Weather Review 104:709-718.

Divins, D.L. and D. Metzger. 2008. NGDC Coastal Relief Model. http://www.ngdc.noaa.gov/mgg/coastal/coastal.html. (Last updated on 06/01/2008), Cited on 6/1/2008,

Dodds, W.K., B.J.F. Biggs and R.L. Lowe. 1999. Photosynthesis-irradiance patterns in benthic microalgae: varialtion as a function of assemblage thickness and community structure. Journal of Phycology 35:42–53.

Dortch, Q., N.N. Rabalais, R.E. Turner and N.A. Qureshi. 2000. Impacts of changing Si/N ratios and phytoplankton species composition. In: Rabalais, N.N. and R.E. Turner, eds. Coastal hypoxia: consequences for living resources. Washington, D.C.: American Geophysical Union. Pp 37-48.

Dortch, Q., N.N. Rabalais, R.E. Turner and G.T. Rowe. 1994. Respiration rates and hypoxia on the Louisiana shelf. Estuaries 17:862-872.

Dortch, Q., R. Robichaux, S. Pool, D. Milsted, G. Mire, N.N. Rabalais, T.M. Soniat, G.A. Fryxell, R.E. Turner and M.L. Parsons. 1997. Abundance and vertical flux of Pseudo-nitzschia in the northern Gulf of Mexico. Marine Ecology Progress Series 146:249-264.

Douglas, B.C., M.S. Kearney and S.P. Leatherman. 2001. Sea Level Rise: History and Consequences. San Diego, CA: Academic Press. 225 pp.

Drake, D.E. and D.A. Cacchione. 1992. Wave Current Interaction in the Bottom Boundary-Layer during Storm and Nonstorm Conditions - Observations and Model Predictions. Continental Shelf Research 12(12):1331-1352.

Drucker, B.S., W. Waskes and M.R. Byrnes. 2004. The US Minerals Management Service Outer Continental Shelf Sand and Gravel program: Environmental studies to assess the potential effects of offshore dredging operations in federal waters. Journal of Coastal Research 20(1):1-5.

Dubois, S., C.G. Gelpi, R.E. Condrey, M.A. Gripo and J.W. Fleeger. In Review. Diversity and composition of macrobenthic community associated with sandy shoals of the Louisiana continental shelf. Biodiversity and Conservation.

Dubois, S., C. Retiere and F. Olivier. 2002. Biodiversity associated with Sabellaria alveolata (Polychaeta : Sabellariidae) reefs: effects of human disturbances. Journal of the Marine Biological Association of the United Kingdom 82(5):817-826.

Eadie, B.J., B.A. McKee, M.B. Lansing, J.A. Robbins, S. Metz and J.H. Trefry. 1994. Records of nutrient-enhanced coastal ocean productivity in sediments from the Louisiana continental shelf. Estuaries 17:754-765.

Earle, M.D., D. McGehee and M. Tubman. 1995. Field wave gaging program, wave data analysis standard. Instruction report CERC-95-1,U.S. Army Corps of Engineers, Waterways Experiment Station. 46 pp.

Eggleston, D.B., G.W. Bell and S.P. Searcy. In Review. Diversity and composition of macrobenthic community associated with sandy shoals of the Louisiana continental shelf. Marine Ecology Progress Series.

Eggleston, D.B., E.G. Johnson, G.T. Kellison, G.R. Plaia and C.L. Huggett. 2008. Pilot evaluation of early juvenile blue crab stock enhancement using a replicated BACI design. Reviews in Fisheries Science 6(1-3):91-100.

Ehrenhauss, S., U. Witte, S.I. Buhring and M. Huettel. 2004. Effect of advective pore water transport on distribution and degredation of diatoms in permeable North Sea sediments. Marine Ecology Progress Series 271:99-111.

Elgar, S., M.H. Freilich and R.T. Guza. 1990. Model-data comparisons of moments of non-breaking shoaling surface gravity waves. Journal of Geophysical Research 95(C9):16055-16063.

Facca, C. and A. Sfriso. 2007. Epipelic diatom spatial and temporal distribution and relationship with main environmental parameters in coastal waters. Estuarine Coastal and Shelf Science 5:35-49.

Fauchald, K. and P.A. Jumars. 1979. The diet of worms: A study of polychaete feeding guilds. Oceanography and Marine Biology, Annual Review 17:193-284.

Finkl, C.W., J.L. Andrews, L. Benedet and T. Campbell. 2005. Geotechnical Investigation for Exploration of Sand Resources in the Lower Mississippi River and South Pass, and Exploration for Sand via Vibracoring in South Pelto Blocks 12 &13. Report Prepared for the Louisiana Department of Natural Resources, Baton Rouge, LA. Boca Raton, Florida: Coastal Planning & Engineering, Inc., 40 pp.

Finkl, C.W. and S.M. Khalil. 2005a. Offshore exploration for sand sources: General guidelines and procedural strategies along deltaic coasts. Journal of Coastal Research SI 44:203-233.

Finkl, C.W. and S.M. Khalil. 2005b. Vibracore. In: Schwartz, M.L., ed. The Encyclopedia of Coastal Science. Dordrecht, The Netherlands: Kluwer Academic. Pp 1272-1284.

Fisher, A.G. 1961. Stratigraphic record of transgressing seas in light of sedimentation on Atlantic coast of New Jersey. AAPG Bulletin-American Association of Petroleum Geologists 45:1656-1667.

Fisk, H.N., E. McFarlan, Jr., C.R. Kolb and L.J. Wilbert, Jr. 1954. Sedimentary framework of the modern Mississippi delta. Journal of Sedimentary Petrology 24:76-99.

Fleeger, J.W., K.R. Carman, P.B. Weisenhorn, H. Sofranko, T. Marshall, D. Thistle and J.P. Barry. 2006. Simulated sequestration of anthropogenic carbon dioxide at a deep-sea site: effects on nematode abundance and biovolume. Deep-Sea Research 53:1135-1147.

Fleeger, J.W., D.S. Johnson, K.A. Galván and L.A. Deegan. 2008. Top-down and bottom-up control of infauna varies across the saltmarsh landscape. Journal of Experimental Marine Biology and Ecology 357:20-34.

Fleeger, J.W. and M.A. Palmer. 1982. Secondary production of the estuarine meiobenthic copepod Microarthridion littorale. Marine Ecology Progress Series 7:157-162.

Fleeger, J.W., T.C. Shirley and J.N. McCall. 1995. Fine-scale vertical profiles of meiofauna in muddy sediments. Canadian Journal of Zoology 73:1453-1460.

Folk, R.L. 1974. Petrology of Sedimentary Rocks. Austin: Hemphill Publishing Company. 182 pp.

Folk, R.L. and W.C. Ward. 1957. Brazos River bar: a study in the significance of grain size parameters. Journal of Sedimentary Petrology 27:3-26.

Forward, R.B., J.H. Cohen, M.Z. Darnell and A. Saal. 2005. The circatidal rhythm in vertical swimming of female blue crabs, Callinectes sapidus, during their spawning migration: A reconsideration. Journal of Shellfish Research 24(2):587-590.

Franco, M.A., K. Soetaert, D. Van Oevelen, D. Van Gansbeke, M.J. Costa, M. Vincx and J. Vanaverbeke. 2008. Density, vertical distribution and trophic responses of metazoan meiobenthos to phytoplankton deposition in contrasting sediment types. Marine Ecology-Progress Series 358:51-62.

Frazier, D.E. 1967. Recent deltaic depositions of the Mississippi River: their development and chronology. Gulf Coast Association of Geological Societies Transactions 27:287-315.

Frazier, D.E. 1974. Depositional Episodes: Their Relationship to the Quaternary Stratigraphic Framework in the Northwestern Portion of the Gulf Basin. Austin, Texas: Bureau of Economic Geology, The University of Texas.

Friedrichs, C.T., L.D. Wright, D.A. Hepworth and S.C. Kim. 2000. Bottom-boundary-layer processes associated with fine sediment accumulation in coastal seas and bays. Continental Shelf Research 20(7):807-841.

Fuller, C.M. and C.A. Butman. 1988. A simple technique for fine-scale, vertical sectioning of fresh sediment cores. Journal of Sedimentary Petrology 58:763-768.

Gaidry, W.J. and C.J. White. 1973. Investigations of commercially important penaeid shrimp in Louisiana estuaries. Louisiana Wildlife and Fisheries Commission Technical Bulletin. Vol. 8. 154 pp.

Gartner, J.W. 2002. Estimation of suspended solids concentrations based on acoustic backscatter intensity: theoretical background. Turbidity and Other Sediment Surrogates Workshop, April 30 – May 2, 2002, Reno, NV. Pp 3.

Gaston, G.R. 1985. Effects of Hypoxia on Macrobenthos of the Inner Shelf Off Cameron, Louisiana. Estuarine Coastal and Shelf Science 20(5):603-613.

Gattuso, J.-P., B. Gentili, C.M. Duarte, J.A. Kleypas, J.J. Middleburg and D. Antoine. 2006. Light availability in the c oastal ocean: impact on the distribution of benthic photosynthetic organisms and their contribution to primary primary production. Biogeoscience 3:489-513.

Georgiou, I.Y., D.M. FitzGerald and G.W. Stone. 2005. The impact of physical processes along the Louisiana coast. Journal of Coastal Research 44:72-89.

Gesteira, J.L.G. and J.C. Dauvin. 2000. Amphipods are good bioindicators of the impact of oil spills on soft-bottom macrobenthic communities. Marine Pollution Bulletin 40:1017-1027.

Giere, O. 1993. Meiobenthology. The Microscopic Fauna in Aquatic Sediments. Berlin, Heidleberg: Springer-Verlag.

Glenn, S.M. and W.D. Grant. 1987. A Suspended Sediment Stratification Correction for Combined Wave and Current Flows. Journal of Geophysical Research 92(C8):8244-8264.

Gordon, L. and A. Lohrmann. 2001. Near-shore Doppler current meter wave spectra. Proceedings of The 4th International Symposium on Ocean Wave Measurement and Analysis, WAVES2001, ASCE. San Francisco, CA. Pp 33-43.

Grant, W.D. and O.S. Madsen. 1986. The Continental-Shelf Bottom Boundary-Layer. Annual Review of Fluid Mechanics 18:265-305.

Gray, J.S. 1974. Animal-sediment relationships. Oceanography and Marine Biology Annual Review 12:223-261.

Gray, J.S. 2000. The measurement of marine species diversity, with an application to the benthic fauna of the Norwegian continental shelf. Journal of Experimental Marine Biology and Ecology 250:23-49.

Green, M.O. 1992. Spectral Estimates of Bed Shear-Stress at Subcritical Reynolds-Numbers in a Tidal Boundary-Layer. Journal of Physical Oceanography 22(8):903-917.

Green, M.O., C.E. Vincent, I.N. McCave, R.R. Dickson, J.M. Rees and N.D. Pearson. 1995. Storm sediment transport: observations from the British North Sea shelf. Continental Shelf Research 15(8):889-912.

Greene, K. 2002. Beach Nourishment: A Review of the Biological and Physical Impacts. ASMFC Habitat Management Series # 7. Washington D.C.: Atlantic States Marine Fisheries Commission. 174 pp.

Grippo, M., J.W. Fleeger, R. Condrey and K.C. Carman. 2009. High Benthic Microalgal Biomass Found on Ship Shoal, North-central Gulf of Mexico.Submitted.

Guillory, V., H. Perry and S. Vanderkooy. 2001. The blue crab fishery of the Gulf of Mexico, United States: A regional management plan. Oceans Springs, Mississippi: Gulf States Marine Fisheries Commission.

Gulf of Mexico Program. 2008. USEPA Gulf of Mexico Program Office. Stennis Space Center, MS. http://www.epa.gov/gmpo/nutrient/hypoxia_pressrelease.html. (Last updated on March 10, 2008), Cited on July 15, 2008.

Hagerman, G.M. and R.M. Rieger. 1981. Dispersal of benthic meiofauna by wave and current action in Bogue Sound, North Carolina, USA. Marine Ecology Progress Series 2:245-270.

Hall, S.J. and M.J.C. Harding. 1997. Physical disturbance and marine benthic communities: The effects of mechanical harvesting of cockles on non-target benthic infauna. Journal of Applied Ecology 34:497-517.

Hanifen, J.C. 2008. 2008 SEAMAP-Gulf of Mexico Marine Directory. Fishery-Independent Survey Activities. Gulf States Marine Fisheries Commission, Ocean Springs, Mississippi. http://www.gsmfc.org/publications/GSMFC%20Number%20153.pdf. 21 pp.

Hard, W.L. 1945. Ovarian growth and ovulation in the mature blue crab, Callinectes sapidus Rathbun. Chesapeake Biological Laboratory (Solomons, Maryland) Contribution 46:3-17.

Hasselmann, K. 1974. On the spectral dissipation of ocean waves due to whitecapping. Boundary-Layer Meteorology 6(1-2):107-127.

Hasselmann, S., K. Hasselmann, J.H. Allender and T.P. Barnett. 1985. Computations and Parameterizations of the Nonlinear Energy-Transfer in a Gravity-Wave Spectrum .2. Parameterizations of the Nonlinear Energy-Transfer for Application in Wave Models. Journal of Physical Oceanography 15(11):1378-1391.

Hayden, B.P. 1999. Climate change and extra-tropical storminess in the United States: An assessment. Journal of the American Water Resources Association 35(6):1387-1397.

Head, E.J.H., B.T. Hargrave and D.V.S. Rao. 1994. Accumulation of a pheophorbide a-like pigment in sediments traps during late stages of a spring bloom: A product of dying algae? Limnology and Oceanography 39:176-181.

Hefley, H.M. and H. Shoemaker. 1952. The occurrence of Branchiostoma (Amphioxus) in Mississippi and Louisiana. Science 115:48.

Hench, J.L., R.B. Forward, S.D. Carr, D. Rittschof and R.A. Luettich. 2004. Testing a selective tidal-stream transport model: Observations of female blue crab (Callinectes sapidus) vertical migration during the spawning season. Limnology and Oceanography 49(5):1857-1870.

Hesp, P. and A. Short. 1999. Barrier morphodynamics. In: Short, A., ed. Handbook of beach and shoreface morphodynamics. New York: John Wiley and Sons. Pp 305-368.

Hester, M.W., E.A. Spalding and C.D. Franze. 2005. Biological Resources of the Louisiana Coast: Part 1. An overview of coastal plant communities of the Louisiana Gulf Shoreline. Journal of Coastal Research SI 44:134-145.

Hill, M.O. 1973. Diversity and evenness : a unifying notation and its consequence. Ecology 54:427-432.

Hillebrand, H., B. Worm and H.K. Lotze. 2000. Marine microbenthic community structure regulated by nitrogen loading and grazing pressure. Marine Ecology Progress Series 204:27-38.

Hines, A.H. 1982. Allometric Constraints and Variables of Reproductive Effort in Brachyuran Crabs. Marine Biology 69(3):309-320.

Hines, A.H., P.R. Jivoff, P.J. Bushmann, J. van Montfrans, S.A. Reed, D.L. Wolcott and T.G. Wolcott. 2003. Evidence for sperm limitation in the blue crab, Callinectes sapidus. Bulletin of Marine Science 72(2):287-310.

Hobbs, C.H., III. 2002. An investigation of potential consequences of marine mining in shallow water: an example from the mid-Atlantic coast of the United States. Journal of Coastal Research 18(1):94-101.

Holthuijsen, L.H. 2007. Waves in Oceanic and Coastal Waters. Cambridge University Press. 404 pp.

Howard, R.J. and I.A. Mendelssohn. 1999. Salinity as a Constraint on Growth of Oligohaline Marsh Macrophytes. I. Species Variation in Stress Tolerance. American Journal of Botany 86(6):785-794.

Hsu, S.A. 1988. Coastal Meteorology. San Diego: Academic Press. 260 pp.

Hsu, S.A. 2003. Estimating overwater friction velocity and exponent of power-law wind profile from gust factor during storms. Journal of waterway Port Coastal and Ocean Engineering 129(4):174-177.

Hsu, S.A. 2006. Measurements of Overwater Gust Factor From NDBC Buoys During Hurricanes. NWA Electric Journal of Operational Meteorology:2006-EJ2.

Huettel, M. and A. Rusch. 2000. Transport and degreadation of phytoplankton in permeable sediment. Limnology and Oceanography 45:534-549.

Hutchings, P.A. 1998. Biodiversity and functioning of polychaetes in benthic sediments. Biodiversity and Conservation 7:1133-1145.

Jahnke, A.R., J.R. Nelson, R.L. Marinelli and J.E. Eckman. 2000. Benthic flux of biogenic elements o the Southeaster US continental shelf: influence of pore water advective transport and benthic microalgae. Continental Shelf Research 20:109-127.

Janssen, P.A.E.M. 1989. Wave-Induced Stress and the Drag of Air-Flow over Sea Waves. Journal of Physical Oceanography 19(6):745-754.

Janssen, P.A.E.M. 1991. Quasi-linear theory of wind-wave generation applied to wave forecasting. Journal of Physical Oceanography 21:1631-1642.

Jeffrey, S.W. and M. Vesk. 1997. Introduction to phytoplankton and their pigment signatures. In: Jeffrey, S.W., R.F.C. Mantoura and S.W. Wright, eds. Phytoplankton pigments in

oceanography: guidelines to modern methods. monographs on oceanographic methodology 10. Paris, France: UNESCO Publishing. Pp 37-84.

Jivoff, P., A.H. Hines and L.S. Quackenbush. 2007. Reproductive biology and embryonic development. In: Kennedy, V.S. and L.E. Cronin, eds. The blue crab Callinectes sapidus. College Park, Maryland: Maryland Sea Grant College. Pp 255-298.

Johnson, H.K., T.V. Karambas, I. Avgeris, B. Zanuttigh, D. Gonzalez-Marco and I. Caceres. 2005. Modelling of waves and currents around submerged breakwaters. Coastal Engineering 52(10-11):949-969.

Jorgensen, B.B., R.N. Glud and O. Holby. 2005. Oxygen distribution and bioirrigation in Arctic fjord sediments (Svalbard, Barents Sea). Marine Ecology-Progress Series 292:85-95.

Jose, F., D. Kobashi and G.W. Stone. 2007. Spectral wave transformation over an elongated sand shoal off south central Louisiana, USA. Journal of Coastal Research SI 50:757-761.

Jose, F. and G.W. Stone. 2006. Forecast of nearshore wave parameters using MIKE 21 spectral wave model. Transactions, Gulf Coast Association of Geological Societies 56:323-327.

Justic, D., N.N. Rabalais and R.E. Turner. 1996. Effects of climate change on hypoxia in coastal waters: A doubled CO2 scenario for the northern Gulf of Mexico. Limnology and Oceanography 41(5):992-1003.

Jutte, P.C., R.F. Van Dolah and P.T. Gayes. 2002. Recovery of benthic communities following offshore dredging, Myrtle Beach, South Carolina. Shore and Beach 70:25-30.

Keim, B.D., R.A. Muller and G.W. Stone. 2007. Spatiotemporal patterns and return periods of tropical storm and hurricane strikes from Texas to Maine. Journal of Climate 20:3498-3508.

Kemp, P.G. 1986. Mud deposition at the shoreface: wave and sediment dynamics on the Chenier plain of Louisiana. Ph.D. Dissertation. Louisiana State University, Baton Rouge. 147 pp.

Kennedy, A.D. and C.A. Jacoby. 1999. Biological indicators of marine environmental health: meiofauna - a neglected benthic component? Environmental Monitoring and Assessment 54:47-68.

Kennedy, V.S. and L.E. Cronin. 2007. The blue crab Callinectes sapidus. College Park, Maryland: Maryland Sea Grant College. 774 pp.

Khalil, S.M. 2004. General Guidelines: Exploration for Offshore Sand Sources., Version-IV. Coastal Engineering Division. OCRM, Louisiana Department of Natural Resources, Baton Rouge, LA.

Khalil, S.M., C. Finkl, J. Andrew and C.P. Knotts. 2007. Restoration-quality sand from Ship Shoal, Louisiana: Geotechnical investigation for sand on a drowned barrier island. Proceedings of Coastal Sediments '07. New Orleans, Louisiana. Pp 685-698.

Khalil, S.M. and C.W. Finkl. 2009 (in press). Regional Sediment Management Strategies for Coastal Restoration in Louisiana, USA. Journal of Coastal Research SI 56:xx-xx.

Khalil, S.M., C.P. Knotts and B. Tate. 2006. Restoration of Louisiana Barrier Islands: Engineering approaches to hazard mitigation by modulating coastal environments. Proceedings of ICCE 2006. Vol. 2, Pp 1951-1963.

Kindinger, J., J. Flocks, M. Kulp, S. Penland and L.D. Britsch. 2001. Sand Resources, Regional Geology, and Coastal Processes for the Restoration of the Barataria Barrier Shoreline. Report to U.S. Army Corps of Engineers, New Orleans District, September 2001. US Geological Survey Open File Report 01-384. St. Petersburg, FL USA. 69 pp.

Kjerfve, B., G.M.E. Perillo, L.R. Gardner, J.M. Rine, G.T.M. Dias and F.R. Mochel. 2002. Morphodynamics of muddy environments along the Atlantic coasts of North and South America. In: Healy, T.R., Y. Wang and J.-A. Healy, eds. Muddy Coasts of the World: Processes, Deposits and Functions. Amsterdam: Elsevier. Pp 219–239.

Knabb, R.D., D.P. Brown and J.R. Rhome. 2005a. Tropical cyclone Report Hurricane Rita. National Hurricane Centre, National Oceanographic and Atmospheric Administration, Miami, Florida. 33 pp.

Knabb, R.D., J.R. Rhome and D.P. Brown. 2005b. Tropical cyclone Report Hurricane Katrina. National Hurricane Centre, National Oceanographic and Atmospheric Administration, Miami, Florida. 43 pp.

Kobashi, D., F. Jose, Y. Luo and G.W. Stone. 2009a. Wind-driven dispersal of fluvial fine sediments for two contrasting storms: extra-tropical and tropical storms, Atchafalaya Bay-Shelf, Louisiana. Marine Geology: In Review.

Kobashi, D., F. Jose and G.W. Stone. 2005. Hydrodynamics and sedimentary responses within bottom boundary layer: Sabine Bank, western Louisiana. Transaction, Gulf Coast Association of Geological Societies 55:392-399.

Kobashi, D., F. Jose and G.W. Stone. 2007a. Heterogeneity and dynamics of sediments on a shoal during spring-winter storm season, south-central Louisiana, USA. Proceedings of Coastal Sediments '07. Pp 921-934.

Kobashi, D., F. Jose and G.W. Stone. 2007b. Impacts of fluvial fine sediments and winter storms on a transgressive shoal, off south-central Louisiana, U.S.A. Journal of Coastal Research SI 50:858-862.

Kobashi, D. and G.W. Stone. 2008a. Two contrasting morpho-hydrodynamics over recurring sandy and muddy bottoms of a shore-parallel Holocene transgressive shoal, south-central Louisiana, USA. Continental Shelf Research: In Review.

Kobashi, D. and G.W. Stone. 2008b. Variability of Surface Water Level and Current Profiles associated with Varying Storm Winds over the Louisiana Inner Shelf and a Holocene Transgressive Shoal, Louisiana, USA: In-Situ Observations and Numerical Model Analyses. In Preparation.

Kobashi, D. and G.W. Stone. 2009. Response of fluvial fine sediment dispersal to storm wind-current effects on a Holocene transgressive shoal, Atchafalaya Shelf, Louisiana, USA: A numerical simulation. In Review.

Kobashi, D., G.W. Stone, F. Jose and A.L. Spaziani. 2008. Dynamics of sediments within the bottom boundary layer over a transgressive shoal influenced by fluvial sediments and winter storms: south–central Louisiana. Ocean Science Meeting, March 2-7, 2008, Orlando, Florida, USA.

Kobashi, D., G.W. Stone, S.M. Khalil and D.R. Kerper. 2009b. Impacts of sand removal from a shore-parallel Holocene transgressive shoal on hydrodynamics and sediment transport, south-central Louisiana, USA. In Preparation.

Komen, G.J., L. Cavaleri, M. Donelan, K. Hasselmann, S. Hasselmann and P.A.E.M. Janssen. 1994. Dynamics and Modelling of Ocean Waves. Cambridge: Cambridge University Press. 532 pp.

Krawiec, W. 1966. Recent sediments of the Louisiana inner continental shelf. Ph.D. dissertation. Rice University, 50 pp.

Kuhl, M., C. Lassen and B.B. Jorgensen. 1994. Light penetration and light intensity in sandy marine sediments measured with irradiance and scalar irradiance fiber-optic microprobes. Marine Ecology Progress Series 105:139-148.

Kulp, M., S. Penland and K. Ramsey. 2001. Ship Shoal: Sand Resource Synthesis Report. Coastal Research Laboratory, Dept. of Geology and Geophysics, University of New Orleans. University of New Orleans, New Orleans, LA. 70 pp.

Kulp, M., S. Penland, S.J. Williams, C. Jenkins, J. Flocks and J. Kindinger. 2005. Geological Framework and Sediment Resources for Restoration of the Louisiana Coastal Zone. Journal of Coastal Research SI 44:56-71.

Langlois, T.J., M.J. Anderson and R.C. Babcock. 2005. Reef-associated predators influence adjacent soft-sediment communities. Ecology 86(6):1508-1519.

Larson, F. and K. Sundbäck. 2008. Role of microphytobenthos in recovery of functions in a shallow-water sediment system after hypoxic events. Marine Ecology Progress Series 357:1-16.

Laska, S., G. Woodell, R. Hagelman, R. Grambling and M.T. Farris. 2005. At Risk: The Human, Community and Infrastructures Resources of Coastal Louisiana. Journal of Coastal Research SI 44:90-111.

Lassuy, D.R. 1983. Species profiles: life histories and environmental requirements (Gulf of Mexico)—brown shrimp. U.S. Fish and Wildlife Service, Division of Biological Services. FWSIOBS-82/11.1. U.S. Army Corps of Engineers, TR EL-82-4, 15 pp.

Le Rouzic, B., G. Vertru and L. Brient. 1995. HPLC analysis of chloropohyll a breakdown products to interpret microalgae dynamics in a shallow bay. Hydrobiologia 302:71-80.

Lee, M.R. and J.A. Correa. 2005. Effects of copper mine tailings disposal on littoral meiofaunal assemblages in the Atacama region of northern Chile. Marine Environmental Research 59:1-18.

Levy, R.V. and B.C. Coull. 1977. Feeding groups and size analysis of marine meiobenthic nematodes from South Carolina. Vie et Milieu 27:1-12.

Li, M.Z., C.L. Amos and D.E. Heffler. 1997. Boundary layer dynamics and sediment transport under storm and non-storm conditions on the Scotian Shelf. Marine Geology 141:157-181.

Li, M.Z. and G. Gust. 2000. Boundary layer dynamics and drag reduction in flows of high cohesive sediment suspensions. Sedimentology 47:71-86.

Light, B.R. and J. Beardall. 1998. Distribution and spatial variation of benthic microalgal biomass in a temperate, shallow-water marine system. Aquatic Botany 61:39-54.

Lindner, M.J. and W.W. Anderson. 1956. Growth, migrations, spawning and size distribution of white shrimp, Penaeus setiferus. Fishery Bulletin, U.S. 56:555-645.

Lipcius, R.N. and W.T. Stockhausen. 2002. Concurrent decline of the spawning stock, recruitment, larval abundance, and size of the blue crab Callinectes sapidus in Chesapeake Bay. Marine Ecology-Progress Series 226:45-61.

Lohrenz, S., G.L. Fahnenstiel, D.G. Redalije, G.A. Lang, M.J. Dagg, T.E. Whitledge and Q. Dortch. 1999. Nutrients, irradiance and mixing as factors regulating primary primary production in coastal waters impacted by the Mississippi River plume. Continental Shelf Research 19:1113-1141.

Louda, W.J., J. Li, L. Liu, M.N. Winfree and E.W. Baker. 1998. Chlorophyll-a degredation during cellular senescence and death. Organic Geochemistry 29(5-7):1233-1251.

Louisiana Department of Wildlife and Fisheries (LDWF). 1992. A fishery management plan for Louisiana penaeid shrimp. Louisiana Department of Wildlife and Fisheries. Office of Fisheries, Baton Rouge, LA. 231 pp.

Louisiana Department of Wildlife and Fisheries (LDWF). 2005. Louisiana comprehensive wildlife conservation strategy. 455 pp.

Lucas, C.H. and P.M. Holligan. 1999. Nature and ecological implications of algal pigment diversity on the Molenplaat tidal flat (Westerschelde estuary, SW Netherlands). Marine Ecology Progress Series 180:51-64.

Maa, J.P.Y., C.H. Hobbs, S.C. Kim and E. Wei. 2004. Potential impacts of sand mining offshore of Maryland and Delaware: Part I - Impacts on physical oceanographic processes. Journal of Coastal Research 20(1):44-60.

MacIntyre, H.L. and J.J. Cullen. 1995. Fines-scale vertical resolution of chlorophyll and photosynthetic parameters in shallow-water benthos. Marine Ecology Progress Series 122:227-237.

MacIntyre, H.L., R.J. Geider and D.C. Miller. 1996. Microphytobenthos: the ecological role of the "secret garden of unvegetated, shallow-water marine habitats. 1. Distribution, abundance and primary primary production. Estuaries 19(2a):186-201.

Madsen, O.S. 1976. Wave climate of the continental margin: Elements of its mathematical description. In: Stanley, D.J. and D.J. Swift, eds. Marine Sediment Transport and Environmental Management. New York: Wiley. Pp 65-87.

Mannino, A. and P.A. Montagna. 1997. Small-scale spatial variation of macrobenthic community structure. Estuaries 20(1):159-173.

Manty, R.E. 1993. Effect of the El Nino/Southern Oscillation on Gulf of Mexico, winter, frontal-wave cyclones: 1960-89. Volume 1. Ph.D. dissertation. Louisiana State University, Baton Rouge, Louisiana. 397 pp.

Marmorino, G.O. 1983. Variability of Current, Temperature, and Bottom Pressure across the West Florida Continental-Shelf, Winter 1981-1982. Journal of Geophysical Research-Oceans and Atmospheres 88(Nc7):4439-4457.

McAnally, W.H., F. C., D. Hamilton, E. Hayter, P. Shrestha, H. Rodriguez, A. Sheremet and A. Teeter. 2007. Management of fluid mud in estuaries, bays and lakes. I: Present state of understanding on character and behavior. Journal of Hydraulic Engineering 133(1):9-22.

McBride, R., M.J. Taylor and M.R. Byrnes. 2007. Coastal morphodynamics and Chenier-Plain evolution in southwestern Louisiana, USA: A geomorphic model. Geomorphology 88:367-422.

McBride, R.A. and M.R. Byrnes. 1997. Regional variations in shore response along barrier island systems of the Mississippi River Delta Plain: Historical change and future prediction. Journal of Coastal Research 13(3):628-655.

McTigue, T.A. and R.J. Zimmerman. 1991. Carnivory vs. herbivory in juvenile Penaeus sefiferus (Linnaeus) and Penaeus aztecus (Ives). Journal of Experimental Marine Biology and Ecology 151:1-16.

Mehta, A.J. 1991. Understanding fluid mud in a dynamic environment. Geo-Marine Letters 11:113-118.

Mehta, A.J., E.J. Hayter, W.R. Parker, R.B. Krone and A.M. Teeter. 1989. Cohesive sediment transport. I: Process Description. Journal of Hydraulic Engineering 115(8):1076-1093.

Mesinger, F., G. DiMego, E. Kalnay, K. Mitchell, P.C. Shafran, W. Ebisuzaki, D. Jovic, J. Woollen, E. Rogers, E.H. Berbery, M.B. Ek, Y. Fan, R. Grumbine, W. Higgins, H. Li, Y. Lin, G. Manikin, D. Parrish and W. Shi. 2006. North American regional reanalysis. Bulletin of the American Meteorological Society 87(3):343-360.

Metaxatos, A. and L. Ignatiades. 2002. Seasonality of algal pigments in the sea water and interstitial water/sediment systems of an eastern Mediterranean coastal area. Estuarine Coastal and Shelf Science 55:415-426.

Michel, J., R. Nairn, J.A. Johnson and D. Hardin. 2001. Development and design of biological and physical monitoring protocols to evaluate the long-term impacts of offshore dredging operations on the marine environment. U.S. Department of Interior, Minerals Management Service. OCS Study MMS 2001-089. 116 pp.

Miller, D.C., R.J. Geider and H.L. MacIntyre. 1996. Microphytobenthos: the ecological role of the "Secret Garden" of unvegetated, shallow-water marine habitats. II. Role in sediment stability and shallow-water food webs. Estuaries 19:202-212.

Milliman, J.D. and R.H. Meade. 1983. World–wide delivery of river sediment to the oceans. Journal of Geology 91(1):1-21.

Minerals Management Service (MMS). 2004. Archaeological Damage from Offshore Dredging: Recommendations for Pre-Oper¬ational Surveys and Mitigation during Dredging to Avoid Adverse Impacts. Washington, DC: US Department of Interior.

Minerals Management Service (MMS). 2008. Louisiana-Sand Management Working Group. Minerals Management Service, U.S. Department of Interior. http://www.mms.gov/sandandgravel/RegionalSandManagementWorkingGroups.htm . Cited on April 25, 2008.

Montagna, P.A. and D.E. Harper. 1996. Benthic infaunal long term response to offshore production platforms in the Gulf of Mexico. Canadian Journal of Fisheries and Aquatic Science 53:2567-2588.

Montagna, P.A. and C. Ritter. 2006. Direct and indirect effects of hypoxia on benthos in Corpus Christi Bay, Texas, USA. Journal of Experimental Marine Biology and Ecology 330(1):119-131.

Moore, G.T., G.W. Stark, L.C. Bonham and H.O. Woodbury. 1978. Mississippi Fan, Gulf of Mexico - Physiography, Stratigraphy and Sedimentational Patterns. In: Bouma, A.H., G.T. Moore and J.M. Coleman, eds. Framework, Facies and Oil-trapping Characteristics of the Upper Continental Margin. American Association of Petroleum Geologists, Studies in Geology No. 7.

More, W.R. 1969. A contribution to the biology of the blue crab Callinectes sapidus Rathbun in Texas, with a description of the fishery. Texas Parks and Wildlife Department, Seabrook, Texas. Technical Series 1:1-31.

Mossa, J. 1996. Sediment dynamics in the lowermost Mississippi River. Engineering Geology 45:457-479.

Muncy, R.J. 1984. Species Profiles: Life Histories and Environmental Requirements of Coastal Fishes and Invertebrates (Gulf of Mexico)—White Shrimp. U.S. Fish and Wildlife Service, FWS/OBS-82/11.20. TR EL-82-4. U.S. Army Corps of Engineers, 19 pp.

Murray, S. 1997. An observational study of the Mississippi-Atchafalaya coastal plume: Final report. U.S. Deptartpemt of the Interior, Minerals Management Service, Gulf of Mexico OCS Region, New Orleans. OCS Study MMS 98-0040. 513 pp.

Murrell, M.C. and J.W. Fleeger. 1989. Meiofauna abundance on the Gulf of Mexico continental shelf affected by hypoxia. Continental Shelf Research 9:1049-1062.

Nairn, R., J.A. Johnson, D. Hardine and J. Michel. 2004. A biological and physical monitoring program to evaluate long term impacts from sand dredging operations in the United States outer continental shelf. Journal of Coastal Research 20:126-137.

National Climatic Data Center. 2006. Climate of 2005 Atlantic Hurricane Season. http://www.ncdc.noaa.gov/oa/climate/research/2005/hurricanes05.html.

National Research Council (NRC). 2006. Drawing Louisiana's New Map, Addressing Land Loss in Coastal Louisiana. Washington, DC: National Academies Press. 190 pp.

Nelson, J.R., J.E. Eckman, C.Y. Robertson, R.L. Marinelli and R.A. Jahnke. 1999. Benthic microalgal biomass and irradiance at the sea floor on the continental shelf of the South Atlantic Bight: spatial and temporal variability and storm effects. Continental Shelf Research 19:477-505.

Nelson, W.G. and G.W. Collins. 1987. Effects of beach nourishment on the benthic macrofauna and fishes of the nearshore zone of Sebastian Inlet State Recreation Area. Unpublished report to Jacksonville District. U. S. Army Corps of Engineers from the Department of Oceanography and Ocean Engineering, Florida Institute of Technology.

Neumann, C.J., B.R. Jarvinen, C.J. McAdie and J.D. Elms. 1993. Tropical cyclones of the North Atlantic ocean, 1871-1992. Historical Climatology Series, 6(2). Asheville, North Carolina: National Climatic Data Centre.

Newcombe, C.L., F. Campbell and A.M. Eckstine. 1949. A Study of the Form and Growth of the Blue Crab Callinectes-Sapidus Rathbun. Growth 13(2):71-96.

Newell, R.C., L.J. Seiderer and D.R. Hitchcock. 1998. The Impact of Dredging Works in Coastal Waters: a Review of the Sensitivity to Disturbance and Subsequent Recovery of Biological Resources on the Sea Bed. Oceanography and Marine Biology: an Annual Review 36:127-178.

Nielsen, P. 1979. Some basic concepts of wave sediment transport. Series paper 20 Institute of Hydrodynamics and Hydraulic Engineering, Technical University of Denmark. 160 pp.

Nielsen, P. 1992. Coastal bottom boundary layer and sediment transport. Advanced Series on Ocean Engineering. Vol. 4. River Edge, N.J.: World Scientific Publishing Co. 324 pp.

NOAA. 2007. Annual Commercial Landing Statistics. National Oceanographic and Atmospheric Administration, National Marine Fisheries Service, Office of Science & Technology, Commercial Fisheries, 1315 East-West Highway, Silver Spring, MD 20910. Available when request "crab, blue; 1950-2007" at: http://www.st.nmfs.noaa.gov/st1/commercial/landings/annual_landings.html.

Nowlin, W.D., Jr., A.E. Jochens, R.O. Reid and S.F. DiMarco. 1998. Texas-Louisiana Shelf Circulation and Transport Processes Study: Synthesis Report, Volume I: Technical Report. U.S. Dept. of the Interior, Minerals Mgmt Service, Gulf of Mexico OCS Region, New Orleans, LA. OCS Study MMS 98-0035. 502 pp.

O'Connel, M.T., C.D. Franze, E.A. Spalding and M.A. Poirrier. 2005. Biological resources of the Louisiana coast: part 2. Coastal animal and habitat associations. Journal of Coastal Research SI 44:146-161.

Ocean Studies Board. 2002. Effects of trawling and dredging on sea floor habitat. Committee on Ecosystems Effects on Fishing, Ocean Studies Board, National Research Council. Washington, D.C.: National Academy Press. 136 pp.

Ohlmann, J.C. and P.P. Niiler. 2005. Circulation over the continental shelf in the northern Gulf of Mexico. Progress in Oceanography 64(1):45-81.

Olmi, E.J. and J.M. Bishop. 1983. Variations in Total Width-Weight Relationships of Blue Crabs, Callinectes-Sapidus, in Relation to Sex, Maturity, Molt Stage, and Carapace Form. Journal of Crustacean Biology 3(4):575-581.

Palmer, T.A., P.A. Montagna and R.B. Nairn. 2008. The effects of a dredged excavation pit on benthic macrofauna in offshore Louisiana. Environmental Management 41:573-583.

Pechenik, J.A. 2005. Biology of the invertebrates. New York: McGray-Hill. 590 pp.

Penland, S., R. Boyd and J.R. Suter. 1988. Transgressive depositional systems of the Mississippi delta plain: A model for barrier shoreline and shelf sand development. Journal of Sedimentary Petrology 58(6):932-949.

Penland, S., P.F. Connor, A. Beall, S. Fearnley and S.J. Williams. 2005. Changes in Louisiana's shoreline: 1855-2002. Journal of Coastal Research 44:7-39.

Penland, S., J.R. Suter and T.F. Moslow. 1985. Stratigraphic development of Ship Shoal, northern Gulf of Mexico. 98th annual meeting of Geological Society of America, October 28-31, Orlando, FL.

Penland, S., J.R. Suter and T.F. Moslow. 1986. Inner-shelf shoal sedimentary facies and sequences: Ship Shoal, Northern Gulf of Mexico. SEPM Core Workshop No.9, Modern and Ancient Shelf Clastics. Pp 73-123.

Pepper, D.A. 2000. Hydrodyanmics, Bottom Boundary layer processes and sediment transport on the south-central Louisiana inner shelf: The influence of extra-tropical storms and bathymetric modification. Ph.D. Dissertation. Louisiana State University, Baton Rouge, LA. 159 pp.

Pepper, D.A. and G.W. Stone. 2002. Atmospheric forcing of fine-sand transport on a low-energy inner shelf: south-central Louisiana, USA. Geo-Marine Letters 22(1):33-41.

Pepper, D.A. and G.W. Stone. 2004. Hydrodynamic and sedimentary responses to two contrasting winter storms on the inner shelf of the northern Gulf of Mexico. Marine Geology 210(1-4):43-62.

Pianka, E.R. 1970. R-Selection and K-Selection. American Naturalist 104(940):592-&.

Pinckney, J.L., K.R. Carman, S.E. Lumsden and S.N. Hymel. 2003. Microalgal - meiofaunal trophic relationships in muddy intertidal estuarine sediments. Aquatic Microbial Ecology 31:99-108.

Pinn, E.H. and M.R. Robertson. 2003. Macro-infaunal biodiversity and analysis of associated feeding guilds in the Greater Minch area, Scottish west coast. Journal of the Marine Biological Association of the United Kingdom 83(3):433-443.

Posey, M. and T. Alphin. 2002. Resilience and stability in an offshore benthic community: responses to sediment borrow activities and hurricane disturbance. Journal of Coastal Research 18(4):681-697.

Posey, M.H., T.D. Alphin, S. Banner, F. Vose and W. Lindberg. 1998. Temporal variability, diversity and guild structure of a benthic community in the northeastern Gulf of Mexico. Bulletin of Marine Science 63(1):143-155.

Prager, M.H., J.R. McConaugha, C.M. Jones and P.J. Geer. 1990. Fecundity of Blue-Crab, Callinectes-Sapidus, in Chesapeake Bay - Biological, Statistical and Management Considerations. Bulletin of Marine Science 46(1):170-179.

Pullen, E.J. and W.L. Trent. 1970. Carapace Width-Total Weight Relation of Blue Crabs from Galveston-Bay, Texas. Transactions of the American Fisheries Society 99(4):795-798.

Qian, P.Y. and F.S. Chia. 1991. Effects of food concentration on larval growth and development of two polychaete worms, *Capitella capitata* (Fabricius) and *Polydora ligni* (Webster). Bulletin of Marine Science 48:477-484.

Qu, W., C. Su, R.J. West and R.J. Morrison. 2004. Photosynthetic characteristics of benthic microalgae and seagrass in Lake Illawarra, Australia. Hydrobiologia 515:147–159.

Quiñones-Rivera, Z.J., B. Wissel, D. Justić and B. Fry. 2007. Partitioning oxygen sources and sinks in a stratified, eutrophic coastal ecosystem using stable oxygen isotopes. Marine Ecology Progress Series 342:69-83.

Rabalais, N.N., N. Atilla, C. Normandeau and R.E. Turner. 2004. Ecosystem history of the Mississippi River-influenced continental shelf revealed through preserved phytoplankton pigments. Marine Pollution Bulletin 49:537-547.

Rabalais, N.N., L.E. Smith, D.E. Harper Jr and D. Justic. 2001. Effects of seasonal hypoxia on continental shelf benthos. In: Rabalais, N.N. and R.E. Turner, eds. Coastal Hypoxia: Consequences for Living Resources and Ecosystems, Coastal and Estuarine Studies. Washington D.C.: American Geophysical Union. Pp 211-240.

Rabalais, N.N., R.E. Turner and D. Scavia. 2002. Beyond science into policy: Gulf of Mexico hypoxia and the Mississippi River. Bioscience 52(2):129-142.

Rabalais, N.N., R.E. Turner, B.K. Sen Gupta, D.F. Boesch, P. Chapman and M.C. Murrell. 2007. Characterization and Long-Term Trends of Hypoxia in the Northern Gulf of Mexico: Does the Science Support the Action Plan? Estuaries and Coasts 30:753-772.

Rabalais, N.N., W.J. Wiseman and R.E. Turner. 1994. Comparison of Continuous Records of near-Bottom Dissolved-Oxygen from the Hypoxia Zone Along the Louisiana Coast. Estuaries 17(4):850-861.

Radziejewska, T., J.W. Fleeger, N.N. Rabalais and K.R. Carman. 1996. Meiofauna and sediment chloroplastic pigments on the continental shelf off Louisiana, U.S.A. Continental Shelf Research 16:1699-1723.

Rakocinski, C.F., S.E. LeCroy, J.A. McLelland and R.W. Heard. 1998. Nested spatiotemporal scales of variation in sandy-shore macrobenthic community structure. Bulletin of Marine Science 63(2):343-362.

RD Instruments Inc. 2004. WAVES PRIMER: Wave Measurements and the RDI ADCP Waves Array Technique. RD Instruments Inc., San Diego, CA. 22 pp.

Rester, J.K., M. Paine and E.O. Serrano. 2007. Annual report of the Southeast Area Monitoring and Assessment Program (SEAMAP). Gulf States Marine Fisheries Commission, Ocean Springs, MS, Electronically available at: http://www.gsmfc.org/pubs.php?s=SEAMAP. 17 pp.

Ricker, W.E. 1975. Computation and interpretation of biological statistics of fish populations. Bulletin of the Fisheries Research Board of Canada 191:382pp.

Risgaard-Petersen, N. 2003. Coupled nitrification-denitrification in autotrophic and heterotrophic estuarine sediments:On the influence of benthic microalgae. Limnology and Oceanography 48:93-105.

Roberts, H.H. 1997. Dynamic changes of the Holocene Mississippi River delta plain: The delta cycle. Journal of Coastal Research 13(3):605-627.

Roberts, H.H., O.K. Huh, S.A. Hsu, L.J. Rouse and D.A. Rickman. 1989. Winter storm impacts on the Chenier Plain coast of southwestern Louisiana. Gulf Coast Association of Geological Societies Transactions 34:515-522.

Roland, R.M. and S.L. Douglass. 2005. Estimating Wave Tolerance of Spartina Alterniflora in Coastal Alabama. Journal of Coastal Research 21(3):453-463.

Rosenzweig, M.L. 1995. Species diversity in space and time. Cambridge: Cambridge University Press. 436 pp.

Rothschild, B.J., J.S. Ault, E.V. Patrick, S.G. Smith, H. Li, T. Maurer, B. Daugherty, G. Davis, C.I. Zhang and R.N. McGarvey. 1992. Assessment of the Chesapeake Bay blue crab stock. Chesapeake Biological Laboratory (Solomons, Maryland) Contribution:136-138.

Rowe, G.T. 2001. Seasonal hypoxia in the bottom water off the Mississippi River Delta. Journal of Environmental Quality 30:281-290.

Rzeznik-Orignac, J., D. Fichet and G. Boucher. 2004. Extracting massive numbers of nematodes from muddy marine deposits: efficiency and selectivity. Nematology 6:605-616.

Saloman, C.H. 1974. Physical, chemical, and biological characteristics of nearshore zone of Sand Key Florida, prior to beach restoration, Vols I and II. National Marine Fisheries Service, Gulf Coast Fisheries Center, Panama City, FL.

Sanders, J.E. and N. Kumar. 1975. Evidence of shoreface retreat and in-place drowning during Holocene submergence of barriers, shelf off of Fire Island, New York. Geological Society of America Bulletin 86:65-76.

Sandoz, M. and R. Rogers. 1944. The effect of environmental factors on hatching moulting, and survival of zoea larvae of the blue crab Callinectes sapidus Rathbun. Ecology 25(2):216-228.

Sarkar, R.K.A., V.K. Aggarwal, V. Bhatt, P.K. Bhaskaran and S.K. Dube. 2000. Ocean wave model- sensitivity experiments. Proceedings of International Conference PORSEC-2000 NIO. Goa, India. Vol. II, Pp 621-627.

SAS Institute Inc. 2004. SAS OnlineDoc® 9.1.3. Carey, NC.

Saucier, R.T. 1994. Geomorphology and Quaternary Geologic History of the Lower Mississippi Valley. Two volumes. Vicksburg, Mississippi: U.S. Army Corps of Engineers, Waterways Experiment Station.

Schaffner, L.C. and R.J. Diaz. 1988. Distribution and Abundance of Overwintering Blue Crabs, Callinectes-Sapidus, in the Lower Chesapeake Bay. Estuaries 11(1):68-72.

Schratzberger, M., K. Warr and S.I. Rogers. 2007. Functional diversity of nematode communities in the southwestern North Sea. Marine Environmental Research 63:368-389.

Schratzberger, M. and R.M. Warwick. 1998. Effects of physical disturbance on nematode communities in sand and mud: a microcosm experiment. Marine Biology 130:643-650.

Scruton, P.C. 1960. Delta building and the deltaic sequence. In: Shepard, F.P., ed. Recent sediments, northwest Gulf of Mexico. Tulsa, OK: American Association of Petroleum Geologists. Pp 82-102.

Serodio, J., S. Vieira, M. Cruz and F. Barroso. 2005. Short-term variability in the photosynthetic activity of microphytobenthos as detected by measuring rapid light curves using variable fluorescence. Marine Biology 146:903–914.

Service, S.K. and S.S. Bell. 1987. Density-influenced active dispersal of harpacticoid copepods. Journal of Experimental Marine Biology and Ecology 114:49-62.

Sheldon, A.L. 1969. Equitability indices: dependence on the species count. Ecology 50:466-467.

Sheremet, A., A.J. Mehta, B. Liu and G.W. Stone. 2005. Wave–sediment interaction on a muddy inner shelf during Hurricane Claudette. Estuarine, Coastal and Shelf Science 63:225-233.

Sheremet, A. and G.W. Stone. 2003. Observations of nearshore wave dissipation over muddy sea beds. Journal of Geophysical Research-Oceans 108(C11):3357. doi: 10.1029/2003JC001885, 2003.

Shields, J.D. and R.M. Overstreet. 2007. Diseases, parasites, and other symbionts. In: Kennedy, V.S. and L.E. Cronin, eds. The blue crab Callinectes sapidus. College Park, Maryland: Maryland Sea Grant College. Pp 299-318.

Simpson, E.H. 1949. Mesurement of diversity. Nature 163:688.

Smith, J.M., A.R. Sherlock and D.T. Resio. 2001. STWAVE: Steady-state spectral wave model. User's manual for STWAVE, version 3.0. ERDC/CHL SR-01-1. Coastal and Hydraulic Laboratory, US Army Corps of Engineers. 81 pp.

Snedden, J.W. and R.W. Dalrymple. 1999. Modern shelf sand ridges: From historical perspective to unified hydrodynamic and evolutionary model. SEPM Special Publication 64. Pp 13-28.

Snelgrove, P.V.R. and C.A. Butman. 1994. Animal-sediment relationships revisited : cause versus effect. Oceanography and Marine Biology: an annual review 32:111-177.

Soetaert, K., A. Muthumbi and C. Heip. 2002. Size and shape of ocean margin nematodes: morphological diversity and depth-related patterns. Marine Ecology Progress Series 242:179-193.

Somerfield, P.J., M. Atkins, S.G. Bolam, K.R. Clarke, E. Garnacho, H.L. Rees, R. Smith and R.M. Warwick. 2006. Relative impacts at sites of dredged-material relocation in the coastal environment: a phylum-level meta-analysis approach. Marine Biology 148:1231-1240.

Somerfield, P.J. and R.M. Warwick. 1996. Meiofauna in marine pollution monitoring programmes: A laboratory manual. Ministry of Agriculture, Fisheries and Food, Directorate of Fisheries, Lowestoft.

SonTek Inc. 1997a. Pulse-coherent Doppler processing and the ADV correlation coefficient. SonTek Technical Notes. San Diego, CA. 5 pp.

SonTek Inc. 1997b. SonTek Doppler Current Meters – Using Signal Strength Data to monitor Suspended Sediment Concentration. SonTek Application Notes. San Diego, California. 7 pp.

SonTek Inc. 2004. PC-ADP - Read Me First! SonTek PC-ADP manual, San Diego, California. 28 pp.

Sorensen, O.R., H. Kofoed-Hansen, M. Rugbjerg and L.S. Sorensen. 2004. A third-generation spectral wave model using an unstructured finite volume technique. Proceedings of International Conference on Coastal Engineering 29. Pp 894-906.

Soulsby, R. 1997. Dynamics of marine sands. London, UK: Thomas Telford Publications. 272 pp.

Steele, P. 1991. Population dynamics and migration of the Blue Crab, Callinectes sapidus, (Rathbun), in the Eastern Gulf of Mexico. Proceedings of The 40th Gulf and Caribbean Fisheries Institute. Pp 241-244.

Sternberg, R.W. 1972. Predicting Initial Motion and Bedload Transport of sediment particles in the shallow marine environment. In: Swift, D.J.P., D.B. Duane and O.H. Pilkey, eds. Shelf sediment transport: Process and Pattern. Stroudsburg, PA: Dowden, Hutchinson, and Ross, Inc. Pp 61-82.

Stone and Webster Environmental Services. 1991. Environmental monitoring of the sand borrow site for the Great Egg Harbor Inlet and Peck Beach, Ocean City, New Jersey Project. Final Report. Prepared for U.S. Army Corps of Engineers. Philadelphia, PA.

Stone, G.W. 2000. Wave climate and bottom boundary layer dynamics with implications for offshore sand mining and barrier island replenishment in south-central Louisiana. U.S. Dept. of the Interior, Minerals Management Service, Gulf of Mexico OCS Region, New Orleans, LA. OCS Study MMS 2000-53. 90 pp.

Stone, G.W. 2001. Mining of Ship Shoal for large-scale barrier island restoration along the Isles Dernieres. Coastal Studies Institute, LSU, Baton Rouge, LA 70803.

Stone, G.W., R. Condrey and J. Fleeger. 2005a. Environmental investigation of long-term use of Ship Shoal sand resources. Year 1 annual report submitted to U.S. Minerals Management Service/Louisiana Department of Natural Resources. 39 pp.

Stone, G.W., R. Condrey and J. Fleeger. 2006. Environmental investigation of long-term use of Ship Shoal sand resources. Year 2 annual report, MMS/LDNR. 62 pp.

Stone, G.W., J.W. Grymes, J.R. Dingler and D.A. Pepper. 1997. Overview and significance of Hurricanes on the Louisiana Coast, USA. Journal of Coastal Research 13(3):656-669.

Stone, G.W., B.P. Kumar, A. Sheremet and D.A. Watzke. 2005b. Complex morpho-hydrodynamic response of estuaries and bays to winter storms: North-central Gulf of Mexico, U.S.A. In: Fizgerald, D.M. and J. Knight, eds. High Resolution Morphodynamics and Sedimentary Evolution of Estuaries. Dordrecht, Netherlands: Springer. Pp 243-267.

Stone, G.W., B.Z. Liu, D.A. Pepper and P. Wang. 2004a. The importance of extratropical and tropical cyclones on the short-term evolution of barrier islands along the northern Gulf of Mexico, USA. Marine Geology 210(1-4):63-78.

Stone, G.W. and R.A. McBride. 1998. Louisiana barrier islands and their importance in wetland protection: Forecasting shoreline change and subsequent response of wave climate. Journal of Coastal Research 14(3):900-915.

Stone, G.W., D.A. Pepper, J.P. Xu and X.P. Zhang. 2004b. Ship shoal as a prospective borrow site for barrier island restoration, coastal south-central Louisiana, USA: Numerical wave modeling and field measurements of hydrodynamics and sediment transport. Journal of Coastal Research 20(1):70-88.

Stone, G.W., A. Sheremet, Y. Zhang and D. Braud. 2003a. Coastal land loss and surge predictions during hurricanes in coastal Louisiana. Final report to Louisiana Department of Natural Resources, U.S. Geological Survey and U.S. Minerals Management Service. 67 pp.

Stone, G.W. and J.P. Xu. 1996. Wave climate modeling and evaluation relative to sand mining on Ship Shoal, offshore Louisiana, for coastal and barrier island restoration. U.S. Dept. of the Interior, Minerals Management Service, Gulf of Mexico OCS Region, New Orleans, LA. OCS Study MMS 96-0059. 170 pp.

Stone, G.W., X. Zhang, J. Li and A. Sheremet. 2003b. Coastal Observing Systems: Key to the future of coastal dynamics investigation. GCAGS/GCSSEPM Transactions 53:783-799.

Stone, G.W., X. Zhang and A. Sheremet. 2005c. The role of barrier islands, muddy shelf and reefs in mitigating the wave field along coastal Louisiana. Journal of Coastal Research SI 44:40-55.

Stone, G.W., X.P. Zhang, W. Gibson and R. Frederichs. 2001. A new wave-current online information system for oil spill contigency planning (WAVCIS). Proceedings of 24th Arctic and Marine Oil spill Program Technical Seminar. Edmonton, Alberta, CANADA. Pp 401-425.

Street, G.T. and P.A. Montagna. 1996. Loss of genetic diversity in Harpacticoida near offshore platforms. Marine Biology 126:271-282.

Suter, J.R., H.L. Berryhill and S. Penland. 1985. Environments of sand deposition on the southwest Louisiana continental shelf. Gulf Coast Association of Geological Societies Transactions 35:495-504.

Suter, J.R., S. Penland and K.E. Ramsey. 1991. Nearshore Sand Resources of the Mississippi River Delta Plain: Marsh Island to Sandy Point. Coastal Geology Technical Report No. 8. Louisiana Geological Survey, Baton Rouge, LA. 130 pp.

Swedmark, B. 1964. The interstitial fauna of marine sand. Biological Reviews Cambridge Philosophical Society 39:1-42.

Swift, D.J.P. 1975. Barrier island genesis: Evidence from the central Atlantic shelf, eastern USA. Sedimentary Geology 14:1-43.

Swift, D.J.P. 1985. Response of the shelf floor to flow. In: Tillman, R.W., D.J.P. Swift and R.G. Wlaker, eds. Shelf Sands and Sandstone Reservoirs. SEPM Short Course Notes 13. Pp 135-241.

Swift, D.J.P. and A.W. Niedoroda. 1985. Fluid and Sediment dynamics on continental shelves. In: Tillman, R.W., D.J.P. Swift and R. Walker, eds. Shelf Sand and Sandstone Reservoirs. Society of Economic Paleontologists and Mineralogists, Short Course 13B, not consecutively paged.

Tagatz, M.E. 1968. Biology of Blue Crab, Callinectes Sapidus Rathbun, in St Johns River, Florida. United States Fish and Wildlife Service Fishery Bulletin 67(1):17-33.

Tankersley, R.A., M.G. Wieber, M.A. Sigala and K.A. Kachurak. 1998. Migratory behavior of ovigerous blue crabs Callinectes sapidus: Evidence for selective tidal-stream transport. Biological Bulletin 195(2):168-173.

Tenore, K.R. 1988. Nitrogen in benthic food chains. In: Sorensen, J. and T.H. Blackburn, eds. Nitrogen cycling in coastal marine environments. New York: Wiley. Pp 191-206.

Thistle, D. 2003. Harpacticoid copepod emergence at a shelf site in summer and winter: implications for hydrodynamic and mating hypotheses. Marine Ecology Progress Series 248:177-185.

Thistle, D., G.L. Weatherly and S.C. Ertman. 1995a. Shelf harpacticoid copepods do not escape into the seabed during winter storms. Journal of Marine Research 53:847-863.

Thistle, D., G.L. Weatherly, A. Wonnacott and S.C. Ertman. 1995b. Suspension by winter storms has an energetic cost for adult male benthic harpacticoid copepods at a shelf site. Marine Ecology Progress Series 125:77-86.

Thompson, C.E.L., C.L. Amos, M. Angelaki, T.E.R. Jones and C.E. Binks. 2006. An evaluation of bed shear stress under turbid flows. Journal of Geophysical Research 111, C04008. doi:10.1029/2005JC003287.

Thornton, E.B. and R.T. Guza. 1983. Transformation of wave height distribution. Journal of Geophysical Research 88(C10):5925-5938.

Thouzeau, G., G. Robert and R. Ugarte. 1991. Faunal Assemblages of Benthic Megainvertebrates Inhabiting Sea Scallop Grounds from Eastern Georges Bank, in Relation to Environmental-Factors. Marine Ecology-Progress Series 74(1):61-82.

Thrush, S.F. and P.K. Dayton. 2002. Disturbance to marine benthic habitats by trawling and dredging: implications for marine biodiversity. Annual review of Ecology and systematics 33:449-473.

Tita, G., M. Vincx and G. Desrosiers. 1999. Size spectra, body width and morphotypes of intertidal nematodes: an ecological interpretation. Journal of the Marine Biological Association of the United Kingdom 79:1-9.

Todaro, M.A., J.W. Fleeger and W.D. Hummon. 1995. Marine gastrotrichs from the sand beaches of the northern Gulf of Mexico: species list and distribution. Hydrobiologia 310:107-117.

Trefry, J.H., S. Metz, T.A. Nelsen, R.P. Trocine and B.J. Eadie. 1994. Transport of Particulate organic carbon by the Mississippi River and its fate in the Gulf of Mexico. Estuaries 17:839-849.

Turner, R.E. and N.N. Rabalais. 1994. Coastal eutrophication near the Mississippi river delta. Nature 368:619-621

Uebelacker, J.M. and P.G. Johnson. 1984. Taxonomic guide to the polychaetes of the northern Gulf of Mexico. Mobile, Alabama: Barry A. Vittor & Associates, Inc.

UN. 2008. UN Atlas of the Oceans. 2008. FAO Fisheries Global Information System (FIGIS) – Species. Species of major importance to fisheries: under blue crab. 2008. Available from: http://www.fao.org/fishery/species/2632.

Unoki, S. 1994. Phyiscal oceanography of coastal waters. Tokyo: Tokai University Press (in Japanese). 672 pp.

USACE. 2001. The New York District's biological monitoring program for the Atlantic Coast of New Jersey, Asbury Park to Manasquan Section beach erosion control project final report. Engineer Research and Development Center, U. S. Army Engineer Waterways Experiment Station, Vicksburg, MS.

Van Dolah, R.F., R.M. Martore, A.E. Lynch, P.H. Wendt, M.V. Levisen, D.J. Whitaker and W.D. Anderson. 1994. Environmental evaluation of the Folly Beach nourishment project. Final Report. Prepared for the U. S. Army Corps of Engineers, Charleston SC. South Carolina Department of Natural Resources, Marine Resources Division, Charleston, SC.

Van Engel, W.A. 1958. The blue crab and its fishery in Chesapeake Bay. Commercial Fisheries Review 20(6):1-17.

Van Hoey, G., S. Degraer and M. Vincx. 2004. Macrobenthic community structure of soft-bottom sediments at the Belgian Continental Shelf. Estuarine Coastal and Shelf Science 59(4):599-613.

Vanaverbeke, J., T. Deprez and M. Vincx. 2007. Changes site in nematode communities at the long-term sand extraction of the Kwintebank (Southern Bight of the North Sea). Marine Pollution Bulletin 54:1351-1360.

Vanaverbeke, J., T. Gheskiere, M. Steyaert and M. Vincx. 2002. Nematode assemblages from subtidal sandbanks in the Southern Bight of the North Sea: effect of small sedimentological differences. Journal of Sea Research 48:197-207.

Vanaverbeke, J., T. Gheskiere and M. Vincx. 2000. The meiobenthos of subtidal sandbanks on the Belgian Continental Shelf (Southern Bight of the North Sea). Estuarine, Coastal and Shelf Science 51:637-649.

Vanaverbeke, J., K. Soetaert and M. Vincx. 2004. Changes in morphometric characteristics of nematode communities during a spring phytoplankton bloom deposition. Marine Ecology Progress Series 273:139-146.

Vanaverbeke, J., M. Steyaert, A. Vanreusel and M. Vincx. 2003. Nematode biomass spectra as descriptors of functional changes due to human and natural impact. Marine Ecology Progress Series 249:157-170.

Vanaverbeke, J. and M. Vincx. 2008. Short-term changes in nematode communities from an abandoned intense sand extraction site on the Kwintebank (Belgian Continental Shelf) two years post-cessation. Marine Environmental Research 66:240-248.

Waggy, G.L., N.J. Brown-Peterson and M. Peterson. 2006. Evaluation of the reproductive life history of the sciaenidae in the Gulf of Mexico and Caribbean Sea: "Greater" vs. "Lesser" strategies. Proceedings of the Gulf and Caribbean Fisheries Institute. Vol. 57, Pp 264-282.

Walker, N.D. 2001. Tropical storm and hurricane wind effects on water level, salinity, and sediment transport in the river-influenced Atchafalaya-Vermilion Bay system, Louisiana, USA. Estuaries 24(4):498-508.

Walker, N.D. and A.B. Hammack. 2000. Impacts of Winter Storms on Circulation and Sediment Transport: Atchafalaya-Vermilion Bay Region, Louisiana, U.S.A. Journal of Coastal Research 16(4):996-1010.

Walker, N.D., R. Jarosz and S.P. Murray. 2001. An investigation of pressure and pressure gradients along the Louisiana/Texas inner shelf and their relationships to wind forcing and current variability. U.S. Dept. of the Interior, Minerals Management Service, Gulf of Mexico OCS region, New Orleans, LA. OCS Study MMS2001-057. 40 pp.

Walker, N.D. and L.J. Rouse, Jr. 1993. Satellite assessment of Mississippi River discharge plume variability. U.S . Dept. of the Interior, Minerals Management Service, Gulf of Mexico OCS Regional Office, New Orleans, LA. OCS Study MMS 93-0044. 50 pp.

Warwick, R.M. 1988. The level of taxonomic discrimination required to detect pollution effects on marine benthic communities. Marine Pollution Bulletin 19:259-268.

Watzke, D.A. 2004. Short-Term Evolution of a Marsh Island System and the Importance of Cold Front Forcing, Terrebonne Bay, Louisiana. M.S. Thesis. Louisiana State University, Baton Rouge, LA. 66 pp.

Welker, C., E. Sdrigotti, S. Covelli and J. Faganeli. 2002. Microphytobenthos in the Gulf of Trieste (Northern Adriatic Sea): Relationship with labile sedimentary organic matter and nutrients. Estuarine Coastal and Shelf Science 55:259–273.

Wells, J.T. and P. Kemp. 1981. Atchafalaya mud stream and recent mudflat progradation: Louisiana chenier plain. Transaction, Gulf Coast Association of Geological Society 31:409-416.

Wetzel, M.A., J.W. Fleeger and S. Powers. 2001. Effects of hypoxia and anoxia on meiofauna: A review with new data from the Gulf of Mexico. In: Rabalais, N.N. and R.E. Turner, eds. Coastal Hypoxia; Consequences for Living Resources. Washington, D.C.: American Geophysical Union. Pp 165-184.

Wheatcroft, R.A. and C.K. Sommerfield. 2005. River sediment flux and shelf sediment accumulation rates on the Pacific Northwest margin. Continental Shelf Research 25(3):311-332.

Whitehouse, R.J.S., R. Soulsby, W. Roberts and H. Mitchener. 2000. Dynamics of Estuarine Muds. London, UK: Thomas Telfort and HR Wallingford.

Whittaker, R.H. 1972. Evolution and measurement of species diversity. Taxon 21:213-251.

Wieking, G. and I. Kroncke. 2005. Is benthic trophic structure affected by food quality? The Dogger Bank example. Marine Biology 146:387-400.

Wieser, W. 1959. The effect of grain size on the distribution of small invertebrates inhabiting the beaches of Puget Sound. Limnology and Oceanography 4:181-194.

Williams, S.J., S. Penland and R.C. Circć. 1989. Distribution and textural character of surficial sediments, Isles Dernieres to Ship Shoal region, Louisiana. Gulf Coast Association of Geological Societies Transactions 39:571-576.

Williams, S.J., S. Penland and A.H. Sallenger. 1992. Louisiana Barrier Island Erosion Study, Atlas of Shoreline Changes in Louisiana from 1853 to 1989, 1-2150-A. U.S. Department of Interior and US Geological Survey, 103 pp.

Williams, S.J., G.W. Stone and A.E. Burrus. 1997. A perspective on the Louisiana wetland loss and coastal erosion problem. Journal of Coastal Research 13(3):593-594.

Wilmott, C.J. 1982. Some Comments on the Evaluation of Model Performance. Bulletin of the American Meteorological Society 63(11):1309-1313.

Wiseman, W.J., Jr., R.E. Turner, F.J. Kelly, L.J. Rouse, JR. and R.F. Shaw. 1986. Analysis of biological and chemical associations near a turbid coastal front during winter 1982. Contributions in Marine Science 29:141-151.

Wolcott, D.L., C.W.B. Hopkins and T.G. Wolcott. 2005. Early events in seminal fluid and sperm storage in the female blue crab Callinectes sapidus Rathbun: Effects of male mating history, male size, and season. Journal of Experimental Marine Biology and Ecology 319(1-2):43-55.

Wright, L.D., C.T. Friedrichs and D.A. Hepworth. 1997a. Effects of benthic biology on bottom boundary layer processes, Dry Tortugas Bank, Florida Keys. Geo-Marine Letters 17(4):291-298.

Wright, L.D. and C.A. Nittrouer. 1995. Dispersal of river sediments in coastal seas: Six contrasting cases. Estuaries 18(3):494-508.

Wright, L.D., C.R. Sherwood and R.W. Sternberg. 1997b. Field measurements of fairweather bottom boundary layer processes and sediment suspension on the Louisiana inner continental shelf. Marine Geology 140(3-4):329-345.

Wu, J. 1982. Wind-stress coefficients over sea surface from breeze to hurricane. Journal of Geophysical Research 87(C12):9704-9706.

Wu, R.S.S. and Y.Y. Or. 2005. Bioenergetics, growth and reproduction of amphipods are affected by moderately low oxygen regimes. Marine Ecology-Progress Series 297:215-223.

Wulff, A., K. Sundbäck, C. Nilsson, L. Carlson and B. Jonsson. 1997. Effect of Sediment load on the microbenthic community of a shallow-water sandy sediment. Estuaries 20(3):547-558.

Wysocki, L.A., T.S. Bianchi, R.T. Powell and N. Reuss. 2006. Spatial variability in the coupling of organic carbon, nutrients, and phytoplankton pigments in surface waters and sediments of the Mississippi River plume. Estuarine Coastal and Shelf Science 69:47-63.

Yonge, C.M. and T.E. Thompson. 1976. Living marine molluscs. London: Collins, St James Place. 288 pp.

Zhang, X.P. 2003. Design and implementation of an ocean observing system: WAVCIS (Wave-current-surge information system) and its application to the Louisiana coast. Ph.D. dissertation. Louisiana State University, Baton Rouge, LA. 194 pp.

Zohar, Y., A.H. Hines, O. Zmora, E.G. Johnson, R.N. Lipcius, R.D. Seitz, D.B. Eggleston, A.R. Place, E.J. Schott, J.D. Stubblefield and J.S. Chung. 2008. The Chesapeake Bay blue crab (Callinectes sapidus): A multidisciplinary approach to responsible stock replenishment. Reviews in Fisheries Science 16(1-3):24-34.

Zühlke, R. 2001. Polychaete tubes create ephemeral community patterns: *Lanice conchilega* (Pallas, 1766) associations studied over six years. Journal of Sea Research 46:261-272.

# APPENDIX

# APPENDIX 10.A

## FAMILIES AND SPECIES IDENTIFIED FROM THE GOMEX BOX CORE SAMPLES. CORE CROSS-SECTIONAL AREA = 0.09 $M^2$. MESH SIZE 500 µM.

| | |
|---|---|
| **Platyhelminthes** | |
| - | *Probusa veneris* |
| Plehniidae | *Discocelides ellipsoides* |
| **Cnidaria** | |
| Actinostolidae | *Paranthus rapiformis* |
| | *burrowing Anemone* sp.2 |
| | *burrowing Anemone* sp.3 |
| **Nemertea** | |
| Lineidae | *Micrura leidyi* |
| - | *Nemertea* sp.1 |
| - | *Nemertea* sp.2 |
| - | *Nemertea* sp.3 |
| **Polychaeta** | |
| Orbiniidae | *Leitoscoloplos fragilis* |
| | *Scoloplos rubra* |
| | *Scoloplos* sp.B |
| | *Phylo felix* |
| Paraonidae | *Cirrophorus forticirratus* |
| | *Aricidea fragilis* |
| | *Aricidea suecica* |
| | *Aricidea alisdairi* |
| | *Aricidea quadrilobata* |
| | *Paraonis pygoenigmatica* |
| Spionidae | *Spiophanes bombyx* |
| | *Boccardiella* sp.A |
| | *Polydora ligni* |
| | *Polydora socialis* |
| | *Dispio uncinata* |
| | *Aonides paucibranchiata* |
| | *Scolelepis texana* |
| | *Scolelepis squamata* |
| | *Paraprionospio pinnata* |
| | *Prionospio cristata* |
| | *Prionospio pygmaea* |
| | *Prionospio cirrobranchiata* |
| | *Spio pettibonea* |
| | *Microspio pigmentata* |
| Magelonidae | *Magelona* sp.A |
| | *Magelona* sp.H |
| Poecilochaetidae | *Poecilochaetus johnsoni* |
| Chaetopteridae | *Spiochaetopterus costarum* |
| | *Mesochaetopterus capensis* |
| Cirratulidae | *Tharyx annulosus* |
| | *Chaetozone* sp.A |
| | *Cirriformia* sp.B |
| Capitellidae | *Mediomastus californiensis* |
| | *Mastobranchus* sp.A |
| | *Notomastus latericeus* |
| Arenicolidae | *Arenicola sp.* |
| Opheliidae | *Armandia maculata* |
| | *Travisia hobsonae* |
| Phyllodocidae | *Phyllodoce mucosa* |
| | *Anaitides groenlandica* |
| Polynoidae | *Malmgreniella* sp.C |
| | *Lepidonotus sublevis* |
| | *Perolepis* sp.A |
| | *Polynoidae* sp. |
| Eulepethidae | *Grubeulepis* sp.A |

| | |
|---|---|
| **Polychaeta (cont.)** | |
| Goniadidae | *Goniada littorea* |
| Nephtyidae | *Nephtys simoni* |
| | *Aglaophamus verrilli* |
| Amphinomidae | *Paramphinome* sp.B |
| Onuphidae | *Diopatra cuprea* |
| | *Onuphis emerita oculata* |
| Lumbrineridae | *Lumbrineris latreilli* |
| | *Lumbrineris tenuis* |
| Oweniidae | *Owenia fusiformis* |
| | *Myriowenia* sp.A |
| Ampharetidae | *Sabellides* sp.A |
| | *Ampharete* sp.A |
| Terebellidae | *Loimia viridis* |
| | *Eupolymnia nebulosa* |
| Sabellidae | *Chone americana* |
| **Mollusca** | |
| Olividae | *Oliva sayana* |
| | *Olivella mutica* |
| Nassariidae | *Nassarius acutus* |
| Fasciolariidae | *Latirus distinctus* |
| Columbellidae | *Anachis obesa* |
| Naticidae | *Polinices duplicatus* |
| | *Natica pusilla* |
| | *Simun maculatum* |
| Litiopinae | *Epitonium multistriatum* |
| Calyptraeidae | *Crepidula plana* |
| Cyclostremellinae | *Cyclostremella humilis* |
| Tellinidae | *Strigilla pisiformis* |
| | *Tellina iris* |
| | *Tellina versicolor* |
| | *Macoma pulleyi* |
| Mactridae | *Mulinia lateralis* |
| | *Raeta plicatella* |
| Cardiidae | *Americardia media* |
| Solecurtidae | *Abra aequalis* |
| Ungulinidae | *Diplodonta soror* |
| Lucinidae | *Parvilucina multilineata* |
| | *Linga amiantus* |
| Veneridae | *Chione clenchi* |
| Solenoidea | *Solen viridis* |
| Dosiniinae | *Dosinia discus* |
| Pandoridae | *Pandora trilineata* |
| Arcidae | *Anadara transversa* |
| **Crustacea** | |
| Haustoriidae | *Acanthohaustorius* sp. A |
| | *Protohaustorius bousfieldi* |
| | *Pseudohaustorius americanus* |
| Synopiidae | *Metatiron triocellatus* |
| | *Metatiron tropakis* |
| Liljeborgiidae | *Listriella barnardi* |
| Isaeidae | *Microprotopus raneyi* |
| Corophiidae | *Monoconophium* sp. A |
| | *Monocorophium tuberculatum* |
| Ampelisca | *Ampelisca* sp. C |
| Oedicerotidae | *Hartmanodes nyei* |
| | *Americhelidium americanum* |
| Ischyroceridae | *Ericthonius brasiliensis* |
| | *Cerapus tubularis* |

| | |
|---|---|
| **Crustacea (cont.)** | |
| Xanthidae | *Xanthidae* sp. |
| Majidae | *Libinia dubia* |
| | *Mithrax acuticormis* |
| Paguridae | *Pagurus annulipes* |
| Albuneidae | *Albunea paretti* |
| | *Lepidopa benedicti* |
| Porcellanidae | *Euceramus praelongus* |
| - | *Thalassinidean* sp. |
| Callianassidae | *Glypturus* nr. *acanthochirus* |
| Pasiphaeidae | *Leptochela serratorbita* |
| Processidae | *Processa hemphilli* |
| Hippolytidae | *Latreutes parvulus* |
| Panaeidae | *Solenocera vioscai* |
| Sergestidae | *Lucifer faxoni* |
| | *Acetes americanus* |
| Ogyrididae | *Ogyrides alphaerostris* |
| Nannosquillidae | *Coronis scolopendra* |
| | *Squilla* sp.A |
| Diastylidae | *Oxyurostylis smithi* |
| Bodotriidae | *Cyclaspis varians* |
| **Echinodermata** | |
| Amphiuridae | *Amphipholis squamata* |
| **Sipuncula** | |
| Golfingiidae | *Phascolion strombi* |
| | *Golfingia tenuissima* |
| Sipunculidae | *Sipunculus* sp. |
| **Echiura** | |
| Echiuridae | *Thalassema* sp. |
| **Phoronida** | |
| Phoronidae | *Phoronis architecta* |
| **Chordata** | |
| Branchiostomatidae | *Branchiostoma floridae* |

| | | | |
|---|---|---|---|
| Sigalionidae | *Thalenessa* cf. *spinosa* | Argissidae | *Argissa hamtipes* |
| | *Fimbriosthenelais minor* | Stenothoidae | *Parametopella cypris* |
| Hesionidae | *Podarke* sp.A | Caprellidae | *Deutella* sp. |
| | *Gyptis brevipalpa* | Platyischnopidae | *Eudevanopus honduranus* |
| Pilargiidae | *Sigambra tentaculata* | Phoxocephalidae | *Trichophoxus* sp. |
| | *Synelmis klatti* | - | *unknown Amphipod* |
| Syllidae | *Streptosyllis pettiboneae* | Portunidae | *Portunus gibbesii* |
| Nereidae | *Neanthes micromma* | | *Ovalipes floridanus* |
| | *Nereis falsa* | | *Callinectes similis* |
| | *Websterinereis tridentata* | | *Portunidae* sp |
| Glyceridae | *Glycera americana* | Pinnotheridae | *Pinnixia chacei* |
| | *Glycera abranchiata* | | *Pinnixia sayana* |

**The Department of the Interior Mission**

As the Nation's principal conservation agency, the Department of the Interior has responsibility of our nationally owned public lands and natural rsources. This includes fostering sound use of our land and water resources; protecting our fish, wildlife, and biological diversity; preserving the environmental and cultural values of our national parks and historical places; and providing for the enjoyment of life through outdoor recreation. The Department assesses our energy and mineral resources and works to ensure that their development is in the best interests of all our people by encouraging stewardship and citizen participation in their care. The Department also has a major responsibility for American Indian reservation communities and for people who live in island territories under U.S. administration.

**The Minerals Management Service Mission**

As a bureau of the Department of the Interior, the Minerals Management Service's (MMS) primary responsibilities are to manage the mineral resources located on the Nation's Outer Continental Shelf (OCS), collect revenue from the Federal OCS and onshore Federal and Indian lands, and distribute those revenues.

Moreover, in working to meet its responsibilities, the Offshore Minerals Management Program administers the OCS competitive leasing program and oversees the safe and environmentally sound exploration and production of our Nation's offshore natural gas, oil and other mineral resources. The MMS Minerals Revenue Management meets its responsibilities by ensuring the efficient, timely and accurate collection and disbursement of revenue from mineral leasing and production due to Indian tribes and allottees, States and the U.S. Treasury.

The MMS strives to fulfil its responsibilities through the general guiding principles of: (1) being responsive to the public's concerns and interests by maintaining a dialogue with all potentially affected parties and (2) carrying out its programs with an emphasis on working to enhance the quality of life for all Americans by lending MMS assistance and expertise to economic development and environmental protection.